The design of
aerostatic
bearings

J. W. Powell

Design of Aerostatic Bearings

BY

J. W. POWELL
B.Sc.(Eng.), Ph.D.

CONTENTS

PREFACE

The technology of gas lubrication has advanced considerably during the past decade. Ten years ago there were virtually no externally pressurized (aerostatic) gas bearings in industrial use in this country, and apart from the pioneering research of G. L. Shires at N.G.T.E. and of Robinson and Sterry at A.E.R.E. very little had been learned about their performance and application. About this time, however, two research programmes began which were to lead to a number of manufacturers marketing products with aerostatic bearings. The first was at the National Engineering Laboratory, where a team led by H. L. Wunsch pioneered the application of air bearings to grinding spindles, machine slideways and form measuring instruments. This work was taken up and developed commercially by the Churchill Machine Tool Co. Ltd., who now supply an air bearing wheelhead as standard equipment on most of their range of precision grinding machines. The second research programme was carried out at the University of Southampton under the leadership of the late Dr. N. S. Grassam. The work was primarily concerned with the problems of operating bearings at very high speeds and in 1962 there evolved the air turbine dental drill, operating at 500 000 r.p.m., which was probably the first mass produced air bearing product. The Dental Manufacturing Co. Ltd. have continued production to the present time and have achieved a peak output of 1 500 units per month. The year 1963 saw the birth of Westwind Turbines Ltd., another offshoot of the Southampton programme, which has ever since devoted itself entirely to the application of air bearings to machine tools and scientific instruments. Several thousand of Westwind's 100 000 r.p.m. drilling spindles are employed in the precision drilling of electronic printed circuit boards throughout the world's computer industries.

Aerostatic bearings have now become firmly established in such applications as precision grinding, micro hole drilling and a variety of instruments such as roundness measuring machines and turbine flowmeters for gases. They are being tried in an ever-increasing range of applications in machine tools, textile spindles and turbo-machinery. The purpose of this book is to place at the disposal of the design engineer who is facing these challenges a survey of the experience gained from the many and diverse applications of aerostatic bearings which have already been successfully accomplished. Most aspects

relating to design have been covered, including basic theory, design methods, materials and manufacture and inspection and installation. In addition to emphasizing the advantages that aerostatic bearings have been shown to possess, stress has also been laid upon their limitations and areas of difficulty. Theory has been kept to a minimum consistent with a proper understanding of design procedures, and emphasis has been placed upon many practical features which have determined the success or failure of past applications. Although this book is primarily intended to assist designers, those engaged in teaching gas lubrication will also find something of value in its pages.

Finally, I would like to express my appreciation of the help that I have received in the preparation of this book from many individuals and organizations. Space considerations preclude a comprehensive list but I am particularly indebted to Mr. W. Kammerling of Westwind Turbines Ltd. and to Dr. N. Tully of Oxford University.

JOHN POWELL

Lytchett Matravers

LIST OF MATHEMATICAL SYMBOLS

α dimensionless factor used in slot-fed bearing analysis

β $\left(= \dfrac{2P_a}{P_o - P_a}\right)$ pressure factor used in slot-fed bearing analysis; angular displacement of rotor axis

γ $\left(= \dfrac{C_p}{C_o}\right)$ ratio of specific heats of gas

δ phase angle by which rotor whirl lags unbalance; pocket depth

ε eccentricity ratio in journal bearing

θ angle measured from load line of journal bearing

ϕ attitude angle in aerodynamic journal bearing

ϕ_H attitude angle in hybrid journal bearing

σ Poissons ratio; squeeze number

ω angular velocity of rotor

ω^* angular velocity of whirl or vibration

ω_1 cylindrical synchronous resonance speed

ω_2 conical synchronous resonance speed

ω_c onset speed of self-excited whirl

μ viscosity; 10^{-6} (e.g. 1 μm $= 10^{-6}$ m)

ρ density: ρ_o at supply condition, ρ_d downstream of feed holes, ρ_a ambient

η $\left(= \dfrac{C}{m_R}\right)$ damping constant per bearing per unit rotor mass

ξ damping ratio

Λ $\left[= \dfrac{\mu\omega}{P_a}\left(\dfrac{a}{h_o}\right)^2\right]$ dimensionless compressibility number for aerodynamic journal bearings

Λ_H $\left[= \dfrac{\mu\omega}{P_m}\left(\dfrac{a}{h_o}\right)^2\right]$ compressibility number for hybrid journal bearings

a radius of journal bearing; inside radius of annular thrust bearing

$\bar{a}$ width of rectangular slot

a_o velocity of sound at gas supply conditions

b outside radius of thrust bearing

c radius of ring of feed holes in annular thrust bearing

d feed hole diameter

d^* optimum feed hole diameter

g gravitational acceleration

h clearance between bearing surfaces

h_o mean radial clearance in journal bearings

k empirical factor for hybrid journal bearing

l distance of feed holes from end of journal bearings

m mass flow of gas through a single feed hole or slot

m_R mass of rotor

n number of feed holes per row in journal bearings;
number of feed holes in thrust bearings

r radius measured from centre of thrust bearing;
radius of whirl orbit

t wall thickness of thin walled hollow rotor;
time

u gas velocity in bearing clearance

v gas velocity in feed hole

x, y rectangular coordinates

z width of feeding slot

A $\left. \begin{array}{l} \left(= \dfrac{\pi d^2}{4} \text{ for pocketed feed holes} \right) \\ (= \pi d h \text{ for annular feed holes}) \end{array} \right\}$ area of feed hole

C damping coefficient

C_D coefficient of discharge of feed hole

C_L $\left(= \dfrac{W}{LDP_o} \right)$ load coefficient

C_{La} load coefficient of axial flow model of aerostatic journal bearing

C_p specific heat at constant pressure

C_Q flow dispersion coefficient

C_v specific heat at constant volume

C_W load dispersion coefficient

D diameter of journal bearing

D_i bore diameter of hollow rotor

E Young's modulus

F friction force

F_d dimensional factor in aerostatic bearing analysis

F_g gas properties factor in aerostatic bearing analysis

F_p pressure factor in aerostatic bearing analysis

F_r friction torque in thrust bearing

F_T tangential friction force on journal surface

$F(\gamma K)$ dimensionless function of pressure ratio across feed hole

G $\quad$ ($= F_d . F_g . F_p$) slot factor

G_o $\quad$ slot factor for concentric journal bearing

G^* $\quad$ optimum value of G

I $\quad$ transverse moment of inertia of rotor

I_o $\quad$ polar moment of inertia of rotor

J $\quad$ half-distance between centres of journal bearings in a two bearing machine

K $\quad$ $\left(= \dfrac{P_d}{P_o}\right)$ absolute pressure ratio across feed hole

$\quad$ $\left(= \dfrac{dW}{dh}\right)$ bearing stiffness constant

K_A $\quad$ axial stiffness

K_a $\quad$ angular or tilt stiffness

K_g $\quad$ $\left(= \dfrac{P_d - P_a}{P_o - P_a}\right)$ gauge pressure ratio

K_{go} $\quad$ gauge pressure ratio for concentric journal bearing

$K_g{}^*$ $\quad$ optimum gauge pressure ratio

L $\quad$ length of journal bearing

M $\quad$ mass flow of gas through bearing

P $\quad$ pressure;

$\quad$ $\left(= \dfrac{W}{LD}\right)$ specific loading

P_a $\quad$ ambient pressure

P_d $\quad$ pressure downstream of feed hole or feed slot

P_{do} $\quad$ $= P_d$ for concentric journal bearing

P_m $\quad$ mean pressure in hybrid journal bearing

P_o $\quad$ supply pressure

R $\quad$ gas constant

S $\quad$ complex stiffness of rubber

T $\quad$ absolute temperature

T_o $\quad$ absolute temperature of supply gas

U $\quad$ linear velocity of bearing surface

W $\quad$ total load on bearing

W_d $\quad$ aerodynamic load vector in hybrid journal bearing;

$\overline{W}_d$ $\quad$ effective aerodynamic load vector in hybrid journal bearing

W_s $\quad$ aerostatic load vector in hybrid journal bearing

X $\quad$ static unbalance of rotor

Y $\quad$ dynamic unbalance of rotor

Subscripts

a $\quad$ ambient

d $\quad$ downstream of feed holes;
$\quad$ aerodynamic

g gauge
H hybrid
o supply;
           concentric bearing
s aerostatic
sf squeeze film

Superscript

*   design or optimum condition

SELECTION OF BEARING TYPE

1.1 Introduction

At a very early stage in the design of any rotating machine the engineer must decide on the type of bearing to be employed. Two basic types have found wide acceptance and will always receive serious consideration: the hydrodynamic oil bearing and the rolling contact bearing. More recently several new kinds have been developed for specialized applications. These have included bearings lubricated by a wide variety of liquids, hydrostatic ones, bearings using solid lubricants such as graphite or molybdenum disulphide, magnetic types, and bearings lubricated by air and other gases.

Two specialized applications stimulated the early development of gas-lubricated bearings. The designers of high precision gyroscopes for use in inertial navigation systems required a spin axis bearing with very low friction and vibration levels and with both independent of time. Gas-lubricated bearings offered a considerable improvement over the precision ball bearings that were previously employed. In nuclear engineering the designers of gas circulators required a bearing that would permit the machine to be sealed into a reactor system and left unattended for up to twenty years. The lubricant also had to be unaffected by high temperature and irradiation. From these specialized beginnings gas bearings and, in particular, air bearings have developed to a stage where they can be used for many applications in general engineering. Air bearings have already successfully been employed in several types of machine tool and their wide utilization is predicted in precision grinding machines of all types and in high-speed drilling machines, hand tools and textile machinery.

The first thing the designer must know when considering the use of air bearings is how they compare with the established types of bearing with which he is already familiar—what are their relative advantages and disadvantages? Before this comparison is attempted even in the broadest terms, it is however necessary to understand the basic methods of operation of gas-lubricated bearings.

1.2 Types of gas bearing

A gas-lubricated bearing can be defined as two accurately machined surfaces separated by a thin film of gas and arranged so that any

tendency to change the clearance between the surfaces is resisted by a change of pressure in the gas film.

Fig. 1.1 shows the three basic types of gas bearing. The aerodynamic kind is often called self-acting because it generates its pressure within the gas film by the mechanism of viscous shearing. The process is similar to that occurring in hydrodynamic oil bearings. Pressure is generated when one surface is moving relative to the other so that the

(a) Aerodynamic   (b) Squeeze film   (c) Aerostatic
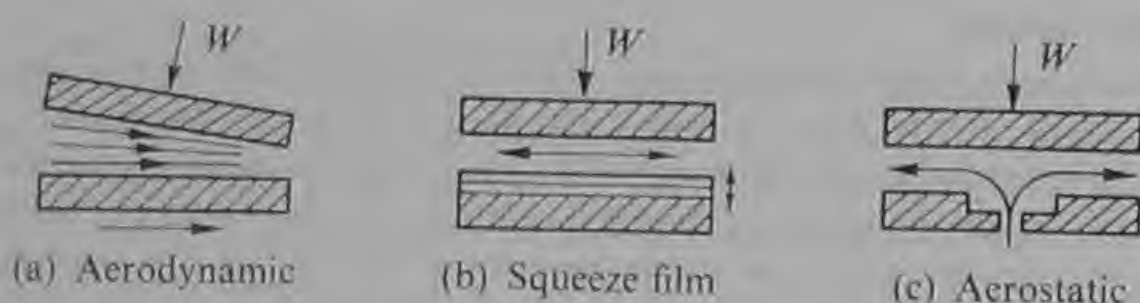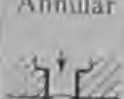
Fig. 1.1 Types of gas bearing

lubricant is dragged into a convergence between the two. The aerodynamic bearing is a simple and elegant concept, being entirely self-contained and independent of any external pressure source or other mechanism. It was this kind that received most of the early development in connection with gyroscopes and nuclear applications, but it has not yet received wide application in general engineering for two reasons. Firstly, the bearings must be manufactured to very high standards of accuracy and therefore their production cost is large. Secondly, their load capacity is proportional to the lubricant viscosity, and, as the viscosity of air is about ten thousand times less than that of an S.A.E. 10 oil, aerodynamic bearings have a maximum load capacity which is typically less than 5 lbf/in^2 (0·35 kgf/cm^2) of plan area. This load capacity would nevertheless be adequate in many applications and as manufacturing techniques are refined aerodynamic bearings should become more widely used.

Like the aerodynamic bearing, the squeeze film bearing is independent of an external supply of gas and generates pressure between the bearing surfaces. In this case, however, the movement producing the pressure is vibratory and normal to the bearing surfaces. The squeeze film bearing has not so far found many practical applications outside the laboratory. This may largely be because the motion required to generate the load-supporting pressure does not derive from the normal functioning of the bearing (such as the rotation of the shaft in the case of the aerodynamic bearing) but must be supplied by an external mechanism such as an electro-mechanical, magnetostrictive or piezo-electric vibration generator.

The aerostatic bearing is often called 'externally pressurized' because the pressure in the gas film is generated at an external source, usually a compressor. The gas from the external source is fed into the clearance space through flow restrictors which are often feed holes in one of the bearing surfaces, and escapes continuously to the atmosphere from the outside edges of the bearing. Relative to the aerodynamic bearing the aerostatic type has the advantage of being able to carry higher loads, and this ability is independent of any relative movement between the bearing surfaces. However, it requires power continuously to be expended in maintaining its supply of pressurized gas, and this feature is a major design consideration since excessive gas flow can render the bearing uneconomical.

Bearings have traditionally been classified according to their function. Those providing radial support for a shaft are called journal bearings and are usually of cylindrical geometry. Bearings which provide

Each square represents a possible bearing type, but the table is not claimed to be comprehensive. However, the shaded areas represent types which have thoroughly been investigated. For these a reliable design basis exists and is presented in this book.

Fig. 1.2 Classification of aerostatic bearings

axial location of the rotor and carry axial or thrust loads are called thrust bearings, and usually have flat bearing surfaces which in plan view are circular or annular. Aerostatic bearings, however, in common with other bearing types, can take the form of combined journal and thrust bearings of conical or spherical geometry.

Aerostatic bearings can also be classified according to the type of flow restrictor through which the gas is fed to the bearing clearance. The most widely used restrictor is a circular feed hole since this is probably the easiest to produce. The restrictor can, however, take the form of a narrow slot, a capillary tube or the porosity of a sintered bearing bush. A classification of types of aerostatic bearing is given in Fig. 1.2.

The present work will be confined mainly to consideration of aerostatic bearings of the feed hole type, sometimes called jet fed, and to bearings with slot feeding. Cylindrical journal bearings and flat thrust bearings will be considered. These types are easier to produce by established manufacturing methods, have a reliable basis for design and have been made and tested in large numbers in many sizes and for many different applications. Their use is therefore based on much experience and future designers may employ them with confidence.

(a) No load on shaft   No pressure difference

(b) Load on shaft   Pressure difference supporting load
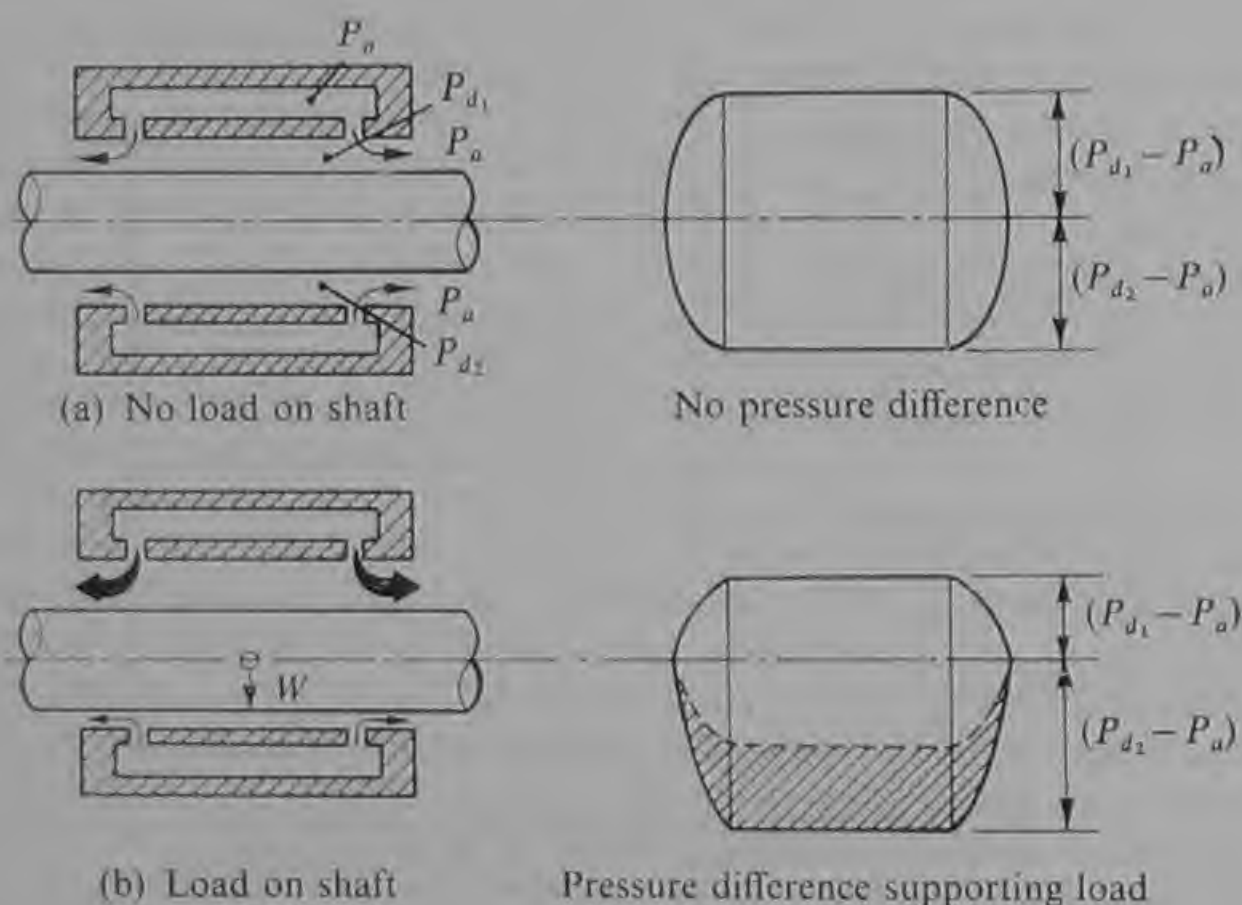
Fig. 1.3 The aerostatic journal bearing

1.3 The aerostatic journal bearing

The mode of operation of an aerostatic journal bearing is explained with reference to the typical jet fed journal bearing of Fig. 1.3. The bearing consists of a cylindrical bush into which are drilled two rows of gas feed holes spaced evenly around the bearing circumference. Compressed gas from an external source is supplied to the reservoir surrounding the bearing. From the reservoir the gas flows through the feed holes into the clearance between the shaft and the bush and then axially to the ends of the bearing where it exhausts to atmosphere. The pressure in the reservoir is the gas supply pressure P_o. The pressure falls as the gas flows through the feed holes and enters the bearing clearance at a pressure P_d, exhausting at the end of the bearing at a pressure P_a.

With no load applied to the shaft (and neglecting its weight), the shaft adopts a concentric position in the bush. In this case there is no variation of pressure circumferentially around the bearing and $P_{d_1} = P_{d_2}$. The pressure forces on the shaft balance.

When a load is applied to the shaft in the vertically downward direction, the shaft deflects in that direction so that the clearance at the top of the bearing is increased, and that at the bottom is reduced. At the top of the bearing the resistance to the flow of gas escaping to atmosphere is thus lessened so that more gas flows in through the top feed holes. This flow increases the pressure drop through the feed holes and the pressure P_{d_1} falls. At the bottom of the bearing the resistance to the flow of gas escaping to atmosphere has been increased so less gas flows through the bottom feed holes. The pressure drop through these feed holes has been reduced and the pressure P_{d_2} rises. A difference of pressure now exists across the shaft to balance the applied load.

For all loads within the capacity of the bearing there is an equilibrium position for the shaft. The eccentricity ratio ε (the actual shaft radial
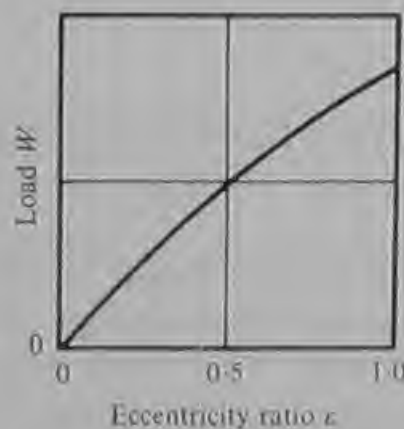
Fig. 1.4 Typical load-eccentricity relationship for an aero-static journal bearing

deflection expressed as a fraction of the mean radial clearance) is an important parameter in all journal bearings. Fig. 1.4 shows a typical load-eccentricity ratio graph for an aerostatic journal bearing. It is usual to express the load capacity of an aerostatic journal bearing in terms of the dimensionless load coefficient C_L where

$$C_L = \frac{W}{(P_o - P_a)LD},$$

where W is the load, L is the length, and D is the diameter of the bearing. The load coefficient at a given eccentricity ratio is dependent upon the gauge pressure ratio K_{go} where

$$K_{go} = \frac{P_d - P_a}{P_o - P_a}$$

for the concentric shaft position. A typical relationship between load coefficient and gauge pressure ratio is shown in Fig. 1.5. The values
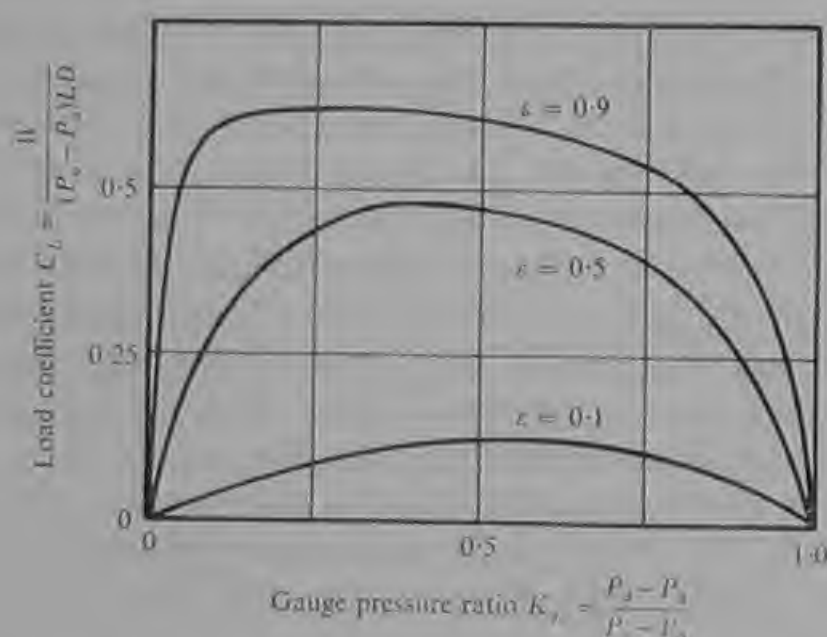
Fig. 1.5 Typical load coefficient-gauge pressure ratio relationship for an aerostatic journal bearing

of load coefficient shown apply to the theoretical case of a short journal bearing with a large number of jets—the load coefficients of real bearings are somewhat lower.

Fig. 3.2 shows the actual load capacity that can be achieved by aerostatic bearings of conservative design at a supply pressure of 100 lbf/in² (7 kgf/cm²) gauge. In most industrial applications the available air supply pressure seldom exceeds this figure and in any case higher pressures would involve greater airflows and for this reason might often be uneconomical. The figure provides a basis of com-

parison with other bearing types and offers a 'rough cut' estimation of the load capacity available to the designer within a given physical size and shape. For another supply pressure P_o the load capacity attainable can be found by multiplying by the ratio

$$\frac{(P_o - P_a)}{100},$$

where $(P_o - P_a)$ is expressed in lbf/in^2.

The stiffness of an aerostatic journal bearing can be seen from Fig. 1.4 to be constant up to an eccentricity ratio of 0·5. The aerostatic stiffness K can therefore be defined as:

$$K = \frac{W}{\varepsilon h_o} \quad \text{(for } \varepsilon < 0\cdot5\text{)},$$

where W is the load, ε the resulting eccentricity ratio and h_o is the mean radial clearance of the bearing. It can be seen that the stiffness is inversely proportional to the clearance and typical values are given in Fig. 1.6 illustrating that the stiffness can be increased by reducing the clearance to a limit determined by the difficulty and cost of manufacture. A typical radial clearance for comparative ease of manufacture

Bearing diameter 2 in; Length 2 in
Supply pressure 100 lbf/in^2 gauge
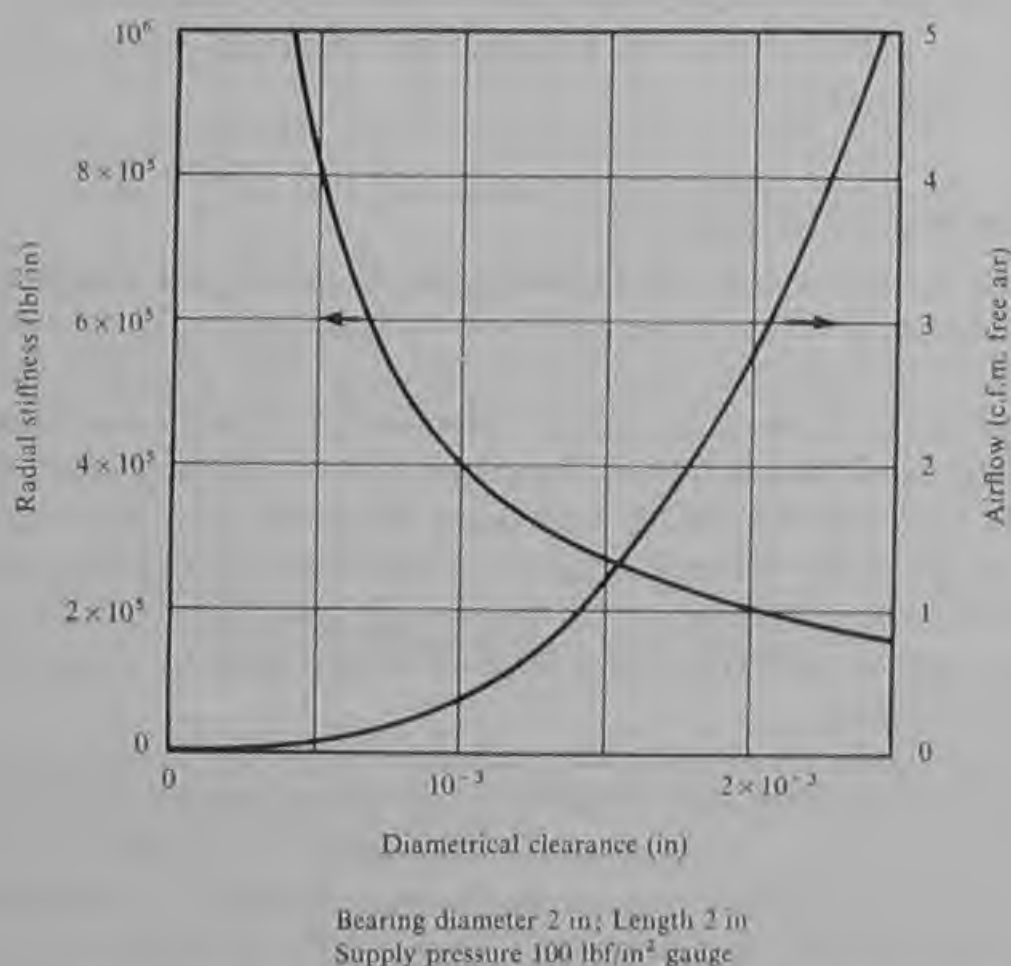
Fig. 1.6 Radial stiffness and airflow of an aerostatic journal bearing

might be 0·000 5 in. At this clearance a journal bearing of 2 in diameter and 2 in long supplied at 100 lbf/in^2 gauge would provide a radial stiffness of about 400 000 lbf/in and a maximum radial load capacity in excess of 150 lbf. It can be seen from Fig. 1.6 that the airflow through this bearing would be 0·34 s.c.f.m. and to supply this flow compressed to 100 lbf/in^2 gauge would require approximately 0·1 h.p. of installed compressor power. The airflow is proportional to the cube of the bearing clearance so that a reduction in clearance provides a significant reduction in the demand for compressor power as well as an increase in radial stiffness.

The power dissipated as heat due to the friction in any full journal bearing operating with a lubricant of viscosity μ is given by $\dfrac{\pi\mu D^3 L\omega^2}{4h_o}$, where ω is the angular velocity in radians per second.

With a knowledge of the method of operation of the aerostatic journal bearing and of the major factors determining its performance it is possible to make a preliminary comparison with other bearing types in order to assess where advantages may be gained from its use. Comparisons will be made with the two established bearing types—the hydrodynamic bearing and the rolling contact bearing—with particular emphasis on load capacity, stiffness, power (friction plus external pumping power), axis definition and wear. The comparison is also extended to include the hydrostatic oil bearing which is finding increasing utilization.

1.4 Comparison of bearing types

In order to focus the discussion and to avoid too great a use of generalizations, for these are difficult to interpret without numerous qualifications, it has been decided to use a specific example to present this comparison of bearing types. The author makes no claim to be an authority on hydrodynamic, hydrostatic or rolling contact bearings but hopes that the following examples illustrate the more important features of all three bearing types. In particular it is hoped that this comparison will highlight both where air bearings can be used to advantage and where their application might lead to difficulties and should be avoided.

The 2 in diameter air bearing already described is compared to a hydrodynamic bearing and a ball bearing which might be chosen for a similar duty such as a wheelhead quill assembly for a precision grinding machine. It is assumed that in each case the bearing should locate within a quill of outside diameter of 4 in and that from a consideration of rigidity the shaft diameter should be at least 1·5 in. The three bearings are shown in Fig. 1.7. The dimensions are self-evident except

SELECTION OF BEARING TYPE   23
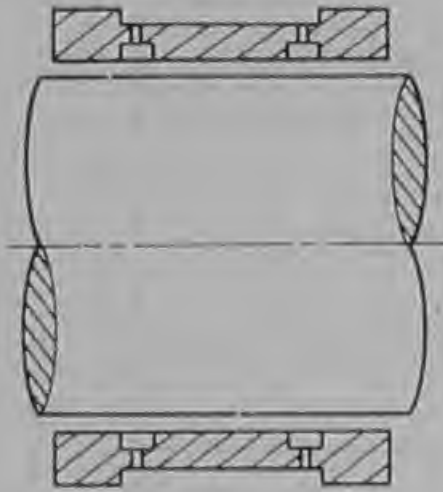
Aerostatic bearing
2 in (5 cm) diameter; 2 in (5 cm) long;
air supply 0·34 s.c.f.m. at 100 lbf/in² gauge;
diametrical clearance 0·001 in (0·0025 cm);
temperature 20°C.
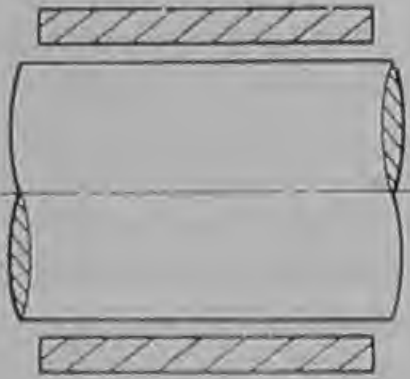
Hydrodynamic bearing
1·5 in (3·7 cm) diameter; 2 in (5 cm) long;
oil–S.A.E. 10; viscosity 3×10^{-6} lbf sec/in²
temperature 40°C;
diametrical clearance 0·001 in (0·0025 cm).

35 lbf
axial preload
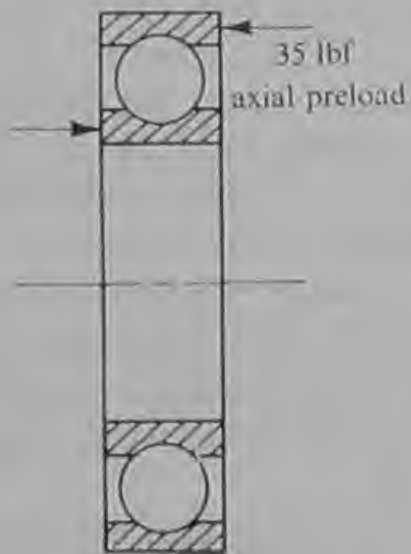
Ball bearing
Outside diameter 3·15 in (80 mm);
inside diameter 1·57 in (40 mm);
width 0·709 in (18 mm);
oil mist lubrication (Esso Univis P38);
temperature 20°C.

Fig. 1.7 Comparison of bearing types

perhaps for the diameter of the hydrodynamic bearing which is normally limited to minimize frictional heating.

(a) *Load capacity* Typical values of radial load capacity for the three bearings are shown in Fig. 1.8. The values for the hydrodynamic bearing are calculated assuming an operating temperature of 40°C at 3 000 rev/min. No value is given at 20 000 rev/min since this speed

Bearing Type	Maximum Radial Load (lbf)	
	at 3 000 rev/min	at 20 000 rev/min
Aerostatic (ε = 0·5)	95	120
Ball bearing	1 050	600
Hydrodynamic	5 000 (40°C)	—
Hydrostatic (ε = 0·5)	1 900	—

Fig. 1.8 Comparison of bearing types—load capacity

would be prohibited by excessive power consumption and heating. The values for the ball bearing are taken from a manufacturer's catalogue and relate to a high quality precision instrument-type bearing. The load capacity of the aerostatic bearing is increased at high speeds by aerodynamic effects, accounting for the higher value given at 20 000 rev/min. The largest ball bearing recommended for a speed of 30 000 rev/min has a maximum radial load capacity of 250 lbf illustrating that at higher speeds, the two bearing types become closer in this respect.

The comparison in terms of load capacity and speed is extended to include other bearing types in Fig. 1.9. The curves for all bearings except the aerostatic bearing are derived from the Institution of Mechanical Engineers Data Sheet No. 65007 (Ref. 1) to which the reader is referred if further information is sought. In each case a shaft diameter of 2 in and a bearing length of 2 in applies.

In this figure, in the case of all types except the aerostatic bearing, a nominal life of 10 000 hours is assumed. The curves are based on normally good engineering practice and commercially available parts. Improved performance is possible with exceptionally high engineering standards or specially produced materials.

It can be seen that both dry rubbing bearings and oil impregnated porous metal bearings can carry greater loads than an aerostatic bearing at speeds up to 300 rev/min and 1 500 rev/min respectively. The rolling bearing can carry a greater load at all speeds up to its maximum of 9 000 rev/min. The hydrodynamic bearing can carry a considerably greater load than the aerostatic bearing at all speeds above about 20 rev/min and both types can theoretically operate at speeds up to the burst limit for a solid steel shaft. However, using a hydrodynamic bearing for speeds approaching this limit presents a considerable cooling problem: the solution would demand a pressurized oil supply recirculating through an efficient cooler and designing the

All bearings are of 2 in shaft diameter and 2 in length, except for rolling bearings which are shorter. A medium viscosity mineral oil is assumed for the hydrodynamic bearings.
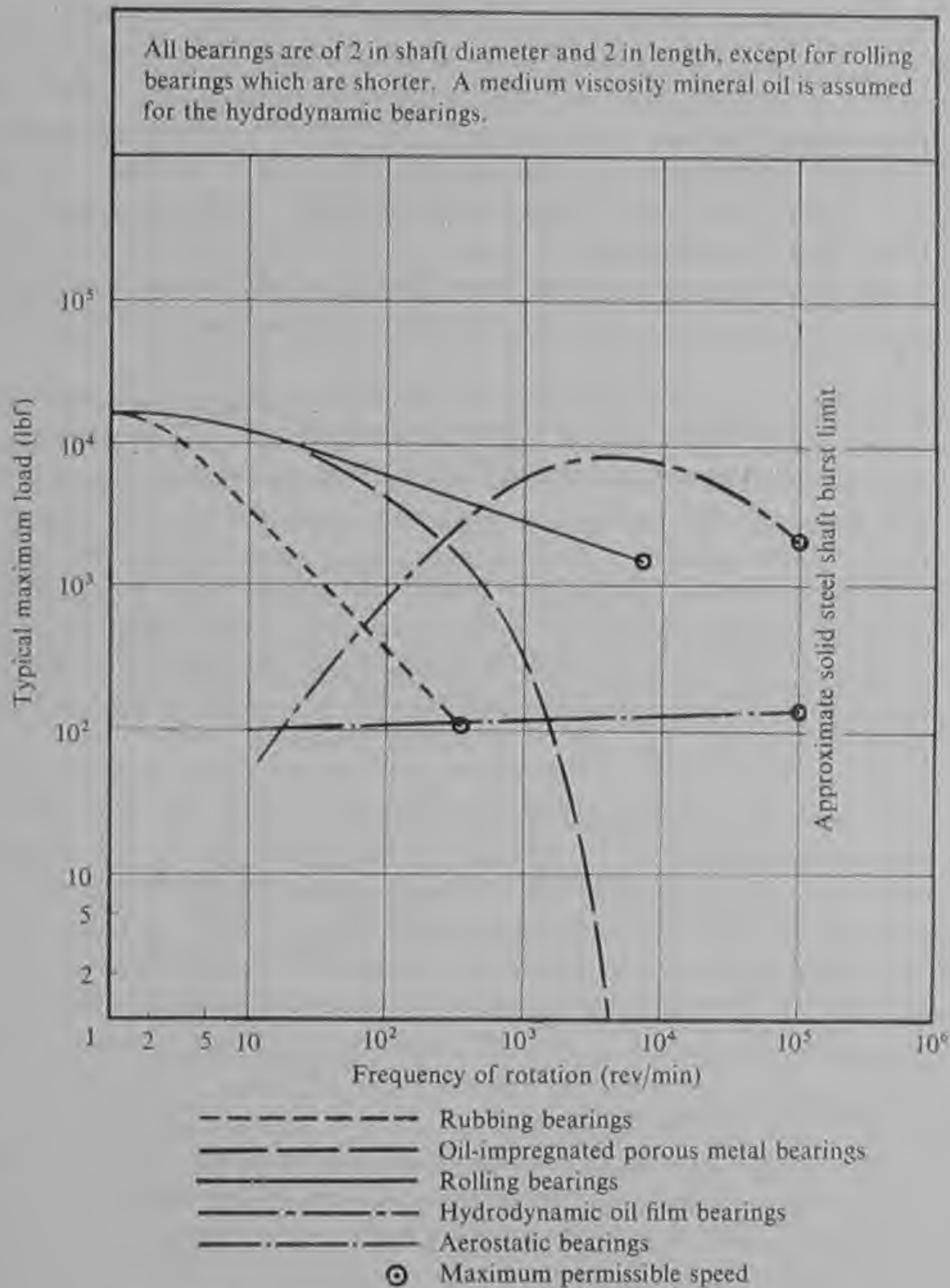
Fig. 1.9 General comparison of bearing types (based on I.Mech.E. data sheet No. 65007)

bearing to permit a maximum heat flow through the bearing wall into a large heat sink.

Boundary lubrication in hydrodynamic bearings enables them to withstand considerable overloading for limited periods. This feature is not shared by other bearing types to anything approaching the same degree and so hydrodynamic bearings are usually preferred for the most arduous applications.

(b) *Radial stiffness* It is extremely difficult to obtain a realistic comparison of journal bearing stiffness. If the lubricant film only is considered the hydrodynamic bearing is undoubtedly much stiffer than the other bearing types. The effective stiffness of a spindle supporting, for example, a grinding wheel is dependent upon a number of other factors. These include the stiffness of the shaft, the bearing bush, the quill body and the support structure. Some of these factors can drastically reduce the overall stiffness of the spindle when a measurement is made in the plane of the grinding wheel, i.e. where the load is actually applied.

In practice, for quill assemblies employing bearings in the size range considered the hydrodynamic bearing provides an overall stiffness in the region of 500 000 to 1 000 000 lbf/in. The aerostatic bearing and the ball bearing will provide comparable stiffness in the region of 250 000 to 500 000 lbf/in. It is stressed that these values are typical of those likely to be measured for an overhung load such as that applied to a grinding wheel mounted at one end of a quill assembly. In overall stiffness the aerostatic bearing gains in relation to the ball bearing because, as illustrated in Fig. 1.10, it permits the use of a shaft
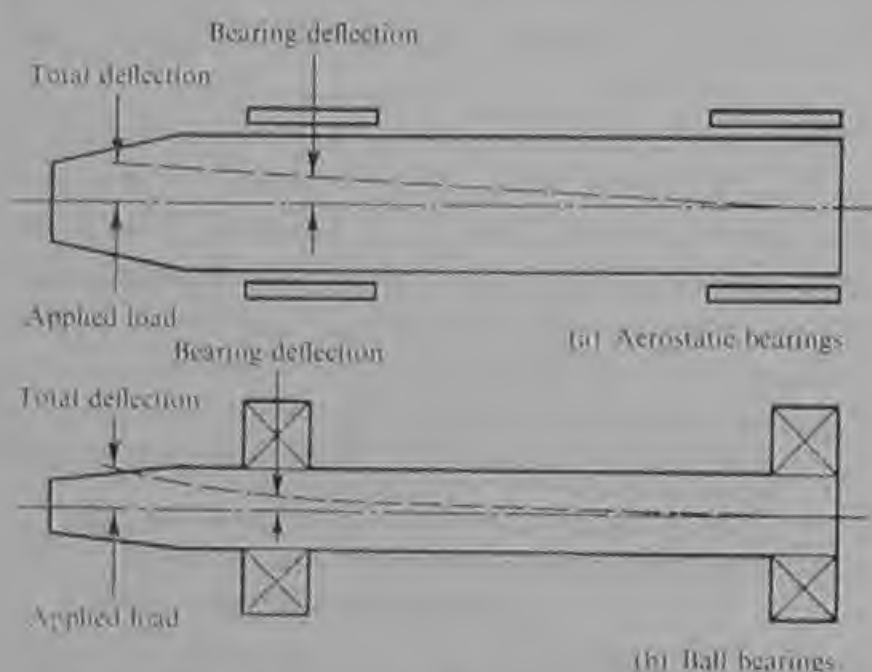
Fig. 1.10 Effective stiffness of machine spindles

of larger diameter and greater rigidity. In many instances in the author's experience it has been possible to provide greater overall stiffness with air bearings than was previously achieved using ball bearings.

(c) *Total power consumption* The total power consumptions for the three bearing types are compared in Fig. 1.11. The aerostatic bearing

Bearing Type	Power Required (h.p.)			
	at 3 000 rev/min		at 20 000 rev/min	
	Friction	Total	Friction	Total
Aerostatic	0·001	0·101	0·045	0·145
Ball bearing	0·007	0·007	0·164	0·164
Hydrodynamic	0·480	0·480	—	—
Hydrostatic	0·200	0·400	—	—

Fig. 1.11 Comparison of bearing types—power consumption

exhibits by far the lowest friction torque and consumes very little power within the gas film. This means that little heat is generated and the aerostatic bearing is the coolest running and seldom has thermal distortion problems. To get a true comparison with other types of bearing it is also necessary however to include the power expended externally to the bearing in the compressor. When this is done it can be seen that the power consumed is still considerably less than that required by the hydrodynamic bearing. At 3 000 rev/min the ball bearing consumes less total power. At this speed grease lubrication can be used and the ball bearing is independent of any external source of power, lubrication or cooling. At 20 000 rev/min the picture changes considerably. Not only is the friction heat produced in the ball bearing much greater than that produced in the aerostatic bearing, but the power consumed exceeds the sum of the friction loss and the compressor power required by the aerostatic bearing. At this higher speed the ball bearing requires oil-mist lubrication which is provided by a lubricator fed from a compressed air supply. Thus the ball bearing also demands compressor power in providing its lubrication and cooling. This additional power however is not included in the comparison given in Fig. 1.11. Thus it can be seen that as the speed increases aerostatic bearings become relatively more efficient and at very high speeds are unrivalled for efficiency and cool running.

(d) *Axis definition* An important requirement of bearings for many precision spindle applications is the ability accurately to define the axis of rotation of the shaft. In an aerostatic bearing the averaging effect of the gas film can reduce the run-out to below a quarter of the roundness error of the shaft surface. Most ground shafts can, with a little care, be produced round to about 20 μin (0·5 μm). With such a shaft supported in aerostatic bearings a run-out of less than

5 μin (0·125 μm) can be realized. If great care is exercised in grinding the shaft a roundness of 5 μin is possible. By this means precision spindles with aerostatic bearings have been produced for use in roundness measuring machines which are capable of defining a true axis to within $1-1\frac{1}{2}$ μin (0·025–0·038 μm).

In respect of axis definition hydrodynamic bearings and ball bearings are undoubtedly inferior to aerostatic bearings. According to the manufacturers' catalogues the best ball races are capable of giving a run-out performance in the region of 20 μin (0·5 μm) and hydrodynamic bearings have a similar limit. The low run-out capabilities of aerostatic bearings can be approached only by hydrostatic bearings which share the same roundness averaging effect. However, even hydrostatic bearings are likely to be inferior to the best aerostatic bearings due to distortion in the shaft and bearings caused by the high pressures employed, and by the friction heating which occurs at all but the lowest speeds. Thus in respect of axis definition the aerostatic bearing has no equal and this feature has been exploited not only in roundness measuring machines but in wheel spindles and work spindles for all types of grinding machines and in spindles for fine hole drilling machines.

(e) *Wear* All rolling contact bearings must be subject to wear since some rubbing contact occurs whenever the shaft is rotating. In the case of the ball bearing chosen for the present example the radial load capacity at various speeds is given for a 500-hour design life. The life is extended by running at lower loads and at lower speeds but the life will always have a definite limit even under ideal conditions.

Hydrodynamic bearings rub at starting and stopping although wear from this source should be very small as long as oil provides boundary lubrication, and as the applied load is low during starting and stopping. However, hydrodynamic bearings experience wear for a number of reasons. The large friction heating raises the temperature and causes oxidation of the oil and corrosion of the bearing surfaces. Deterioration of the bearing surfaces by corrosion can lead to solid particles circulating in the oil and increasing the wear rate. Breaking down of the bearing surfaces is accelerated by high pressures resulting from high loading. However, hydrodynamic bearings can operate effectively for many years if they are adequately cooled and the oil is well filtered and changed frequently.

The aerostatic bearing is theoretically not subject to wear. No rubbing contact ever occurs and most pure gases will cause neither corrosion or erosion of the bearing surfaces. However, it must be emphasized that this is an ideal condition and will only be approached in practice if attention is given to detail in the design both of the

bearing and of the complete air supply installation. The bearing must not be subjected to loads beyond its capacity, and it must be constructed of stainless materials. The gas supply must be filtered to remove solid particles of a size likely to cause damage (say less than half the least clearance) and to reduce any excessive liquid contamination. Finally it may be necessary to make provision to safeguard the bearing in the event of gas pressure failure. This often takes the form of automatically cutting-off the drive and providing an adequate storage volume to support the shaft until rotation ceases. A detailed consideration of installation design is given in Chapter 11.

1.5 Aerostatic and hydrostatic bearings

Before concluding this preliminary comparison of bearing types some mention must be made of hydrostatic oil bearings. These are now the subject of concentrated research and development activity and are finding increasing application particularly in the field of machine tools. Design in formation on hydrostatic bearings is given in reference 29. Future designers may often be faced with the problem of choosing between an aerostatic and a hydrostatic bearing.

The principle of operation of the hydrostatic journal bearing is essentially similar to that of the aerostatic journal bearing. The oil is supplied from a high pressure source and is fed through flow restrictors to enter the bearing clearance at points arranged symmetrically around the bearing in one or two axial planes. However, the flow restrictors are not jets drilled within the bearing bush but often take the form of a coil of fine bore tubing mounted externally to the bearing. The flow through the restrictors is laminar and the pressure drop occurs by the mechanism of viscous shearing.

In hydrostatic bearings the lubricant must be recirculated and this involves collecting the oil exhausting from the bearing, suitably sealing the shaft to avoid losses, and providing a return pipe to the pump. These factors add to the cost of the hydrostatic bearing system and, with the high cost of the pump, help to make them relatively more expensive to provide than aerostatic bearings.

When comparing hydrostatic and aerostatic bearings there are two fundamental differences in the lubricant properties which must be borne in mind. Firstly the oil can be considered to be incompressible, and secondly its viscosity is usually between 100 and 1 000 times greater than the viscosity of air. These two factors mean that in practice very much higher supply pressures can be used with oil before flow rates become excessive and before the demand for pumping power becomes prohibitive. Thus one finds that hydrostatic bearings operate typically at supply pressures in the range 1 500–3 000 lbf/in^2, and even higher pressures may be used in the future.

The maximum load capacity of any externally pressurized bearing is proportional to the supply pressure. A hydrostatic bearing is therefore capable of carrying a very much higher load than an aerostatic bearing of the same size and shape. It is also much stiffer. Therefore in applications where bearing loads are very high, or where a very high lubricant film stiffness is required, the hydrostatic bearing competes with the hydrodynamic bearing and the aerostatic bearing is not seriously considered.

One basis for comparing aerostatic and hydrostatic bearings is in considering that equal pumping power is required to supply the bearings. Assuming that the two bearings are the same size and shape and have the same clearance, and neglecting the compressibility of the gas, this condition is represented by the equation:

$$\frac{(P_o - P_a)^2}{\mu} = \text{constant}.$$

The load capacity is proportional to $(P_o - P_a)D^2$, giving

$$\frac{\text{Hydrostatic load capacity}}{\text{Aerostatic load capacity}} = \sqrt{\frac{\mu_{oil}}{\mu_{air}}}.$$

The friction power loss is proportional to $\mu\omega^2$, giving

$$\frac{\text{Hydrostatic power loss}}{\text{Aerostatic power loss}} = \frac{\mu_{oil}}{\mu_{air}},$$

for the same speed.

These equations highlight the superiority of the hydrostatic bearing in terms of load capacity and the aerostatic bearing in terms of friction. At higher speeds the friction power loss in the hydrostatic bearing rapidly becomes prohibitive.

A second basis for comparison is in terms of equal load capacity. This will occur for geometrically similar bearings when

$$(P_o - P_a)D^2 = \text{constant},$$

giving

$$D_{hydro} = \left[\frac{(P_o - P_a)_{aero}}{(P_o - P_a)_{hydro}}\right]^{\frac{1}{2}} D_{aero}.$$

or for a ratio of supply pressures of twenty,

$$D_{hydro} = 0.224 D_{aero}.$$

On this basis of comparison and for constant speed the friction power loss is proportional to $\dfrac{\mu}{(P_o - P_a)^2}$, and for a viscosity ratio of 200 one has

$$\frac{\text{Friction power loss in hydrostatic bearing}}{\text{Friction power loss in aerostatic bearing}} = \frac{1}{2}.$$

Thus it is theoretically possible to produce a hydrostatic bearing of equal load capacity and stiffness and lower friction power loss. However, this performance may not be practicable owing to the fact that the smaller diameter shaft is often of inadequate rigidity. Hydrostatic bearings are also more expensive to produce and this difference is greater at small sizes. A major cost factor is the hydrostatic pump and this cost does not decrease proportionately with size. Thus hydrostatic bearings are best suited to applications where speeds are relatively low and where arduous operating conditions demand their high load carrying capacity. In applications involving high speeds or requiring low friction or cool running the aerostatic bearing will generally offer a simpler and more economical solution.

Load and power consumption data are included in Figs. 1.8 and 1.11 for a typical hydrostatic bearing which could be considered for the same application. A supply pressure of 2 000 lbf/in^2 is assumed and the viscosity of the oil is taken to be 200 times greater than that of air. The same bearing dimensions apply as in the case of the aerostatic bearing—namely 2 in diameter and 2 in length. Once again it is seen that compared to the aerostatic bearing the hydrostatic bearing carries a considerably higher load and consumes considerably more power.

1.6 Advantages and limitations of aerostatic bearings

The advantages of aerostatic bearings can be summarized as follows:

(a) low friction giving low power loss and cool running characteristics;

(b) capability of operating at very high rotational speeds;

(c) precise axis definition;

(d) low or zero wear rate giving a long life;

(e) little or no need for periodic maintenance;

(f) capability of operating at very high and very low temperatures; and

(g) low noise and vibration levels.

All these advantages are not necessarily easily obtained in any one particular application. For example, the maximum operating speed may be determined by the onset of self-excited whirl instability or the friction level may be raised by liquid impurities in the gas supply. The following chapters attempt to describe how, with the benefit of the available design data and practical experience, these ideals can be approached.

In addition to the advantages already listed, air bearings possess advantages of convenience which, although mostly self evident, are nevertheless often overlooked by those inexperienced at using air as a lubricant. Air is universally available with a nearly constant chemical composition and well established physical properties and behaviour.

Compressed air is widely used and is available in the majority of factories and industrial plants. On a very large number of machines compressed air is employed to drive motors and turbines, to actuate pneumatic cylinders, to lubricate ball bearings by carrying oil mist, and for cooling or use in air dusters. In many of these machines the incorporation of air bearings, using the existing compressed air supply, often seems a logical development.

With the possible limited exception of water, air and its constituent gases are the only lubricants that can freely be exhausted to atmosphere without danger or risk of harmful pollution. This permits an open cycle lubrication system of great simplicity compared to recirculating oil systems.

Finally, and particularly important in relation to prototype and research machines, air bearings have an inherent cleanliness and general convenience which can be appreciated fully only through first-hand experience.

Aerostatic bearings can solve some lubrication problems which would be insoluble or extremely difficult to solve by any other means. Examples of these demand operation at very high or very low temperatures with very low friction at high rotational speeds. However, in many applications two or more types of bearing can be used, each type offering some small performance or manufacturing cost advantage, but with no clear-cut superiority. In this introductory chapter the author has attempted to present a realistic basis of comparison by which to choose or to reject aerostatic bearings. However, a great deal of care and attention to detail will be needed if aerostatic bearings are successfully to be employed. If equal diligence were always applied to the application of conventional bearing types an equally effective solution might often be realized. For example, a hydrodynamic bearing can be manufactured or a ball bearing can be installed to the same degree of precision as the aerostatic bearing, and their lubrication systems can be planned as thoroughly as the compressed air supply system. They can also be mounted into the machine structure with equal care to minimize distortion due to clamping stresses.

It is not meant to imply that many designers employing conventional bearing systems neglect refinements in design and manufacture, but rather that, since familiarity does in many cases tend to breed contempt, any new bearing system tends to be applied with greater care than the old. Often an improvement in performance can result from the care as much as from the novelty.

The author has included this reflection to counterbalance any natural enthusiasm or bias which must inevitably colour his writings in favour of aerostatic bearings. It is intended to prompt the designer to take a second look at his present bearing system and to make his

comparison with the new bearing while keeping in mind all possible refinements to the design, manufacture and installation of the old.

In all engineering design it is at least as important to appreciate the disadvantages and limitations of a mechanism or technique as to understand its advantages. The latter are often immediately apparent while the former are often overlooked. Thus it is important before proceeding to deal with design in detail that the disadvantages and limitations of aerostatic bearings are given close consideration. By this means unsuitable applications will quickly be identified and the designer will avoid joining the ranks of those prejudiced against a new technique through an unfortunate and ill-conceived initial experience. It is to be regretted that the history of gas lubrication lists many such disillusionments.

A major consideration with aerostatic bearings is always their limited load-carrying capacity. It is essential that before commencing any bearing design calculations all the applied loads are accurately estimated. There are many sources of such applied loads including:

(a) rotor weight;

(b) static and dynamic unbalance;

(c) applied cutting loads in machine tool spindles;

(d) electro-magnetic forces in motors;

(e) pressure forces on turbines or compressor wheels; and

(f) transmission forces through a belt, coupling or gearing.

These forces must correctly be combined to give the maximum total load to be carried by the bearing at each operating condition. At this stage the physical location of the bearings should carefully be considered since by proper adjustment the effective applied load can often be reduced. Any possible overload or accident condition must carefully be considered and the bearing should be designed to give a generous safety margin in all possible cases. Where some accidental contact of the bearing surfaces cannot be avoided full consideration must be given to the choice of bearing materials so that the damage and wear are minimized.

The other major limitation which must always be borne in mind concerns the cleanliness of the air supply. This aspect is considered in detail in a later chapter but it is important to note at this stage that the design clearance and feed jet or slot dimensions are likely to be dictated in many cases by considerations of blockage by solid and liquid impurities in the gas supply rather than by considerations of gas flow or stiffness.

Finally, the designer must resist the temptation to design a super bearing at a small clearance demanding an impossible degree of

precision in manufacture and an impossibly high quality of air filtration. The designer is advised to start in the machine shop by finding out exactly what degree of precision can be achieved with the available equipment. A wise man having arrived at a tolerance will then often double it to arrive at a practical and successful design.

THEORY OF AEROSTATIC LUBRICATION

2.1 Introduction

It is not the author's intention to burden the design engineer with a great deal of advanced mathematical analysis or to pursue academic discussions of phenomena which, while they might be of great intrinsic interest, are of little or no practical importance. It is rather the purpose of this chapter to give some understanding of the basic physical behaviour of gases upon which the design of aerostatic bearings is based. Those already well read in fluid mechanics will find little new and will quickly pass on to the following chapters dealing with design. However, the newcomer to the field will make better use of the design information if he has a basic understanding of the theory upon which it is based. An attempt has been made to limit this treatment to essentials and to keep the mathematics simple so that the information is meaningful to the greatest possible number. Wider ranging and more advanced treatments of the theory of aerostatic lubrication will be found in the various references given in the bibliography. It is left to these to satisfy the specialist and the researcher.

2.2 Flow between parallel plates

(a) *Rectangular slot* In almost all practical bearings the flow in the bearing clearance is laminar and pressure losses occur due to viscous shearing in the gas film. It is of fundamental interest therefore to understand the laminar flow of gases between flat and parallel plates. In this simplified treatment a number of assumptions are made.

(a) Inertia forces due to acceleration can be neglected compared with frictional forces due to viscous shearing.
(b) Laminar flow conditions exist at all points in the gas film.
(c) Pressure is constant over any section normal to the direction of flow.
(d) There is no slip at the boundaries between the fluid and the plates.

In the following analysis the dimensions and co-ordinates are shown in Fig. 2.1. Using this nomenclature and applying the stated conditions to the well known Navier Stokes equations the following expression results:

$$\frac{\partial^2 u}{\partial y^2} = \frac{1}{\mu}\frac{\partial P}{\partial x},$$

$$\tag{1}$$
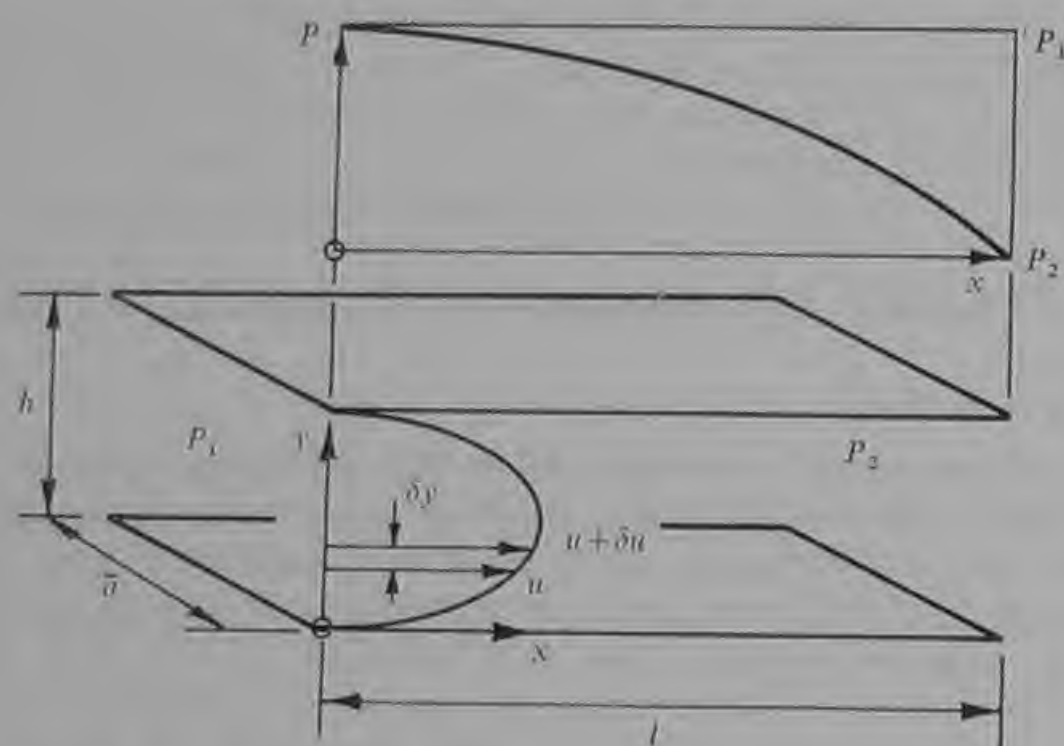
Flow occurs in the x direction due to pressure P_1 being higher than pressure P_2. The velocity distribution across the film in the y direction follows a parabolic curve and the gas in contact with each plate is stationary.

Fig. 2.1 Flow between parallel plates

This equation connects the pressure gradient in the x direction with the resulting velocity distribution in the y direction. Here u is the velocity of the gas at any point, P is the pressure at that point, and μ is the viscosity of the gas.

Integrating equation (1) gives

$$\frac{du}{dy} = \frac{1}{\mu}\frac{dP}{dx}y + A,$$

where A is a constant; integrating again yields

$$u = \frac{1}{\mu}\frac{dP}{dx}\frac{y^2}{2} + Ay + B.$$

If h is the clearance between the plates, then $u = 0$ at $y = 0$ and at $y = h$; substituting these boundary conditions gives

$$B = 0$$

and

$$A = -\frac{1}{2\mu}\frac{dP}{dx}h$$

and so

$$u = \frac{1}{2\mu}\frac{dP}{dx}y(y-h). \tag{2}$$

Equation (2) gives the velocity of the gas at any given position across the gas film and it will be noted that the velocity distribution is parabolic.

The greatest velocity is at the centre of the clearance, i.e. at $y = \dfrac{h}{2}$.

The mass of gas flowing between plates of width $\bar{a}$ is given by:

$$m = \bar{a}\rho \int_0^h u \, dy,$$

where m is the mass flow rate of gas and ρ is the density of the gas; which upon substituting for u from equation (2) becomes

$$m = \bar{a}\,\frac{\rho}{2\mu}\,\frac{dP}{dx}\int_0^h (y^2 - yh)\,dy$$

and

$$m = -\frac{\bar{a}\rho h^3}{12\mu}\,\frac{dP}{dx},$$

whence rearranging gives:

$$\frac{dP}{dx} = -\frac{12\mu m}{\bar{a}\rho h^3}.\tag{3}$$

Equation (3) gives the relationship between the mass flow rate and the pressure gradient between the plates in the direction of flow. The density ρ has so far been assumed constant in the y direction and equation (3) applies to both liquids and gases. However, the density of a gas is dependent upon the pressure and as the pressure varies in the x direction equation (3) cannot be integrated to give the pressure distribution in the x direction until some relationship is established between the gas density and the pressure. It is reasonable to assume that the gas behaviour is isothermal since the heat generated in the gas film is small, and the bearing walls are usually metal and therefore of high thermal conductivity. At isothermal conditions

$$\frac{P}{\rho} = RT,\tag{4}$$

where R is the gas constant and T the absolute temperature. Substituting for ρ in equation (3) and separating the variables gives:

$$P\,dP = -\frac{12\mu m RT}{\bar{a}h^3}\,dx.$$

Then

$$P_1^2 - P_2^2 = \frac{24\mu m RT l}{\bar{a}h^3}.\tag{5}$$

Equation (5) is of fundamental importance to the understanding of aerostatic bearings. It expresses the pressure drop along the slot in

terms of the mass flow, the gas properties and the slot dimensions. Some bearings, both journal and thrust, employ slot feeding. That is the gas is fed through a slot before entering the bearing clearance. To such slots equation (5) can be applied directly provided that the slots are rectangular, i.e. $\bar{a}$ is constant. In this case P_1 will be the gas supply pressure P_o, and P_2 will be the pressure in the bearing at the point of entry which is usually denoted by P_d. Thus, for a rectangular feeding slot of length y and clearance z equation (5) can be written:

$$P_a^2 - P_d^2 = \frac{24\mu m R T y}{\bar{a} z^3}. \tag{6}$$

In journal bearing analysis it is usual to divide the bearing into a number of 'equivalent slots' each supplied with gas from a feed hole or a feed slot. This arrangement is shown in Fig. 2.2. The slot width in this case is given by:

$$\bar{a} = \frac{\pi D}{n},$$

where D is the diameter of the bearing and n is the number of feed
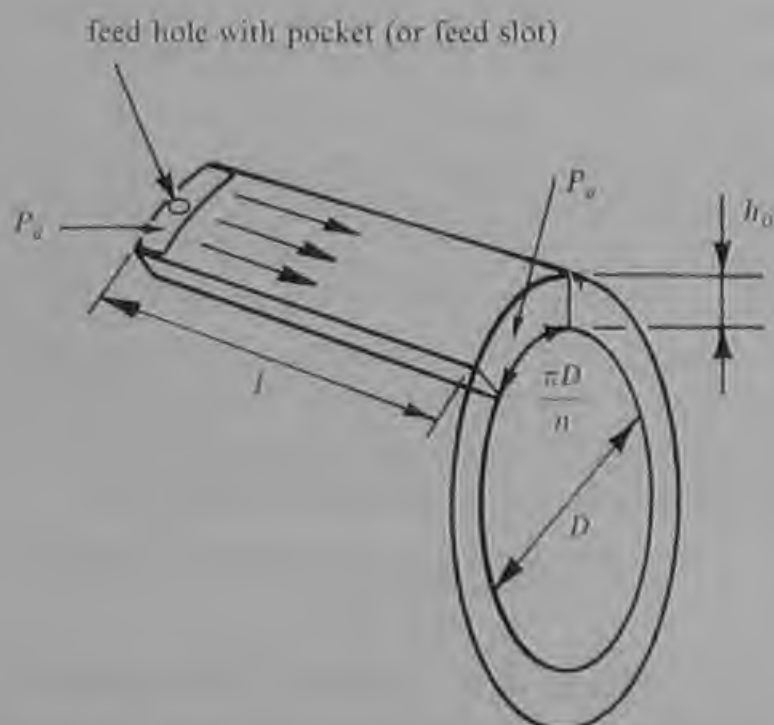
Fig. 2.2 Equivalent slot in a journal bearing

holes in a row around the bearing. When the shaft is concentric in the bearing the film thickness for all the slots is the mean radial clearance h_o. Thus for an equivalent slot equation (5) can be written as

$$P_d^2 - P_a^2 = \frac{24\mu m n R T l}{\pi D h_o^3}, \tag{7}$$

where P_a is the ambient pressure where the gas exhausts from the end of the bearing.

If one considers the complete 360° journal bearing, this can be rearranged to yield the total mass flow of gas from both ends of the bearing thus

$$M = \frac{(P_d^2 - P_a^2)\pi D h_o^3}{12\mu R T l}.$$ (8)

It can be seen that the flow is proportional to the cube of the bearing clearance. This fact is often of considerable economic importance since even a small increase in clearance can involve a considerable penalty in terms of increased flow and pumping power requirement.

(b) *Circular plates* The laminar flow in a rectangular slot has been considered and it has been shown how this theory can be applied to feed slots and to segments of journal bearings. Another important case occurs in thrust bearings where the gas is fed into the centre of two circular plates and flows radially outwards. This arrangement is shown in Fig. 2.3. In this case assuming laminar flow and with the other

Fig. 2.3 The simple aerostatic thrust bearing with central feed hole and pocket

assumptions as before the Navier Stokes equations can be written as:

$$\frac{\partial^2 u}{\partial y^2} = \frac{1}{\mu} \frac{\partial P}{\partial r},$$

where r is some radius from the centre of the plates which is greater than the pocket radius a and less than the bearing radius b. Integrating twice and applying the same boundary conditions as before yields

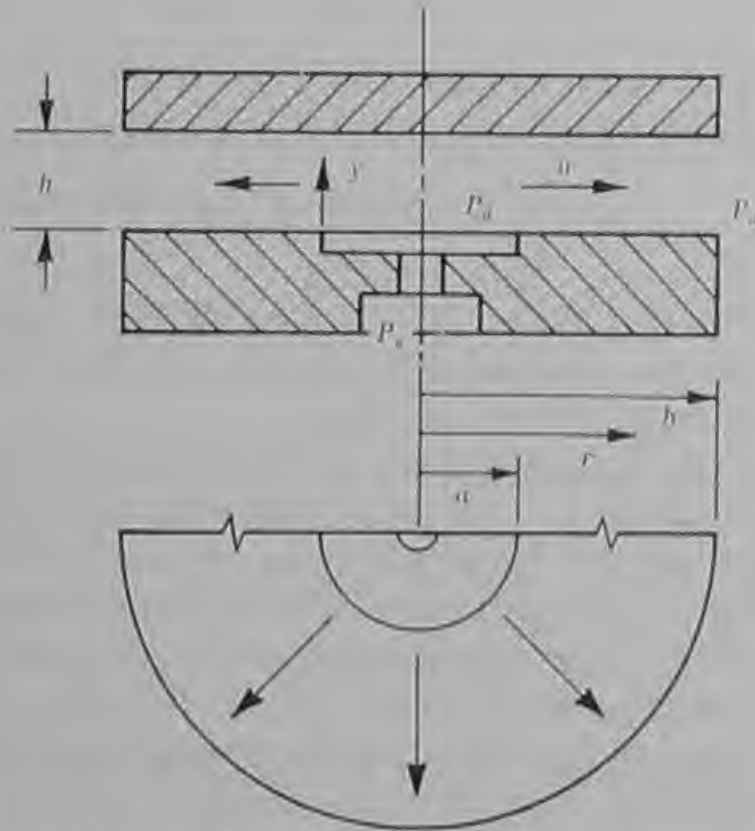$$u = \frac{1}{2\mu}\frac{dP}{dr}\,y(y-h). \tag{9}$$

Then the mass flow through annulus of width h and radius r is given by

$$m = 2\pi r\rho \int_0^h u\,dy.$$

Substituting for u from equation (9) and integrating gives

$$\frac{dP}{dr} = -\frac{6\mu m}{\pi r\rho h^3}. \tag{10}$$

In equation (10), as in equation (3), the negative sign implies that the pressure is falling in the direction of flow, i.e. in the positive r or the positive x direction. Again assuming isothermal conditions in the gas film and separating the variables gives:

$$P\,dP = -\frac{6\mu m R T}{\pi h^3}\cdot\frac{dr}{r}, \tag{11}$$

and integrating from the pocket where $r = a$ and $P = P_d$ to the outer edge of the bearing where $r = b$ and $P = P_a$ gives:

$$P_d^2 - P_a^2 = \frac{12\mu m R T}{\pi h^3}\log_e\left(\frac{b}{a}\right). \tag{12}$$

Equation (12) can be rearranged to give the flow and it can be seen that the flow is proportional to the cube of the clearance in thrust bearings as well as in journal bearings.

Fig. 2.4 shows a more common and practical type of aerostatic thrust bearing. This bearing is of annular plan form with a central hole of radius a through which a shaft may pass. A ring of feed holes supplies a pocket or groove in the form of a circle of some intermediate radius c. However, the same analysis also applies if the gas is fed into the bearing through a circular slot at the same radius. In either case the pressure at radius c is P_d and the gas flows radially inwards and radially outwards to exhaust at pressure P_a at the inner radius a and the outer radius b. Equation (11) can be integrated to give the pressure at any radius r:

$$P^2 - P_d^2 = -\frac{12\mu m_1 R T}{\pi h^3}\log_e\left(\frac{r}{c}\right) \tag{13}$$

for the region of outward flow, and

$$P^2 - P_d^2 = -\frac{12\mu m_2 R T}{\pi h^3}\log_e\left(\frac{c}{r}\right) \tag{14}$$
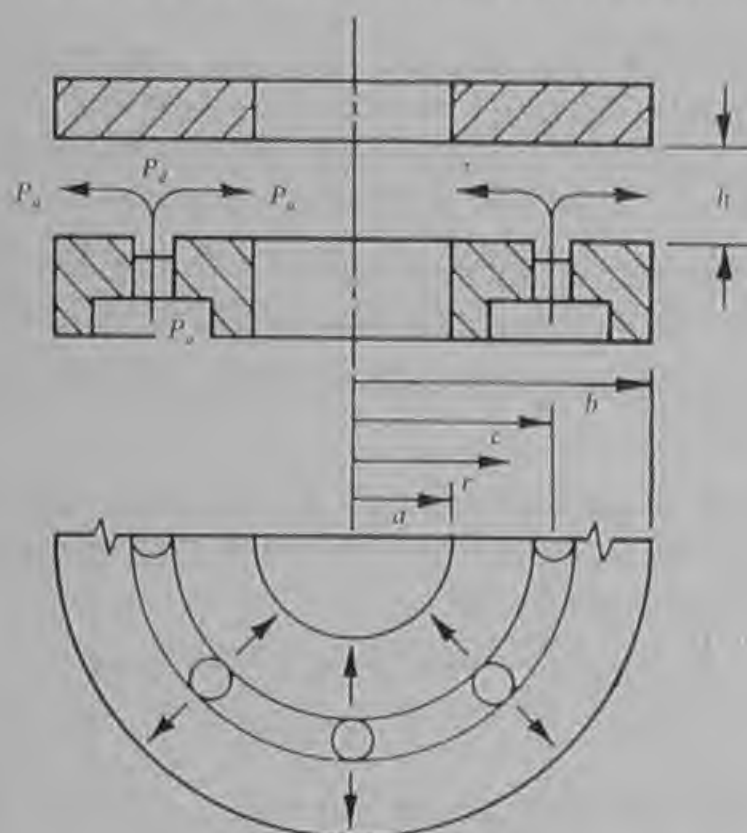
Fig. 2.4 The annular aerostatic thrust bearing with jets
feeding an annular groove

for the region of inward flow. By substituting $P = P_a$ at $r = b$ in
equation (13) the outward flow m_1 is given by

$$m_1 = \frac{(P_d^2 - P_a^2)\pi h^3}{12\mu RT \log_e \left(\dfrac{b}{c}\right)} \qquad (15)$$

and by substituting $P = P_a$ at $r = a$ in equation (14) the inward flow m_2
is given by

$$m_2 = \frac{(P_d^2 - P_a^2)\pi h^3}{12\mu RT \log_e \left(\dfrac{c}{a}\right)}. \qquad (16)$$

It can be seen that the inward flow will be equal to the outward flow
when

$$\frac{b}{c} = \frac{c}{a}$$

or $c^2 = ab.$

This is the usual design condition for annular thrust bearings and
applies to the design data given in Chapter 4.

2.3 Flow through feed holes

In many aerostatic bearings the gas is supplied to the bearing clearance through feed holes drilled in the bearing wall. In considering the flow through feed holes the following assumptions can be made:

(a) there are no pressure losses upstream of the throat of the jet, i.e. the pressure at the entry to the jet is the supply pressure P_o;

(b) the pressure immediately downstream of the jet is the static pressure in the throat of the jet.

Then considering the flow through a nozzle of the same throat diameter as the jet, the relationship between supply pressure and static pressure at the throat is given by:

$$\frac{P_d}{P_o} = \left[1 - \frac{\gamma - 1}{2} \left(\frac{v}{a_o} \right)^2 \right]^{\frac{\gamma}{\gamma - 1}}$$

where P_d is the static pressure at the throat,
     v is the velocity at the throat,
     a_o is the speed of sound at the supply conditions,
     γ is the ratio of specific heats for the gas.

and then

$$v^2 = \frac{2a_o^2}{\gamma - 1} \left[1 - \left(\frac{P_d}{P_o} \right)^{\frac{\gamma - 1}{\gamma}} \right].$$

The mass flow through the jet

$$m = C_D \rho_d A v,$$

where C_D is the coefficient of discharge,
     ρ_d is the density at the throat,
     A is the cross section area of the throat.

Then for isentropic expansion

$$\rho_d = \rho_o \left(\frac{P_d}{P_o} \right)^{\frac{1}{\gamma}}$$

and therefore

$$m^2 = C_D^2 \rho_o^2 A^2 \left(\frac{P_d}{P_o} \right)^{\frac{2}{\gamma}} v^2$$

$$= \frac{2 C_D^2 A^2 \rho_o^2 a_o^2}{\gamma - 1} \left[\left(\frac{P_d}{P_o} \right)^{\frac{2}{\gamma}} - \left(\frac{P_d}{P_o} \right)^{\frac{\gamma + 1}{\gamma}} \right]$$

Then substituting for the speed of sound at the supply condition

$$a_o = (\gamma R T_o)^{\frac{1}{2}}$$

and rearranging, gives the mass flow through a jet as:

$$m = C_D A \rho_o (2RT_o)^{\frac{1}{2}} \left[\frac{\gamma}{\gamma-1} \left\{ \left(\frac{P_d}{P_o}\right)^{\frac{2}{\gamma}} - \left(\frac{P_d}{P_o}\right)^{\frac{\gamma+1}{\gamma}} \right\} \right]^{\frac{1}{2}}. \tag{17}$$

The value of the coefficient of discharge C_D is usually taken to be 0·8 in design calculations. However, C_D varies with the pressure ratio $\frac{P_d}{P_o}$ as shown in Fig. 2.5. It can be seen that the value of C_D falls
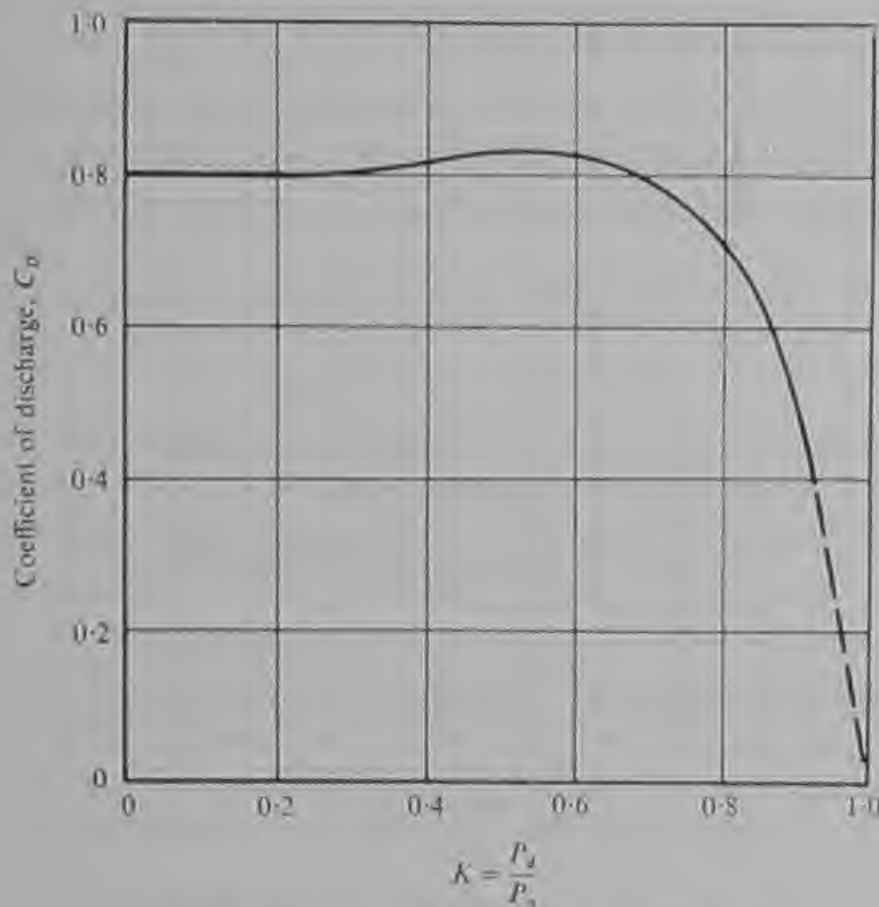
Fig. 2.5 Variation of C_D with K—typical values

at pressure ratios above 0·7 and this has sometimes been taken into account, for example, when considering the ultimate load capacity of thrust bearings (see Ref. 3).

Equation (17) can be simplified by writing

$$F(\gamma K) = \left[\frac{\gamma}{\gamma-1} \left\{ \left(\frac{P_d}{P_o}\right)^{\frac{2}{\gamma}} - \left(\frac{P_d}{P_o}\right)^{\frac{\gamma+1}{\gamma}} \right\} \right]^{\frac{1}{2}}, \tag{18}$$

where

$$K = \frac{P_d}{P_o}.$$

$F(\gamma K)$ varies with K as shown in Fig. 2.6. The function reaches a maximum value at the choked jet condition obtained by differentiating

$$F(\gamma K) = \left[\frac{\gamma}{\gamma-1}(K^{2/\gamma} - K^{(\gamma+1)/\gamma})\right]^{1/2}$$
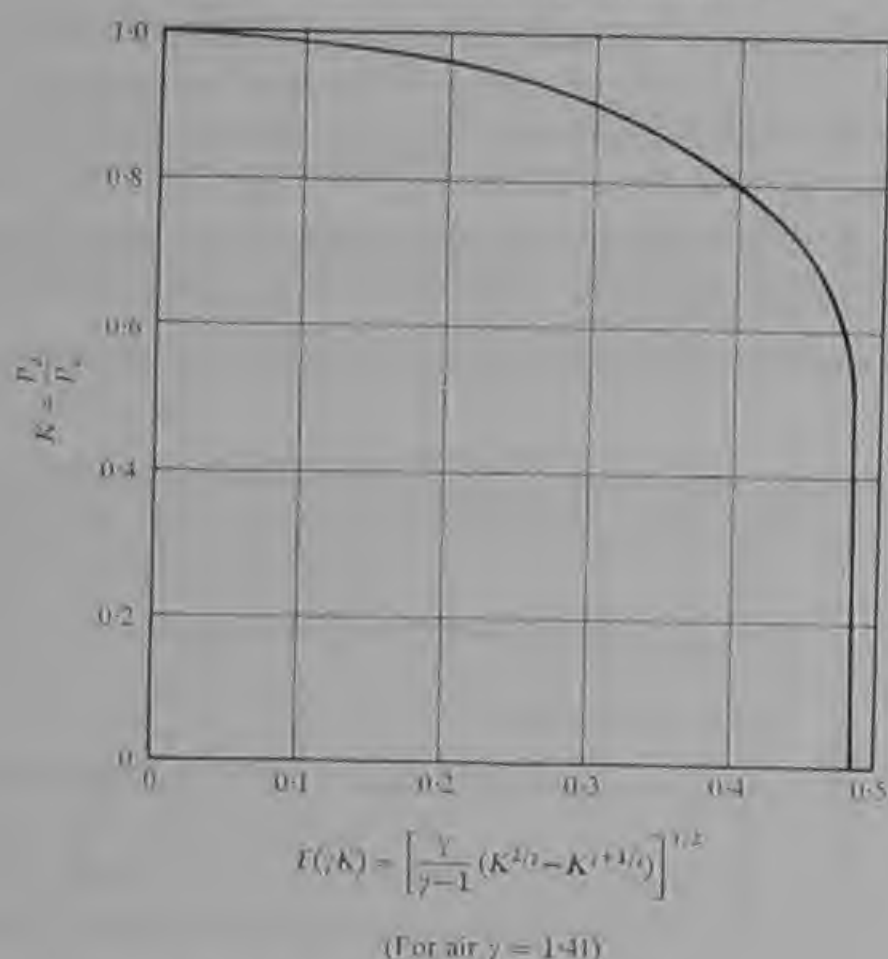
(For air $\gamma = 1\cdot41$)

Fig. 2.6 Variation of $F(\gamma K)$ with K

equation (18) with respect to pressure ratio and equating to zero, when

$$\frac{P_d}{P_o} = \left(\frac{2}{\gamma+1}\right)^{\frac{\gamma}{\gamma-1}}.$$

(19)

At all values of K below that defined by equation (19) $F(\gamma K)$ has a constant value of $0\cdot484$ for air ($\gamma = 1\cdot41$).

The value of the area A of the throat of the jet will depend upon the type of feed hole used. The two types commonly used are shown in Fig. 2.7. For a simple orifice the smallest flow area occurs in the bore
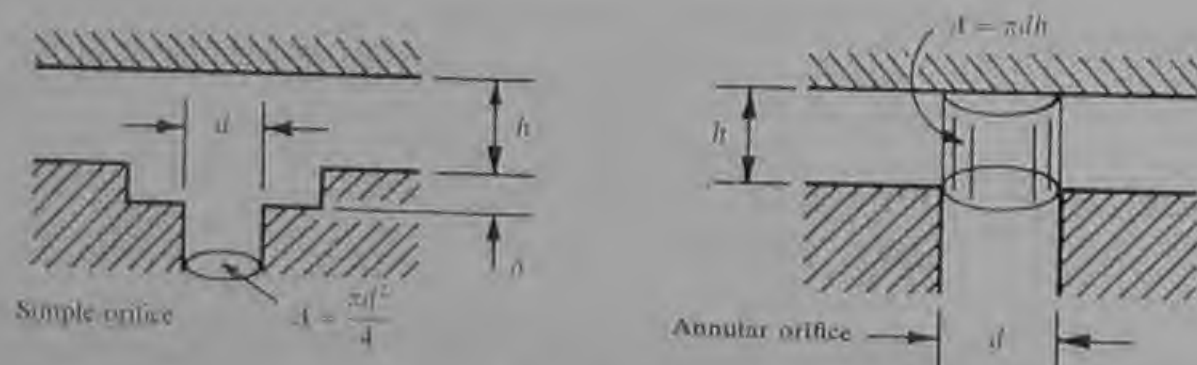
Fig. 2.7 Types of feed hole

of the feed hole and

$$A = \frac{\pi d^2}{4},$$

where d is the diameter of the feed hole. The smallest flow area with an annular orifice occurs in the outlet to the bearing clearance and in this case

$$A = \pi d h,$$

where h is the local clearance. It can be seen that the two areas will be equal when $h = \frac{d}{4}$ and for all larger clearances the jet can only operate as a simple orifice. However, in practice such large clearances are very rare and simple orifice compensation is achieved by exhausting the feed hole into a pocket. The minimum effective pocket depth δ is then given by

$$\delta = \frac{d}{4},$$

since the feed hole must still operate as a simple orifice as the local clearance reduces to zero. Simple orifices always give a greater gas film stiffness than annular orifices because the throat area is independent of the local clearance. The annular orifice reduces in area as the bearing surfaces approach and as a result the downstream pressure does not increase as rapidly as it would if the throat area remained constant. However, for a given clearance the annular orifice diameter is usually larger and it is occasionally preferred to use annular orifices to facilitate manufacture in a bearing where stiffness is of secondary importance.

2.4 Jet and slot combinations

(a) *Journal bearings* It has already been described how a journal bearing can be considered as being composed of a number of rectangular slots arranged circumferentially around the shaft. This concept was shown in Fig. 2.2. It is usual to consider that the number of slots is equal to the number of feed holes in a row around the bearing. In this case, for a bearing with two rows of feed holes, the flow through the slot is equal to the flow through one feed hole. For a bearing with a single central row of feed holes the flow in the slot is equal to half the flow through a feed hole, since each feed hole supplies two slots with gas exhausting at both ends of the bearing.

Considering a bearing with two rows of feed holes, the flow through the feed hole given in equation (17) can be substituted into equation (5)

for the flow in the slot to give:

$$P_d^2 - P_a^2 = \frac{24\mu RTl . C_D A \rho_o (2RT_o)^{\frac{1}{2}} F(\gamma K)}{\bar{a}h^3}.$$

Now

$$P_d^2 - P_a^2 = (P_d - P_a)(P_d + P_a)$$

$$= \frac{P_d - P_a}{P_o - P_a}(P_d + P_a)(P_o - P_o)$$

$$= K_g \left(\frac{P_d}{P_o} + \frac{P_a}{P_o}\right)\left(1 - \frac{P_a}{P_o}\right) P_o^2,$$

where

$$K_g = \frac{P_d - P_a}{P_o - P_a}.$$

Also putting

$$\rho_o = \frac{P_o}{RT_o}$$

and assuming

$$T_o = T$$

(i.e., the supply temperature is equal to the temperature in the slot) then

$$K_g = \frac{24\mu(2RT)^{\frac{1}{2}} l C_D A F(\gamma K)}{\left(\dfrac{P_d}{P_o} + \dfrac{P_a}{P_o}\right)\left(1 - \dfrac{P_a}{P_o}\right) P_a \bar{a}h^3}. \tag{20}$$

The calculation of the load capacity of the aerostatic journal bearing requires the solution of equation (20) for each jet and slot combination. When load is applied to the shaft it moves to an eccentric position in the bearing. It can be seen from Fig. 2.8 that at an angle θ to the load line, the local bearing clearance is given by

$$h = h_o(1 - \varepsilon \cos \theta),$$

where ε is the eccentricity ratio. Thus for any given mean radial clearance h_o and eccentricity ratio ε, the mean clearance of each slot can be calculated and substituted in equation (20) to obtain the pressure at the point where the gas enters the bearing. Then assuming that the pressure falls parabolically to the ends of the bearing and that the pressure between adjacent jets in two rows is constant, the pressure forces of the slots on the shaft can be summed vectorially to yield the load on the shaft (see Fig. 2.10).

However, equation (20) is not explicit in terms of P_d or K_g and hence its solution is a matter of successive approximations which are both
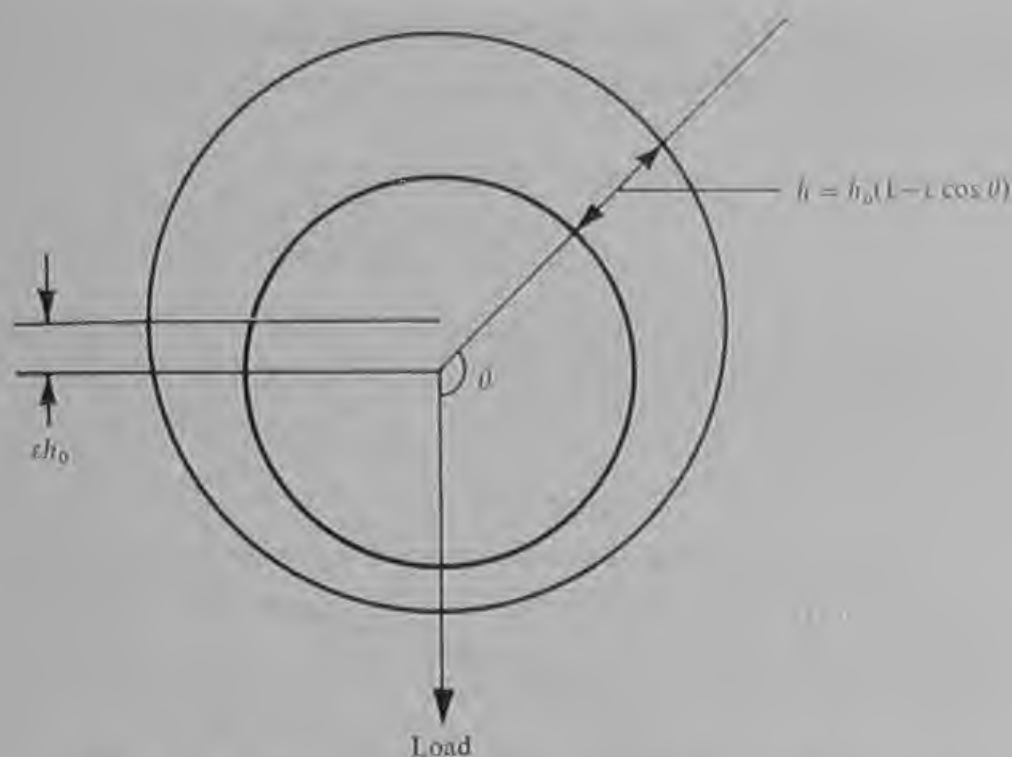
Fig. 2.8 Variation of clearance around a loaded journal
bearing

lengthy and tedious. Shires (Ref. 4) noticed that as $\dfrac{P_d}{P_o}$ approaches
unity, equation (20) reduces to

$$K_g = G(1 - K_g)^{\frac{1}{4}}$$

since $F(\gamma K)$ reduces to

$$\left(1 - \frac{P_d}{P_o}\right)^{\frac{1}{4}} = \left[\left(1 - \frac{P_a}{P_o}\right)\left(1 - \frac{P_d - P_a}{P_o - P_a}\right)\right]^{\frac{1}{4}}$$

$$= \left(1 - \frac{P_a}{P_o}\right)^{\frac{1}{4}} (1 - K_g)^{\frac{1}{4}}.$$

The slot factor G is given by

$$G = \frac{P_a/P_o}{\left(1 + \dfrac{P_a}{P_o}\right)\left(1 - \dfrac{P_a}{P_o}\right)^{\frac{1}{4}}} \cdot \frac{24\mu(2RT)^{\frac{1}{4}}}{P_a} \cdot \frac{IC_D A}{\bar{a}h^3} \qquad (21)$$

$$= \qquad F_p \qquad . \qquad F_g \qquad . \qquad F_d$$

where F_p is the pressure factor,
        F_g is the gas properties factor,
and F_d is the dimensional factor.

Shires calculated the variation of K_g with G for both compressible and
incompressible flow and for various values of γ. The results are shown

graphically in Fig. 2.9. For incompressible flow K_g can be expressed explicitly in terms of G as

$$K_g = \frac{2}{1 + \left(1 + \dfrac{4}{G^2}\right)^{\frac{1}{2}}}.$$

Fig. 2.9 can be used to provide a rapid solution of equation (20). If K_{go} is the gauge pressure ratio for the concentric bearing, i.e. when
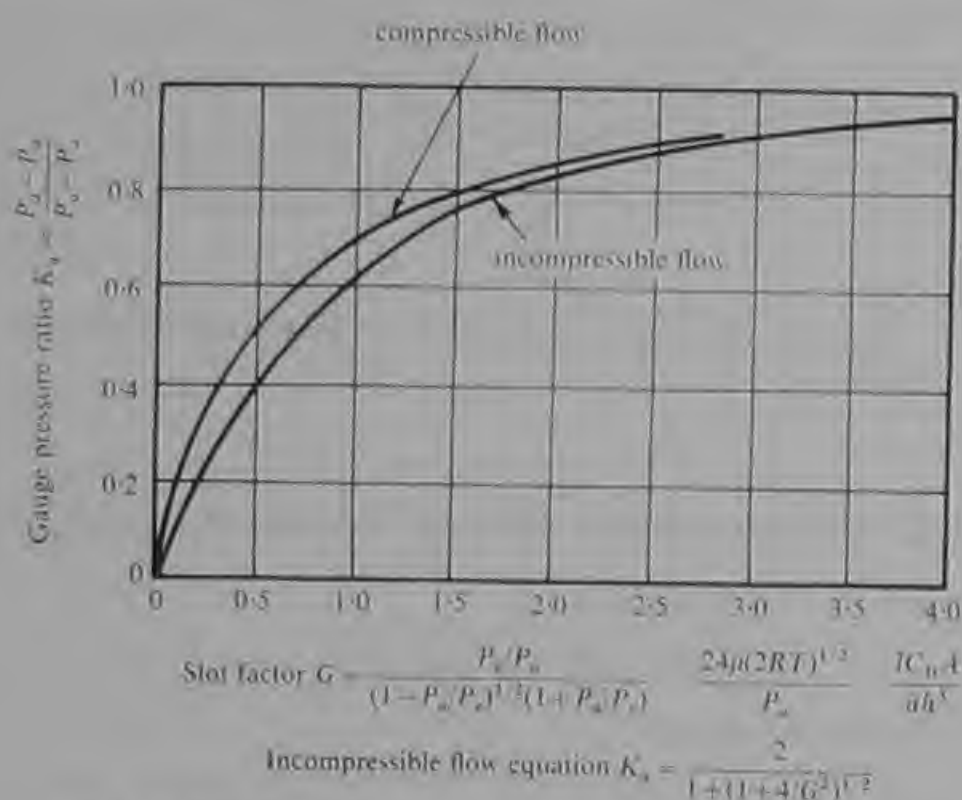
Fig. 2.9 Theoretical characteristics of the jet and slot combination (after Shires, Ref. 11)

$h = h_o$, and the corresponding value of G is G_o, then the value of G for any slot at angle θ to the load line in a bearing at eccentricity ratio ε is given by

$$\frac{G}{G_o} = \left(\frac{h_o}{h}\right)^3$$

$$= \frac{1}{(1 - \varepsilon \cos \theta)^3}. \tag{22}$$

Thus it is only necessary to make one full calculation of G_o for the concentric bearing; then by calculating the value of G for each slot from equation (22), the corresponding values of K_g can be found from Fig. 2.9. In this way the pressure distribution in the bearing can be found for any eccentricity ratio and the corresponding load

capacity can be calculated as shown in Fig. 2.10. A typical variation of load coefficient C_L with K_{go} and ε is shown in Fig. 1.5.

Pressure from each feed hole is felt over a chord of width $D \sin \dfrac{\pi}{N}$

$$P_{dm_3} = \tfrac{2}{3}(P_{d_3} - P_a) + P_a$$

position of rows of feed holes

$$P_{dm_1} = \tfrac{2}{3}(P_{d_1} - P_a) + P_a$$
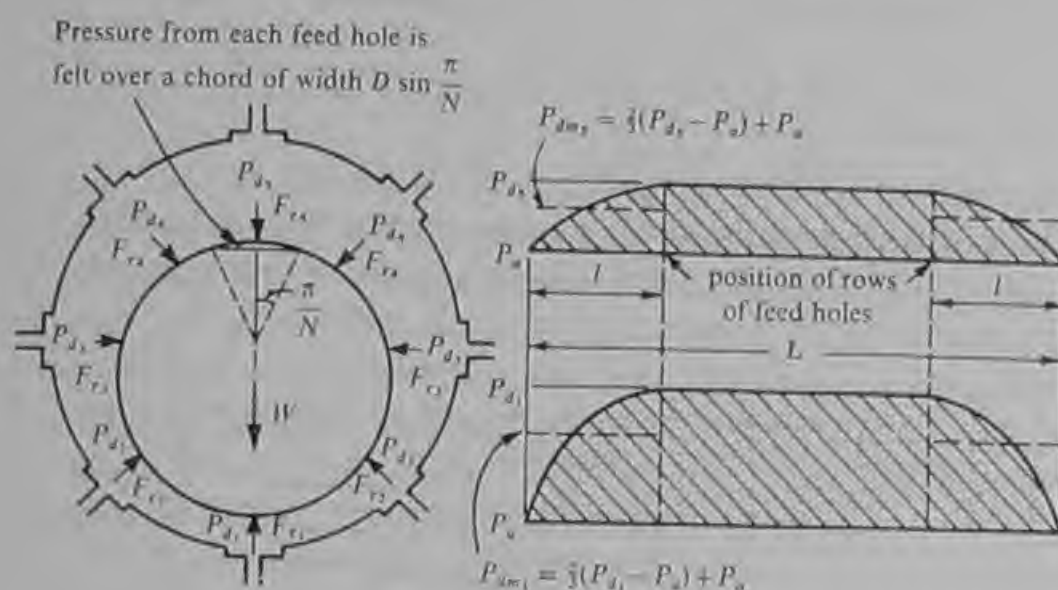
Radial pressure force from each full length axial slot

$$F_r = P_a(L - 2l)D \sin \frac{\pi}{N} + 2\left[\tfrac{2}{3}(P_d - P_a)lD \sin \frac{\pi}{N}\right]$$

and resolving vertically the total load

$$W = F_{r_1} - F_{r_3} + 2(F_{r_3} - F_{r_4}) \cos \frac{\pi}{4}$$

for eight feed holes per row, i.e. $N = 8$.

Fig. 2.10 Load capacity of aerostatic journal bearing—axial flow model

However, the load capacity calculated by this method will be greater than that achieved in practice due to two factors which have not yet been considered but which distort the pressure distribution (Fig. 2.11).

gas flow lines

pressure distributions

(a) Axial flow model

(b) Real bearing
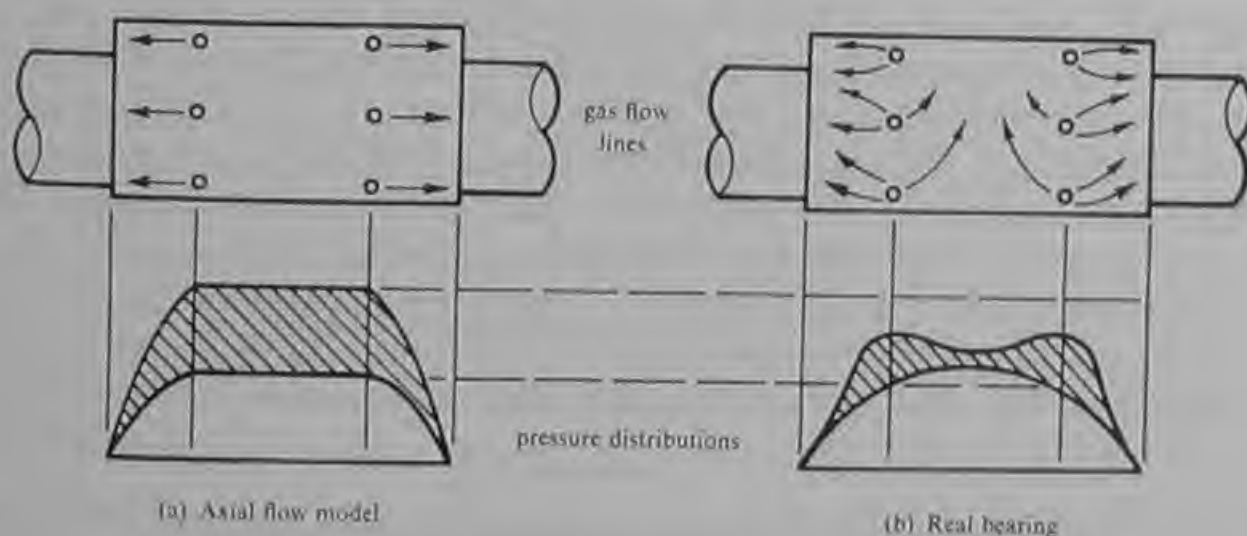
Fig. 2.11 The effects of dispersion and non-axial flow

The first of these is the effect of dispersion as the gas flow diverges from around the feed jet. Dudgeon and Lowe (Ref. 5) have studied the effects of dispersion and have shown that the theoretical load is reduced by a factor called the load dispersion coefficient C_W given by

$$C_W = 0.89 \left(\frac{dn}{\pi D}\right)^{0.21} \left(\frac{Ln}{\pi D}\right)^{0.42} \left(\frac{P_d}{P_a}\right)^{0.0505} \left(\frac{\pi D}{nd}\right)^{0.379} \left(\frac{\pi D}{nL}\right)^{0.758} \quad . \quad (23)$$

Some typical values of load dispersion coefficients are given in Fig. 2.12 and some typical values of flow dispersion coefficients C_Q are given
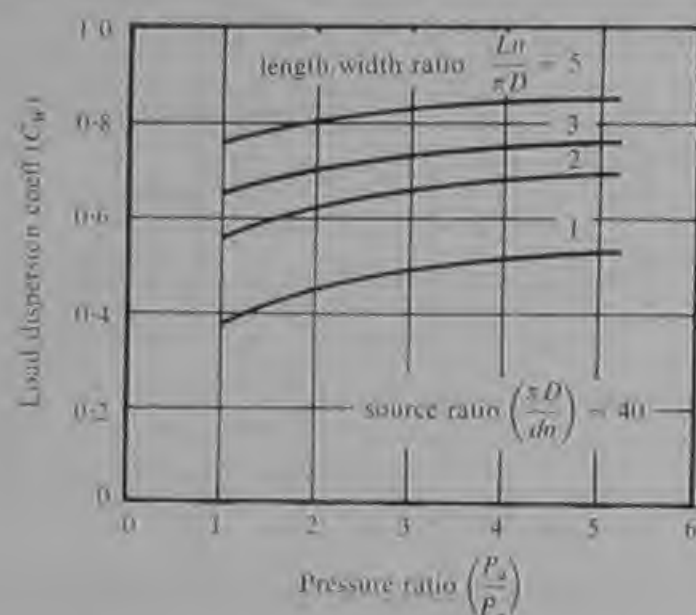
Fig. 2.12 Typical load dispersion coefficients (after Dudgeon and Lowe, Ref. 5)
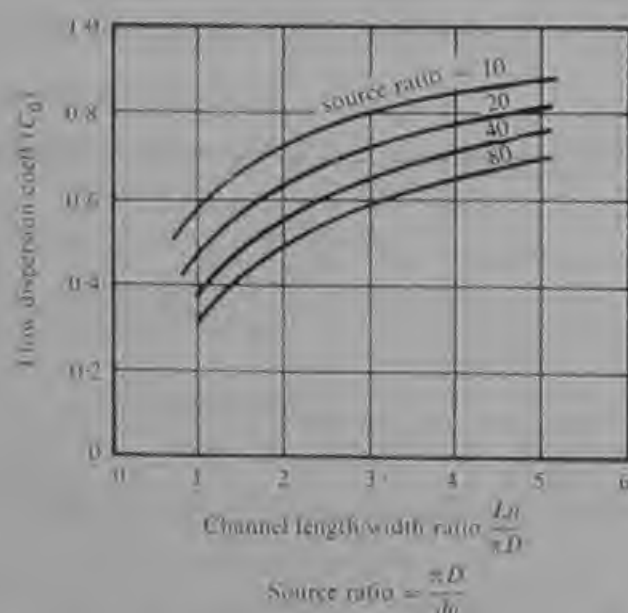
Fig. 2.13 Flow dispersion coefficients (after Dudgeon and Lowe, Ref. 5)

in Fig. 2.13. It can be seen that the effects of dispersion will be greatest in short bearings and bearings with few jets per row. In these cases the gas flow may not be fully dispersed to fill the whole of the bearing circumference before it exhausts to atmosphere at the ends of the bearings. It will be seen that bearings with circumferential slot feeding do not suffer from dispersion effects and this constitutes one of their major advantages.

The second factor affecting load capacity not yet considered is non-axial flow. So far it has been assumed that in each slot around an eccentric journal bearing the gas flows axially from the plane of the feed hole to the end of the bearing. Yet in practice the circumferential pressure distribution causes the gas to flow around the bearing from the region of high pressure to the region of low pressure. The effect of this non-axial flow is to reduce the pressure differential across the shaft and hence to reduce the load capacity.

No simple analytical solution exists for the effects of non-axial flow. Dudgeon and Lowe (Ref. 5) give a computer programme for calculating its effect to which the reader is referred for a more rigorous treatment of this aspect of journal bearing design. Shires has deduced a semi-empirical correction factor for non-axial flow in which the constant was derived from a series of experimental results by Robinson (Ref. 6). Shires' correction factor also makes some allowance for dispersion since Robinson's results must have included this effect. Shires gives

$$\frac{C_L}{C_{L_o}} = 0.315 \frac{\left[\dfrac{\cosh (6.36l/D) - 1}{\sinh (6.36l/D)} + \tanh \left(6.36 \dfrac{L - 2l}{D} \right) \right]}{\left(\dfrac{L - l}{D} \right)}, \quad (24)$$

where C_{L_o} is the load coefficient based on the axial flow model previously considered and C_L is the load coefficient corrected for non-axial flow.

The design data given in Chapter 3 is based on the work of Shires and of Dudgeon and Lowe and on much experimental data. Though less precise in any particular case than a numerical computer solution the design data derived by this method enables the effect of variation in the different parameters rapidly to be evaluated. It has been found that design load capacities and stiffnesses are predicted to within ten per cent in most cases for bearings of length-to-diameter ratio below two and of near optimum design. Longer bearings are seldom used because the effect of non-axial flow increases as the bearing length-to-diameter ratio increases and thus long bearings are very inefficient load supporters.

(b) *Thrust bearings* Thrust bearings can be treated in a similar way to the journal bearing equivalent slot already considered. In the case

of the simple thrust bearing with central feed hole shown in Fig. 2.3, the flow through the feed hole given by equation (17) can be equated to the flow in the clearance space given in equation (12). However, once again the resulting equation is not explicit in terms of P_d and a bearing slot factor is introduced.

$$G = \frac{P_a/P_o}{(1 - P_a/P_o)^{\frac{1}{2}}(1 + P_a/P_o)} \cdot \frac{24\mu(2RT)^{\frac{1}{2}}}{P_a} \cdot \frac{C_D d^2 \log_e (b/a)}{8h^3} \quad (25)$$

$$= \qquad F_p \qquad , \qquad F_g \qquad , \qquad F_d$$

The factors F_p and F_g are identical with those used in the journal bearing theory. In aerostatic thrust bearings the effects of compressibility on the pressure distribution in the clearance space is small and is often neglected. In this case the incompressible relationship between K_g and G applies:

$$K_g = \frac{2}{1 + \left(1 + \dfrac{4}{G^2}\right)^{\frac{1}{2}}}. \quad (26)$$

The total load which the bearing will support is proportional to K_g and is obtained by integrating the pressure over the whole of the

$$P = \left(P_d^2 - \frac{12\mu\omega RT}{\pi h^3} \ln \left(\frac{r}{a}\right)\right)^{1/2}$$

Total load $W = \pi a^2 P_d + \int_a^b 2\pi r P dr - \pi b^2 P_a$

$$= (P_d - P_a)\frac{\pi(b^2 - a^2)}{2 \ln (b/a)}$$
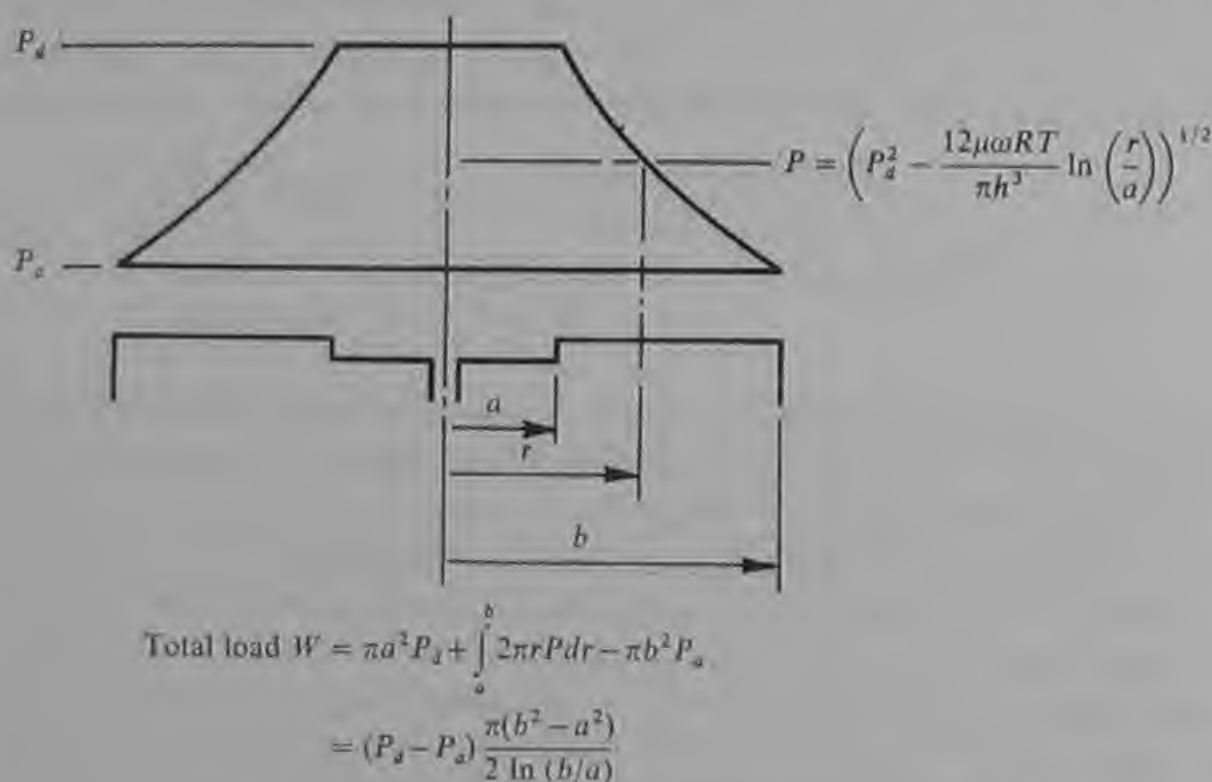
Fig. 2.14 Load carried by circular thrust bearing with central feed hole

thrust plate (Fig. 2.14). The solution is

$$W = K_g(P_o - P_a)\frac{\pi(b^2 - a^2)}{2 \log_e (b/a)}. \quad (27)$$

Since G is a function of the clearance h, K_g may be plotted against h for a particular design to illustrate the shape of the load versus clearance curve. Fig. 2.15 shows this transformation of equation (26). The shape
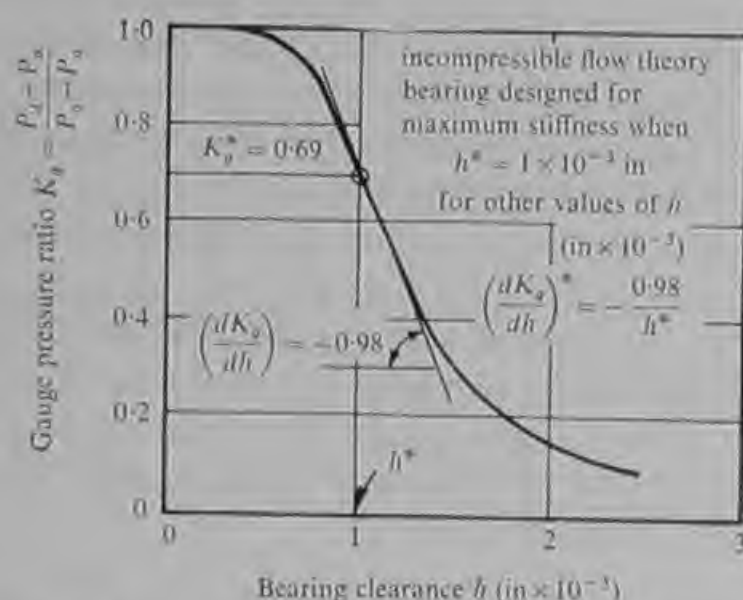
Fig. 2.15 Variation of thrust bearing gauge pressure ratio with clearance

of the curve is typical of all aerostatic thrust bearings. K_g increases as h is reduced, slowly at large clearances, then more rapidly and finally slowly again. The point of greatest slope is the point of maximum bearing stiffness. For incompressible flow the maximum stiffness occurs when

$$K_g^* = 0.69$$

and

$$G^* = 1.25,$$

under which conditions

$$\left(\frac{dK_g}{dh}\right)^* = -\frac{0.98}{h^*}$$

and

$$\left(\frac{dW}{dh}\right)^* = -\frac{0.69(P_o - P_a)\pi(b^2 - a^2)}{h^* \, 2\log_e(b/a)}. \tag{28}$$

Under these conditions the load capacity is given by

$$W^* = \frac{0.69(P_o - P_a)\pi(b^2 - a^2)}{2\log_e(b/a)} \tag{29}$$

and the mass flow by

$$M^* = \frac{\pi(h^*)^3[(P_d^*)^2 - P_a^2]}{12\mu RT \log_e(b/a)}, \tag{30}$$

where P_d^* corresponds to $K_g^* = 0.69$. In practice the assumption of incompressible flow means that predicted loads and stiffnesses are between ten and twenty percent less than those measured experimentally for actual bearings. This means that the design charts given in Chapter 4 tend to underestimate bearing performance and therefore incorporate some margin of safety. The basic theory for symmetrically loaded thrust bearings does not neglect any factors of major importance corresponding to dispersion or non-axial flow in journal bearings.

The annular thrust bearing supplied by a ring of feed holes can be treated in a similar way by equating the total flow through the feed holes to the total flow in the clearance given by equations (15) and (16). It is assumed that the inward and outward flows are equal which is the condition defined by

$$c^2 = ab.$$

In this case the slot factor is given by

$$G = F_p . F_g . F_d,$$

where F_p and F_g are as before and

$$F_d = \frac{C_D n d^2 \log_e (b/a)}{32h^3}, \tag{31}$$

where n is the number of feed holes of diameter d. The incompressible relationship given in equation (26) can again be applied and the values for maximum stiffness of K_g^*, G^* and $(dK_g/dh)^*$ are the same as before. The total load capacity is obtained by integrating the pressure given in equations (13) and (14) over the surface of the bearing between radius a and radius b. The load is given by

$$W = \frac{K_g(P_o - P_a)\pi(b-a)^2}{\log_e (b/a)}. \tag{32}$$

The maximum stiffness is

$$\left(\frac{dW}{dh}\right)^* = -\frac{0.69(P_o - P_a)\pi(b-a)^2}{h^* \log_e (b/a)}, \tag{33}$$

at which condition the load is

$$W^* = \frac{0.69(P_o - P_a)\pi(b-a)^2}{\log_e (b/a)} \tag{34}$$

and the mass flow is

$$M^* = \frac{\pi(h^*)^3[(P_d^*)^2 - P_a^2]}{3\mu R T \log_e (b/a)}. \tag{35}$$

By comparing equations (30) and (35) it can be seen that with all other factors equal the mass flow of gas through the annular thrust

bearing is four times as great as for the simple thrust bearing with a central feed. Therefore in order to minimize the pumping power required the simple thrust bearing is used wherever other design factors permit. The annular thrust bearing must be used wherever a shaft projects beyond the bearing assembly. The annular bearing also provides greater resistance to tilting. In most practical machines with aerostatic bearings the single bearing element demanding the greatest individual gas flow is almost always an annular thrust bearing. Equation (35) shows that in order to minimize this flow the ratio b/a should be as large as possible.

2.5 Flow through slots in series

(a) *Journal bearings* A journal bearing in which the supply gas is fed to the clearance space through narrow slots in the bearing sleeve is shown in Fig. 2.16. The bearing clearance can be divided into a number
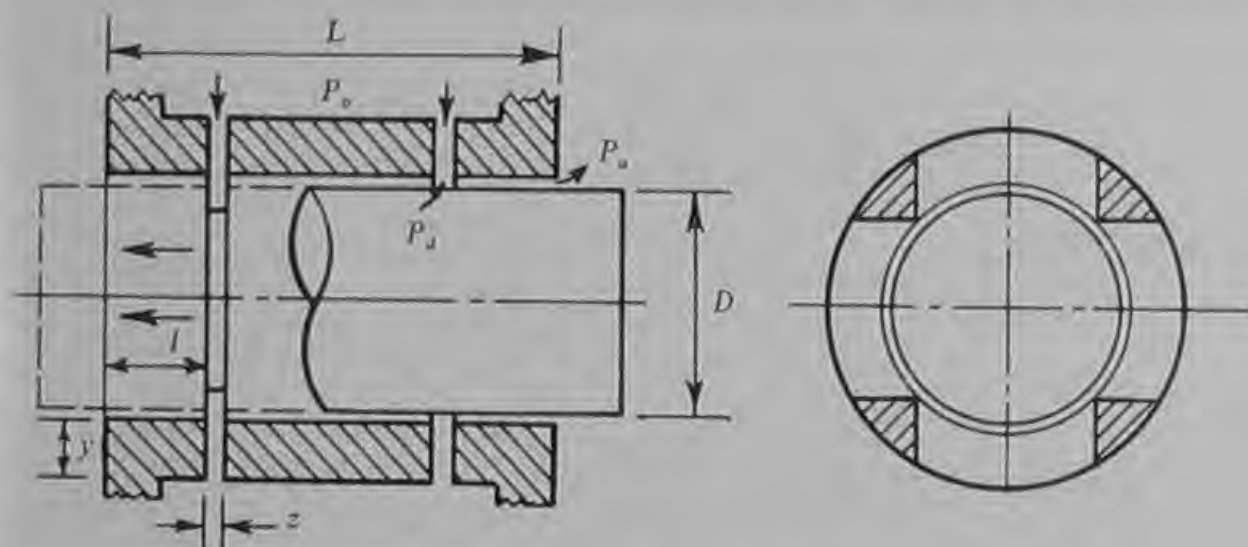
Fig. 2.16 Journal bearing with circumferential inlet slots

of equivalent slots equal to the number of feed slots, and each two-slot combination can be treated in a similar way to the jet and slot combination already considered.

Rewriting equation (5) for the flow through a slot in terms of the dimensions given in Fig. 2.16 gives the following expressions for the flow from P_o to P_d in the feed slot and from P_d to P_a in the bearing slot.

$$P_o^2 - P_d^2 = \frac{24\mu R T m y}{z^3} \cdot \frac{n}{\pi D} \qquad (36)$$

where y is the length of the feed slot (usually the thickness of the bearing sleeve),

  z is the thickness of the feed slot,

   n is number of feed slots giving the width of the slot as $\dfrac{\pi D}{n}$

and

$$P_d^2 - P_a^2 = \frac{24\mu R T m l}{h^3} \cdot \frac{n}{\pi D}. \qquad (37)$$

By eliminating the mass flow m (and incidentally μRT too), equations (36) and (37) are combined to give:

$$\frac{P_d^2 - P_a^2}{P_o^2 - P_a^2} = \frac{1}{1 + \left(\dfrac{y}{l}\right)\left(\dfrac{h}{z}\right)^3}$$

$$= \frac{1}{1 + \alpha}. \qquad (38)$$

Equation (38) can be rearranged to give

$$\frac{P_d - P_a[(P_d - P_a) + 2P_a]}{P_o - P_a[(P_o - P_a) + 2P_a]} = \frac{1}{1 + \alpha},$$

then

$$K_g\left(K_g + \frac{2P_a}{P_o - P_a}\right) = \frac{(P_o - P_a) + 2P_a}{(P_o - P_a)(1 + \alpha)},$$

whence putting

$$\beta = \frac{2P_a}{P_o - P_a}$$

gives

$$K_g^2 + \beta K_g - \frac{1 + \beta}{1 + \alpha} = 0.$$

This has a real solution:

$$K_g = \left[\left(\frac{\beta}{2}\right)^2 + \frac{1 + \beta}{1 + \alpha}\right]^{\frac{1}{2}} - \frac{\beta}{2}. \qquad (39)$$

It should be noted that for a single ring of feed slots

$$\alpha = 2\left(\frac{y}{l}\right)\left(\frac{h}{z}\right)^3$$

and for two rings of feed slots

$$\alpha = \left(\frac{y}{l}\right)\left(\frac{h}{z}\right)^3$$

because in the former case one feed slot feeds two bearing slots.

Equation (39) can be used to determine the pressure P_d for each slot, and, once again assuming a parabolic pressure distribution from the slot to the end of the bearing and constant pressure between two adjacent slots, the radial pressure force on the shaft from each bearing

slot can be calculated. The radial forces can then be summed vectorially to yield the load on the shaft. For short bearings the bearing characteristics shown in Fig. 2.17 can be derived.
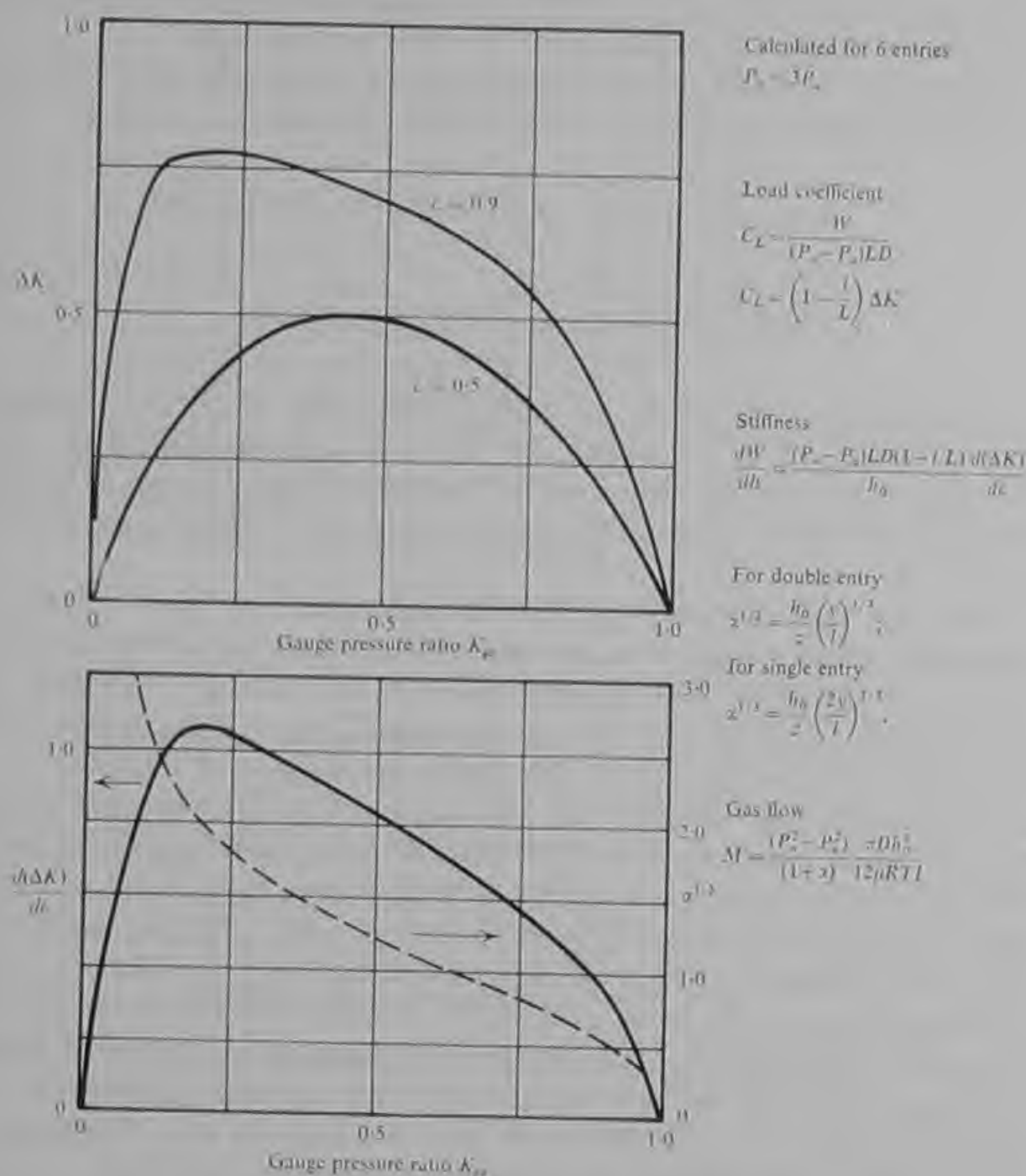
Fig. 2.17 Characteristics of short journal bearings with circumferential slots (after Shires and Dee, Ref. 7)

One significant feature of all bearings with inlet slots is that the load capacity and stiffness are functions of the dimensions and fluid pressures only. Unlike bearings with metering orifices gas properties and temperature do not influence the performance. Furthermore, the choice of optimum dimensions, which can be expressed simply as ratios of linear dimensions, is not significantly affected by the level either of the supply pressure or of the ambient pressure over normal working

ranges. In fact a bearing designed for pressurizing with a gas will also work at the same gauge pressure ratio with a liquid. This is because the bearing depends for its operation on the pressure drop through two successive slots of similar dimensions and at the same temperature. A change in fluid density or viscosity changes each pressure drop by the same factor so that the pressure ratio remains constant.

In the case of short journal bearings with circumferential inlet slots the critical design parameter is the ratio of dimension α where

$$\alpha = \left(\frac{h_o}{z}\right)^3 \left(\frac{y}{l}\right) \quad \text{for two rings of slots, and}$$

$$\alpha = \left(\frac{h_o}{z}\right)^3 \left(\frac{2y}{l}\right) \quad \text{for one ring of slots.}$$

For maximum stiffness at an eccentricity ratio of 0·5, α should be approximately equal to eight. In practice it is sometimes necessary to design at smaller values of α (for example to keep z large to simplify manufacture) and there is little deterioration in performance down to $\alpha = 2$.

Bearings with circumferential inlet slots will not be weakened by dispersion effects since the gas is introduced to the clearance space evenly around the whole circumference of the bearing. However, the load capacity will be reduced by the effects of non-axial flow and a correction is made for this in the design data given in Chapter 3.

Slot-fed journal bearings can take a variety of forms with circumferential slots, axial slots and combinations of both types. Bearings with axial inlet slots can be analysed by the same basic method already used for jet-fed bearings and for bearings with circumferential inlet slots. An estimate of the load capacity of the bearing can be obtained by considering the bearing as a series of strip bearings each fed by a single slot. Shires (Ref. 7) has considered the axial pressure distribution in such a strip for an incompressible fluid and his conclusions are shown in Fig. 2.18 (although this does not include any allowance for dispersion). Two cases are considered, an axial slot, OA, over the complete bearing length and an axial slot, OB, over the central half only. The load coefficients for journal bearings with six axial slots have been calculated using this one dimensional model and are shown in Fig. 2.18(b). The maximum load coefficient occurs for a combination of geometric parameters which are independent of slot length, namely

$$\alpha = \left(\frac{h_o}{z}\right)^3 \left(\frac{4\pi D y}{n L^2}\right)$$

$$= 0.42 \tag{40}$$

One dimensional model

Pressure distribution

$J = 0.4$ for OA

$J = 0.3$ for OB

Mean non-dimensional pressure J

Incompressible fluid

$\varepsilon = 0.5$

$$\phi = \left\{ \frac{L^2}{4ay} \left(\frac{z}{h_0} \right)^3 \right\}^{1/2}$$
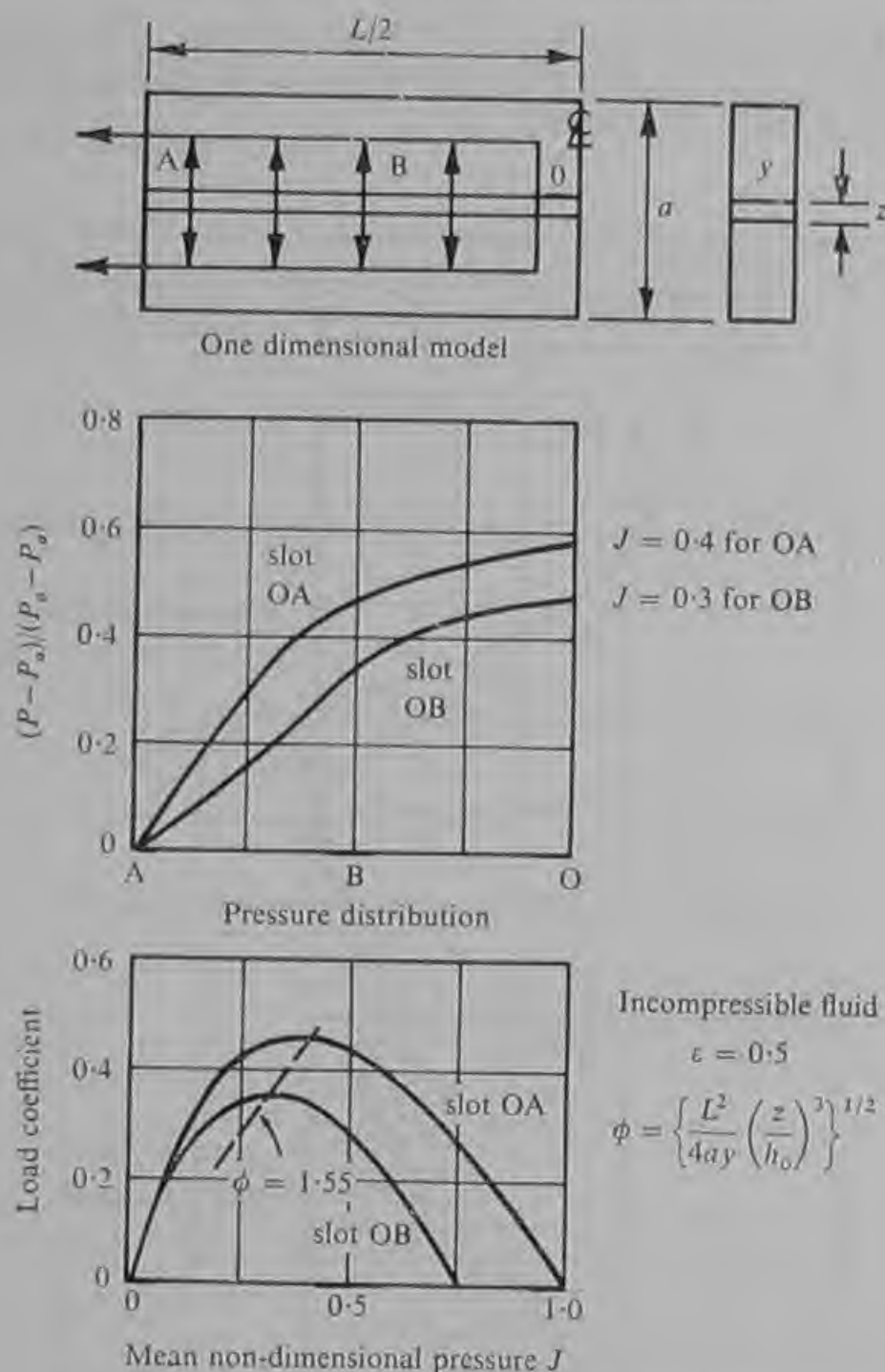
Fig. 2.18 Characteristics of axial inlet slots (after Shires and Dee, Ref. 7)

where L is the bearing total length,

$\dfrac{\pi D}{n}$ is the circumferential distance between inlet slots,

n is the number of slots,

y is the depth of the inlet slot,

and z is the width of the inlet slot.

Although the total length of axial inlet slot in a bearing may be greater than that of the equivalent circumferential slot the mass flow requirement may not be significantly higher. This is because the flow

from the axial slot is concentrated towards the ends. A comparison of the mass flow from bearings with the same clearance is given in Fig. 2.19, which illustrates this point.
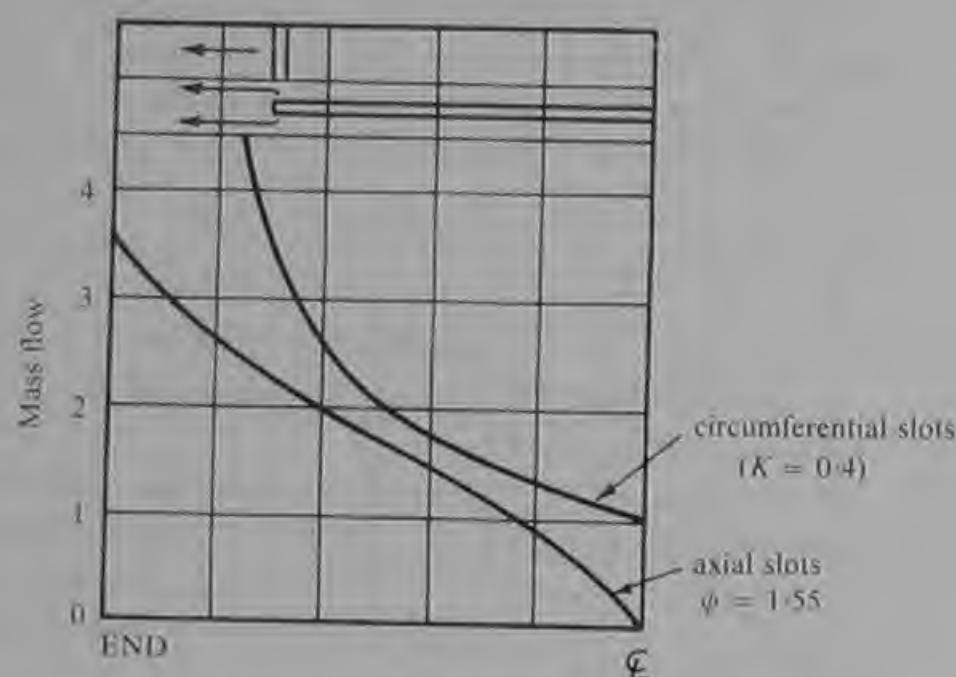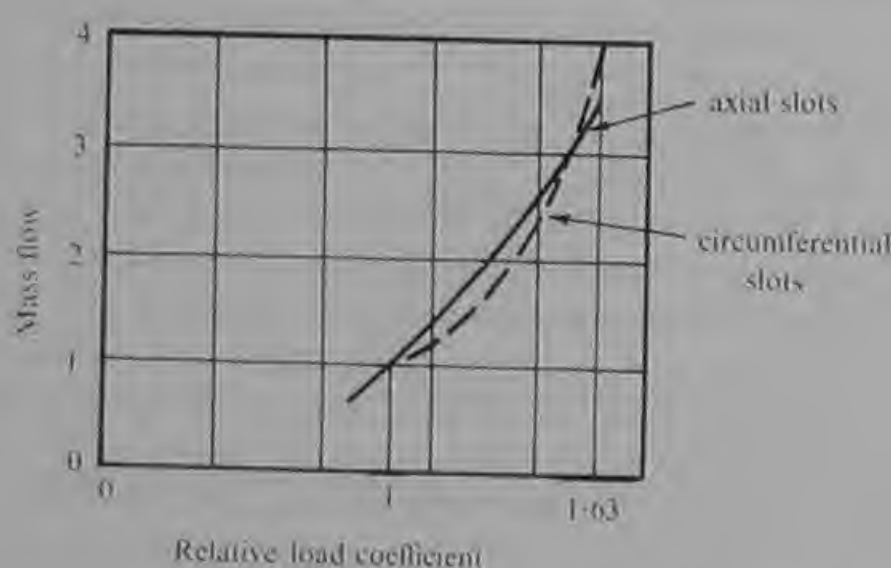
Fig. 2.19 Comparison of mass flow requirements of axial and circumferential inlet slots (after Shires and Dee, Ref. 7)

Bearings with axial slots will be weakened by the effects of dispersion. However, axial slots do offer a means of limiting or even nullifying the effects of non-axial flow. This is a particularly valuable feature in cases where a bearing of large length-to-diameter ratio must be used. It has also been suggested that axial slots, perhaps even angled tangentially to the journal surface, may increase the dynamic stability of bearings for high speed applications. This possibility is discussed

more fully in Chapter 7. To date few applications of bearings with axial slots have however been proposed and the available design and experimental data are limited.

(b) *Annular thrust bearing with circular inlet slots* An annular thrust bearing with circular inlet slots is shown in Fig. 2.20. From equation (15) it can be seen that

$$P_d^2 - P_a^2 = \frac{12\mu m_1 RT}{\pi h^3} \log_e \left(\frac{b}{c} \right) \tag{41}$$

for the outward flow region between the radius of the slot c and the
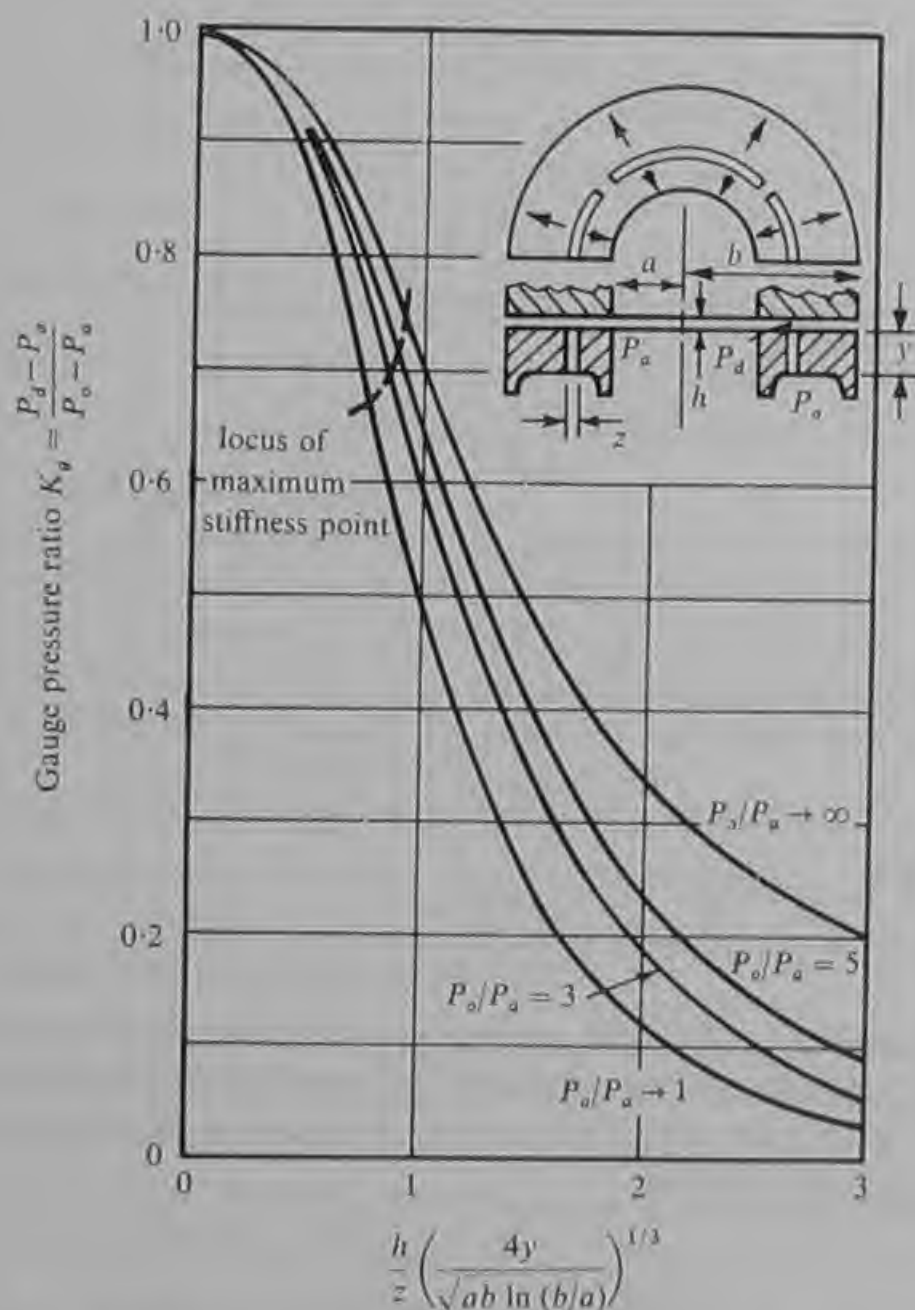
Fig. 2.20 Characteristics of thrust bearings with circular inlet slots (after Shires and Dee, Ref. 7)

outer radius b. From equation (16) it can also be seen that

$$P_d^2 - P_a^2 = \frac{12\mu m_2 RT}{\pi h^3} \log_e \left(\frac{c}{a}\right) \qquad (42)$$

for the inward flow region between the slot and the inner radius a. Once again it is assumed that the inward and outward flows are equal and therefore $c^2 = ab$. Then by adding equations (41) and (42) and putting the total flow $M = m_1 + m_2$ we find

$$P_d^2 - P_a^2 = \frac{3\mu RTM}{\pi h^3} \log_e \left(\frac{b}{a}\right). \qquad (43)$$

The flow through the inlet slot is given by equation (6) for a mass flow M as

$$P_o^2 - P_d^2 = \frac{12\mu RTMy}{\pi(ab)^{\frac{1}{2}}z^3}, \qquad (44)$$

where the length of the slot

$$\bar{a} = 2\pi c$$
$$= 2\pi(ab)^{\frac{1}{2}}.$$

Equations (42) and (43) can be combined to give

$$\frac{P_d^2 - P_a^2}{P_o^2 - P_a^2} = \frac{1}{1 + \left(\dfrac{h}{z}\right)^3 \left(\dfrac{y}{(ab)^{\frac{1}{2}}}\right) \dfrac{4}{\log_e (b/a)}}$$

$$= \frac{1}{1 + \alpha}, \qquad (45)$$

and as before for journal bearings

$$K_g = \left(\frac{1+\beta}{1+\alpha} + \frac{\beta^2}{2}\right)^{\frac{1}{2}} - \frac{\beta}{2} \qquad (39)$$

where again

$$\beta = \frac{2P_a}{P_o - P_a}.$$

The relationship between K_g and the load on the bearing is independent of the type of feeding and equation (32) also applies to annular bearings with slot feeding assuming incompressible flow in the bearing clearance. The stiffness is given by

$$\frac{dW}{dh} = \frac{(P_o - P_a)\pi(b-a)^2}{\log_e (b/a)} \left(\frac{dK_g}{dh}\right). \qquad (46)$$

An alternative expression for the load carried by an annular thrust bearing can be obtained by assuming a linear fall in pressure from

the slot or ring of jets to the inner and outer edges of the bearing. The resulting expression for load is

$$W = K_g \frac{\pi}{2} (b^2 - a^2)(P_o - P_a) \tag{47}$$

and for stiffness

$$\frac{dW}{dh} = \frac{\pi}{2} (P_o - P_a)(b^2 - a^2) \frac{dK_g}{dh} \tag{48}$$

Equation (32) tends slightly to underestimate the bearing load and equation (47) tends to overestimate it. For most design purposes equation (32) is generally the more reliable.

By differentiating K_g with respect to h for the slot-fed annular thrust bearing the following values were obtained by Shires.

Supply pressure ratio, P_o/P_a	2	3	5
Optimum value of α	0·65	0·72	0·77
Corresponding value of K_g	0·68	0·69	0·70
Corresponding value of dK_g/dh	−0·64	−0·61	−0·58

The negative sign indicates that K_g increases as h decreases. It is interesting to note how close the value of K_g for optimum stiffness is to the value of 0·69 previously obtained for jet-fed bearings. However, the theoretical stiffness of the slot-fed bearing is lower than that of the jet-fed bearing and this can be seen by comparing the value of the numerical constant $\left(\frac{dK_g}{dh} = -0{\cdot}69 \right)$ in equation (33) with the values in the table above. However, as the stiffness of the jet-fed bearing may be slightly reduced by the effects of dispersion the difference will be less in practice.

The variation of K_g with α is shown in Fig. 2.20. It is noteworthy that the optimum ratio of bearing dimensions for maximum stiffness is insensitive to pressure level.

The mass flow of gas through the bearing is given by equation (43) as

$$M = \frac{\pi h^3}{3\mu R T \log_e \left(\frac{b}{a} \right)} (P_d^2 - P_a^2)$$

which can be rearranged to give

$$M = \frac{\pi h^3}{3\mu RT \log_e \left(\frac{b}{a}\right)} \cdot \frac{P_o^2 - P_a^2}{1+\alpha} \tag{49}$$

2.6 Friction in bearings

When one surface of a fluid film bearing is moved relative to the other a resisting force is set up by the shearing of the fluid. The magnitude of the force depends upon the viscosity of the fluid but the mechanism is essentially similar for both liquids and gases.

Fig. 2.21 shows two parallel flat plates separated at a distance h by a fluid of viscosity μ. The upper plate is stationary and the lower plate
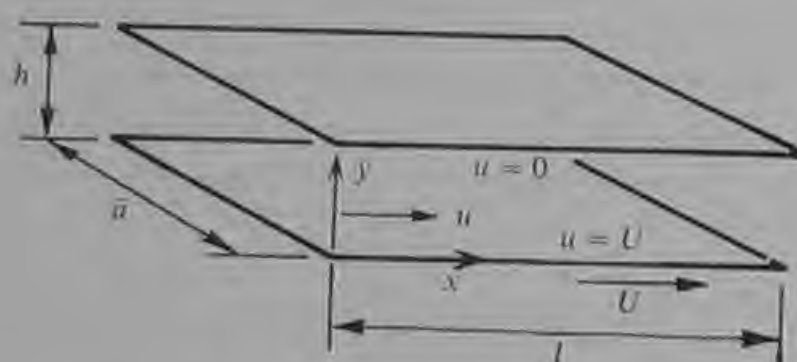
Fig. 2.21 Simple slider bearing

is moving at velocity U. The equation defining viscosity states that the force opposing the motion is given by

$$F = -\mu A \frac{du}{dy} \tag{50}$$

at any plane parallel to the surfaces within the fluid film. A is the area of the plates $(A = \bar{a}l)$ and u is the velocity of the gas at any position y in the film.

Assuming that there is no pressure variation in the x direction, the direction of motion, equation (1) reduces to

$$\frac{d^2u}{dy^2} = 0.$$

Integrating gives

$$\frac{du}{dy} = B \quad \text{(constant)}$$

and

$$u = By + C \quad \text{(constant)}.$$

Substituting the boundary conditions

$$u = U \quad \text{at } y = 0$$

and

$$u = 0 \quad \text{at } y = h$$

gives

$$\frac{du}{dy} = B = -\frac{U}{h}$$

and substituting in equation (50) gives

$$F = \mu \bar{a} l \frac{U}{h}. \tag{51}$$

Equation (51) expresses the frictional resistance of a flat pad bearing. It has little direct practical use although it can be applied to certain slideway bearings that have been used in machine tools. However, the frictional resistance of the concentric journal bearing can simply be derived from equation (51) by imagining the fluid film to be wrapped around a cylindrical journal of diameter D and length L rotating with angular velocity ω.

Then

$$l = \pi D,$$

$$U = \frac{\omega D}{2},$$

$$h = h_o,$$

and

$$\bar{a} = L,$$

and the tangential force on the surface of the journal

$$F_T = \frac{\mu \pi D^2 L \omega}{2h_o}$$

or the friction torque

$$F_T \frac{D}{2} = \frac{\mu \pi D^3 L \omega}{4h_o}$$

and the friction power loss is given by

$$\frac{\mu \pi D^3 L \omega^2}{4h_o}. \tag{52}$$

Equation (52) applies to all full concentric cylindrical journal bearings. The friction increases slightly in an eccentric bearing but the increase can be ignored for almost all practical purposes and certainly at eccentricity ratios below 0·5.

Fig. 2.22 shows an annular thrust bearing with parallel surfaces separated at a distance h by a fluid of viscosity μ. The inner radius

D.A.B.
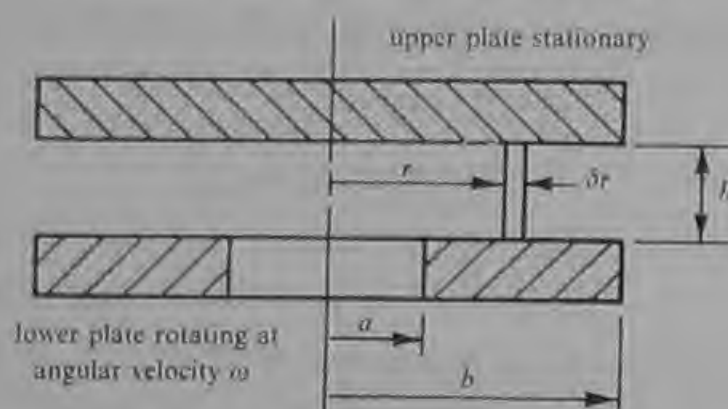
Fig. 2.22 Friction torque in a circular thrust bearing

of the film is a and the outer radius of the film is b. This model corresponds to both the annular thrust bearing and the simple thrust bearing with central feed hole and pocket since in the latter case the pocket depth will make the friction negligible over the area of the pocket.

Considering an annulus of radius r and width δr, equation (51) can be substituted as follows

$$\bar{a} = \delta r,$$

$$l = 2\pi r$$

and

$$U = r\omega,$$

therefore

$$F = \frac{\mu 2\pi r^2 \omega \delta r}{h}$$

or the torque

$$F_r = \frac{\mu 2\pi \omega r^3 \delta r}{h}.$$

Then integrating from $r = a$ to $r = b$ gives

$$\text{friction torque} = \frac{\mu \pi \omega}{2h} (b^4 - a^4)$$

$$\text{and the friction power loss} = \frac{\mu \pi \omega^2}{2h} (b^4 - a^4) \tag{53}$$

Equation (53) can be used to estimate the friction power loss in almost all circular thrust bearings and can be applied to all aerostatic thrust bearings described in this book.

2.7 Uses of the theory of aerostatic bearings

The design information given in the next two chapters is based upon the theory presented here. An understanding of the foregoing will assist the designer in making the correct interpretation of the design data and in appreciating their limitations and range of application.

It will facilitate the extending of the design data to bearings of similar geometry which are excluded. It will also indicate a method of approach to the analysis of bearings of other geometrical forms, such as those with conical or spherical surfaces, which are not included in the present work.

CHAPTER 3

DESIGN OF JOURNAL BEARINGS

3.1 Feasibility study

All designs must begin with a feasibility study. At this stage the designer attempts to build a bridge out from the known boundary limitations towards the required operating performance. In the case of aerostatic journal bearings the design usually has boundary limitations imposed by the following factors:

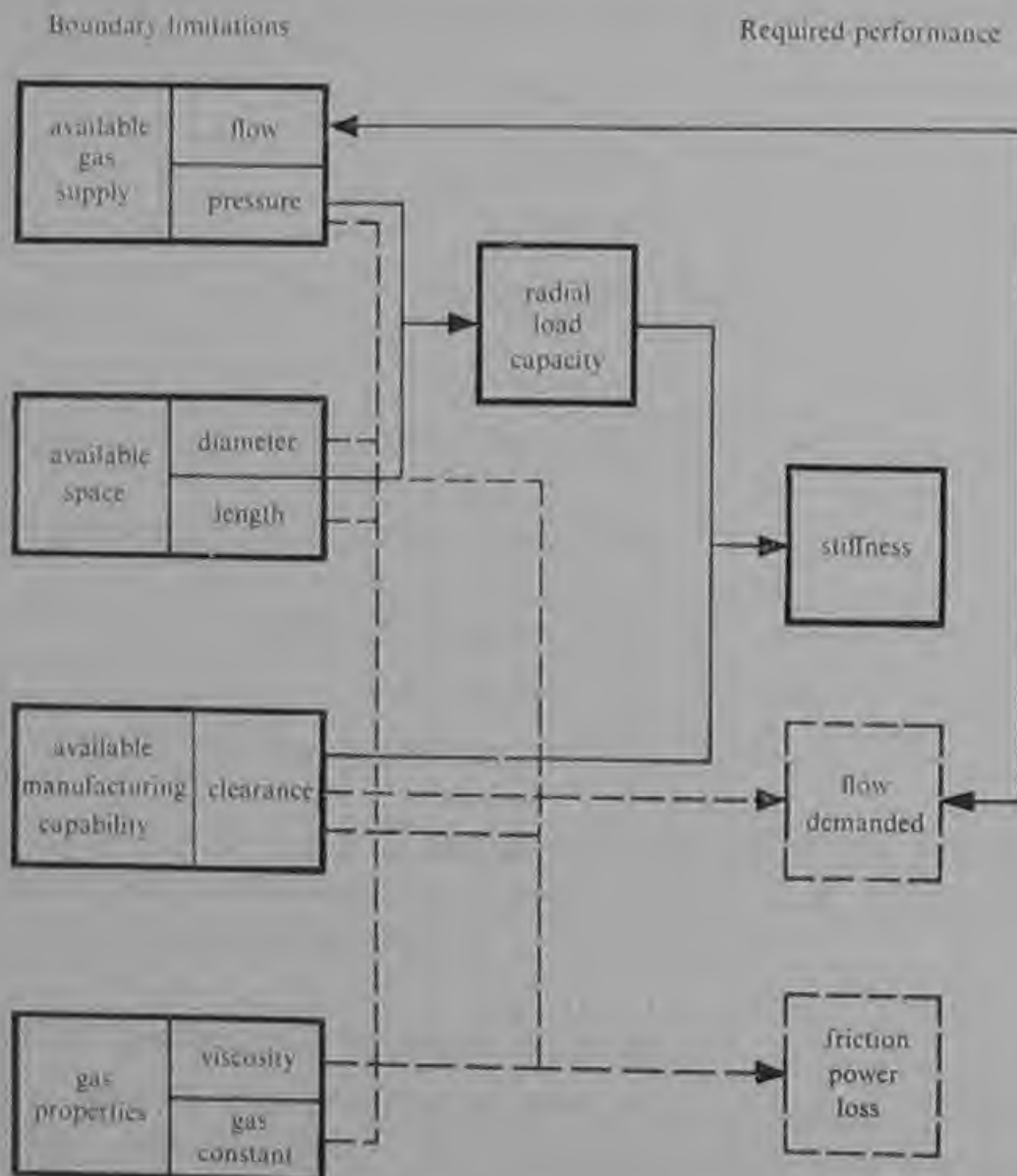(a) the available gas supply in terms of pressure and flow;

Fig. 3.1 Design of journal bearings—feasibility study

68

(b) the space available in which to engineer the bearing which will limit the length, diameter and plan area;

(c) the available manufacturing capability which will determine the minimum practical clearance. (In practice the limiting factor could be jet diameter or slot width and these could be determined by manufacturing difficulty or by problems of filtering the gas supply. In any case the result is to impose a lower limit on the bearing clearance.)

The stages in the feasibility study for an aerostatic journal bearing are shown diagrammatically in Fig. 3.1. Before beginning the designer will have made some estimation of the load the bearing must carry and of the required stiffness. The importance of including all possible loads which might arise has already been stressed. It is advisable at this stage to tend to overestimate the loading or to include a generous factor of ignorance. If the feasibility cannot be established it may be necessary to go back and recalculate the loads more accurately prior to a second attempt. However, if the feasibility is established the bearing can always be trimmed at a later stage of design to operate at a lower supply pressure or to take up less space in the machine.

The first step in the feasibility study will be to estimate the maximum radial load capacity. This will involve consideration of the available supply pressure and the length and diameter of the bearing. This step can often be achieved by referring to Fig. 3.2. This gives an estimate of the load capacity of bearings of up to 6 in in diameter and 6 in in length supplied at 100 lbf/in^2 gauge. The graphs of load capacity relate to all gas bearings with two rows of jets and the values given tend to slightly underestimate the performance which can be achieved by a bearing of good design and manufacture at an eccentricity ratio of 0·5.

The second step in the feasibility study involves the estimated radial load capacity and mean bearing clearance in an estimation of stiffness. For most aerostatic bearings the stiffness is constant up to an eccentricity ratio of 0·5 and can be calculated from equation (54).

Radial stiffness

$$\text{Radial stiffness } K = \frac{2W}{h_o} \, (\varepsilon = 0 \cdot 5) \text{ for } 0 < \varepsilon < 0 \cdot 5. \tag{54}$$

Data are given at an eccentricity ratio of 0·5 for two reasons. Firstly, most bearings operate linearly up to this eccentricity ratio and so the load values taken together with the clearance permit an accurate estimation of radial stiffness. Secondly, most designers choose to operate a bearing under normal working conditions at eccentricity ratios up to 0·5 or 0·6 and to make use of higher eccentricity ratios to provide capacity to withstand overload or accident conditions.

$\kappa = 0.5$
$K_{go} = 0.4$
$n = 8$
$P_a = 14.7$ psi
$P_o - P_a = 100$ psi
$\dfrac{l}{L} = \dfrac{1}{4}$
zero speed

0.34 c.f.m.

$W = 600$ lbf

500 lbf

400 lbf

300 lbf

0.23 c.f.m.

200 lbf

150 lbf

100 lbf

50 lbf

0.17 c.f.m.

25 lbf

0.11 c.f.m.

0.68 c.f.m.

0.45 c.f.m.

Airflow given in free volume
at 15°C for $2h_0 = 0.001$ in

Diameter (in)

Length (in)
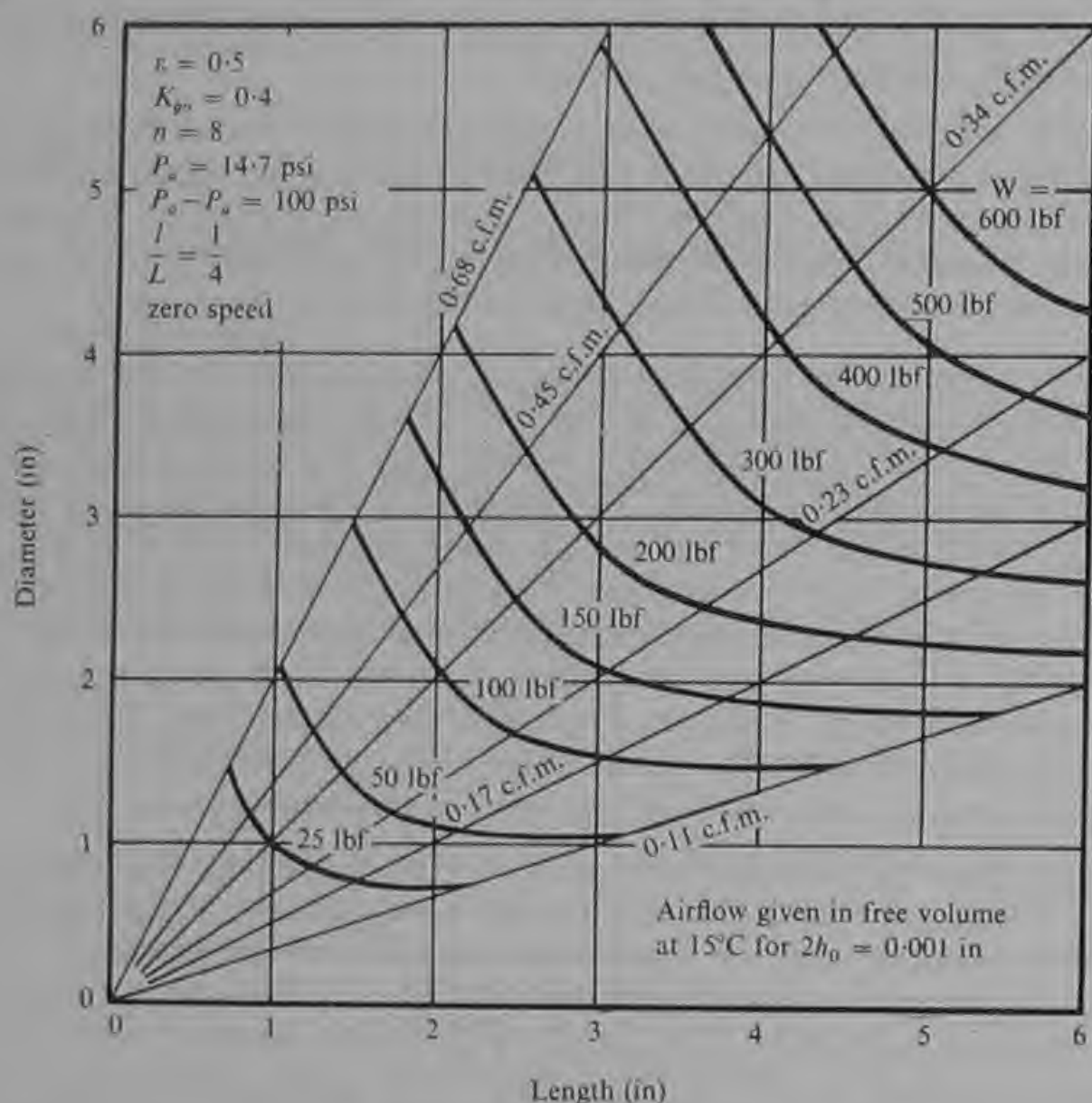
For other supply pressures multiply load by $\dfrac{(P_o - P_a)}{100}$

at $P_o - P_a = 75$ lbf/in² multiply flow by 0.65
at $P_o - P_a = 50$ lbf/in²   „   „   „ 0.27
at $P_o - P_a = 25$ lbf/in²   „   „   „ 0.14

For other clearances multiply flow by $\left(\dfrac{2h_0}{0.001}\right)^3$.

Radial stiffness $K = \dfrac{2W}{h_0}$.   Tilt stiffness $= \dfrac{KL^2}{16}$.

For other values of K_{go} see Fig. 3.12

Fig. 3.2 General performance of air journal bearings with
simple orifice feeding at quarter stations

At this stage, since it affects the chosen value of the mean radial
clearance, it is of interest to consider the effect of the geometric error
which will remain after manufacture. This is illustrated with reference
to Fig. 3.3. It can be seen that, as the stiffness reduces at high values
of eccentricity ratio the major proportion of the available load capacity
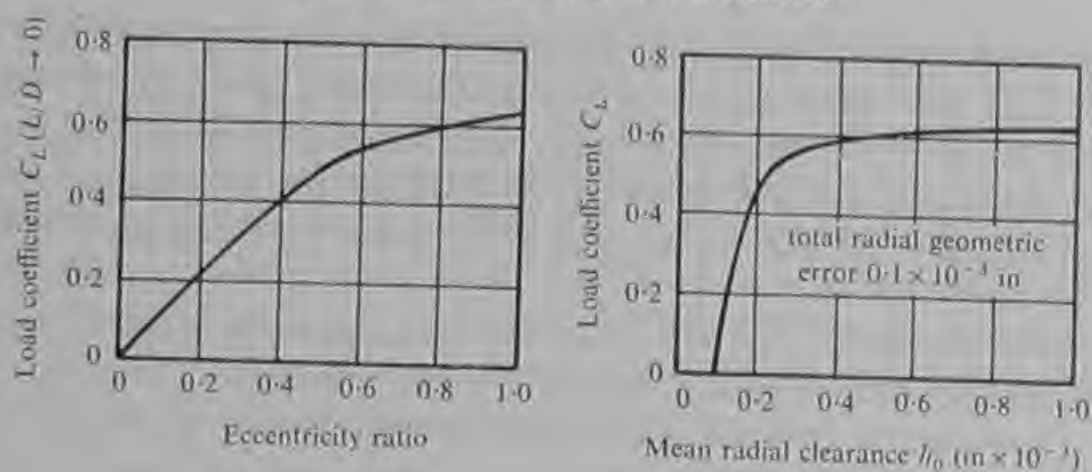
Fig. 3.3 Influence of manufacturing error on selection of journal bearing clearance

Length L (in)
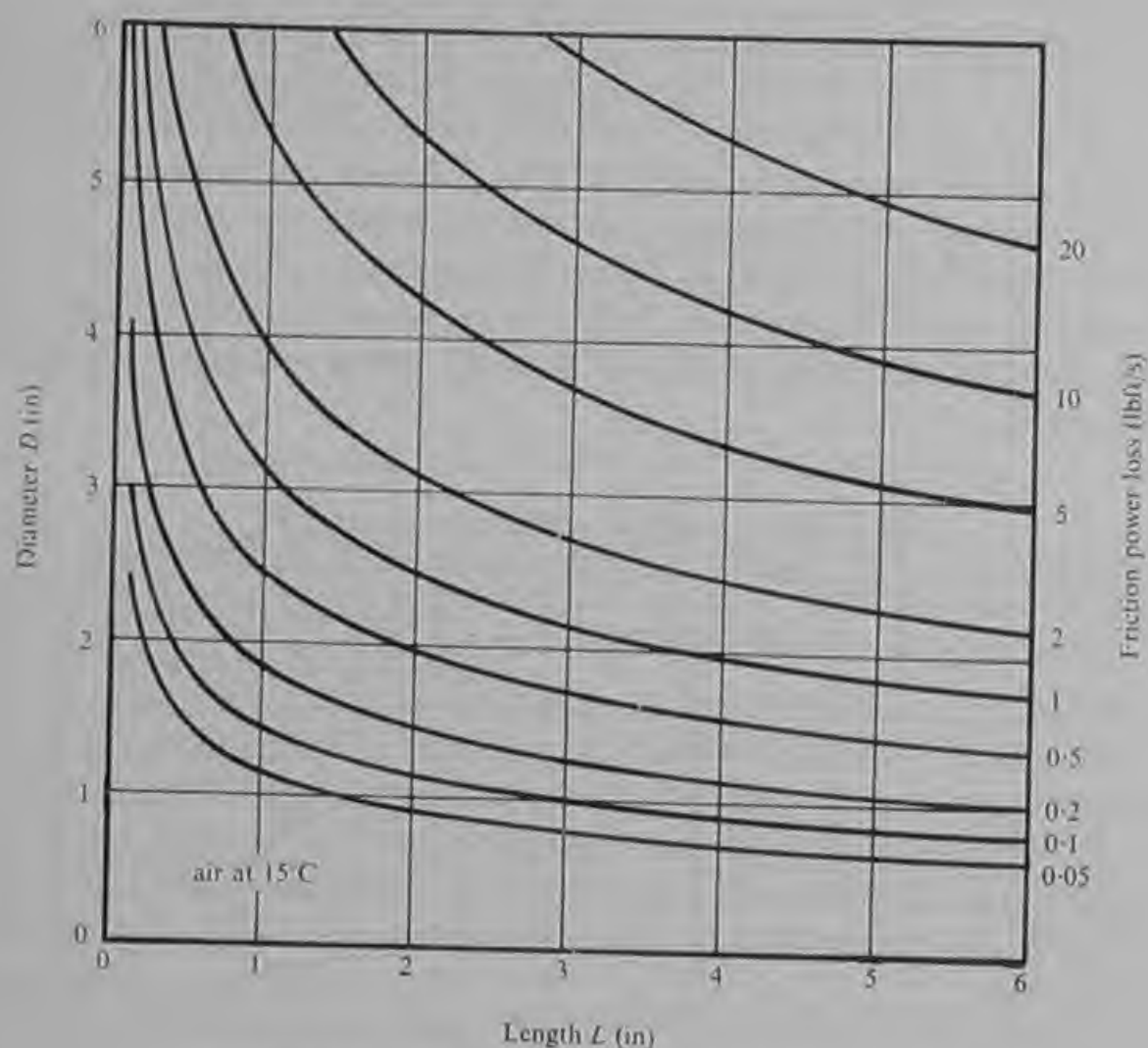
Curves plotted for 3 000 rev/min, 0·001 in diametrical clearance ($2h_0$).

For other speeds multiply by $\left(\dfrac{N}{3\,000}\right)^2$ (where N is speed in rev/min).

For other clearances multiply by $\left(\dfrac{0\cdot001}{2h_0}\right)$.

For other gases and temperatures multiply by the gas viscosity relative to air at 15°C.

(Viscosity data for some gases are given in Appendix 1.)

Fig. 3.4 Friction power loss in air journal bearings

can be achieved at a mean radial clearance only three or four times greater than the total radial error in the bearing surfaces. Thus if the total radial error resulting from misalignment, taper, ovality and so on is estimated to be 0·000 1 in (0·000 25 cm), an efficient bearing could be designed at any mean radial clearance greater than 0·000 3 in (0·000 75 cm).

Gas bearings offer such low friction in comparison with other types of bearings that the friction power loss is often ignored in the feasibility study. However, it may be important in applications demanding very low friction such as in dynamometers, gyroscopes, turbine flowmeters, balances and other instruments, or in high speed machines where the friction power loss can become a significant part of the power input to the machine. The friction power loss can be quickly estimated by reference to Fig. 3.4.

The final step in the feasibility study involves consideration of the supply pressure and the chosen clearance in an estimation of the gas flow required by the bearing. This flow value can then be compared with that available in the supply. Fig. 3.2 can be used to estimate the flow through air bearings. However, while the load capacities obtained from Fig. 3.2 can be taken to apply for any gas and at any temperature the airflow values relate only to air at 15°C. The table below gives multiplication factors for some common gases at various temperatures.

Mass flow of gases relative to air at 15°C

Gas	Temperature °C	$\dfrac{Mass\ flow\ of\ gas}{Mass\ flow\ of\ air\ at\ 15°C}$
Air	300	0·31
CO_2	15	1·88
H_2	15	0·14
He	15	0·13
H_2O	100	0·87
A	15	1·13
CO	15	0·95
C_3H_8	15	3·5
O_2 and N_2	15	1·0

In practice it will usually be necessary to repeat each of the stages of the feasibility study several times before the feasibility is established and an outline design is evolved. However, the designer should arrive at this stage with an approximate but useful knowledge of the size and shape of the bearing, its clearance, load capacity, stiffness, friction and gas consumption. It is now possible to proceed to study alternative designs in some detail; to select a jet-fed or slot-fed bearing and to investigate the effect of variations in the jet or slot dimensions and arrangement on the performance of the bearing.

3.2 Jet-fed bearings

The load capacity and stiffness of an aerostatic journal bearing depend primarily upon the design value of the gauge pressure ratio K_{go}. Fig. 1.5 shows a typical variation of load coefficient with K_{go} and it can be seen that the optimum value of K_{go} varies with eccentricity ratio as shown in the following table.

ε	Optimum value of K_{go}
0·1	0·6
0·5	0·4
0·9	0·35

From these data Shires recommended designing at a gauge pressure ratio of 0·4. However, there are advantages in using somewhat higher values of K_{go} and in fact the designer has a fairly wide choice.

One factor which often establishes a lower limit to the choice of K_{go} is the consideration of choking of the feed holes. This occurs at a condition defined by equation (19). Bearings operating with choked feed holes have often been observed to exhibit an aerostatic instability, which has been called air hammer, and the condition is avoided for this reason. For air the critical pressure ratio across the feed hole is given by:

$$\frac{P_{do}}{P_o} = 0.528.$$

This value applies to all diatomic gases such as oxygen, nitrogen, hydrogen, etc., which have a ratio of specific heats of 1·4. Monatomic gases such as argon and helium with a ratio of specific heats above 1·6 have a critical pressure ratio of 0·486. Triatomic gases such as carbon dioxide and dry superheated steam have a ratio of specific heats of around 1·3 and a critical pressure ratio of 0·546. Polyatomic gases

such as propane which have a ratio of specific heats of 1·13 have critical pressure ratios around 0·59.

The gauge pressure ratio at which the feed holes become choked can be obtained for air from the equation:

$$K_{go} = \frac{0 \cdot 528 - P_a/P_o}{1 - P_a/P_o}. \tag{55}$$

This limitation is shown in Fig. 3.5 for bearings exhausting to atmosphere ($P_a = 14 \cdot 7$ lbf/in²). It can be seen that air bearings will have choked feed holes at $K_{go} = 0 \cdot 4$ at supply pressures in excess of 55 lbf/in² gauge, and therefore at higher supply pressures a higher value of K_{go} is recommended.
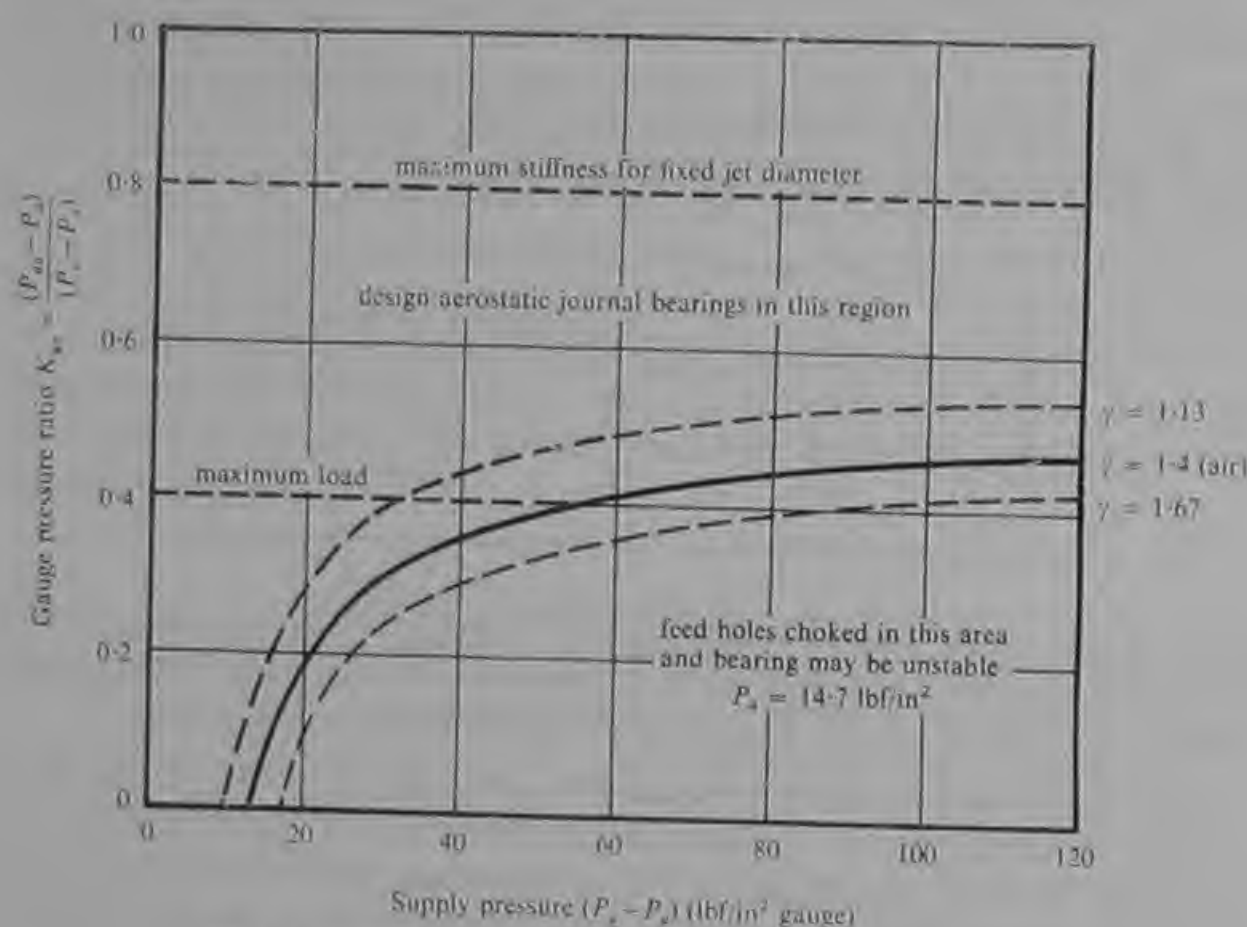
Fig. 3.5 Journal bearing design—choice of gauge pressure ratio

If no other considerations affect the choice, the designer wishing for optimum radial load capacity will design at a gauge pressure ratio of 0·4 or as near this condition as a consideration of choked feed holes will permit. This will almost certainly be the case with large clearance bearings, say $2h_o > 0 \cdot 002$ in (0·005 cm). However, in bearings designed at smaller clearances, with the aim of limiting gas consumption or achieving high stiffness, the difficulty of producing small feed holes or of avoiding feed hole blockage may become the limiting factor. It is worth while therefore to consider a bearing in

which the smallest practical feed hole size is employed and to investigate the variation of radial stiffness with gauge pressure ratio as the clearance is varied. The results of this exercise are shown in Fig. 3.6. It can be seen that the maximum stiffness occurs at $K_{go} = 0.8$. No advantage is gained at higher gauge pressure ratios, i.e. at smaller clearances, and manufacturing difficulties increase. The value $K_{go} = 0.8$ can therefore be taken as an upper limit for practical design purposes.

Gauge pressure ratio $K_{go} = \dfrac{P_{do} - P_a}{P_s - P_a}$.
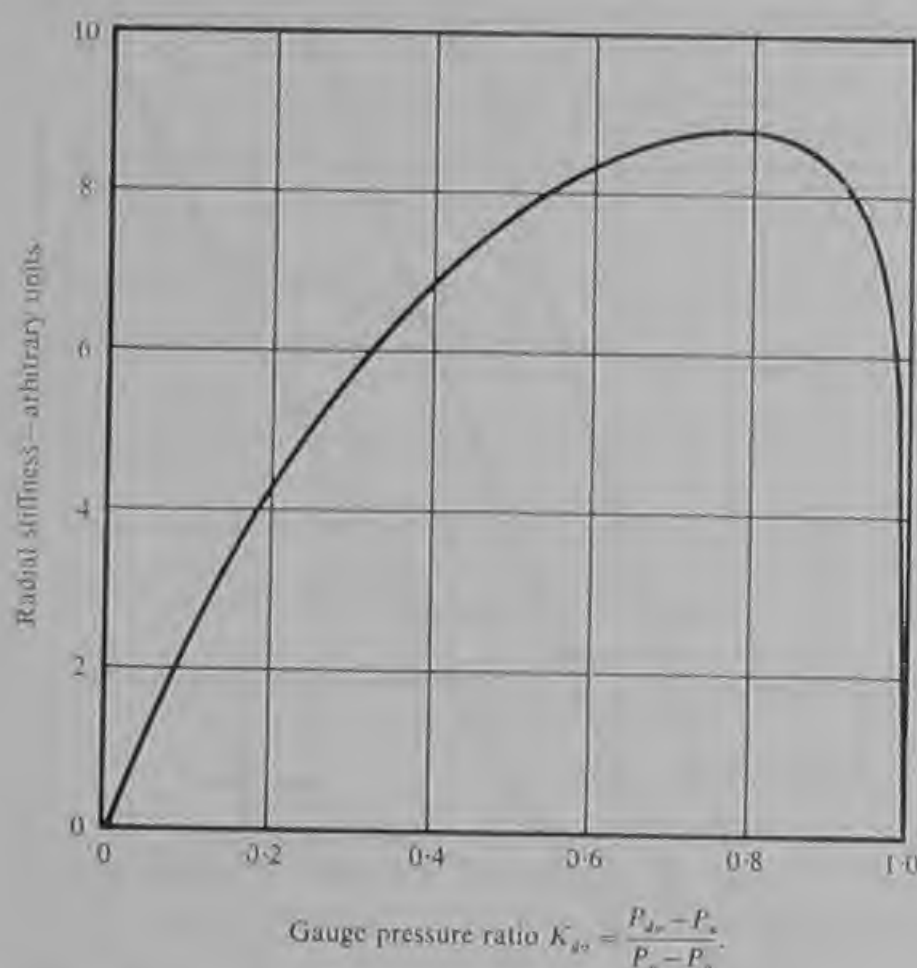
Fig. 3.6 Variation of radial stiffness with gauge pressure
ratio by variation of clearance only

The designer is interested in the range of gauge pressure ratios between 0·4, or the critical value for choking in the lower limit, and 0·8 in the upper limit. This region is shown for bearings exhausting to atmosphere in Fig. 3.5. The problem is correctly to match the feed hole size and arrangement to the bearing clearance in order to achieve a suitable value of gauge pressure ratio.

Matching jet size to clearance Fig. 3.7 shows the corresponding values of jet diameter and diametrical clearance for an air bearing with simple orifice feeding operating at gauge pressure ratios of 0·4, 0·6 and 0·8. The bearing chosen is of typical design and will be used as a standard of reference. It has a length-to-diameter ratio of unity and is supplied
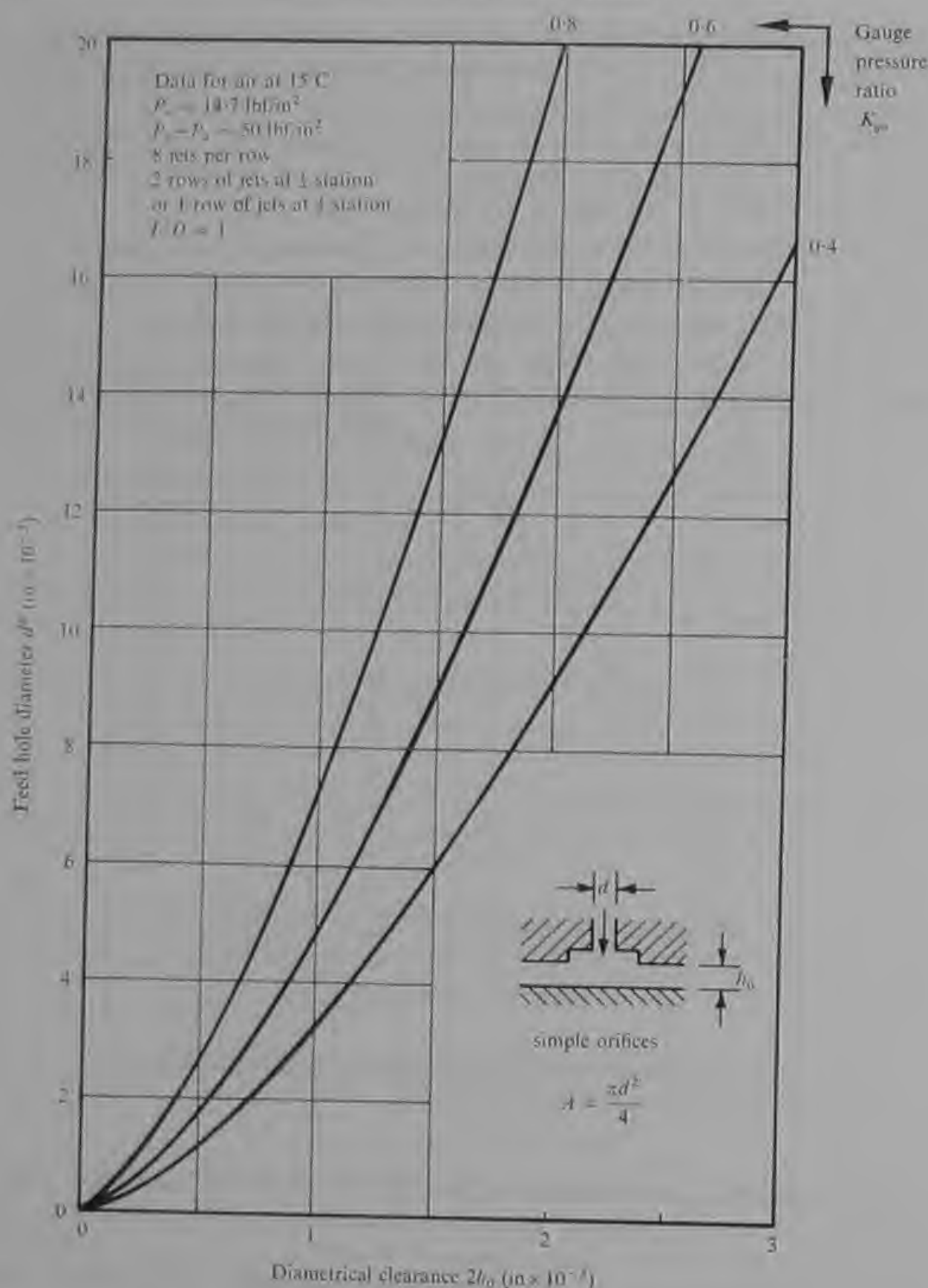
Fig. 3.7 Jet diameter versus clearance for simple orifices

at 50 lbf/in^2 gauge through two rows of eight feed holes at quarter stations or one row of eight feed holes at half station. The exhaust pressure is taken as 14·7 lbf/in^2 and a uniform temperature of 15°C is assumed.

(a) Supply pressure $(P_o - P_a)$ lbf/in^2

$$d = d^* \sqrt{\frac{8}{n}}$$

(b) Number of jets per row n

$$d = d^* \sqrt{\frac{1}{L/D}}$$

(c) Length-to-diameter ratio L/D

$$d = d^* \sqrt{\frac{1}{4(l/L)}}$$

(d) Jet station for two row bearings l/L
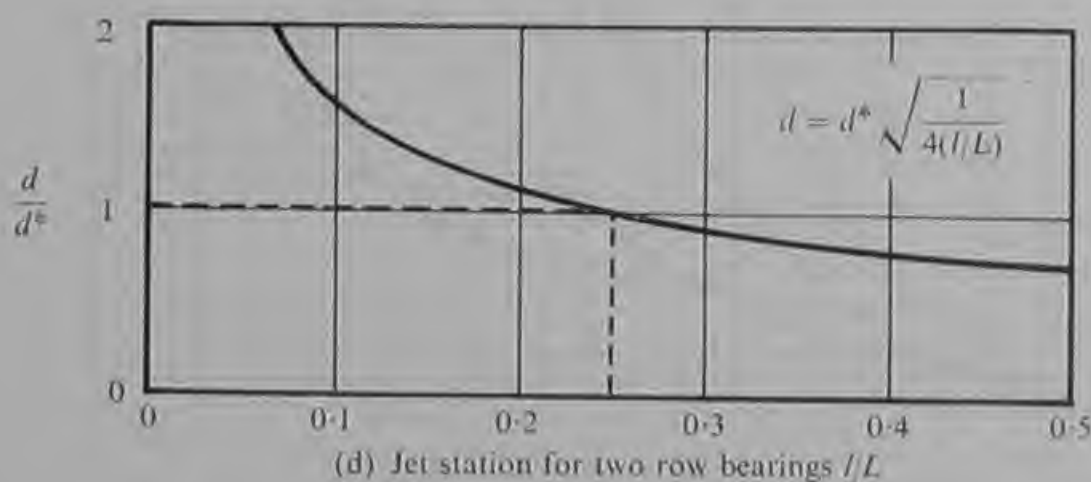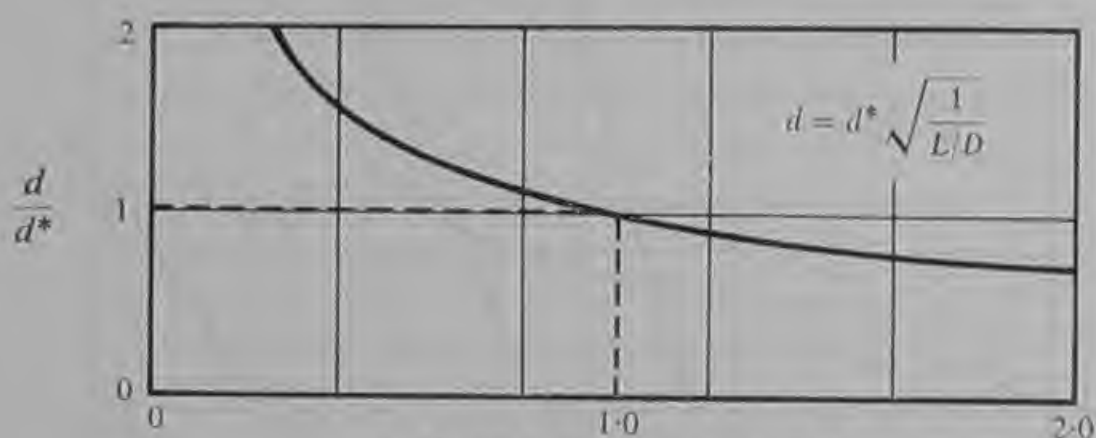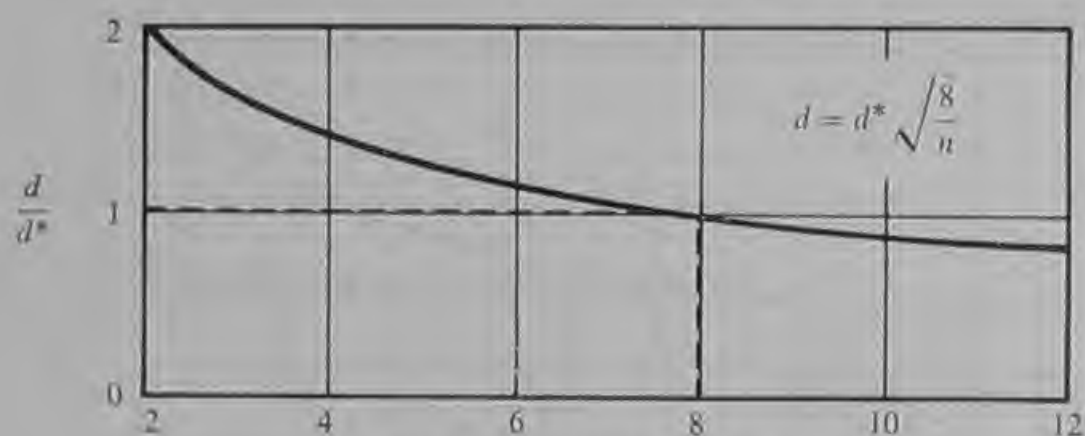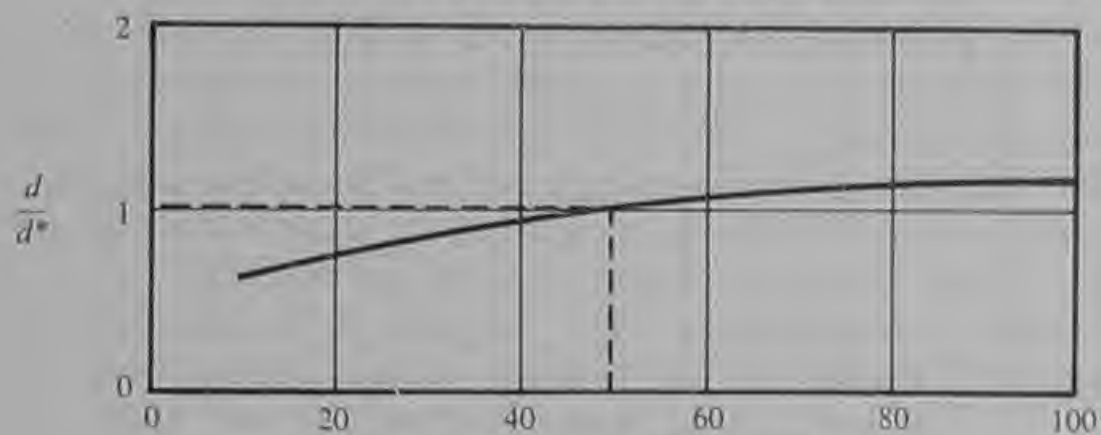
Fig. 3.8 Variation of jet diameter with various parameters
—simple orifices

The various correction factors given in Fig. 3.8 can be used to allow for variation in supply pressure, number of feed holes per row, length-to-diameter ratio and the distance of the rows of feed holes from the ends of the bearing. Figs. 3.7 and 3.8 taken together permit the correct choice of bearing parameters to achieve the desired gauge pressure ratio in most simple orifice compensated air bearings exhausting to atmosphere. Figs. 3.9 and 3.10 provide the corresponding information for air bearings with annular orifice compensation. Within their scope these four figures will assist with the design of almost all jet-fed air bearings for industrial and commercial applications.

Fig. 3.9 Jet diameter versus clearance for annular orifices

(a) Supply pressure $(P_o - P_a)$ (lbf/in²)

$$d = d^* \frac{8}{n}$$

(b) Number of jets per row n

$$d = d^* \frac{1}{L/D}$$

(c) Length-to-diameter ratio L/D

$$d = d^* \frac{1}{4(l/L)}$$

(d) Jet station for two row bearings l/L

Fig. 3.10 Variation of jet diameter with various parameters—annular orifices

At this stage it is worth noting a few basic differences between simple orifices and annular orifices. For a given clearance and gauge pressure ratio the annular orifice is invariably larger in diameter and therefore easier to produce. However, it has already been remarked that since the orifice area is dependent on the local bearing clearance the annular orifice produces a bearing of lower stiffness. Annular orifices are also liable to become smeared over in bearings in which rubbing takes place due to overloading. For these reasons simple orifices are to be preferred and should be used in preference to annular orifices whenever possible. However, simple orifices require pockets to be formed in the bearing surface around t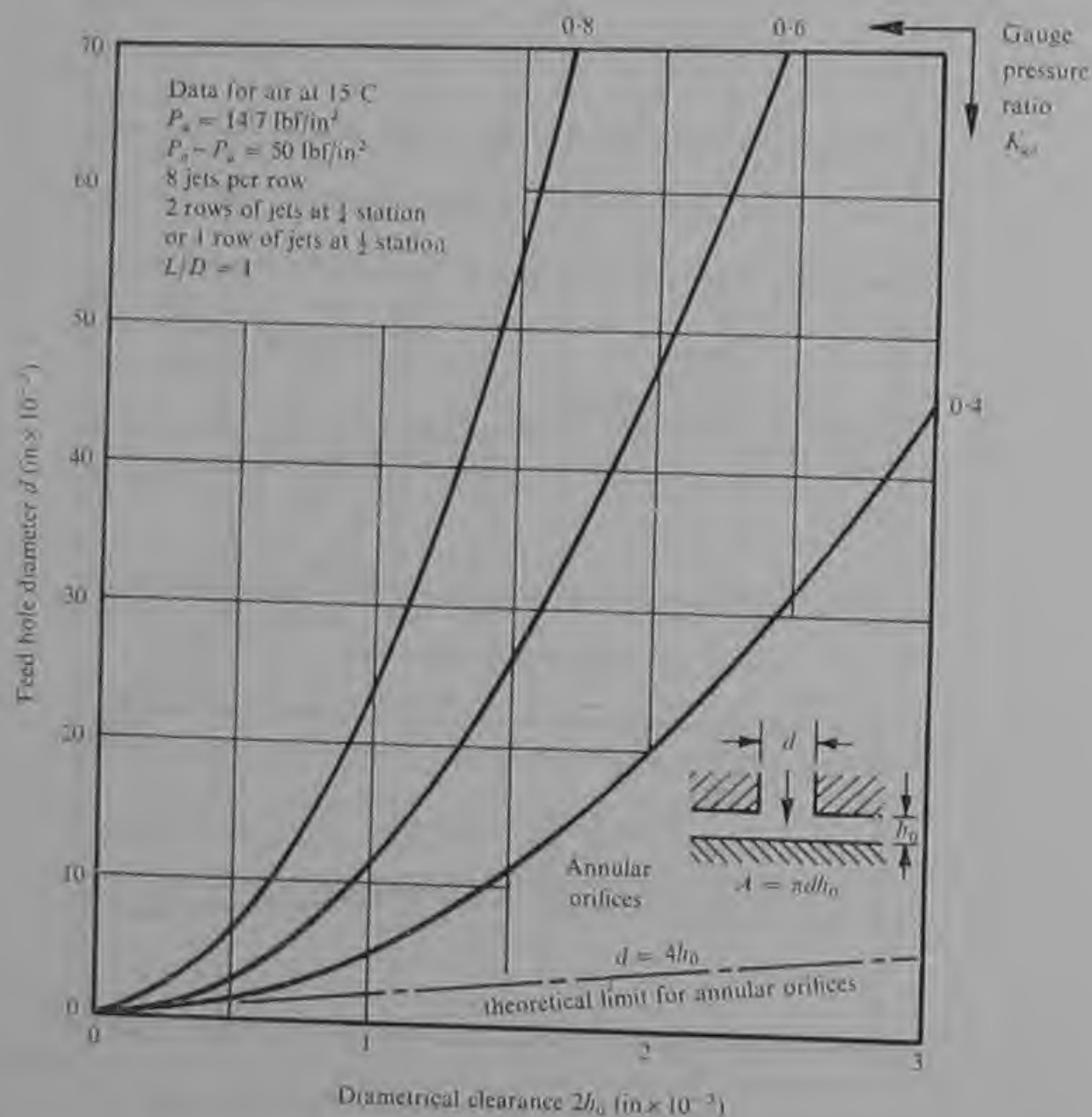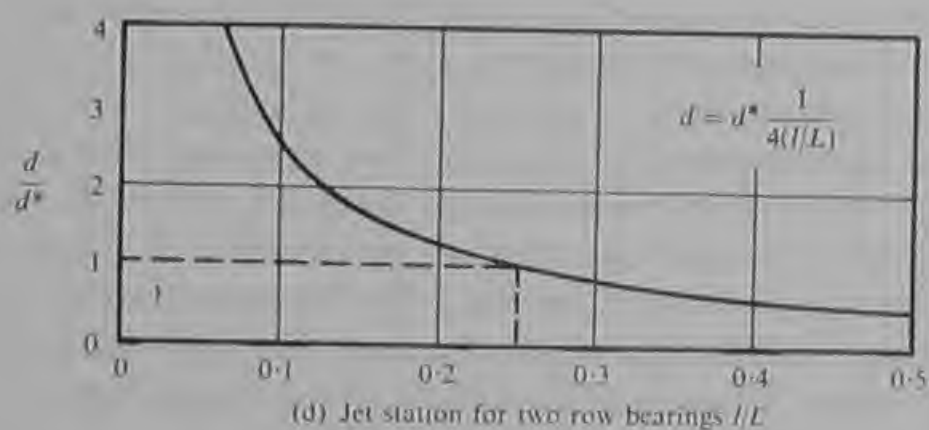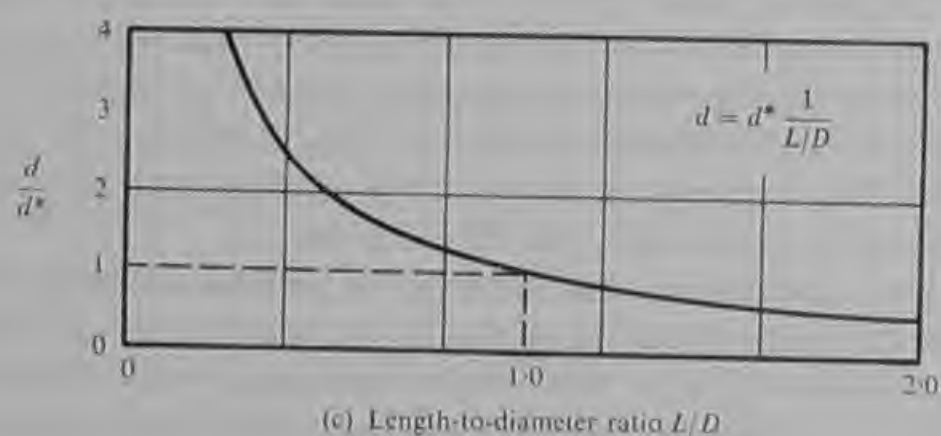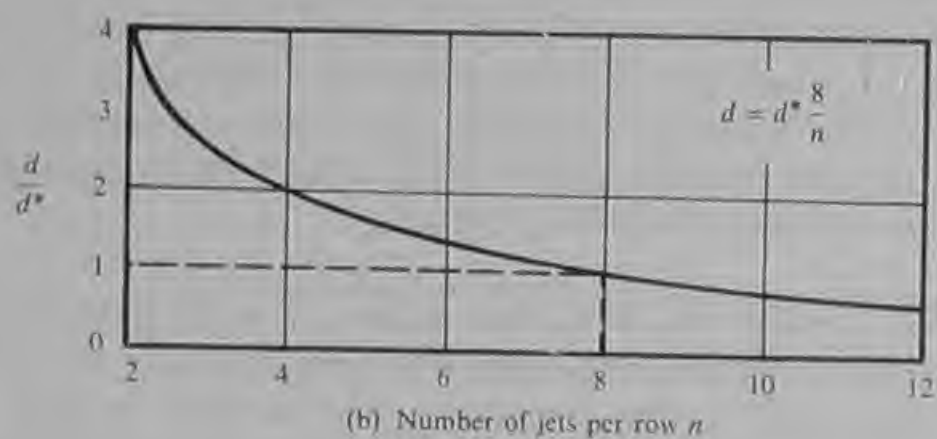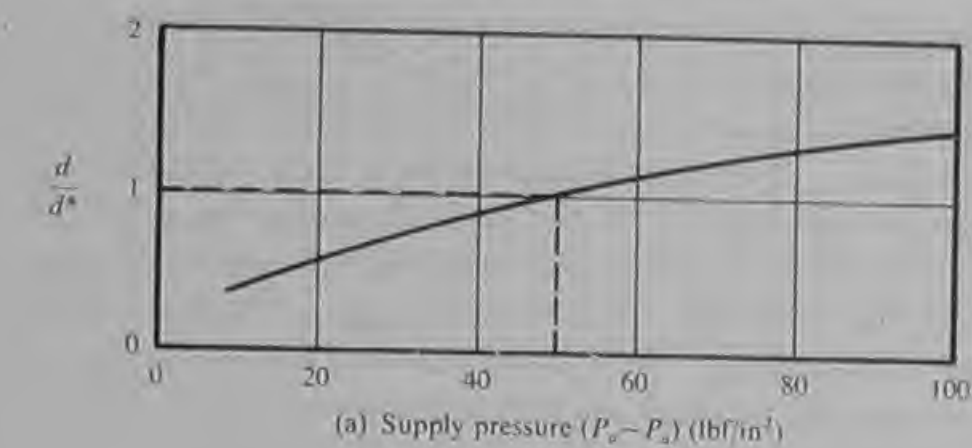he feed holes and this sometimes presents difficulties particularly in small bearings and in very hard materials. It is interesting to note that in one of the most successful commercial applications of air bearings, the high speed air turbine dental drill, the 0·186 in diameter bearing bushes made of sintered tungsten carbide employ annular orifices of 0·006 in diameter.

Types of simple orifice With simple orifices the pockets can take a variety of forms. Probably the easiest to manufacture, and therefore the most widely used, is the circular pocket shown in Figs. 3.11(a) and 3.11(b). The pocket is formed by fixing a round plug in which the jet is already drilled into a hole drilled radially through the bearing bush. The jet plug must be sealed to prevent leakage, and this can be accomplished by screwing in the plug against a ring seal or gasket (Fig. 3.11(a)) or by soldering or brazing (Fig. 3.11(b)). Robinson and Sterry in their early work on aerostatic bearings used circumferential pockets similar to those shown in Fig. 3.11(c).

According to the theoretical analysis of journal bearings assuming purely axial flow, the load capacity of a bearing should be almost independent of the type of feed hole. Bearings with simple orifices are estimated to provide maximum load coefficients approximately ten percent higher than bearings with annular orifices, but the theory makes no distinction between the performance of simple orifice compensated bearings with different types of pocket. In practice the choice of feed hole type is somewhat more critical. Annular orifice compensated bearings are found to be some thirty percent weaker than bearings with feed holes with circular pockets. This is due to two factors. Firstly, the pockets reduce the effects of dispersion and, though not fully effective in making the source diameter effectively equal to the pocket diameter, they do make a significant contribution. Secondly, in cases where inertia effects are of significance owing to high pressure ratios across the orifices forming shock waves around the feed holes the load capacity of annular orifice compensated bearings can be reduced. However, as the shock waves usually extend

(a) Screwed jet plug

(b) Soldered jet plug

(c) Jet with circumferential pocket (as used by Robinson and Sterry)
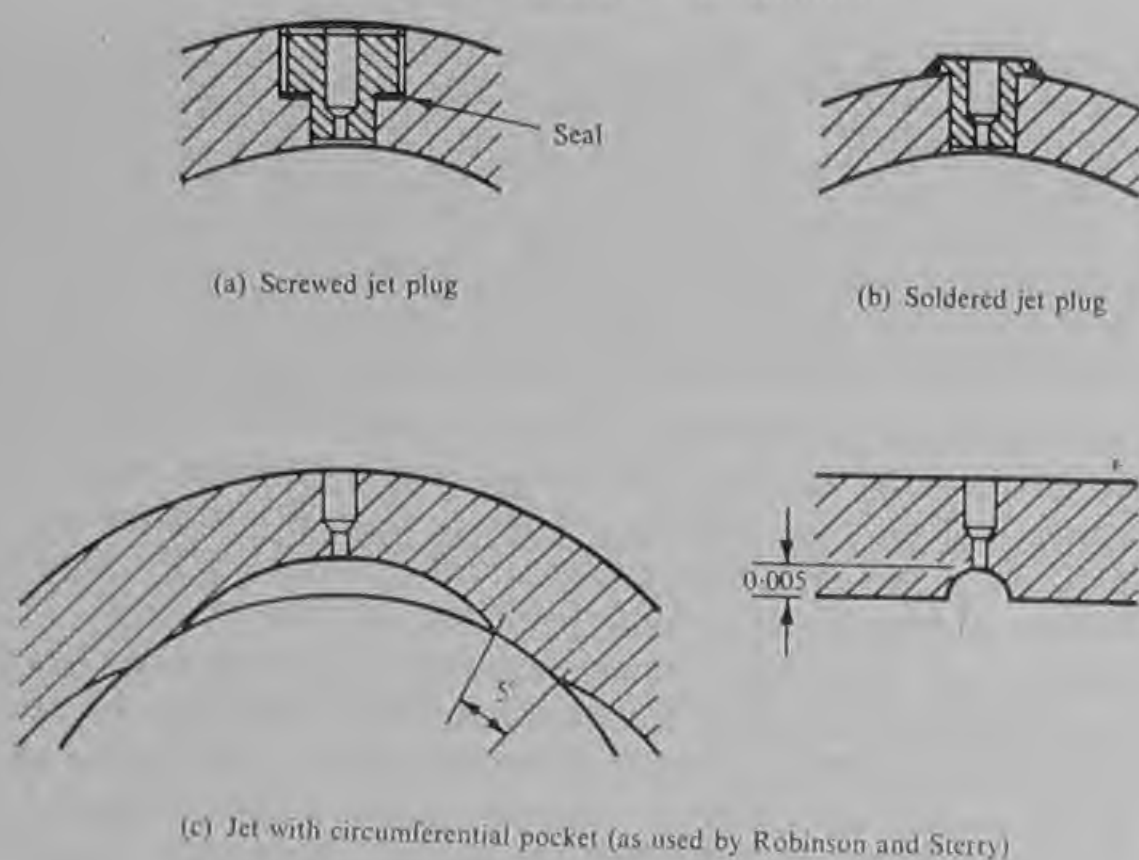
Fig. 3.11 Some practical forms of simple orifices

only a few orifice diameters, their effects are lost within the pockets of simple orifice compensated bearings. The effect of pocket type on the load capacity of simple orifice compensated bearings is less certain. Robinson and Sterry (Ref. 6) reported that circumferential pockets could provide up to twenty-five percent greater load capacity than circular pockets. However, Whitley (Ref. 8) reviewing work by Robinson and Sterry and Allen and Stokes concludes that, within the experimental error, the bearings with circumferential pockets were no better than those with circular pockets. It is probable that in most applications the additional manufacturing complexity involved in producing circumferential pockets would be difficult to justify in terms of increased load capacity or stiffness.

Circumferential pockets and other more complex forms of pockets should always be applied with caution. If incorrectly designed they can lead to a weakening rather than a strengthening of the bearing. They can also constitute a large storage volume for gas within the bearing which is a condition which can lead to instability. A good general rule for all aerostatic bearings is to keep all pocket volumes to a minimum and this consideration often helps to determine the type of pocket finally chosen. Whatever type of pocket is used, provided that they do not extend axially towards the bearing ends much beyond the plane of the feed holes, the jet diameters can be determined from Figs. 3.7 and 3.8.

Designing at high gauge pressure ratios From Fig. 3.7 the advantage in terms of jet diameter of designing at high gauge pressure ratios is immediately apparent. In practice the use of higher gauge pressure ratios does not incur such a large proportional loss of load capacity as the axial flow theory shown in Fig. 1.5 implies. This is possibly due to the higher axial pressure gradients reducing the circumferential flow of the gas and hence reducing the weakening effect of non-axial flow. The penalty incurred from the use of high gauge pressure ratios is the increased gas consumption shown in Fig. 3.12. If the smallest possible jet diameter is used and a high gauge pressure ratio chosen to optimize stiffness, the gas flow is lower than if the same size jets were used at a lower gauge pressure ratio achieved by increasing clearance or moving the jets closer to the ends of the bearing.

The theory of aerostatic journal bearings assuming axial gas flow enables a useful relationship to be established between the various design parameters for the purpose of designing at a given value of K_{go}. The various parameters can be adjusted using Figs. 3.7 and 3.8 or Figs. 3.9 and 3.10 to yield a practical design. However, in order to

$$K_{go} = \frac{P_d - P_a}{P_s - P_a}$$

$$M \propto (P_s - P_a)^2 \left[K_{go}^2 + \frac{2P_a}{P_s - P_a} K_{go} \right]$$
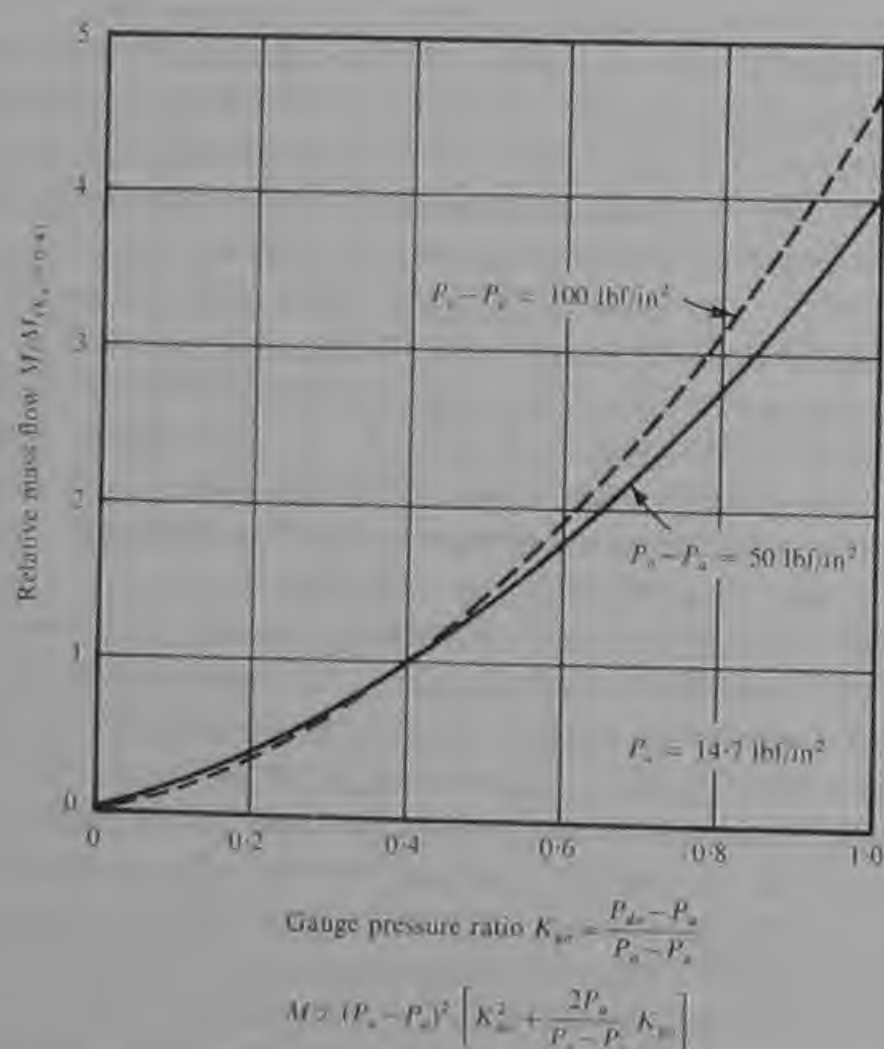
Fig. 3.12 Variation of mass flow with gauge pressure ratio

take some account of the effect of dispersion it is necessary to consider its influence upon the choice of the number of jets per row. It is also necessary to consider the influence of non-axial flow upon the choice for the length-to-diameter ratio and the distance of the jets from the ends of the bearing. Having weighed the influence of these two factors upon the various bearing parameters against manufacturing considerations, a design compromise can be evolved with the bearing dimensions finally decided.
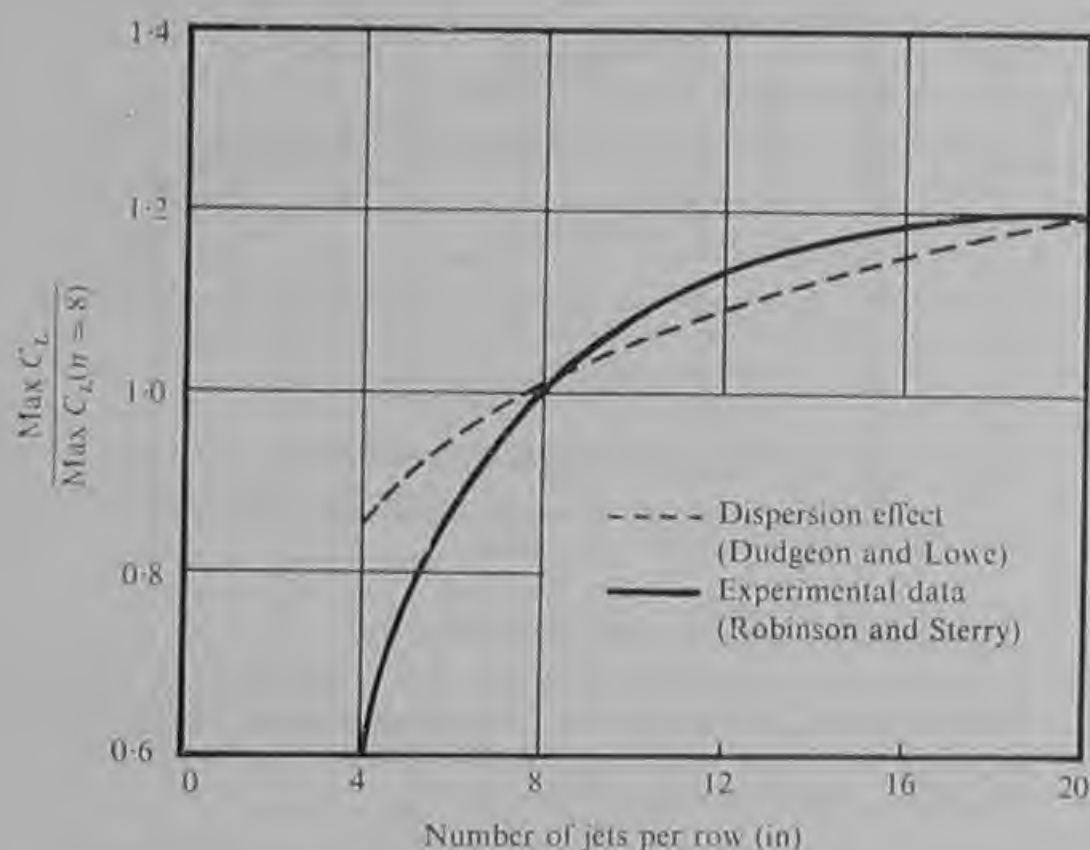
Fig. 3.13 Influence of number of jets on load coefficient

Influence of dispersion Fig. 3.13 illustrates the influence of the number of jets per row upon the bearing load capacity. One curve is derived from the theory of Dudgeon and Lowe which has been referred to in Chapter 2. The effect of dispersion in reducing the load capacity of the bearing decreases as the number of jets increases. Doubling the number of jets from eight to sixteen yields a sixteen percent increase in load capacity. This prediction is supported by experimental data obtained by Robinson and Sterry (Ref. 6). The agreement is fairly good for more than eight jets per row. The load capacity of the real bearing falls more rapidly at low numbers of jets and the correction based on dispersion can be seriously in error where less than six jets are used. Most practical aerostatic journal bearings employ between

six and twelve jets per row, the number of jets tending to increase at
low length-to-diameter ratios. Manufacturing considerations usually
determine that the larger the journal diameter the larger must be the
mean radial clearance although not necessarily in direct proportion.
The result is that with larger bearings the designer often chooses to
compensate for the increased clearance by increasing the number of
jets with or without increasing their diameter.
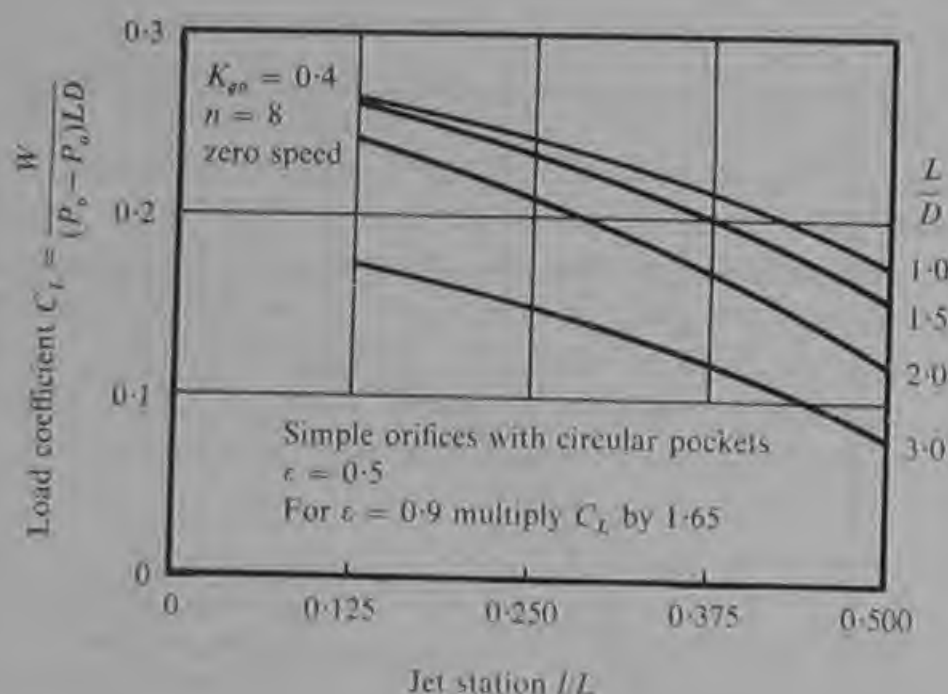
Based on theory of Dudgeon and Lowe and substantiated by several
experimenters for air with $P_a = 14.7$ lbf/in², $(P_o - P_a)$ in range 20 to
100 lbf/in², and $2h_0$ in range $0.6-3.0 \times 10^{-3}$ in.

Fig. 3.14 Influence of jet position on journal bearing load
coefficient

Influence of non-axial flow The influence of non-axial flow in deter-
mining the choice of length-to-diameter ratio and the position of the
rows of jets is shown in Figs. 3.14 and 3.15. Fig. 3.14 shows the
influence of the jet position on load coefficient. It can be seen that the
highest load coefficients are realized when the rows of jets are stationed
between a quarter and one eighth of the bearing length from the ends
of the bearings. Since for a given value of K_{go} the gas flow is greater the
nearer are the jets to the end of the bearing, there is much in favour
of standardizing on quarter station bearings. The temptation to move
the jets closer to the bearing ends in short bearings should be resisted
since this will often involve considerable dispersion losses. For bearings
of length-to-diameter ratio of 0.5 and less, jet-fed bearings are inferior
to slot-fed bearings and the latter should be employed wherever possible.
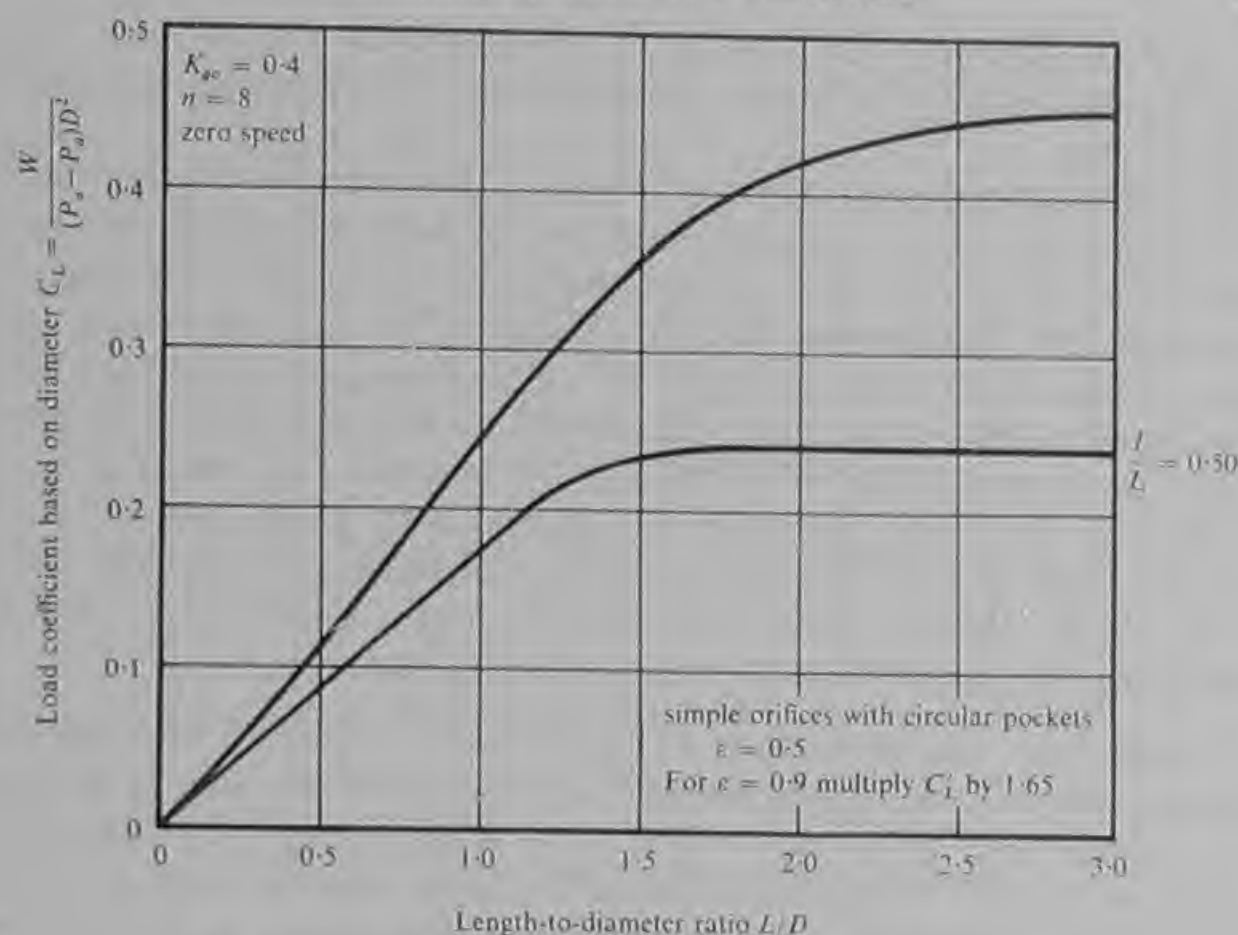
Fig. 3.15 Influence of length-to-diameter ratio on journal bearing load coefficient

Fig. 3.15 shows the influence of the length-to-diameter ratio on journal bearing load capacity. In this case the load coefficient based on diameter C_L' is used where

$$C_L' = \frac{W}{(P_o - P_a)D^2}.$$

The data presented enable the estimation of the optimum bearing length for a given diameter. It can be seen that there is little or nothing to be gained in terms of total load capacity in producing quarter station bearings at length-to-diameter ratios greater than 2·0 or half station bearings at length-to-diameter ratios greater than 1·5.

For the same clearance and gauge pressure ratio the half station bearing consumes only half the gas flow of the quarter station bearing. Therefore in cases where gas flow must be minimized and particularly where short bearings are employed (L/D between 0·5 and 1·0) the gas flow can be reduced by fifty percent for a twenty-five percent loss of load capacity by changing to a bearing with a single row of feed holes.

Where load capacity and stiffness are of primary importance two rows of jets at quarter station bearings are usually preferred. It is of value to note that due to the superiority of short bearings in terms

of load coefficient it is sometimes advantageous to use two short bearings separated by a narrow exhaust recess in preference to a single long bearing.

The data presented in Figs. 3.14 and 3.15 are based on the theory of Dudgeon and Lowe and take account of both dispersion and non-axial flow. They have been substantiated by the results of numerous experimenters including Allen and Stokes (Ref. 10), Robinson and Sterry (Ref. 6) and Powell (Ref. 9). The data can be applied with confidence to all air bearings exhausting to atmosphere and designed within the stated range of variables. In practice the measured load coefficients have been found to be insensitive to gauge pressure ratio over the range 0·4 to 0·8 and the majority of bearings tested have been found to be within −10% and +20% of the stated values of load coefficient for gauge pressure ratios in this range.

Air mass flow The mass flow of air through a bearing of length-to-diameter ratio of unity operating at a gauge pressure ratio of 0·4 and zero eccentricity is given in Fig. 3.16 plotted against diametrical clearance. The correction factors for other gauge pressure ratios were given in Fig. 3.12. The mass flow is independent of the number of jets and is inversely proportional to the length-to-diameter ratio and the feed hole station. These latter factors can be quickly accounted for by reference to Fig. 3.17. For gases other than air the multiplication factors given in the table on page 72 can be used.
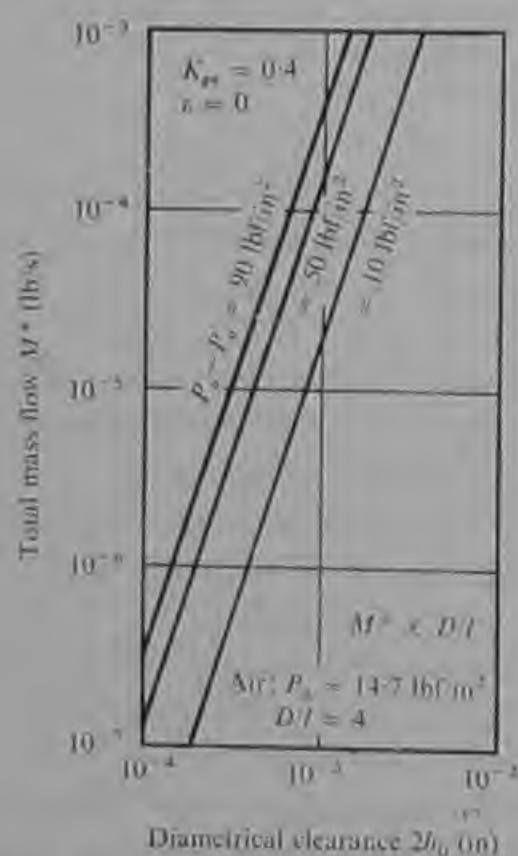
Fig. 3.16 Mass flow as a function of diametrical clearance

(a) Length-to-diameter ratio L/D

(b) Jet station for two row bearings l/L
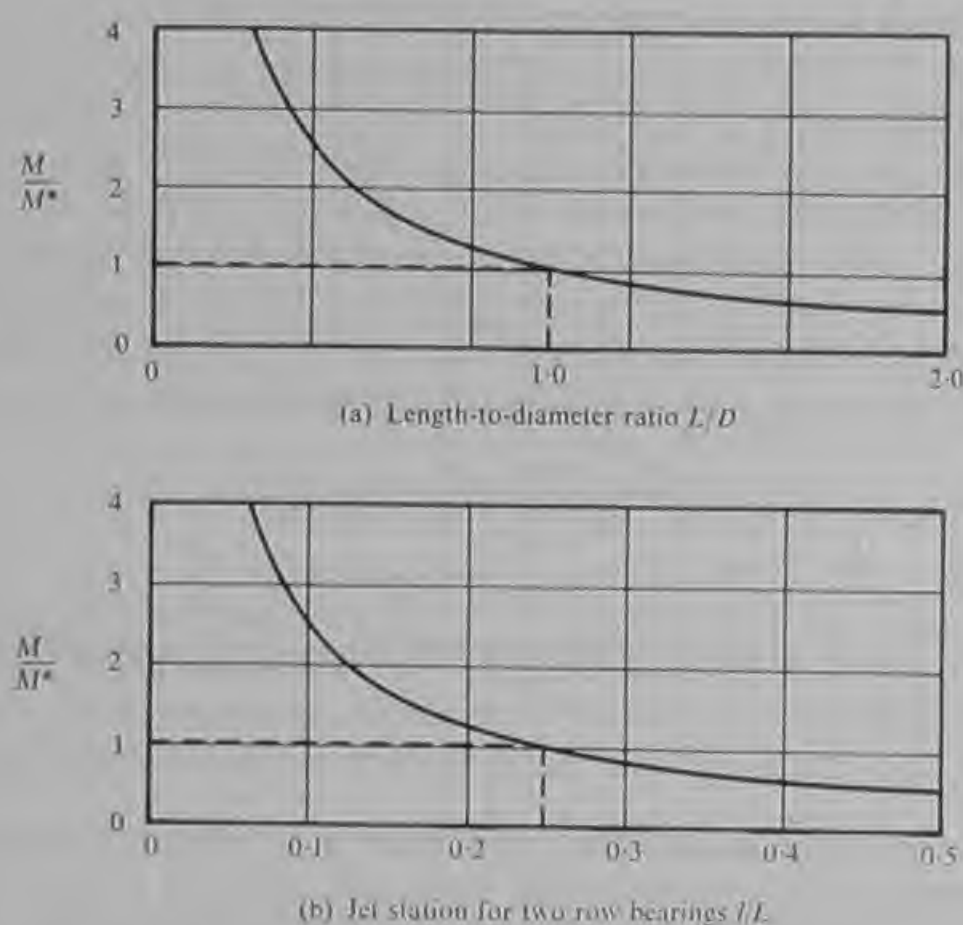
Fig. 3.17 Variation of mass flow with bearing geometry

Non-atmospheric conditions The information so far given will permit the design of most jet-fed air journal bearings operating at atmospheric temperature, supplied at normal workshop air pressures (up to 100 lbf/in^2 gauge), and exhausting to atmosphere. Probably upwards of ninety-five percent of future aerostatic gas bearings will operate under these conditions. However, there are applications of aerostatic bearings where both supply and exhaust pressures and temperature can be widely different from those so far considered. For example, air bearings in aircraft ancillary equipments must operate at altitudes where ambient pressures and temperatures are very low. There are also numerous applications for aerostatic bearings in flowmeters, compressors and circulators for use in chemical plants where both supply and exhaust pressures can be of the order of several hundreds of poundsforce per square inch and temperatures of several hundreds of degrees Celsius are common. Many of these potential applications will involve the use of gases other than air, and in particular an important group will consist of bearings operating on steam.

Fig. 3.18 is useful in assisting the optimization of the various bearing parameters for bearings operating at elevated or reduced pressures. It shows the variation of the bearing slot factor G_o with the ratio of exhaust to supply pressures for a gauge pressure ratio of 0·4. It also
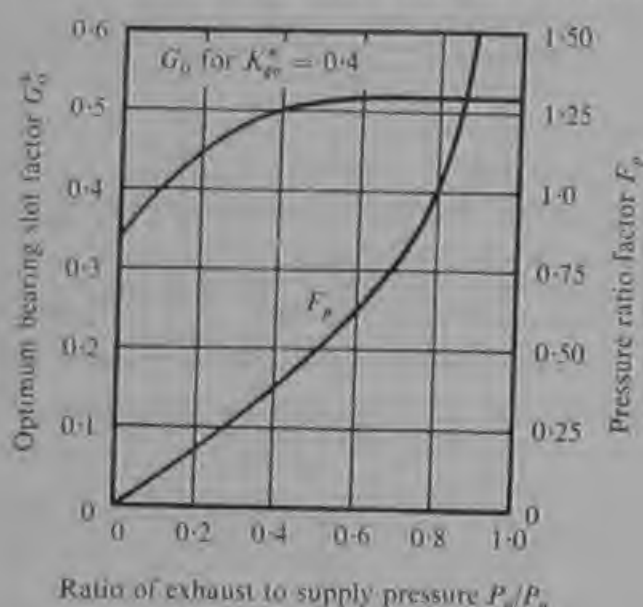
Fig. 3.18 Effect of pressure ratio on optimum bearing slot factor

shows the variation of the pressure factor F_p. Since F_p increases more rapidly than G_o, to maintain the required value of G_o for a constant gauge pressure ratio, it is necessary for the jet area to be reduced as the pressure ratio rises. The basic design charts shown in Figs. 3.7 and 3.9 are calculated for $P_a = 14.7$ and $P_o = 64.7$ lbf/in². Therefore the ratio $\dfrac{P_a}{P_o} = 0.227$. Using this condition as the standard of reference,
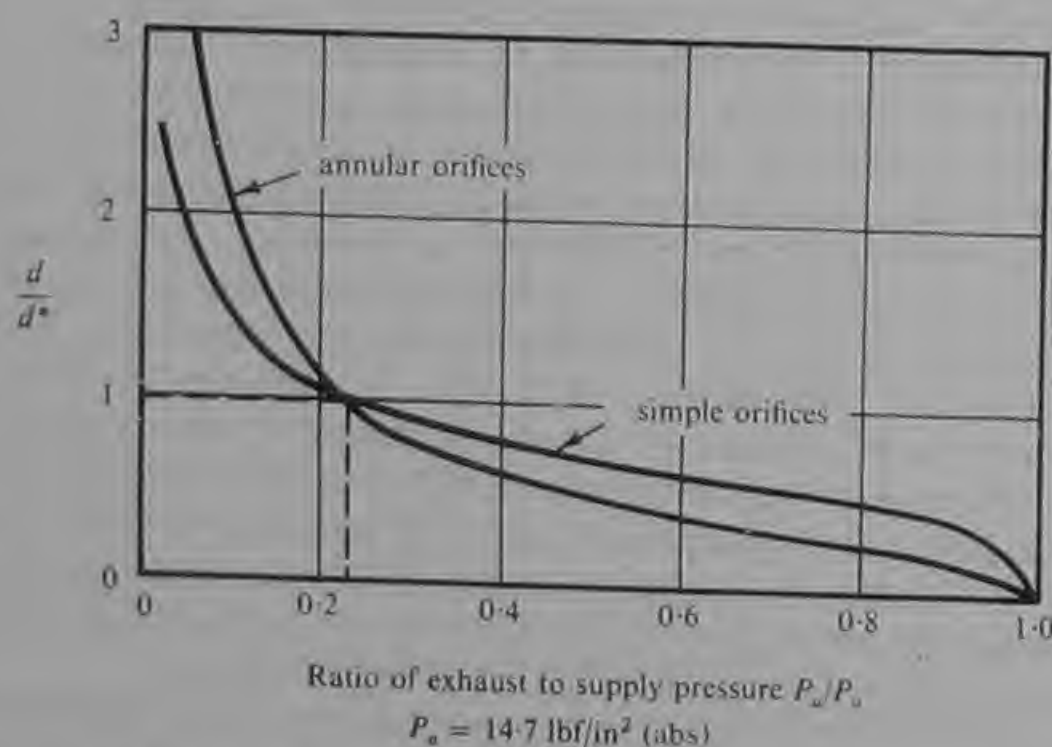
Fig. 3.19 Variation of optimum jet diameter with pressure ratio

at which the jet diameter $d = d^*$, the value obtained from Fig. 3.7 or Fig. 3.9, correction factors for other supply pressures can be calculated and these are plotted in Fig. 3.19. Fig. 3.19 can be used with Fig. 3.7 or Fig. 3.9 to obtain the desired relationship between jet diameter and clearance at any supply pressure. However, for other exhaust pressures the effect of P_a in the denominator of the gas properties factor F_g must also be taken into account.

The influence of temperature on the design of the bearing can be deduced from a study of the gas properties factor F_g which is given by

$$F_g = \frac{24\mu(2RT)^{\frac{1}{2}}}{P_a}.$$

In addition to occurring directly in the equation as absolute temperature it must be remembered that the gas viscosity is also temperature-dependent. It is preferable therefore to include temperature with the gas properties in assessing the influence on the bearing design. For constant slot factor G_o the product of F_g and F_d, i.e. $\frac{lC_D A}{ah_o}$, must remain constant. Thus varying the jet area alone and keeping all other factors in F_d constant gives

$$A \propto \frac{1}{\mu(RT)^{\frac{1}{2}}}.$$

Thus for annular orifices

$$\frac{d}{d^*} = \frac{[\mu(RT)^{\frac{1}{2}}]_{\text{air at } 15^\circ\text{C}}}{[\mu(RT)^{\frac{1}{2}}]},$$

and for simple orifices

$$\frac{d}{d^*} = \left\{ \frac{[\mu(RT)^{\frac{1}{2}}]_{\text{air at } 15^\circ\text{C}}}{[\mu(RT)^{\frac{1}{2}}]} \right\}^{\frac{1}{2}}.$$

From a knowledge of the gas properties and the operating temperature a correction factor for jet diameter can thus be obtained. Some correction factors which have been used in various aerostatic bearings are given in Fig. 3.20. More information on gas properties is given in Appendix 1.

The mass flow of gas through a bearing is also dependent upon the supply and exhaust pressures, temperature and gas properties. From equation (8) it can be deduced that for a concentric bearing of fixed dimensions:

$$M \propto \frac{P_d^2 - P_a^2}{\mu RT},$$

which can be rearranged to yield:

$$M \propto \frac{(P_o - P_a)^2}{\mu R T} \left[K_{go}^2 + \frac{2P_a}{(P_o - P_a)} K_{go} \right].$$

This proportionality can be used to take account of any variation in supply pressure, ambient pressure, gauge pressure ratio, gas properties and temperature.

Gas	Temperature T (°C)	Fg (ft $\times$ 10^6)	d/d^* air at 15°C	
			simple	annular
Air	15	5·66	1·00	1·00
Air	300	13·4	0·66	0·44
CO_2	15	3·44	1·28	1·64
H_2	15	10·3	0·74	0·55
He	15	16·9	0·59	0·35
He	−261	0·145	6·23	38·90
H_2O	100	5·85	0·98	0·97

Fig. 3.20 The influence on gas properties on optimum jet diameter

Friction The friction in gas bearings is independent of pressure and depends only on bearing dimensions and the gas viscosity which is in turn temperature dependent. Thus the friction power loss in most bearings can be estimated by reference to Fig. 3.3. For bearings beyond the size range covered a simple correction factor can be derived from equation (52) as follows:

$$\text{Friction power loss} \propto D^3 L.$$

The fact that friction power losses increase with the cube of diameter can introduce a practical limitation in high speed applications. In some cases friction power can become significant and an appreciable temperature rise can result. When this happens, an increase in journal diameter to increase bearing load capacity or shaft stiffness may often be difficult to achieve unless some thought is given to cooling the bearings. In air-turbine driven machines this has often been achieved by effective utilization of the cold turbine exhaust (Chapter 6).

Angular stiffness In addition to the radial stiffness of a journal bearing it is sometimes important to know the angular or tilt stiffness. This is particularly so with bearings which are flexibly mounted and which must therefore possess a degree of self-aligning ability. Bearings with two rows of feed holes or slots possess greater angular stiffness than those with a single central row. The optimum feed station lies between one-quarter and one-eighth of the bearing length from the ends of the bearing. For quarter station bearings the angular stiffness K_a is related to the linear radial stiffness by equation (56):

$$K_a = \frac{KL^2}{16}. \tag{56}$$

Equation (56) is easily derived by assuming that the forces in the bearing act in the feeding planes. This method gives accurate predictions of angular stiffness only with quarter station bearings. One-eighth station bearings exhibit approximately five percent higher angular stiffness which is seldom justified on account of the doubling of gas flow.

The practical effect of equation (56) is frequently to ensure that a flexibly mounted bearing is designed at a higher length-to-diameter ratio than if it were rigidly mounted.

3.3 Slot-fed bearings

Designing journal bearings with slot feeding permits some degree of control over the two factors tending to reduce the load capacity and stiffness of jet-fed bearings. Circumferential feed slots can eliminate the effects of dispersion but are still affected by non-axial flow. Axial inlet slots can reduce the effects of non-axial flow but still suffer from dispersion. Thus circumferential feed slots can be applied to advantage in short journal bearings where the effect of non-axial flow is least. Axial slots can be applied to advantage where a long bearing must be used and some control of non-axial flow is essential in maintaining load capacity and stiffness.

It might seem from the above that slot-fed bearings are always to be preferred to jet-fed bearings. However, this is not the case since jet-fed bearings, of the simple orifice type at least, possess a higher theoretical load capacity and stiffness based on the axial-flow model. Thus although the effects of dispersion and non-axial flow are greater in jet-fed bearings they subtract from a greater initial strength and consequently jet-fed bearings can be superior in some cases.

Journal bearings with circumferential slots are compared to bearings with simple orifice feeding jets in Fig. 3.21. In each case the feeding is in the quarter station planes. It can be seen that for length-to-
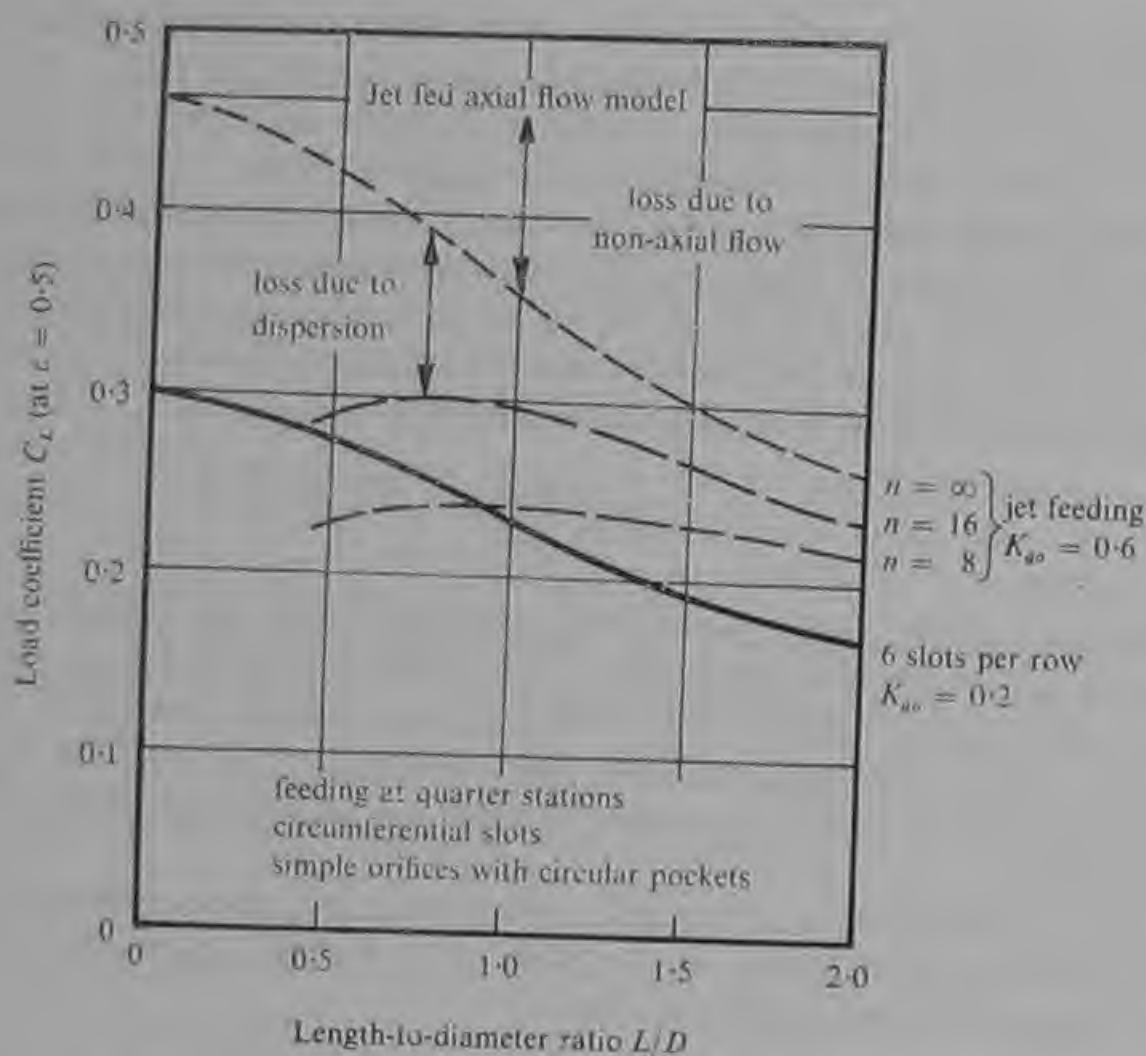
Fig. 3.21 Comparison of jet fed and slot fed journal bearings

diameter ratios of less than 0·5 the bearing with circumferential slots is superior. However, at length-to-diameter ratios in excess of 1·0 the jet-fed bearings are superior when eight or more jets per row are employed. The higher load capacity of bearings with more jets is due to the reduced effect of dispersion. The rise in the load coefficient with length-to-diameter ratios of less than 1·0 is due to the effect of dispersion reducing more rapidly than the effect of non-axial flow is increasing.

It is more difficult to compare jet-fed bearings with bearings with axial slots since the only published data on load coefficients (shown in Fig. 2.18) takes no account of dispersion of full-length slots or of dispersion and non-axial flow of half-length slots. At present no reliable experimental data on bearings with axial slots are available. However, from their low 'axial flow model' load coefficient it appears that bearings with half-length axial slots are unlikely to offer any load capacity advantage when compared to bearings with jets or circumferential slots at practical length-to-diameter ratios (say up

to 3·0). Full-length axial slots undoubtedly offer higher load coefficients in bearings of high length-to-diameter ratios. This advantage is offered at the expense of higher gas flow (Fig. 2.19) and considerably greater difficulty of manufacture when compared to bearings with jets or circumferential slots.

It is the author's opinion that journal bearings of low length-to-diameter ratios with circumferential slot feeding will be used widely. They can be produced in a range of materials, including refractories for high temperature applications, and when produced in metal are unlikely to be much more expensive to produce than jet-fed bearings. However, bearings with axial slots are seldom likely to offer sufficient advantage to justify their high cost of manufacture and will find only limited application. Some researchers claim an advantage for axial slot bearings in terms of stability at high rotational speeds. (This aspect is discussed more fully in Chapter 8.) This advantage, however, is at best only marginal and is unlikely to promote the widescale use of this type of bearing.

The advantages of bearings with circumferential inlet slots may be summarized as follows.

(a) The aerostatic performance is independent of fluid temperature and properties even to the extent that they can be operated with liquids as well as gases. The optimum choice of bearing dimensions is independent of temperature and fluid properties, and is insensitive to pressure level.

(b) The manufacture of the bearings involves no drilling, permitting the easier use of refractory materials as alternatives to metals. Bearings made from tungsten carbide or silicon nitride will withstand surface contact at high speed without damage. Silicon nitride remains chemically inert and dimensionally stable at temperatures up to 1 200°C.

(c) Circumferential inlet slots approach the ideal conditions of a line source and eliminate the loss of load capacity and stiffness associated with flow dispersion. The gain is greatest at low length-to-diameter ratios and offers the possibility of bearings having an aspect ratio similar to that of ball races.

Design of bearings with circumferential slots It has been shown in Chapter 2 that the design of journal bearings with circumferential feeding slots depends only on the correct matching of the slot dimensions and the bearing clearance dimensions. The important factor, α, is given by

$$\alpha = \left(\frac{h_o}{z}\right)^3 \left(\frac{y}{l}\right) \quad \text{for two rings of slots, and}$$

$$\alpha = \left(\frac{h_o}{z}\right)^3 \left(\frac{2y}{l}\right) \quad \text{for one ring of slots;}$$

where h_a = radial clearance at zero eccentricity,

z = width of inlet slot,

y = radial length of inlet slot,

l = distance of slot from end of bearing.

The optimum value of α for stiffness and load capacity is eight. However, such a high value may often be difficult to attain. For bearings with two rings of slots it is unlikely that $\dfrac{y}{l}$ will often exceed unity. This requires that $\dfrac{h_o}{z} = 2$ for $\alpha = 8$. Since in the majority of bearings h_o will be of the order 0·001 in or less the manufacture of the width of the slot z at half of this value can present great difficulties. Thus in practice it is usual to make h_o and z almost equal and to compromise at a value of α between one and two. The variation in load coefficient with α is shown for half station and quarter station feeding in Figs. 3.22 and 3.23. The curves are drawn for a length-to-diameter ratio of 0·5. For other length-to-diameter ratios we may multiply by the factors given in the table below.

L/D	Multiplication Factor
0·25	1·06
0·75	0·91
1·0	0·84
1·5	0·71
2·0	0·61

For other feed hole stations multiply the values given in Fig. 3.23 by the following factors

$1/L$	Multiplication Factor
0·125	1·167
0·333	0·890

Since the bearing design is not influenced by gas properties or temperature and is insensitive to pressure level the data given will permit the design of almost all bearings with circumferential slot feeding which can be envisaged.
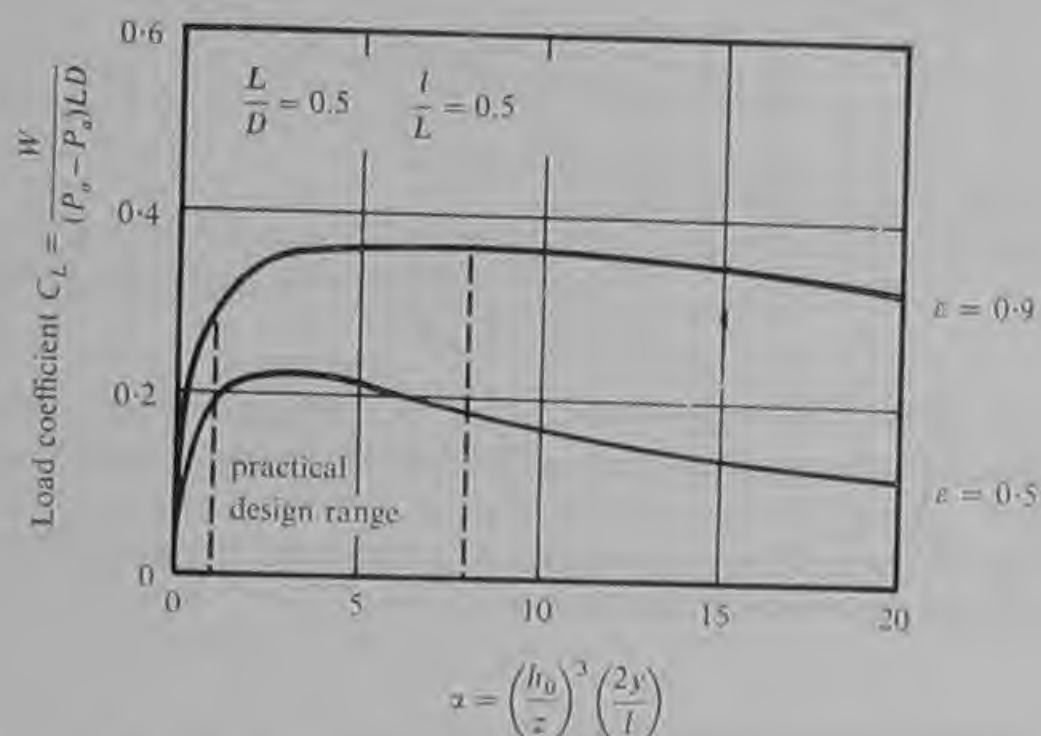
Fig. 3.22 Load capacity of bearings with circumferential slots—half station feeding
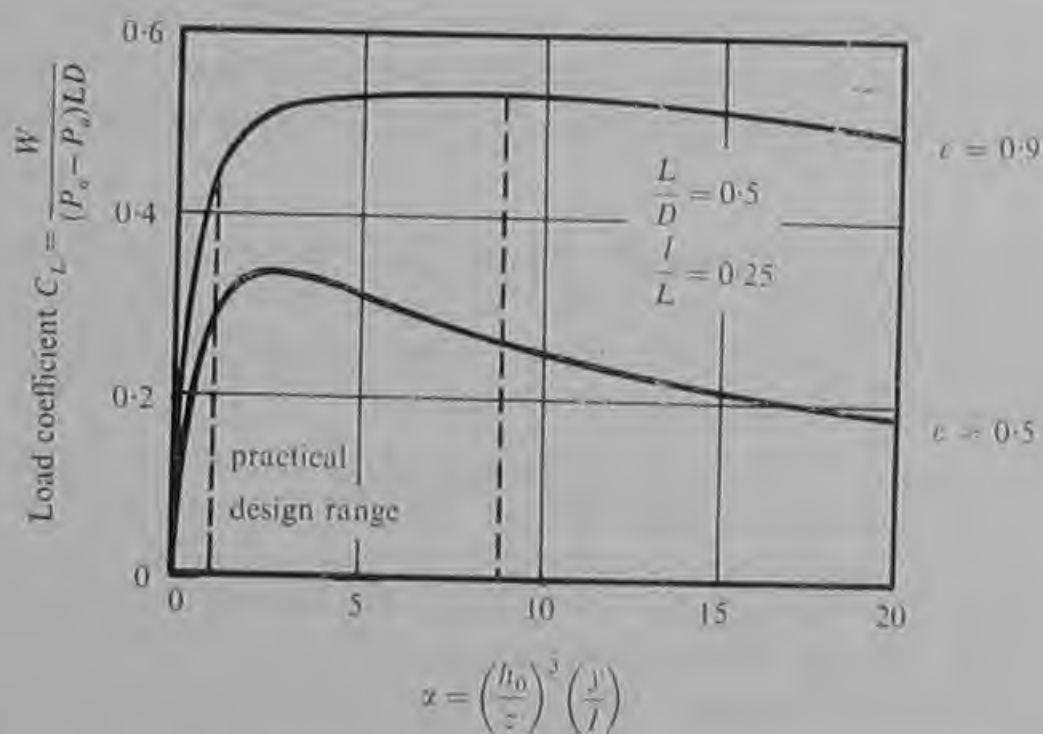
Fig. 3.23 Load capacity of bearings with circumferential slots—quarter station feeding

In all bearings the mean aerostatic radial stiffness for eccentricities up to 0·5 is given by

$$K = C_{L(\epsilon=0\cdot5)} \frac{2LD(P_o - P_a)}{h_o}.$$

The mass flow of gas is given by:

$$M = \frac{(P_o^2 - P_a^2)}{(1+\alpha)} \frac{\pi D h_o^3}{12\mu R T l}.$$

The gas flow is therefore lower at $\alpha = 8$ than at lower values of α and a considerable penalty is incurred by designing at values of $\alpha = 2$ and below. This penalty as well as the loss of load capacity and stiffness must often be accepted in arriving at a practical design which can be manufactured by existing techniques.

3.4 Example of design procedure

Problem An air-lubricated journal bearing must be designed to carry a load of 100 lbf at an eccentricity ratio of 0·5. Its radial stiffness should exceed 400 000 lbf/in. A workshop airline is available at 75 lbf/in² gauge. The airflow should not exceed 0·50 s.c.f.m. A consideration of the manufacturing facilities available suggest that geometric errors may total 0·000 2 in in relation to the diametrical clearance and holes down to 0·005 in diameter can be drilled. The machine design limits the bearing diameter to 2 in but does not restrict the bearing length.

Feasibility A study of Fig. 3.2 shows that a bearing of 2 in diameter and 3 in long could carry a load of about 145 lbf at $\varepsilon = 0\cdot5$ on a supply pressure of 100 lbf/in² gauge. Thus supplied at 75 lbf/in² gauge its load capacity would be given as follows:

$$145 \times \frac{75}{100} = 109 \text{ lbf.}$$

A diametrical clearance of 0·001 in would require an airflow of 0·23 s.c.f.m. at 100 lbf/in² gauge and a flow of $0\cdot23 \times 0\cdot65 = 0\cdot15$ s.c.f.m. at 75 lbf/in² gauge. This is acceptable and so is the fact that the clearance chosen is five times greater than the manufacturing error.

It is then necessary to confirm that this clearance will give adequate radial stiffness. From the equation

$$K = \frac{2W}{h_o}$$

DESIGN OF JOURNAL BEARINGS

one has

$$K = \frac{2 \times 109}{5 \times 10^{-4}} \frac{\text{lbf}}{\text{in}}$$

$$= 437\,000 \text{ lbf/in}.$$

From this study it can be concluded that a suitable bearing can be designed with the following dimensions:

diameter	2 in
length	3 in
diametrical clearance	0·001 in

It is now necessary to decide upon the type of feeding. This decision is usually made after considering the performance and manufacturing difficulties of the various alternatives.

Simple orifice feeding From Fig. 3.7 it can be seen that using one central row of eight feed holes or two rows of eight feed holes at quarter stations requires the following feed hole diameters.

$K_g = 0·4$ $3·2 \times 10^{-3}$ in at 50 lbf/in² gauge and $L/D = 1$
$K_g = 0·6$ $4·8 \times 10^{-3}$,, ,, ,,   ,,   ,,   ,,   ,,   ,, ,,
$K_g = 0·8$ $7·2 \times 10^{-3}$,, ,, ,,   ,,   ,,   ,,   ,,   ,, ,,

From Fig. 3.8 it can be found that these diameters corrected for the length-to-diameter ratio of 1·5 and the supply pressure of 75 lbf/in² gauge become

at $K_g = 0·4 = 3·2 \times 10^{-3} \times 1·1 \times 0·82 = 2·9 \times 10^{-3}$ in
$K_g = 0·6$ $= 4·3 \times 10^{-3}$ in
$K_g = 0·8$ $= 6·5 \times 10^{-3}$ in.

It can further be seen that to design at $K_g = 0·4$ is impossible since only three feed holes of 5×10^{-3} in diameter could be drilled and so few feed holes would seriously impair the load capacity (Fig. 3.13). A practical design would use either six or eight feed holes per row of either 5×10^{-3} in or 6×10^{-3} in diameter, all alternatives providing a gauge pressure ratio between 0·6 and 0·8. The choice of six or eight feed holes per row and one or two rows of feed holes can now be decided as follows.

At an eccentricity ratio of 0·5 the required load coefficient is given by

$$\frac{100}{75 \times 3 \times 2} = 0·222.$$

Fig. 3.14 shows that this value will only be exceeded by a bearing with two rows of feed holes at between one quarter station and one eighth station. Thus a half station bearing will not meet the specification. This is confirmed by reference to Fig. 3.15. The load coefficient based on diameter is given by

$$C'_L = \frac{100}{75 \times 2 \times 2}$$

$$= 0.33.$$

It can be seen that this coefficient is not reached by half station bearings. It would not be reached even if twenty feed holes were used since Fig. 3.15 shows that only a twenty percent increase in load would result, giving for a half station bearing the maximum possible $C'_L = 0.24 \times 1.2 = 0.288$ only.

For a bearing with two rows of eight feed holes at quarter station Fig. 3.15 gives:

$$C_L = 0.355.$$

Fig. 3.13 indicates a loss of load capacity of ten to twelve percent if six feed holes are used and so this possibility also is eliminated. Two rows of eight or more feed holes must be used and the final choice is decided by a consideration of airflow.

Fig. 3.2 indicated an airflow of 0.15 s.c.f.m. for a bearing with two rows of feed holes at quarter station operating at a gauge pressure ratio of 0.4. Fig. 3.12 shows that the airflow will be three times greater if the bearing operates at a gauge pressure ratio of 0.8. Thus one has—

at $\dfrac{l}{L} = \frac{1}{4}$ $K_g = 0.8$ airflow $= 0.45$ s.c.f.m.

Using Fig. 3.17 to examine the effect on airflow of employing one eighth station feeding yields—

$\dfrac{l}{L} = \frac{1}{8}$ $K_g = 0.6$ airflow $= 0.57$ s.c.f.m.

$\dfrac{l}{L} = \frac{1}{8}$ $K_g = 0.8$ airflow $= 0.9$ s.c.f.m.

Both of these alternatives are eliminated on the basis of excessive airflow. Thus the final choice will be two rows of eight feed holes at quarter station. A feed hole diameter of 5×10^{-3} in is to be preferred, providing the lowest gauge pressure ratio and airflow. However, feed holes of up to 6.5×10^{-3} in might be used and still keep the bearing within specification.

The final design is as follows:

diameter	2 in
length	3 in
diametrical clearance	0·001 in
feeding	2 rows of 8 simple orifices at quarter station
feed hole diameter	5×10^{-3} in

Performance on a supply pressure of 75 lbf/in² gauge:

radial load capacity (at $\varepsilon = 0.5$)	107 lbf
radial stiffness ($0 < \varepsilon < 0.5$)	428 000 lbf/in
airflow	0·35 s.c.f.m.

Annular orifice feeding In this design example bearings with annular orifice feeding could be eliminated since they would not provide adequate load capacity. Annular orifice bearings have thirty percent lower load capacity than a simple orifice bearing of similar size, shape and feed arrangement.

Slot feeding Fig. 3.21 clearly indicates that a slot-fed bearing with six slots would not give the required load coefficient at a length-to-diameter ratio of 1·5 and a gauge pressure ratio of 0·2. However, the possibility of employing a slot-fed bearing must be examined more closely. A gauge pressure ratio of 0·2 is chosen because it offers the highest load capacity at large eccentricity ratios and the highest radial stiffness. This can be seen in Fig. 2.17. It can also be seen that a higher load capacity is obtained at an eccentricity ratio of 0·5 by designing at a gauge pressure ratio of 0·4. Thus for very short bearings with quarter station feeding the load coefficient

$$C_L = (1 - \tfrac{1}{4})0.5$$

$$= 0.375.$$

Then allowing for the effect of non-axial flow this value is reduced at a length-to-diameter ratio of 1·5 to

$$C_L = 0.375 \times \frac{0.195}{0.30} = 0.244 \quad \text{(from Fig. 3.21).}$$

Thus the load carried by the slot-fed bearing

$$= 0.244 \times 75 \times 3 \times 2 \text{ lbf}$$

$$= 110 \text{ lbf}$$

and the mean radial stiffness up to this eccentricity ratio for a diametrical clearance of 0·001 in.

$$K = \frac{110 \times 2}{5 \times 10^{-4}} \text{ lbf/in}$$

$$= 440\,000 \text{ lbf/in}.$$

At an eccentricity ratio of 0·9 the load capacity of the slot-fed bearing would be 160 lbf, from Fig. 2.17, and the load capacity of the simple orifice compensated bearing would be 176 lbf, from Fig. 3.15. Thus the load capacity and stiffness of the two bearings are closely comparable.

Fig. 2.17 also shows that to design the slot-fed bearing at a gauge pressure ratio of 0·4 requires that

$$\alpha^{\frac{1}{4}} = 1·4,$$

$$\alpha = \frac{h_o}{z}\left(\frac{y}{l}\right)^{\frac{1}{4}}$$

thus

$$\alpha = 2·75$$

Now $h_o = 5 \times 10^{-4}$ in and $l = 0·75$ in and putting $y = 0·75$ in (it could scarcely be larger) gives

$$z = \frac{5 \times 10^{-4}}{2·75} \text{ in}$$

$$= 1·8 \times 10^{-4} \text{ in}.$$

This example highlights the difficulty in making slot-fed bearings. Accurately manufacturing such fine slots requires the utmost precision and is often prohibitively expensive. Moving the slots closer to the ends of the bearing eases the manufacturing problem a little. For example, with one eighth station feeding

$$z = \frac{5 \times 10^{-4}}{2·75}\left(\frac{0·75}{0·375}\right)^{\frac{1}{4}} \text{ in}$$

$$= 2·3 \times 10^{-4} \text{ in}.$$

However, since the bearing is designed at a gauge pressure ratio of 0·4 the airflow is still within the design limits with one-eighth station slot feeding. With one-quarter station feeding and $K_g = 0·4$ the airflow is the same as for the jet-fed bearing, namely 0·15 s.c.f.m. Moving to one-eighth station feeding doubles the flow to 0·3 s.c.f.m. This consideration tempts the designer to consider higher gauge pressure ratios to give wider slots and to sacrifice some airflow. Designing at $K_g = 0·6$ gives $\alpha^{\frac{1}{4}} = 1$ and feeding at quarter station gives

$$z = 5·0 \times 10^{-4} \text{ in}.$$

This change reduces the load capacity at $\varepsilon = 0.5$ to barely 100 lbf and increases the airflow to 0·28 s.c.f.m.

It can be concluded that a slot-fed bearing could be designed to meet this requirement but that its manufacture would present some difficulty. Most designers would probably choose the simple orifice bearing unless some special circumstance, such as the need for ceramic bearings to withstand high temperature, made the problem of drilling jets more acute than the slot production problem.

CHAPTER 4

DESIGN OF THRUST BEARINGS

4.1 Introduction

The basic theory of aerostatic thrust bearings described in Chapter 2 provides a reliable basis for design in respect of load capacity, stiffness and gas consumption. The simplifying assumption of an incompressible pressure distribution in the bearing clearance yields values of load capacity and stiffness which are invariably exceeded in practice by up to ten percent. The load-carrying performance is not appreciably reduced by dispersion or by any effect corresponding to non-axial flow in journal bearings. Thus as far as calculating load capacity and stiffness are concerned thrust bearings are rather easier to design than journal bearings. However, there are two areas which present considerably more difficulty in thrust bearings than in journal bearings. These are proneness to a self-exciting instability sometimes called 'air hammer', and high gas consumption. Both these conditions are aggravated where a thrust bearing in the form of a narrow annulus must be used.

The problem of aerostatic instability is dealt with more fully in a later chapter. In the design of thrust bearings, however, the problem must be kept in mind from the outset. It is generally true to say that designed at random most thrust bearings would be unstable. Many difficulties can be avoided by observing the following rules.

(a) single groove

(b) double groove—
double feed

(c) double groove—
single feed
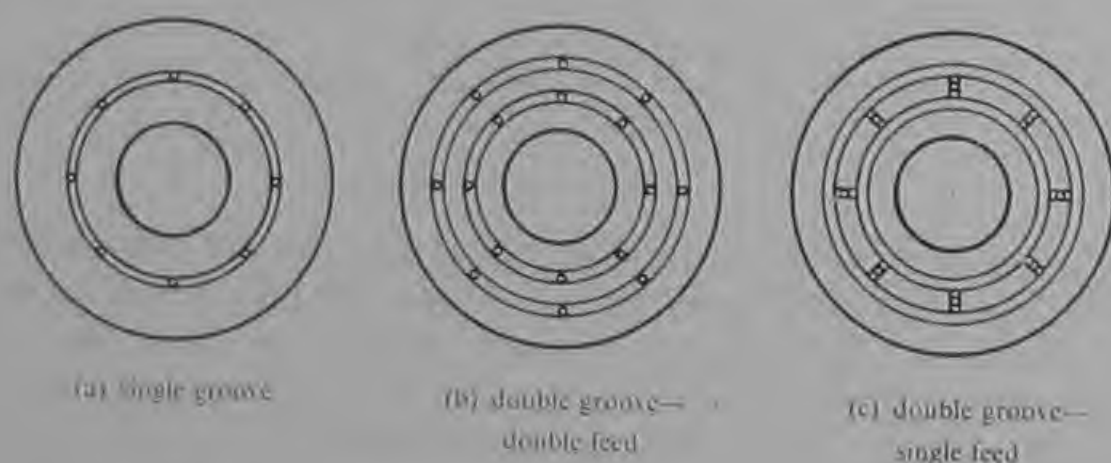
Type (a) demands the least gas flow
Types (b) and (c) provide greater load capacity and axial stiffness at
the expense of greater gas flow
Type (b) provides a high tilt stiffness

Fig. 4.1 Grooved annular thrust bearings

(a) In all annular thrust bearings keep the ratio of outside to inside diameter as large as possible.

(b) Keep the volume of all pockets and grooves to a minimum by limiting both depth and width. Avoid using pockets wherever possible and instead outline any desired pocket area by narrow grooving as shown in Fig. 4.1.
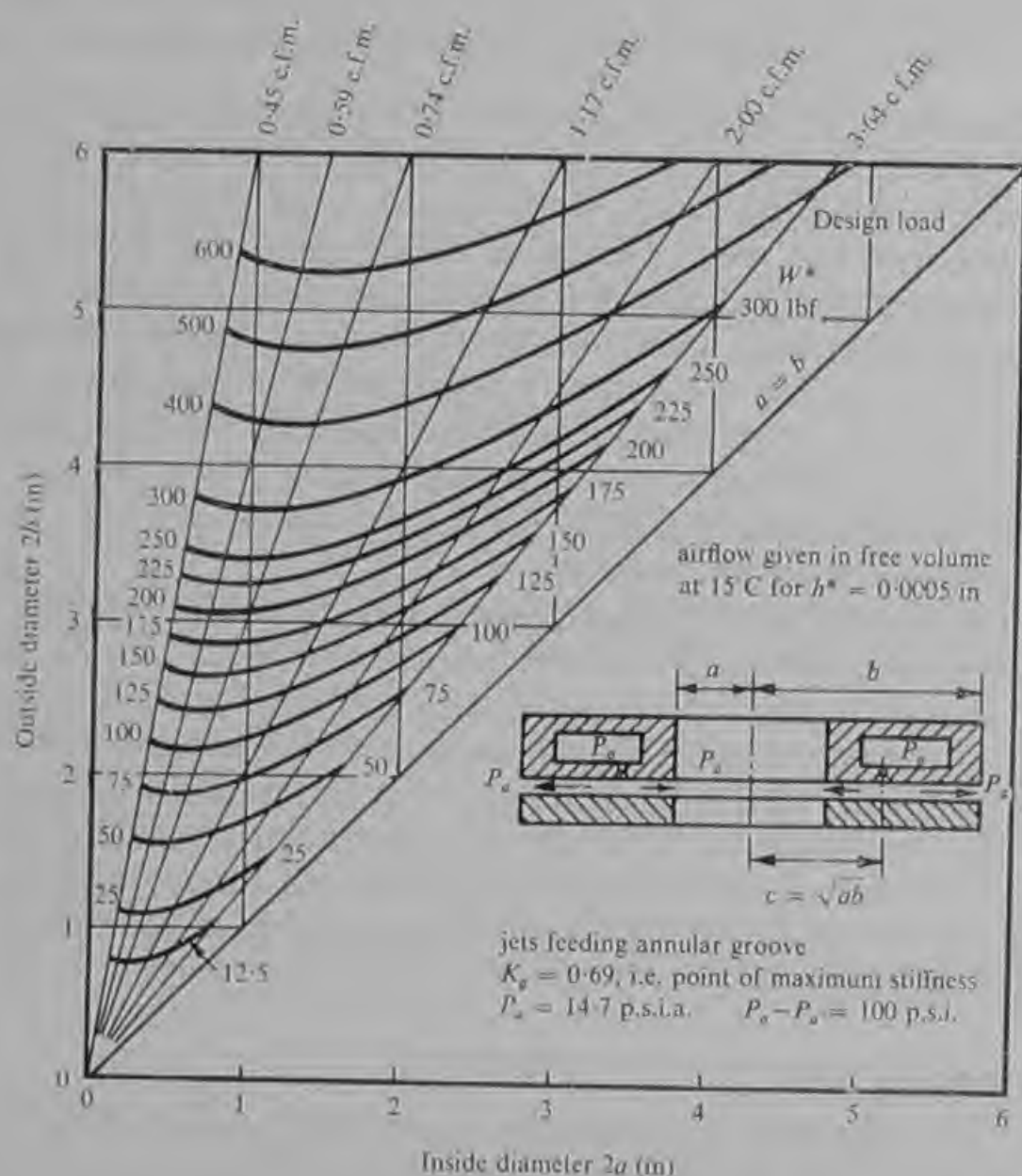
For other supply pressures multiply load by $\dfrac{(P_s - P_a)}{100}$.

For ultimate load multiply by 1·45.

At $P_s - P_a = 75$ lbf/in² multiply flow by 0·625;

  ,, ,, = 50 ,, ,, ,, ,, 0·325;

  ,, ,, = 25 ,, ,, ,, ,, 0·170.

For other clearances multiply flow by $\left(\dfrac{2h^*}{0\cdot001}\right)^3$.

Axial stiffness $K = 1\cdot44\,\dfrac{W^*}{h^*}$. Tilt stiffness $= \dfrac{K(b+a)^2}{8}$.

Fig. 4.2 General performance of annular air thrust bearings with a ring of jets

(c) Where two thrust bearings are employed these should be loaded one against the other so that with no applied external load each bearing is operating near the design condition of $K_g = 0.69$. Always avoid choked feed hole conditions.

(d) Wherever possible channel the exhaust gas from the thrust bearings to the atmosphere through a single hole. This will not prevent instability, but should instability occur in the prototype machine a restrictor or throttling orifice placed in the exhaust hole can afford a considerable degree of control without seriously impairing the bearing performance.

A comparison of Fig. 4.2 for annular thrust bearings with Fig. 3.2 for journal bearings quickly reveals the considerably higher gas flows required by thrust bearings. Both figures are plotted for the same supply pressure and mean clearance. Once again it is indicated that narrow annular thrust bearings should be avoided. Unfortunately the designer often has little room to manoeuvre since the outside diameter of the thrust bearing is limited by the external dimensions of the machine, and the inside diameter is determined by the shaft diameter. For this reason the single groove thrust bearing shown in Fig. 4.1(a) is by far the most widely used since the double groove arrangements further increase the flow required.

The simplest form of circular thrust bearing with a single central feed hole and pocket is by far the most economical. It can provide comparable or higher load capacity and stiffness for only twenty-five percent of the flow required by an annular thrust bearing of the same outside diameter. Its only weakness is in terms of tilt stiffness and this is not important in the majority of applications. Most machine designs, however, do not permit more than one simple thrust bearing to be used and those with the shaft protruding at both ends prohibit their use entirely.

4.2 Feasibility study

The basic approach to feasibility is the same as that described for journal bearings. It consists of seeking a compromise between the conflicting demands of performance, the available gas supply and the manufacturing capability.

The load capacity, stiffness, gas flow and friction power can quickly be estimated by reference to Figs. 4.2, 4.3 and 4.4. Although the data are given for air, the load capacity and stiffness values apply for any gas. The data are presented for a supply pressure of 100 lbf/in² gauge and atmospheric exhaust conditions, and correction factors are given for other supply pressures. The standard clearance of 0.000 5 in corresponds to that used for journal bearings in Fig. 3.2. Correction factors are given for other clearances. With a little practice the designer
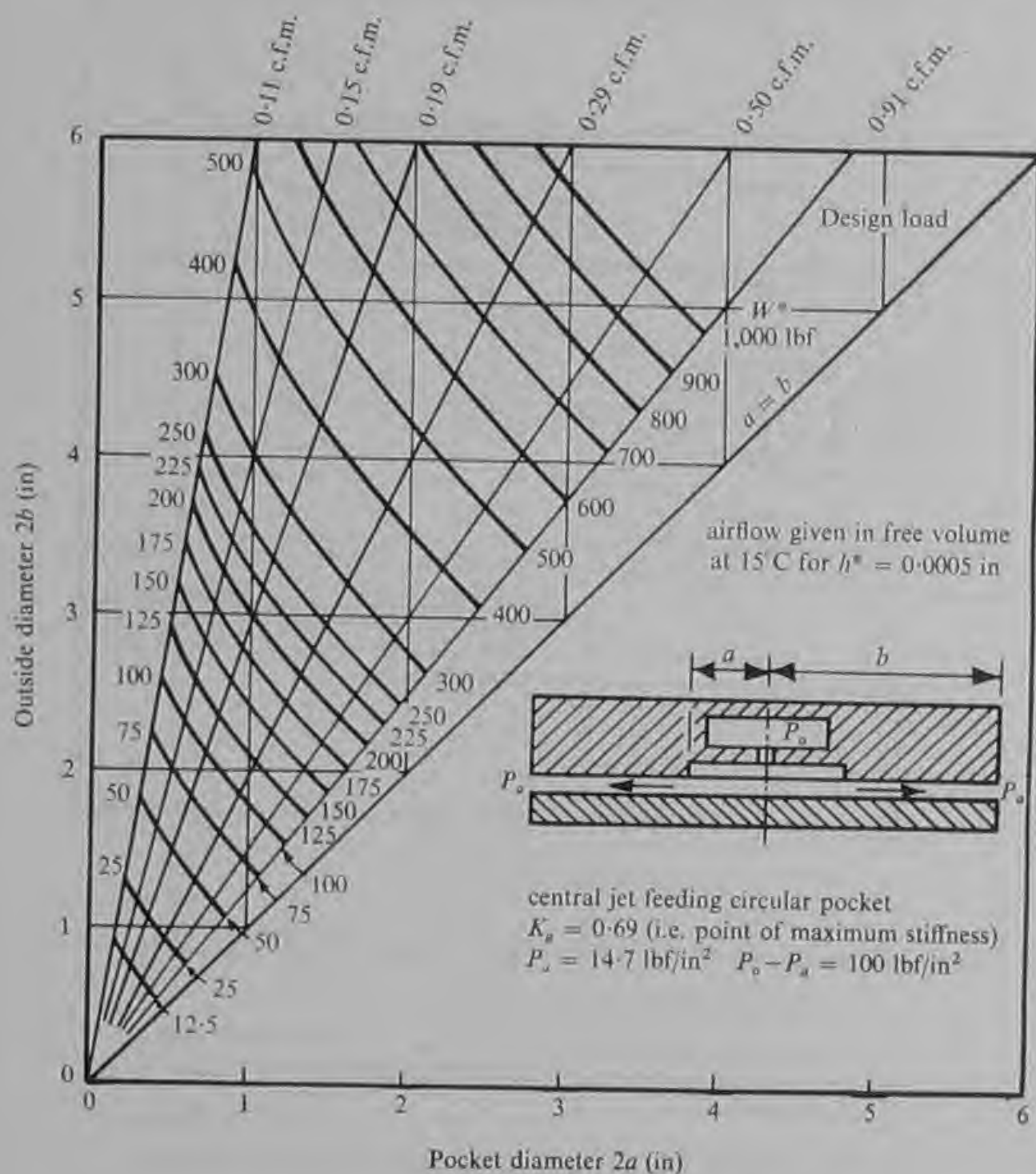
For other supply pressures multiply load by $\dfrac{(P_o - P_a)}{100}$;

for ultimate load multiply by 1·45;

at $P_o - P_a = 75$ lbf/in^2 multiply flow by 0·625;

,,   ,, $= 50$,,   ,,   ,,   ,, 0·325;

,,   ,, $= 25$,,   ,,   ,,   ,, 0·17;

for other clearances multiply flow by $\left(\dfrac{2h}{0·001}\right)^3$.

Axial stiffness $K = 1·44 \dfrac{W^*}{h^*}$.

Fig. 4.3 General performance of air thrust bearings with central feed hole and circular pocket
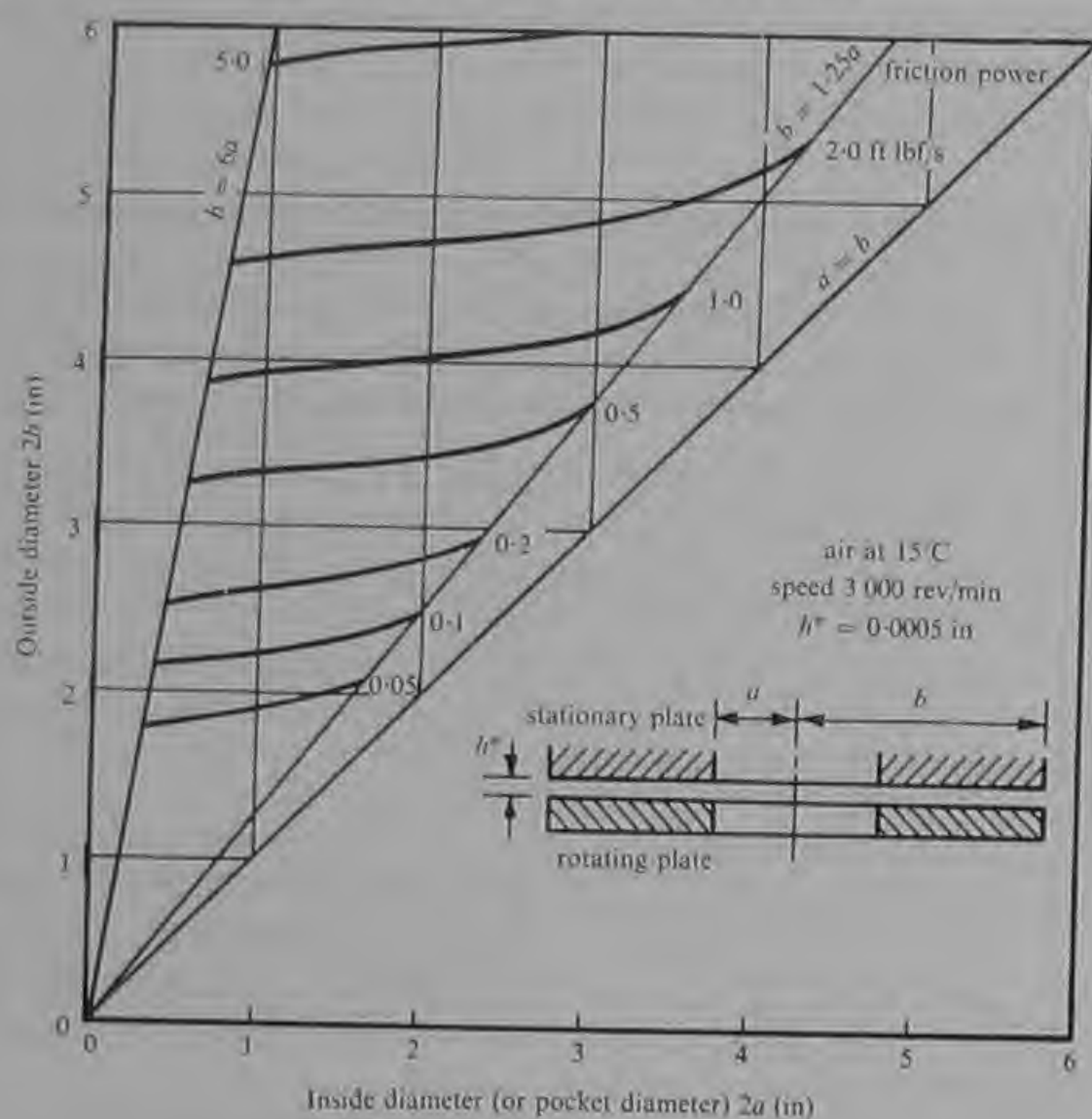
For other speeds multiply by $\left(\dfrac{N}{3\,000}\right)^2$ (with N in rev/min);

for other clearances multiply by $\dfrac{0 \cdot 001}{2h}$;

for other gases and temperatures multiply by the gas viscosity relative to air at 15°C. (Viscosity data for the more common gases are given in Appendix 1.)

Fig. 4.4 Friction power consumed by aerostatic thrust bearings

will find that, at least for air bearings, Figures 4.2 to 4.4 will permit the effect of changes in design parameters quickly to be evaluated. It must be emphasized that Figures 4.2 and 4.3 give the load capacity at the point of maximum stiffness ($K_g = 0 \cdot 69$) and that the ultimate load capacity for perfectly flat and parallel plates is forty-five percent higher.

The load coefficients of centre-fed and annular thrust bearings are compared in Fig. 4.5. The figure illustrates how the load coefficient varies with the ratio of the outside to inside radii $\left(\dfrac{b}{a}\right)$. The very high
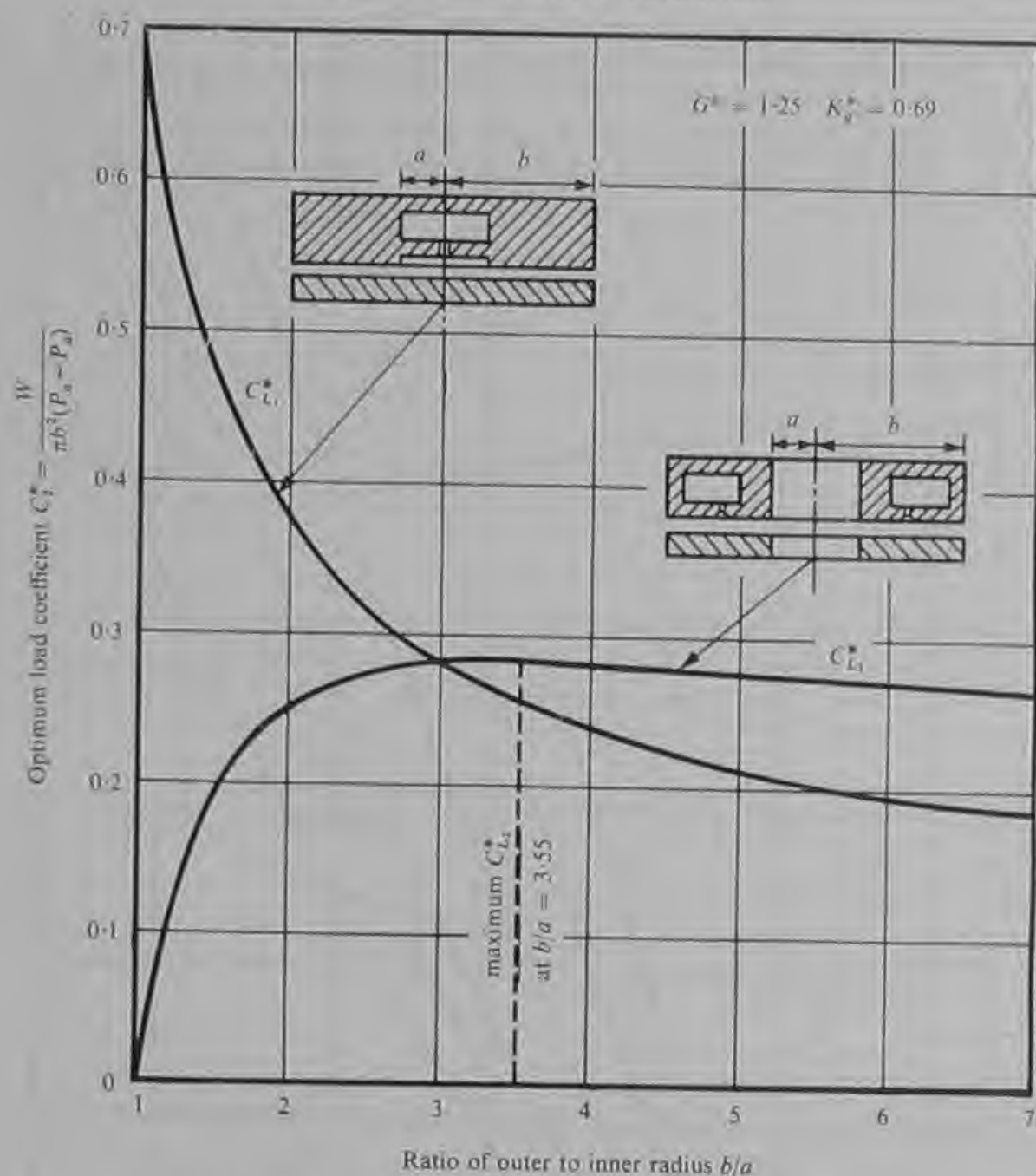
Fig. 4.5 Optimum load coefficient of thrust bearings (after Shires, Ref. 11)

load coefficients of centre-fed bearings of low ratio are not often usable in practice since the large pocket volume renders the bearing prone to instability.

Once the size and shape of the bearing have been established from consideration of the load capacity, stiffness, gas flow and friction power it is possible to proceed to obtain the required jet diameter. This can be done by reference to Fig. 4.6. The optimum jet diameter for the simple thrust bearing with single jet is plotted against clearance for various ratios of outside radius to pocket radius. The data are given for air at 15°C, supplied at 50 lbf/in² gauge and exhausting to atmosphere. These conditions correspond to those for journal bearings used in Fig. 3.7 and the range of clearance (0–0·001 5 in) is also
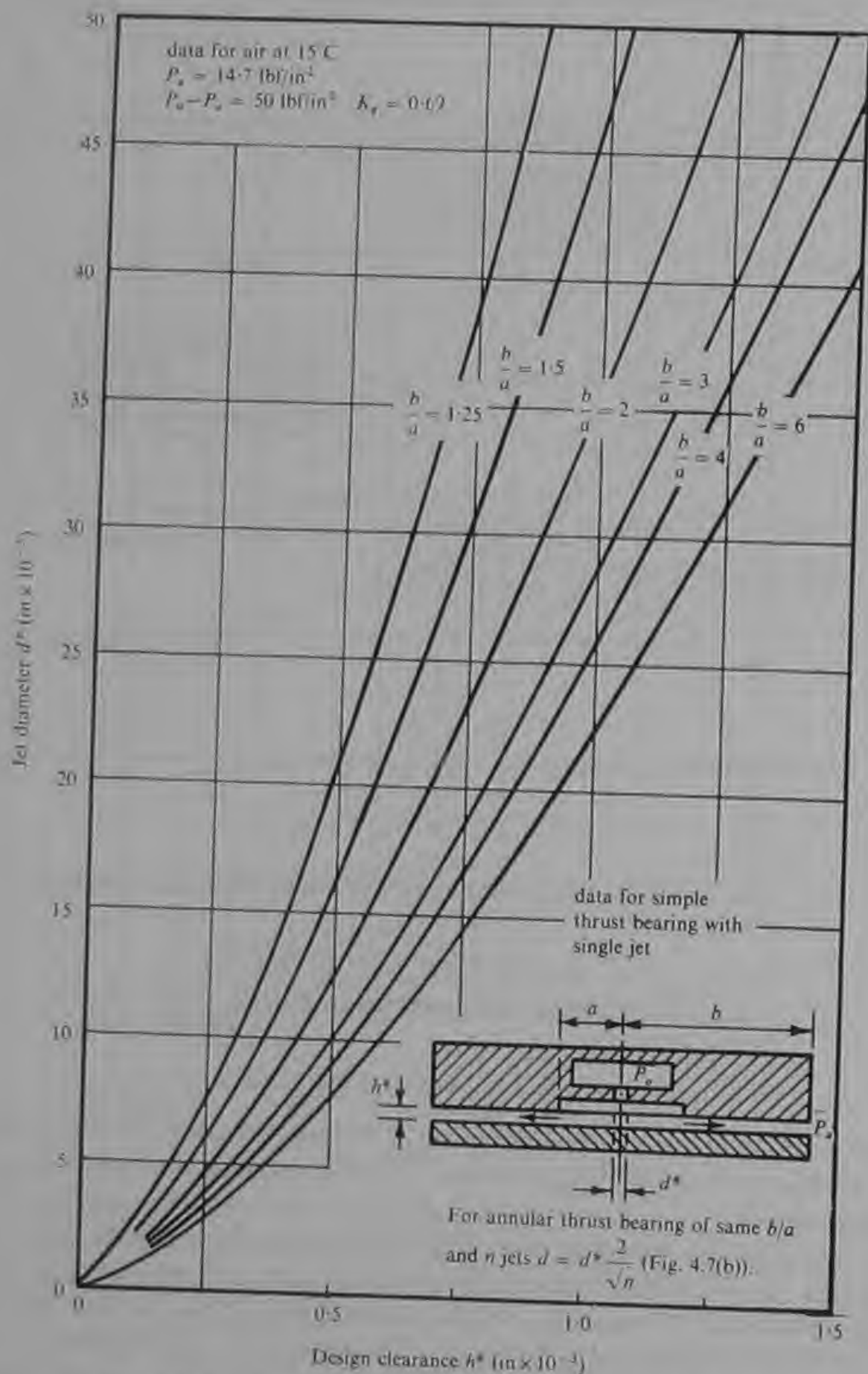
Fig. 4.6 Jet diameter versus clearance for simple thrust bearing

the same for both journal and thrust bearings. In Fig. 4.7(a) correction factors are given for other supply pressures in the range 10 to 100 lbf/in² gauge and in Fig. 4.7(b) correction factors are given for annular bearings with between four and twenty-four jets.

(a) Supply pressure $(P_s - P_a)$ (lbf/in²)

$$d = d^* \cdot \frac{2}{\sqrt{n}}$$

(b) Number of jets in annular bearing of same $\dfrac{b}{a} - n$.
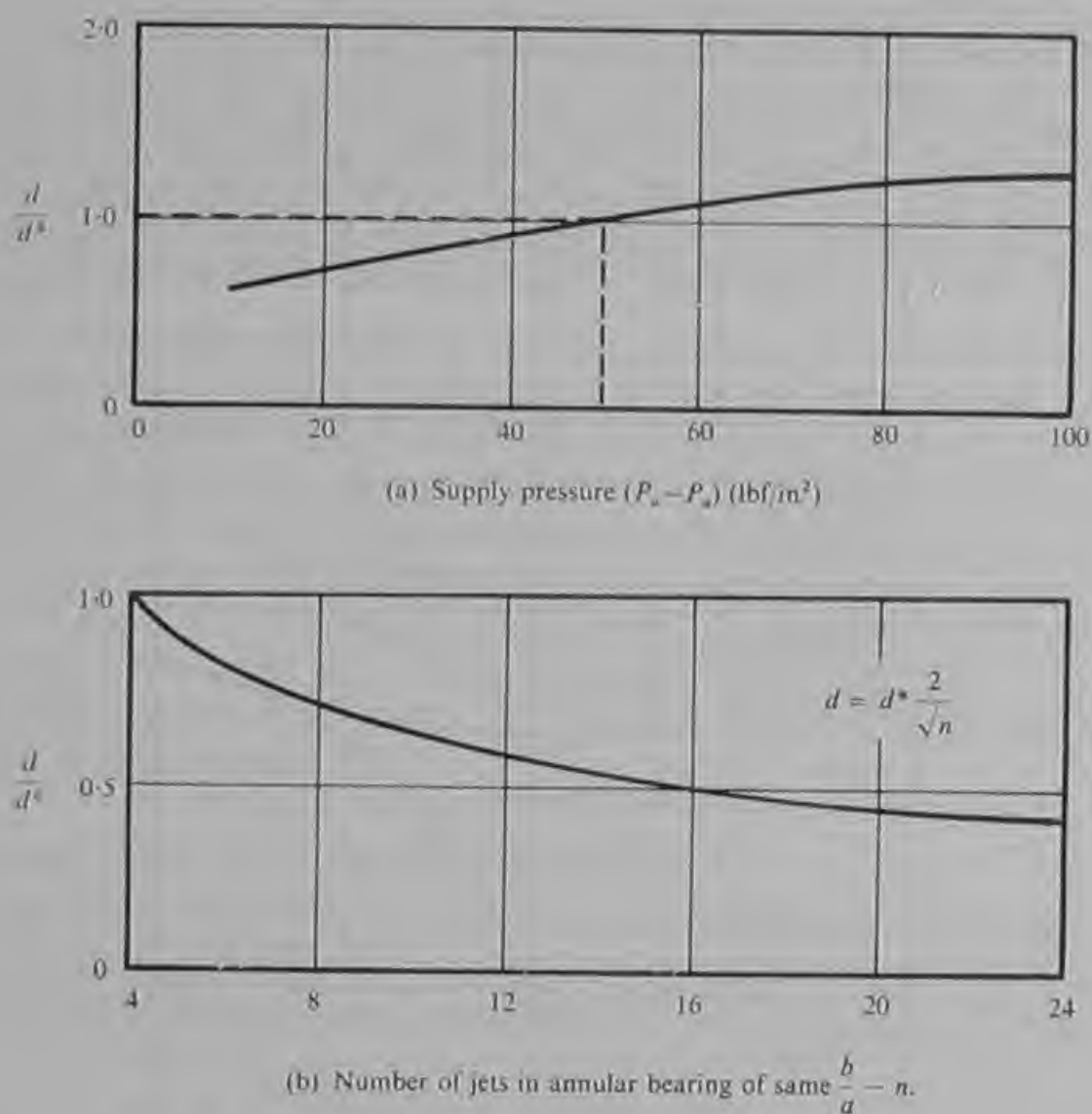
Fig. 4.7 Variation of optimum jet diameter with supply pressure and number of jets in annular bearings

The influences of pressure, temperature, and gas properties on the optimum jet diameter are the same for thrust bearings as for journal bearings. Thus Fig. 3.19 can be used to adjust the jet diameter for other supply pressures. Similarly the correction factors for simple orifices given in Fig. 3.20 for various gases and temperatures can be applied to thrust bearings designed to operate under these conditions. The mass flow of gas through thrust bearings is also influenced in the same way by variations in pressure, temperature and gas properties, as is the mass flow of gas through journal bearings, and the proportionality given in Chapter 3 can again be applied.

4.3 Combination of two thrust bearings

In the majority of machines it is necessary to employ two thrust bearings, either because axial loading can arise in both directions, or because the rotor must be located axially as precisely and rigidly as possible. Thus it is important to consider the combination of two thrust bearings in opposition.

The greatest axial stiffness is realised if the two bearings are loaded against one another at the design condition $K_g = 0.69$. This condition is illustrated in Fig. 4.8. With no externally applied loads the bearings apply to each other the design load W^* given by Fig. 4.2 or 4.3. The stiffness at this point is twice as high as that provided by one isolated bearing under the same load. When external load is applied in one
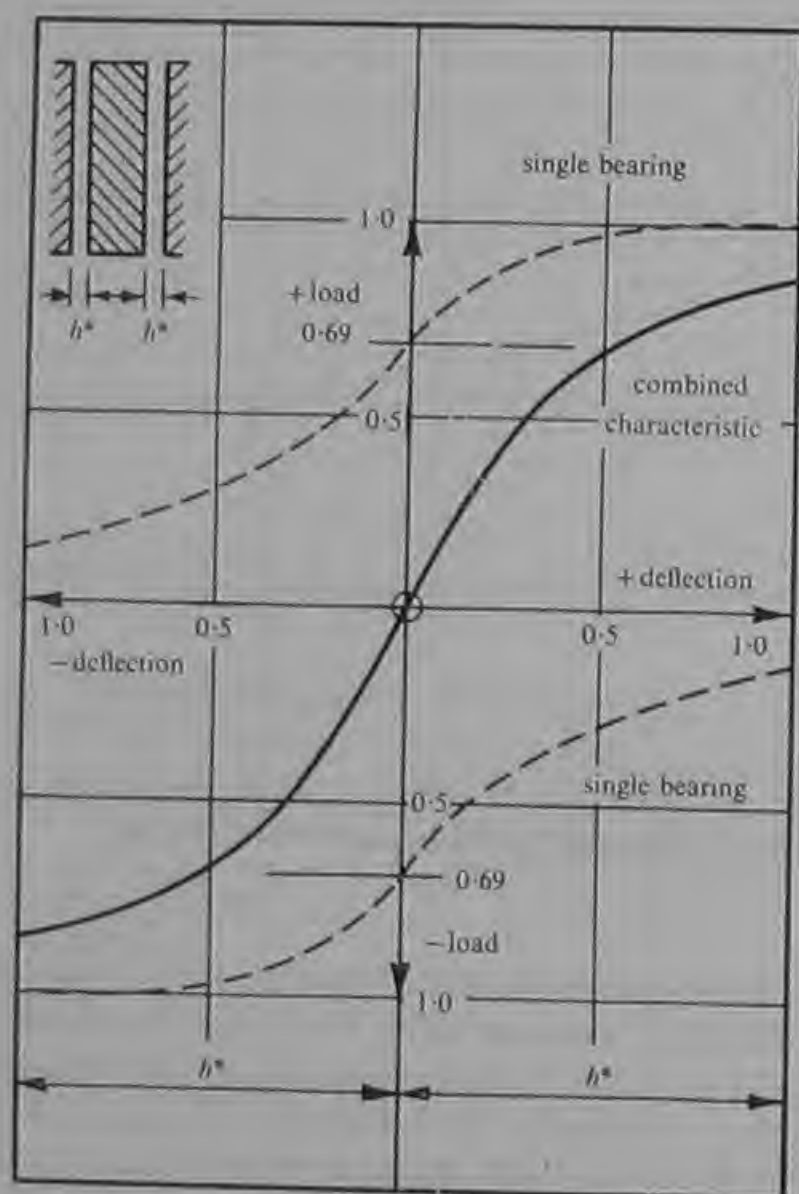
Ultimate load in both directions $= 1 \cdot 25 W^*$
where W^* is the design load of a single bearing at $K_g = 0.69$.
Stiffness $k_a = 2 \cdot 88 \dfrac{W^*}{h^*}$ at central position.

Fig. 4.8 Combination of two thrust bearings

direction the resulting movement of the bearing surfaces causes the pressure in one bearing to rise and the other to fall. The ultimate load when the bearings surfaces come into contact is twenty-five percent higher than the design load $W*$ if perfect geometry is assumed. The ultimate axial load capacity is slightly increased if a greater free axial movement (end float) is used so that the bearings are more lightly preloaded. However, three disadvantages are incurred for this marginal gain in load capacity. The gas flow is higher, the stiffness is lower and the tendency to aerostatic instability is increased. With these considerations in mind most designers tend to design at or below the end float corresponding to the $K_g = 0.69$ condition. They also ensure that manufacturing tolerances tend to reduce the end float rather than increase it.

It is sometimes necessary to use two unequal thrust bearings. In this case with no axial load only one bearing can operate at the $K_g = 0.69$ condition. It is necessary to calculate the load deflection curve for each bearing and to combine the two curves in the manner of Fig. 4.8 for several different values of end float. Fig. 2.15 can be used to determine the load deflection curves using a value of the design load $W*$ from Fig. 4.2 or 4.3 as an anchor point at $K_g = 0.69$. From the various combinations of the two load deflection curves the best compromise emerges in terms of ultimate load in both directions, stiffness and gas flow.

4.4 Thrust faces fed by journal exhaust gas

It has been emphasized that in most machines with aerostatic bearings the thrust bearings use by far the larger part of the total gas consumption. One method of eliminating this large gas consumption
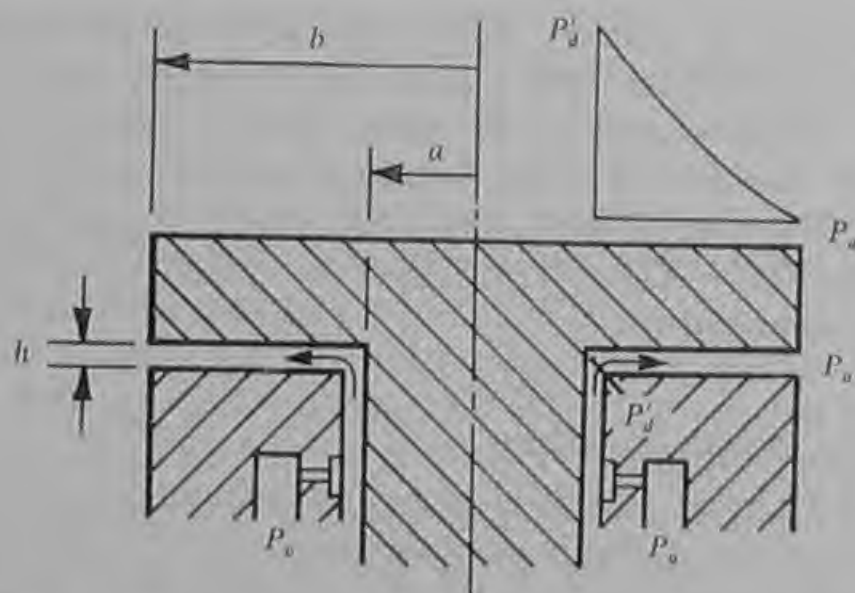

Fig. 4.9 Thrust bearing fed by journal bearing exhaust

which can be used where thrust loads are small is to feed the thrust clearance space from the exhaust of the journal bearing. This arrangement is shown in Fig. 4.9. As the gas flows radially outwards between the thrust faces its pressure falls from P'_d at radius a to P_a at radius b. The load carried by the thrust bearing is given by

$$W = (P'_d - P_a)\pi \, \frac{[b^2 - a^2(2 \log_e (b/a) + 1)]}{2 \log_e (b/a)}. \qquad (57)$$

P'_d is now the exhaust pressure of one end of the journal bearing and if it is allowed to rise too high it will seriously reduce the differential pressure $(P_o - P'_d)$ across that end of the bearing and will reduce its radial load capacity. Equation (57) can be rewritten as

$$W = K'_g(P_o - P_a)\pi \, \frac{[b^2 - a^2(2 \log_e (b/a) + 1)]}{2 \log_e (b/a)}.$$

In practice K'_g seldom exceeds 0·3 which can be taken to give the ultimate load capacity for most design purposes. Higher values are difficult to attain for two reasons: the gas flow increases towards the other end of the journal bearing, reducing the flow available to feed the thrust bearing, and geometric errors have a large effect at the small thrust clearances dictated by the low flow under high load conditions. It is usual to make the thrust bearing clearance under no load conditions of the same order as, or slightly larger than, the clearance in the journal bearing.

It is important to ensure that there is an absolute minimum of any undercutting or chamfering in the corner between the journal bearing clearance and the thrust clearance. Any appreciable storage volume located within the combined bearing clearance can give rise to aerostatic instability which is extremely difficult to eliminate.

Thrust faces fed by journal exhaust gas have found limited applications in small machines in which a low gas consumption is of primary importance. Some examples of these are discussed in Chapters 6 and 12. They should, however, be applied with caution and are not suitable where large axial loads must be carried or where a large axial stiffness is needed. These considerations rule them out for most machine tool applications.

4.5 Example of design procedure

Problem   Two thrust bearings must be provided on an aerostatic machine to carry thrust loads in both directions of up to 100 lbf. The air supply pressure available is 50 lbf/in² gauge and the airflow must be limited to 0·5 s.c.f.m. The outside diameter must be limited

to 3 in and one thrust bearing must have a central hole of 1·5 in diameter to permit access for the shaft. Axial stiffness should exceed 500 000 lbf/in for small axial loads.

Feasibility Fig. 4.9 indicates that for a combination of two thrust bearings the ultimate load is twenty-five percent higher than the design loads given in Figures 4.2 and 4.3 for single thrust bearings. Then since Figures 4.2 and 4.3 give the load capacity for bearings supplied at 100 lbf/in² gauge the equivalent load is given by

$$\frac{100}{1·25} \times \frac{100}{50} \text{ lbf} = 160 \text{ lbf}.$$

Fig. 4.2 indicates that an annular thrust bearing of 3 in outside diameter and 1·5 in inside diameter supplied at 100 lbf/in² gauge would carry a load of 175 lbf at the design clearance of 0·000 5 in. The airflow at 100 lbf/in² gauge would be 1·17 s.c.f.m. and at 50 lbf/in² gauge would be 1·17 × 0·325 s.c.f.m. = 0·38 s.c.f.m. Thus an annular thrust bearing can be designed to provide the necessary load capacity and a combination of two identical bearings would provide an axial stiffness (from Fig. 4.8) of

$$K_A = \left(\frac{175}{2} \times 1·25\right) \times \frac{2·88}{5 \times 10^{-4}} \text{ lbf/in}$$

$$= 500\,000 \text{ lbf/in}.$$

This stiffness is up to requirements and represents the maximum stiffness for small axial loads, that is in operation near the point of equal clearance for the two thrust bearings.

However, two annular thrust bearings would require an airflow of 0·76 s.c.f.m. and this is in excess of the design allowance. Therefore it is necessary to consider using a thrust bearing with a central feed hole and pocket to carry the load in one direction. Identical load capacity is required in both directions and so using Fig. 4.3 it is necessary to find a bearing that will match the annular thrust bearing already chosen. Once again Fig. 4.3 relates to a supply pressure of 100 lbf/in² gauge and so an equal load capacity of 175 lbf must be sought. It can be seen that this is achieved by a bearing with a pocket diameter of 0·8 in. This bearing would consume 0·16 s.c.f.m. at 100 lbf/in² gauge and 0·16 × 0·325 s.c.f.m. = 0·05 s.c.f.m. at 50 lbf/in² gauge.

Thus the feasibility study shows that a combination of an annular thrust bearing and a central feed thrust bearing will meet the design requirements. The principal dimensions and performance data are as in the following table.

	Annular Thrust Bearing	Central Feed Thrust Bearing	
Outside diameter	3 in		3 in
Inside diameter	1·5 in	(Pocket diameter)	0·8 in
Design clearance	0·000 5 in		0·000 5 in
Ultimate load	109 lbf		109 lbf
Airflow	0·38 s.c.f.m.		0·05 s.c.f.m.

Combined axial stiffness   500 000 lbf/in
Combined airflow   0·43 s.c.f.m.

Feed hole size and arrangement   Fig. 4.6 can be used to determine the feed hole diameter of the centre fed bearing.   The ratio of outside diameter to pocket diameter is

$$\frac{3 \cdot 0}{0 \cdot 8} = 3 \cdot 75.$$

Thus it can be seen that for a design clearance of $0 \cdot 5 \times 10^{-3}$ in the feed hole diameter is 9×10^{-3} in.   No correction is needed for supply pressure since Fig. 4.6 is plotted for 50 lbf/in² gauge.

The ratio of outside to inside diameter for the annular thrust bearing is $\frac{3 \cdot 0}{1 \cdot 5} = 2$.   Thus the single jet diameter would be $12 \cdot 5 \times 10^{-3}$ in. However, in this case multiple jets will be arranged feeding into a circular groove of radius given thus:

$$c^2 = 1 \cdot 5 \times 0 \cdot 75 = 1 \cdot 12$$

$$c = 1 \cdot 06 \text{ in.}$$

The number of feed holes will be determined in the limit by the smallest size that can be drilled.   Fig. 4.7(b) shows the variation in feed hole diameter with the number of feed holes.   The practical choice of most designers would lie between eight and sixteen and possibly the best compromise between considerations of aerostatic instability and manufacturing difficulty would be to use twelve feed holes of $7 \cdot 2 \times 10^{-3}$ in diameter.

CHAPTER 5

HYBRID JOURNAL BEARINGS

5.1 Aerodynamic journal bearings

In Chapter 1 mention was made of aerodynamic bearings in which the load-carrying pressure is generated by the relative motion of the bearing surfaces. Pressure changes occur by the mechanism of viscous shearing in an essentially similar manner to that occurring in hydrodynamic oil bearings. The simplest form of aerodynamic journal bearing consists of a cylindrical shaft rotating in a cylindrical bush
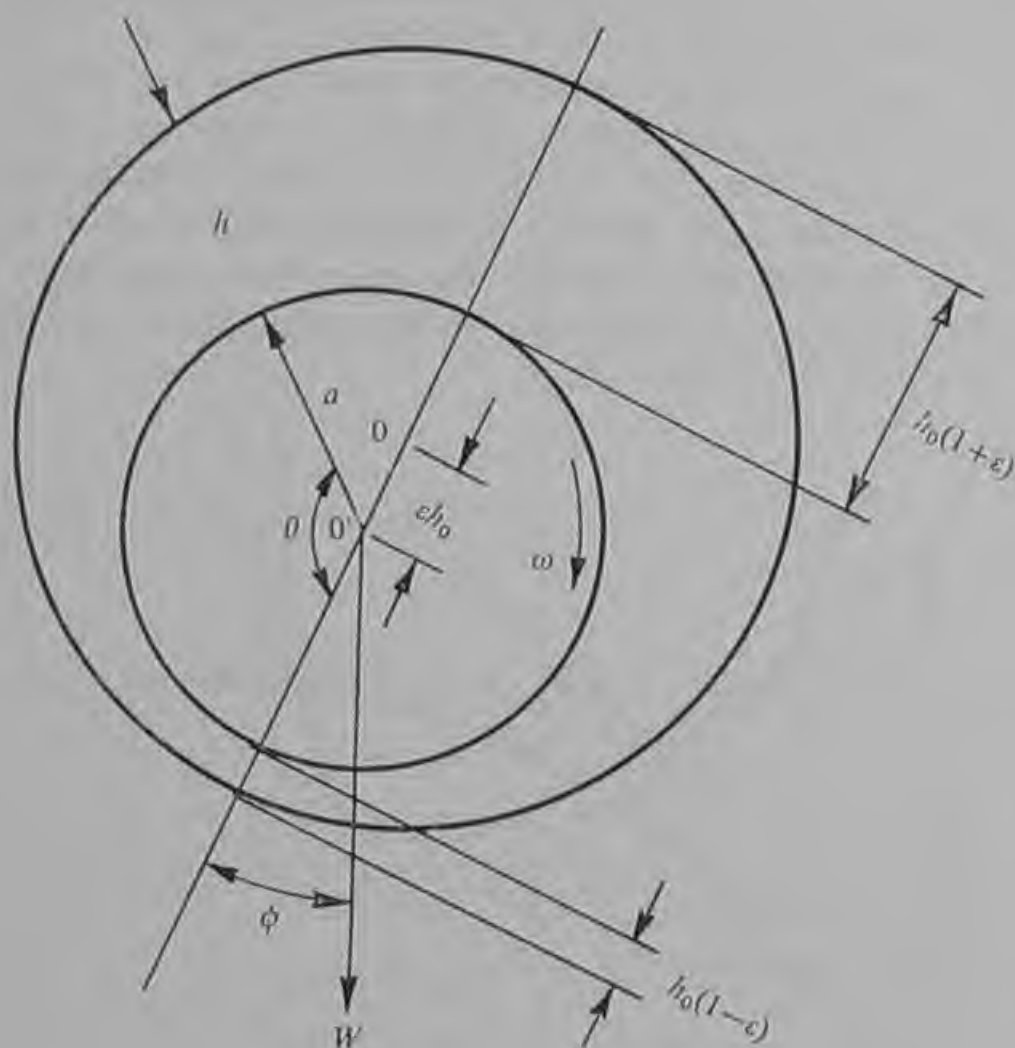
Clearance at angle θ $h = h_0(1 - \varepsilon \cos \theta)$

Compressibility No. $\Lambda = \dfrac{\mu \omega}{P_a} \left(\dfrac{a}{h_0} \right)^2$

Fig. 5.1 Aerodynamic journal bearing

with no pockets, grooves or any other feature machined in either surface. A section through such a bearing is shown in Fig. 5.1. The centre of the bearing bush is at O and the shaft rotates about its centre O' with angular velocity ω. A load W applied to the shaft deflects the shaft a distance εh_o at some angle ϕ to the load line.

The performance of the bearing depends primarily on the compressibility number Λ defined by:

$$\Lambda = \frac{\mu\omega}{P_a}\left(\frac{a}{h_o}\right)^2, \tag{58}$$

where μ is the viscosity of the gas, and P_a is the ambient pressure, while a is the radius of the shaft and h_o is the mean radial clearance as before. The latter is very small compared to a so that $\frac{a}{h_o}$ usually exceeds 10^3, and in a typical design might be $2 \cdot 5 \times 10^3$.

The load capacity of the aerodynamic journal bearing increases with increasing compressibility number as shown in Fig. 5.2. At low values of Λ the increase in load capacity is linear as in a hydrodynamic bearing with an incompressible lubricant. However, with a compressible lubricant the rate of increase of load capacity falls and at high values of Λ the load capacity becomes independent of Λ. In most aerodynamic journal bearings the linear region extends roughly up to $\Lambda = 0 \cdot 15$ and the load capacity becomes effectively independent of Λ at values in excess of $\Lambda = 4$.
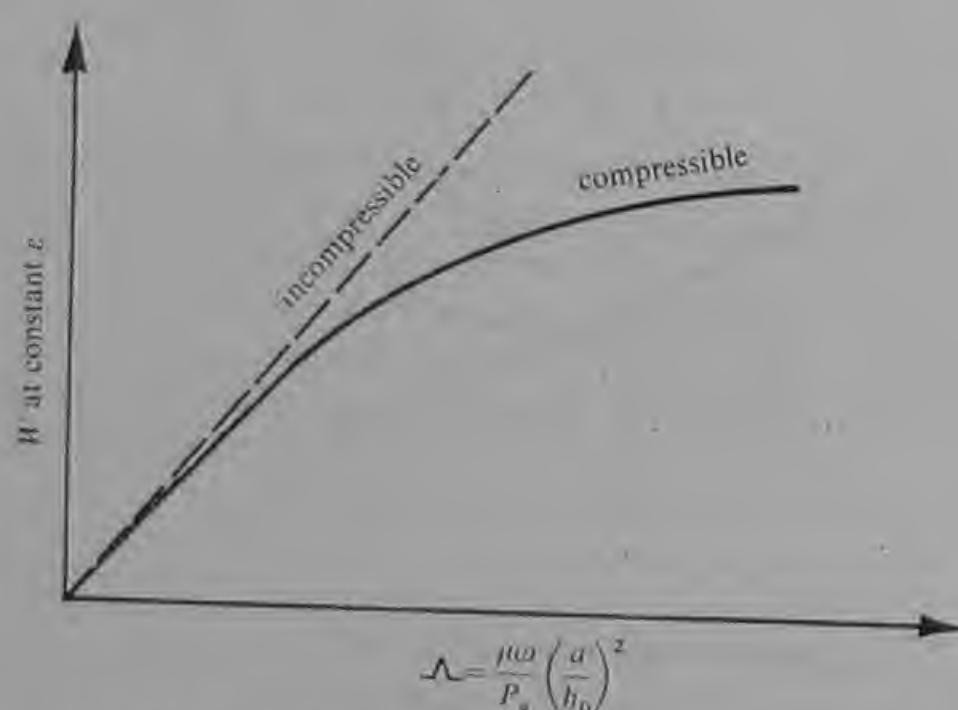
Fig. 5.2 Variation of load capacity with compressibility number in an aerodynamic journal bearing

The value of the compressibility number also has an influence on the size of the attitude angle ϕ; that is the angle between the direction of the applied load and the resulting deflection. The theoretical limits are

$$\text{at} \quad \Lambda = 0, \quad \phi = 90°, \quad \text{and}$$

$$\text{at} \quad \Lambda = \infty, \quad \phi = 0°,$$

	Load (lbf)	Speed (rev/min)	+ve press. ratio	Λ
1	61·4	11 200	1·71	0·2
2	30·4	5 600	1·32	0·1
3	16·4	2 800	1·16	0·05

degrees around bearing from load line in direction of rotation
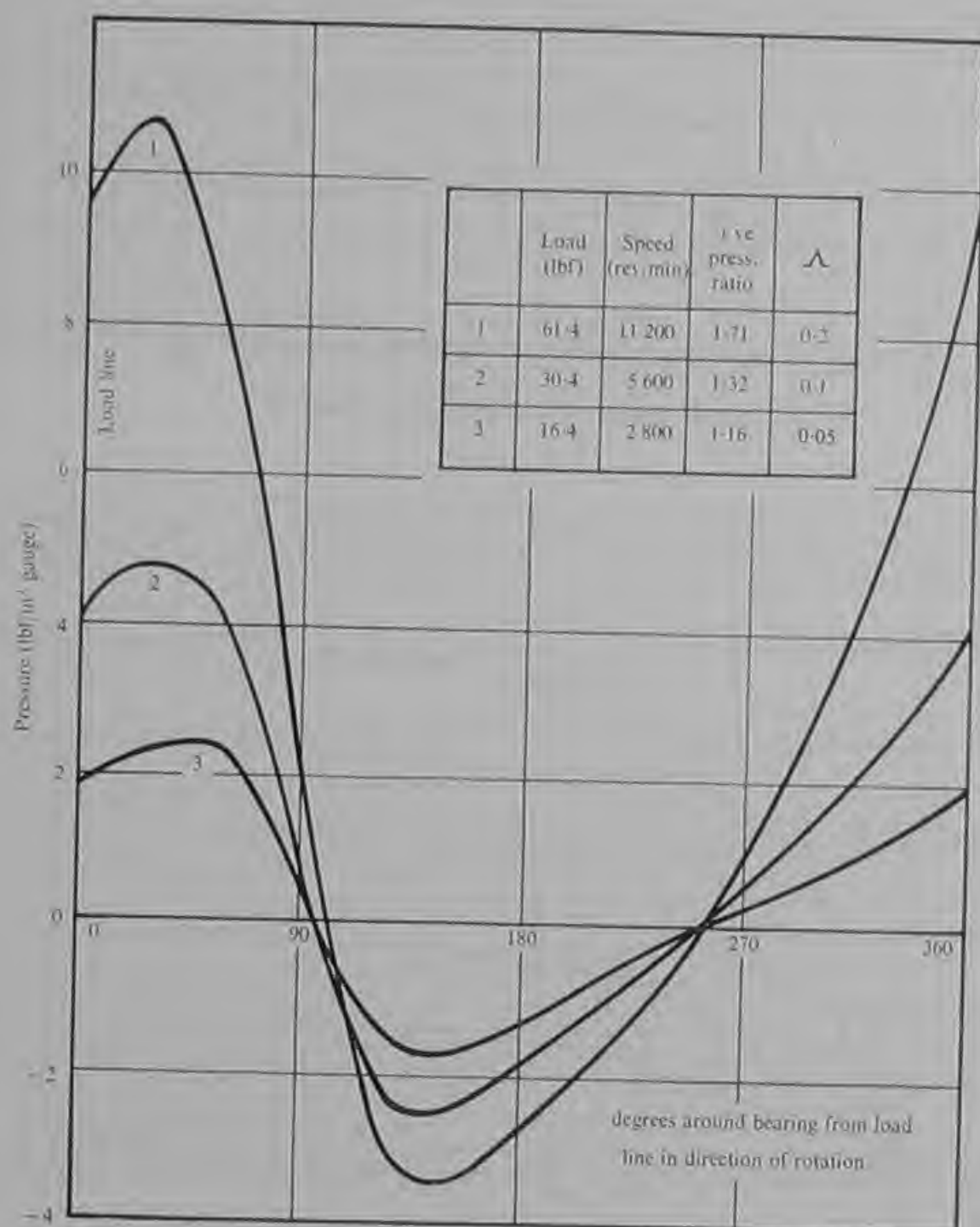
Experimental data for bearing of 2 in diameter
4 in length
0·001 05 in mean radial clearance
0·5 eccentricity ratio

Fig. 5.3 Experimental pressure distribution around the centre of an aerodynamic journal bearing

(a)

(b)
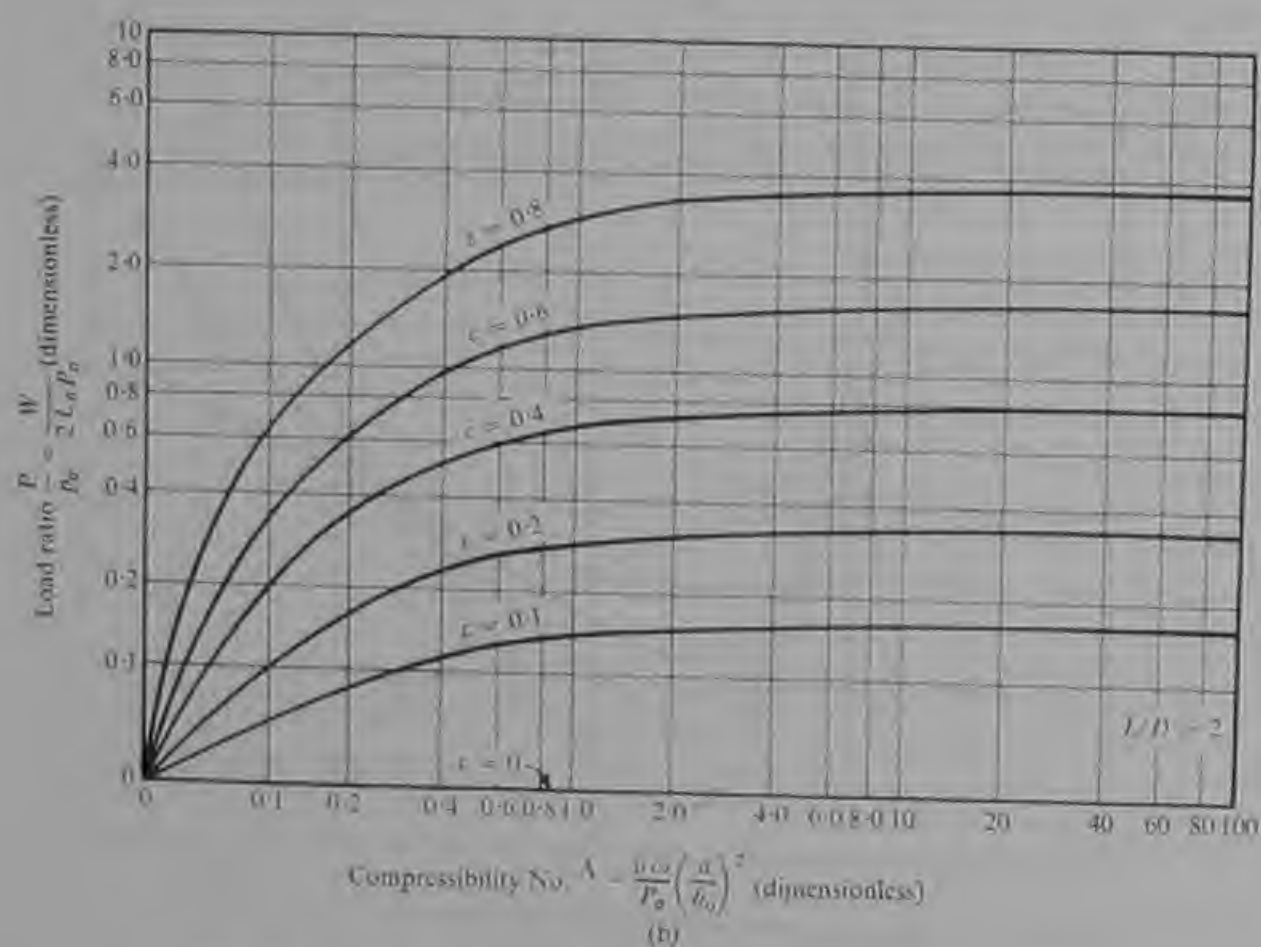
Fig. 5.4a Design charts for load capacity of a 360 degree
cylindrical journal bearing $L/D = \infty$

Fig. 5.4b Design charts for load capacity of a 360 degree
cylindrical journal bearing $L/D = 2$
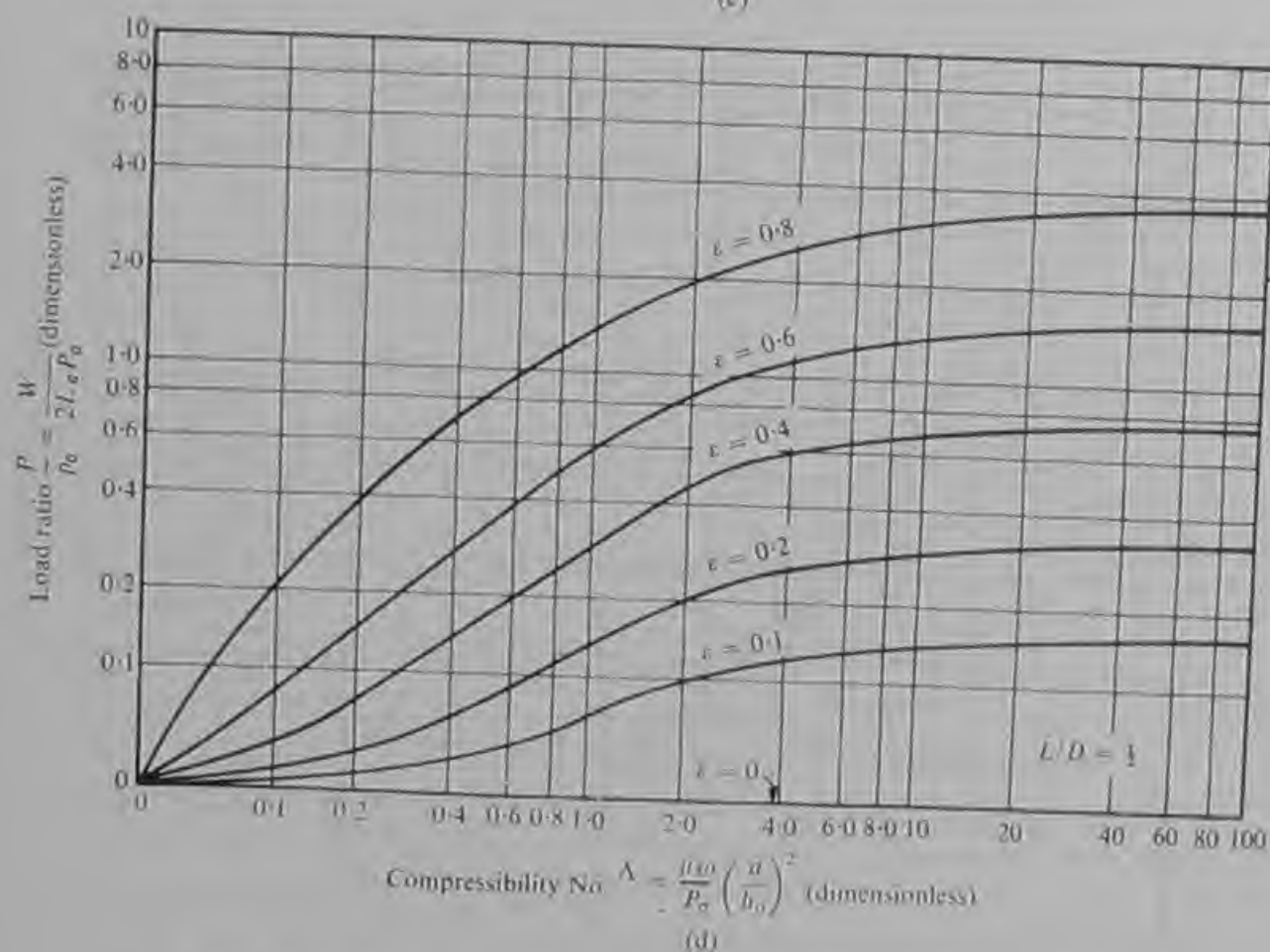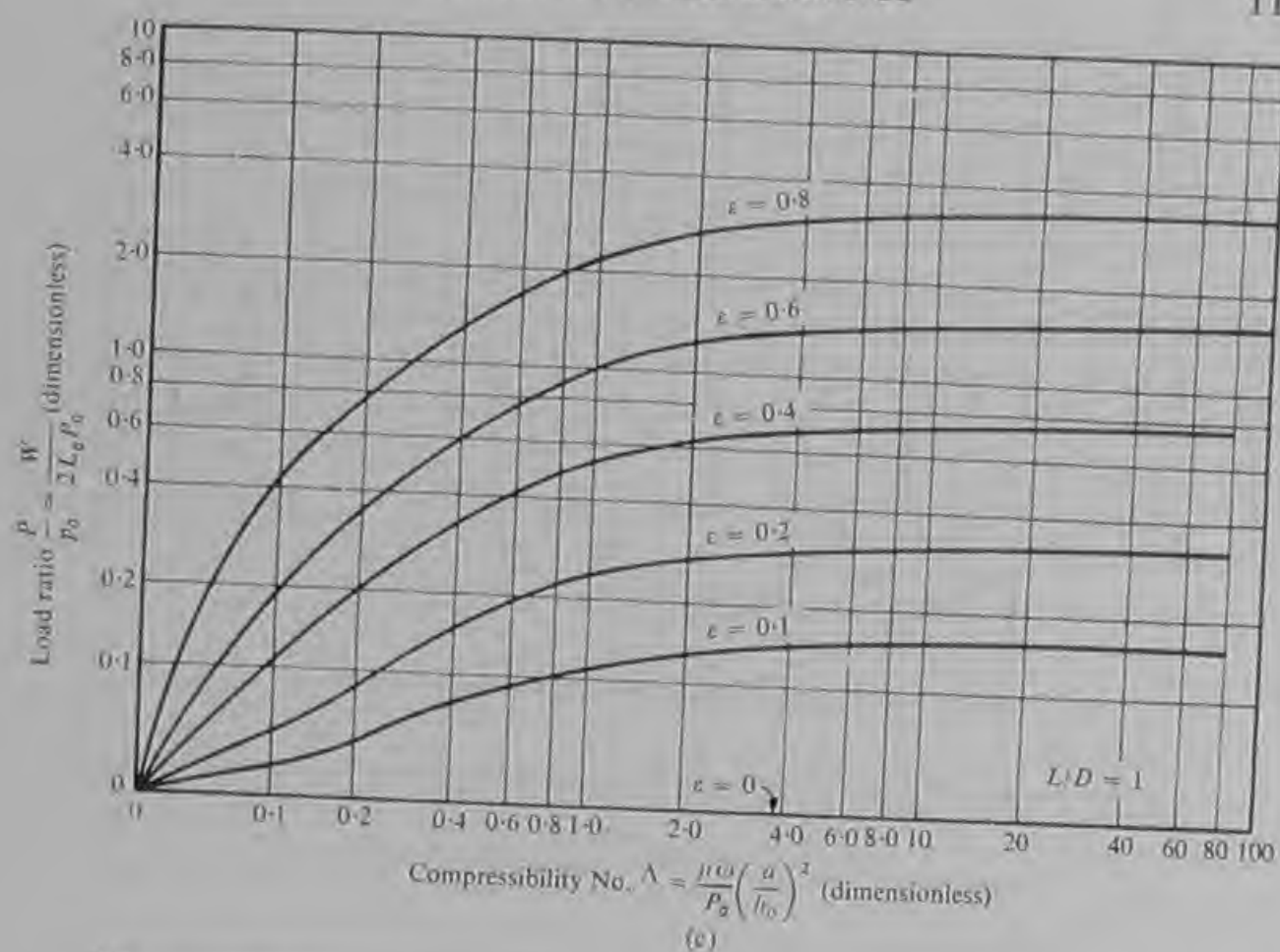
Fig. 5.4c Design charts for load capacity of a 360 degree
cylindrical journal bearing $L/D = 1$

Fig. 5.4d Design charts for load capacity of a 360 degree
cylindrical journal bearing $L/D = \frac{1}{2}$

Fig. 5.5a Design charts for attitude angle in a 360 degree
cylindrical journal bearing $L/D = \infty$

Fig. 5.5b Design charts for attitude angle in a 360 degree
cylindrical journal bearing $L/D = 2$

Fig. 5.5c Design charts for attitude angle in a 360 degree
cylindrical journal bearing $L/D = 1$

Fig. 5.5d Design charts for attitude angle in a 360 degree
cylindrical journal bearing $L/D = \frac{1}{2}$
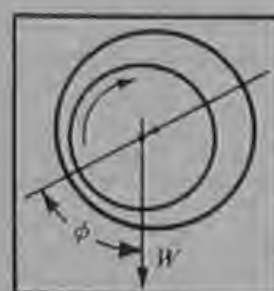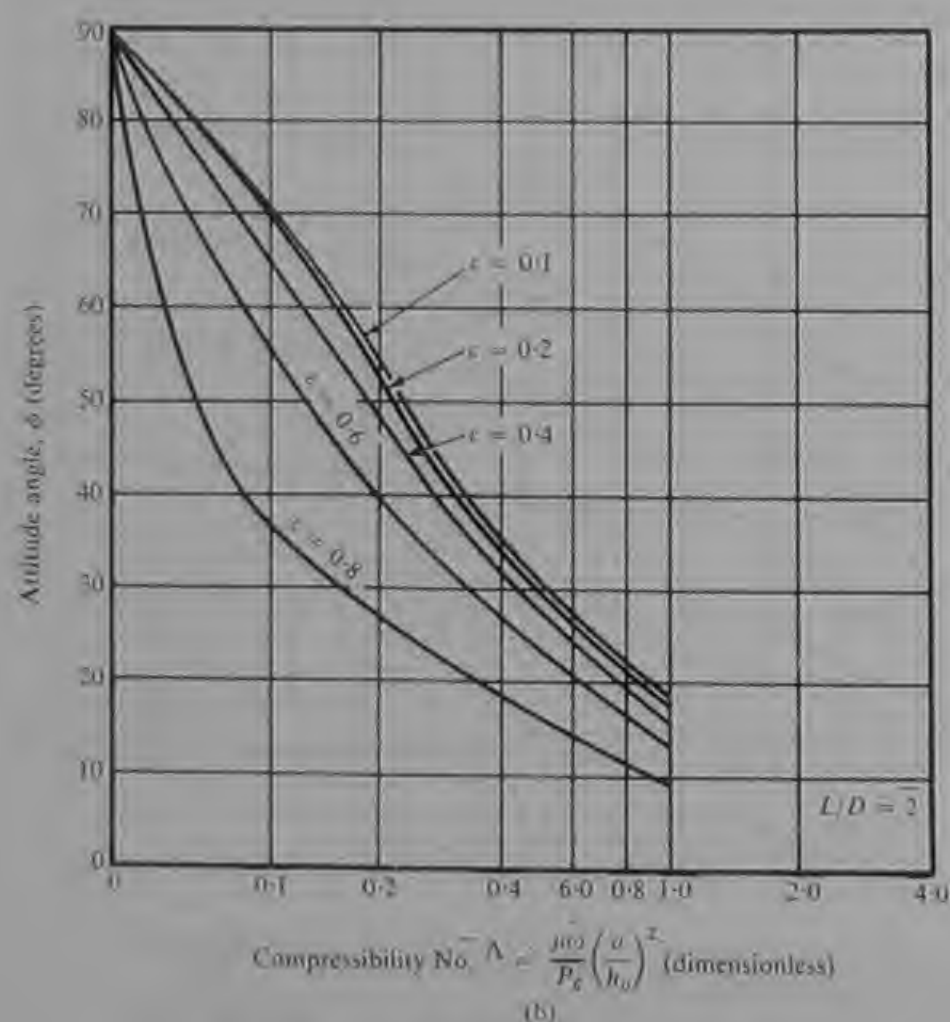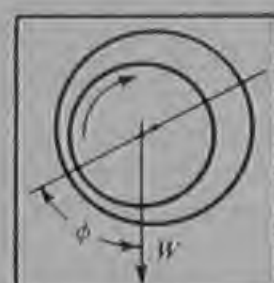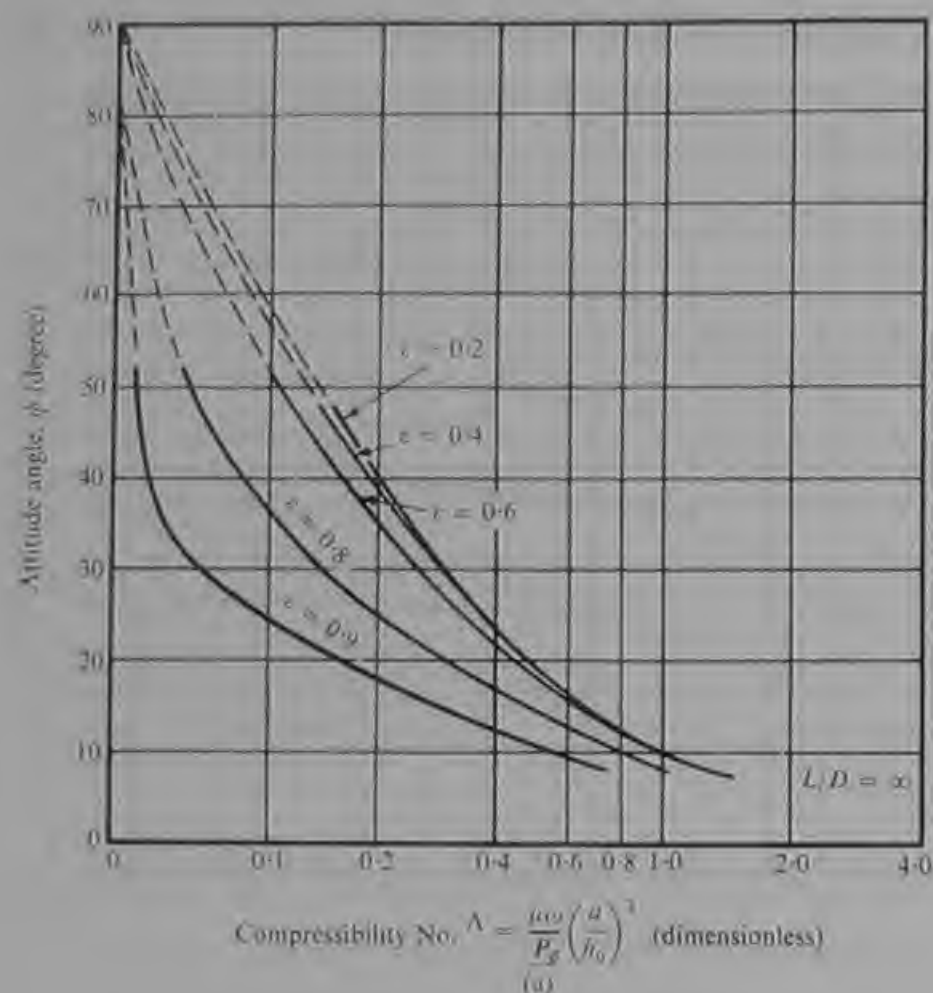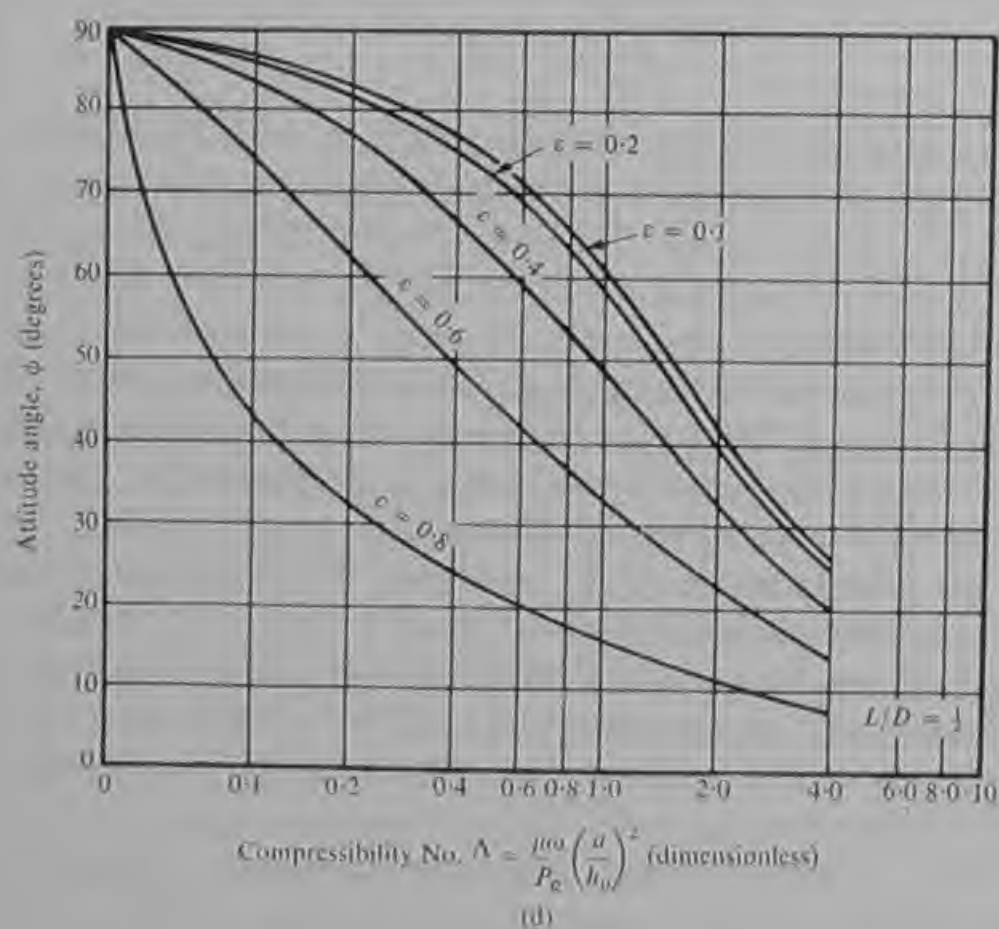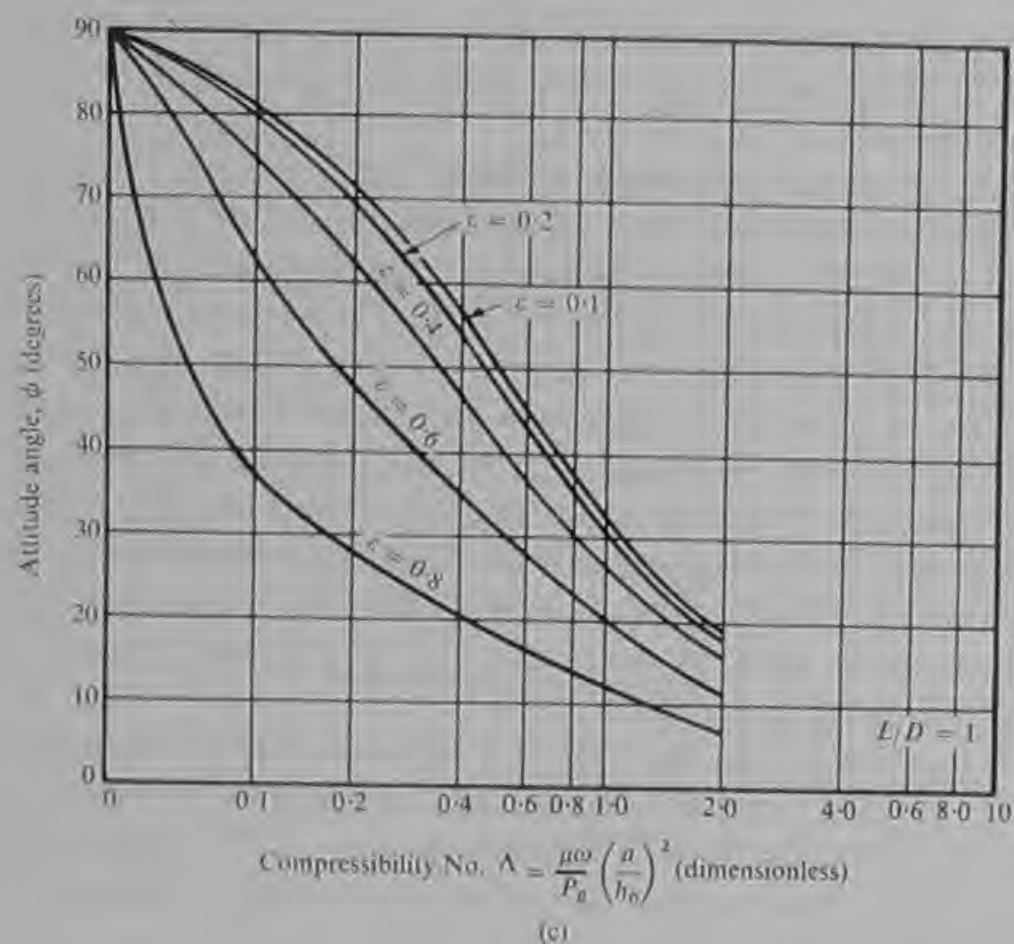
Thus at low values of Λ the deflection is almost at right angles to the applied load and at high values of Λ the deflection is almost in line with the applied load.

The load capacity of an aerodynamic journal bearing is also dependent upon the length-to-diameter ratio of the bearing. Long bearings are more efficient for load carrying than short bearings owing to the lessened effect of end leakage. Typical pressure distributions around the centre of a loaded aerodynamic journal bearing are shown in Fig. 5.3. Considerable pressure variation is generated extending both above and below the ambient pressure P_a. At the ends of the bearing gas is forced out from the bearing in the region of high pressure and drawn into the bearing in the region of low pressure. By this means the pressure difference is greatly reduced at the ends of the bearing and the resulting reduction in load capacity is proportionately greater in short bearings than in long bearings.

Design charts for aerodynamic journal bearings have been computed by Raimondi (Ref. 13) and these are reproduced in Figures 5.4 and 5.5. The former gives the variation of the dimensionless load P/P_a against Λ for various eccentricity ratios and for length-to-diameter ratios of ∞, 2, 1, and $\frac{1}{2}$, where

$$P = \frac{W}{LD}.$$

Fig. 5.5 gives the variation of the attitude angle ϕ with Λ for the same eccentricity ratios and length-to-diameter ratios.

5.2 Hybrid journal bearings

Early experimenters found that aerostatic journals could be made to function at relatively large clearances, whereas aerodynamic journal bearings required small clearances if a suitably large value of Λ and a useful load capacity were to be achieved. Thus early aerostatic bearings showed little or no aerodynamic effect and their load capacity was considered to be effectively independent of speed. However, as aerostatic bearings became made at smaller clearances, in order to provide greater stiffness and lower gas consumption, it was discovered that their load capacity increased with speed. It was also found that although the shaft deflection occurred in the direction of the applied load in a stationary aerostatic bearing, when the shaft was rotating an attitude angle developed which increased with speed. These two effects are shown in Fig. 5.6 for an experimental bearing tested by Powell (Ref. 9). The bearing was tested at a constant load and the increasing load capacity was manifested by a reducing eccentricity ratio as the speed increased.

Fig. 5.6 Variation of eccentricity ratio and attitude angle
with speed for a hybrid journal bearing at constant load

It was found that the same bearing could operate in three modes: purely aerostatically if fed at some pressure above ambient but with no rotation; purely aerodynamically when rotating but with no pressure feeding; and in a hybrid mode when both pressure feeding and rotation occurred together. These three modes of operation are compared in Fig. 5.7 which also illustrates the large effect that radial clearance exercises upon the aerodynamic and hybrid performance of the bearing. The aerostatic performance was measured for constant jet diameter but with jet diameter optimized for clearance the aerostatic load capacity would be independent of clearance. It was found that in bearings of small clearance the aerodynamic effect could increase the load capacity to two or three times the aerostatic load capacity. It is essential therefore that this effect is taken into account in the design of bearings for operation at high speeds.

5.3 Design of hybrid bearings

The first step in considering the aerodynamic effect in a hybrid gas bearing is to define a compressibility number:

$$\Lambda_H = \frac{\mu\omega}{P_m}\left(\frac{a}{h_o}\right)^2. \tag{59}$$
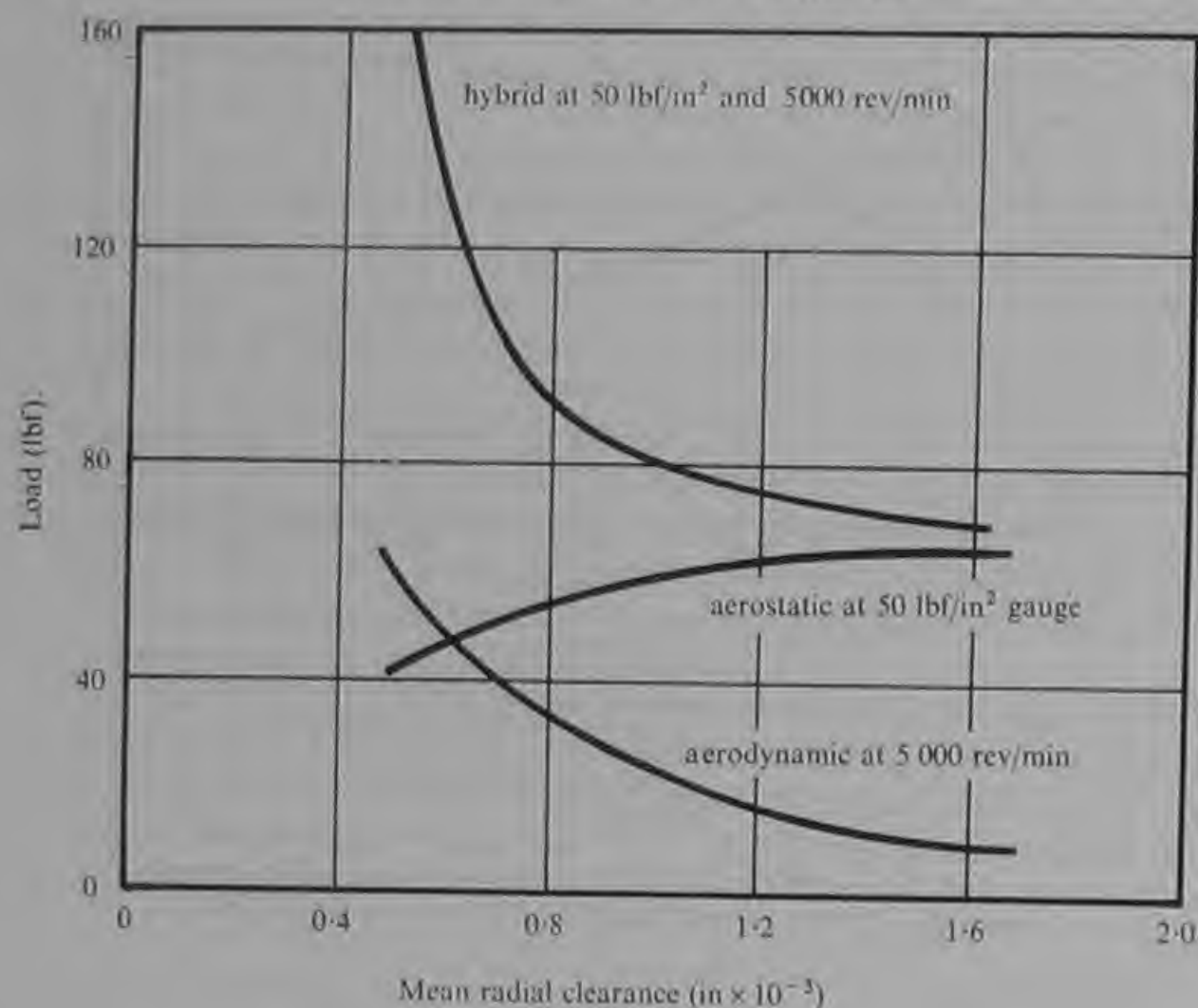
Experimental data: Bearing diameter—2 in
                   Length—4 in
                   Six pocketed jets of 0·017 in diameter
                   at half station
                   Constant eccentricity ratio, $\varepsilon = 0·4$

Fig. 5.7 Variation of load capacity with mean radial clearance

A difficulty lies in defining a mean pressure P_m. However, when typical values of the various parameters are substituted into equation (59) it becomes apparent that P_m must be large compared to the atmospheric value of P_a and that consequently values of Λ_H tend to be low. This means that hybrid bearings mostly operate in the near incompressible region where the load capacity is almost independent of P_m. Consequently small variations in P_m have little effect on the load capacity of the bearing and for simplicity it is usual to define P_m by the equation:

$$P_m = \frac{P_o + P_a}{2}.$$

$$(60)$$

It has been shown experimentally by Powell (Ref. 9) that the magnitude of the aerodynamic effect in increasing the load capacity of the bearing is related to the compressibility number.

While there is little theoretical justification for presenting the operation of the hybrid bearing in this way, the designer will find that Fig. 5.8 assists in an attempt to visualize the interaction of the aerostatic

(a) displacement diagram   (b) force diagram
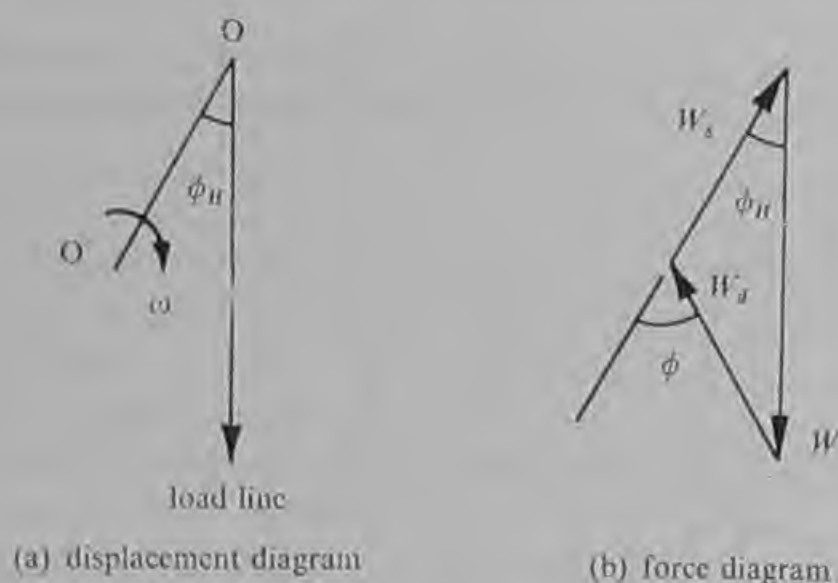
Fig. 5.8 Quasi-static equilibrium in a hybrid journal bearing

and aerodynamic effects. A shaft rotating with angular velocity ω about a centre O' is deflected by a load W a distance $OO' = \varepsilon h_o$ from the centre of the bearing O. The deflection occurs at some angle ϕ_H (hybrid attitude angle) to the direction of the applied load. The resultant pressure force acting on the shaft must be equal and opposite to the applied load. We can consider this resultant force to be made up from two components, one derived aerostatically and the other derived aerodynamically. The aerostatic effect produces a force in the direction opposite to the deflection of the shaft and is denoted in Fig. 5.8 by W_s. The aerodynamic effect produces a force at some angle ϕ to the deflection which is denoted by W_d in the figure. The three forces W_s, W_d and W are shown in equilibrium in Fig. 5.8. Solving the triangle of forces yields

$$W = W_s \cos \phi_H + W_d \cos (\phi - \phi_H) \tag{61}$$

and

$$\cot \phi_H = \frac{W_s}{W_d \sin \phi} + \cot \phi. \tag{62}$$

For eccentricity ratios less than 0·5 the load-displacement characteristic is close to linear in all three modes. Thus for design purposes

equation (61) is often more conveniently written as:

$$\frac{W}{\varepsilon} = \frac{W_s}{\varepsilon}\cos\phi_H + \frac{W_d}{\varepsilon}\cos(\phi - \phi_H). \tag{63}$$

W_s can be calculated by the methods given in Chapter 3 to give the load-carrying performance of the bearing at low speeds. To estimate the load capacity at higher speeds it is necessary to be able to calculate W_d and ϕ.

Fig. 5.9 can be used to assist in a preliminary estimation of the compressibility number in a hybrid air bearing. The curves are plotted
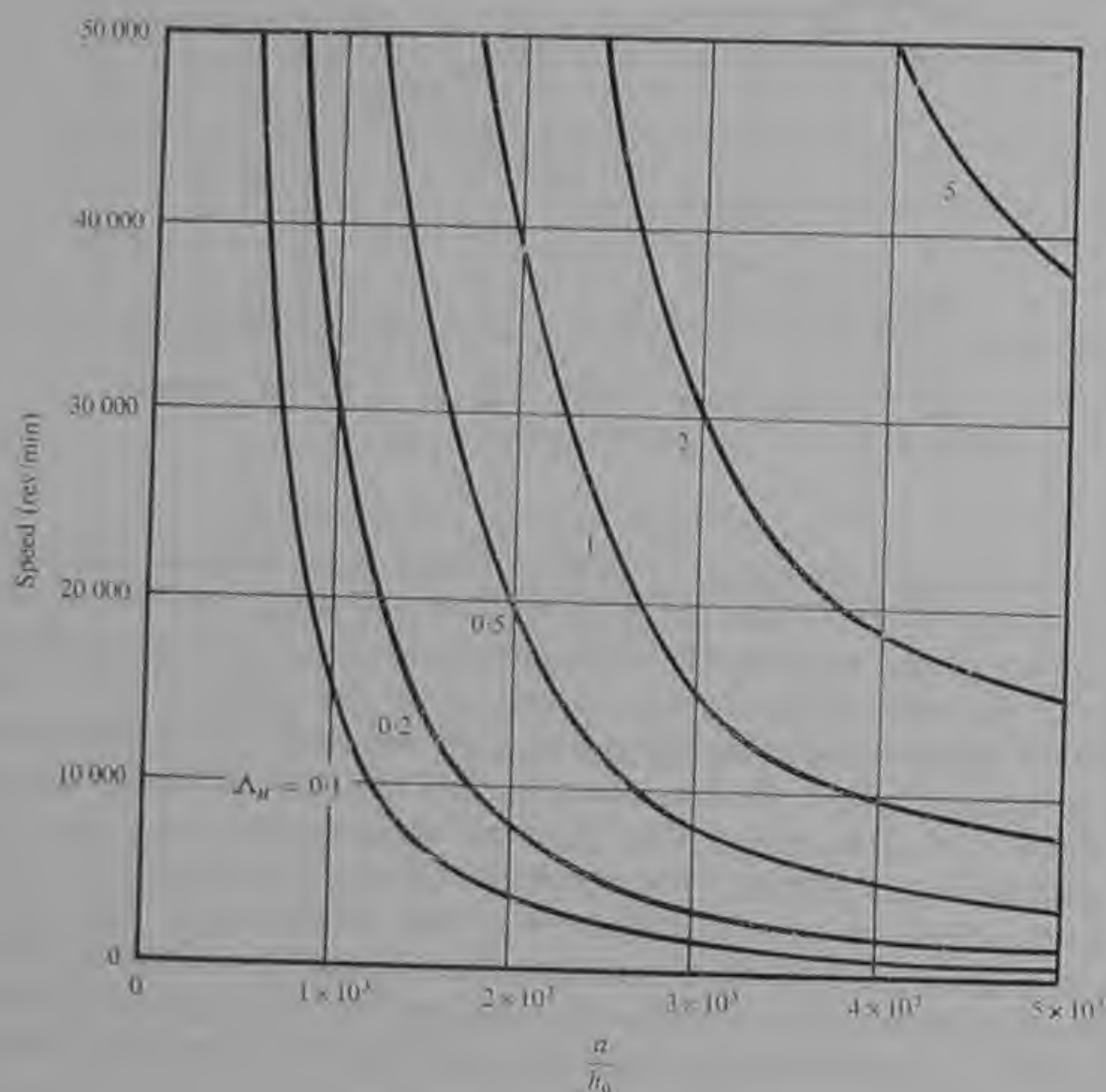
Curves plotted for $P_u - P_a = 50$ lbf/in²
$P_a = 15$ lbf/in²
$P_m = \dfrac{P_u + P_a}{2} = 40$ lbf/in²

Hybrid compressibility number $\Lambda_H = \dfrac{\mu\omega}{P_m}\left(\dfrac{a}{h_0}\right)^2$

Fig. 5.9 Compressibility number in hybrid air journal bearings

for a bearing supplied at 50 lbf/in² gauge and exhausting to atmosphere. Using the appropriate value of Λ_H a value of $\overline{W}_d$ can be obtained from Fig. 5.4. For a hybrid bearing the load ratio becomes $\dfrac{P}{P_m}$ and $\overline{W}_d = \left(\dfrac{P}{P_m}\right) LDP_m$. The bar denotes that the full aerodynamic effect is not realized and so one has

$$W_d = k\overline{W}_d,$$

where k is an empirically derived factor.

Tests carried out by Powell (Ref. 9) indicate that for bearings of length-to-diameter of two the value of k can be taken as 0·7. Within the range of variables tested the value of k did not vary appreciably with feed hole diameter or gauge pressure ratio. Little experimental evidence is available at other length-to-diameter ratios and the value of 0·7 must be applied with caution. However, the performances of some bearings designed at length-to-diameter ratios of unity or below have suggested that the value of $k = 0·7$ can be used at least in an approximate estimation of hybrid load capacity.

5.4 Design examples

A miniature high speed bearing One early example of the application of this design method serves to illustrate the design procedure. Details of an air bearing for a high-speed air turbine dental drill were as follows:

operating speed	500 000 rev/min
bearing diameter	0·187 in ⎱ length-to-diameter
bearing length	0·150 in ⎰ ratio = 0·8
diametrical clearance	0·000 6 in
air supply pressure	50 lbf/in² gauge
design cutting load	3 ozf
ratio of cutting load to front bearing load	0·46
design load for front bearing	6·5 ozf.

In order to allow some excess load capacity to carry out-of-balance loads it was desirable to carry the design cutting load at an eccentricity ratio of 0·5. In a small bearing of this type the bearing surfaces might be expected to touch down at an eccentricity ratio of about 0·7 particularly when the cutting load is applied overhung beyond the bearing.

From Fig. 3.15 it can be seen that the aerostatic performance of the bearing would provide a load coefficient based on diameter of 0·19

at $\varepsilon = 0.5$. Thus the aerostatic load capacity

$$W_s = 0.19 \times 0.187^2 \ (\text{in}^2) \times 50 \ (\text{lbf/in}^2) \times 16 \ \text{oz/lb}$$
$$= 5.3 \ \text{ozf.}$$

This load capacity applies for two rows of eight simple orifices at quarter stations. In fact two rows of six annular orifices at one-eighth station were used. Thus for annular orifices the load is reduced by thirty percent, i.e. a factor of 0.7; for six feed holes per row the load is reduced by a factor of 0.88 (from Fig. 3.13); for one-eighth station feed holes the load is increased by a factor of $\frac{2.6}{2.4} = 1.08$ (from Fig. 3.14). Thus the final aerostatic load capacity

$$W_s = 5.3 \times 0.7 \times 0.88 \times 1.08 \ \text{ozf}$$
$$= 3.5 \ \text{ozf,}$$

which is barely half of the required load capacity at $\varepsilon = 0.5$ and even if an eccentricity ratio of 0.9 could be achieved the load capacity would be only about 5.7 ozf.

The hybrid compressibility number

$$\Lambda_H = 1.2 \times 10^{-5} \ (\text{lb/ft s}) \times \frac{1}{40} \ (\text{in}^2/\text{lbf}) \times \frac{2\pi \times 500\,000}{\text{min}}$$

$$\times 9.7 \times 10^4 \times \frac{\text{min}}{60 \ \text{s}} \times \frac{\text{lbf sec}^2}{32.2 \ \text{lb ft}} \times \frac{\text{ft}^2}{144 \ \text{in}^2}$$

$$= 0.33.$$

Applying this value of Λ_H to Fig. 5.4 yields, at $\varepsilon = 0.5$,

$$\frac{P}{P_m} = 0.38 \quad \text{for} \quad \frac{L}{D} = 1.0$$

and

$$\frac{P}{P_m} = 0.15 \quad \text{for} \quad \frac{L}{D} = 0.5.$$

Taking a value of 0.3 by linear interpolation for $\frac{L}{D} = 0.8$ gives

$$\overline{W}_d = 0.3 \times 0.187 \times 0.150 \times 40 \times 16 \ \text{ozf}$$
$$= 5.4 \ \text{ozf,}$$

while Fig. 5.5 yields

$$\phi = 45° \quad \text{for} \quad \frac{L}{D} = 1.0$$

$$\phi = 63° \quad \text{for} \quad \frac{L}{D} = 0.5.$$

Taking a value of $\phi = 50°$ and a value of $W_d = 0.7\ \overline{W}_d = 3.8$ ozf gives by substitution in equation (62)

$$\cot \phi_H = \frac{3\cdot5}{3\cdot8 \sin 50°} + \cot 50°$$

$$= \frac{3\cdot5}{3\cdot8 \times 0\cdot766} + 0\cdot839$$

$$= 2\cdot04.$$

$$\phi_H = 26\cdot1°.$$

Alternatively equation (62) can be solved quickly but approximately by the use of Fig. 5.10. Substituting in equation (61) gives

$$W = 3\cdot5 \cos 26\cdot1° + 3\cdot8 \cos 23\cdot9°\ \text{ozf}$$

$$= 3\cdot5 \times 0\cdot898 + 3\cdot8 \times 0\cdot914\ \text{ozf}$$

$$= 6\cdot6\ \text{ozf}.$$
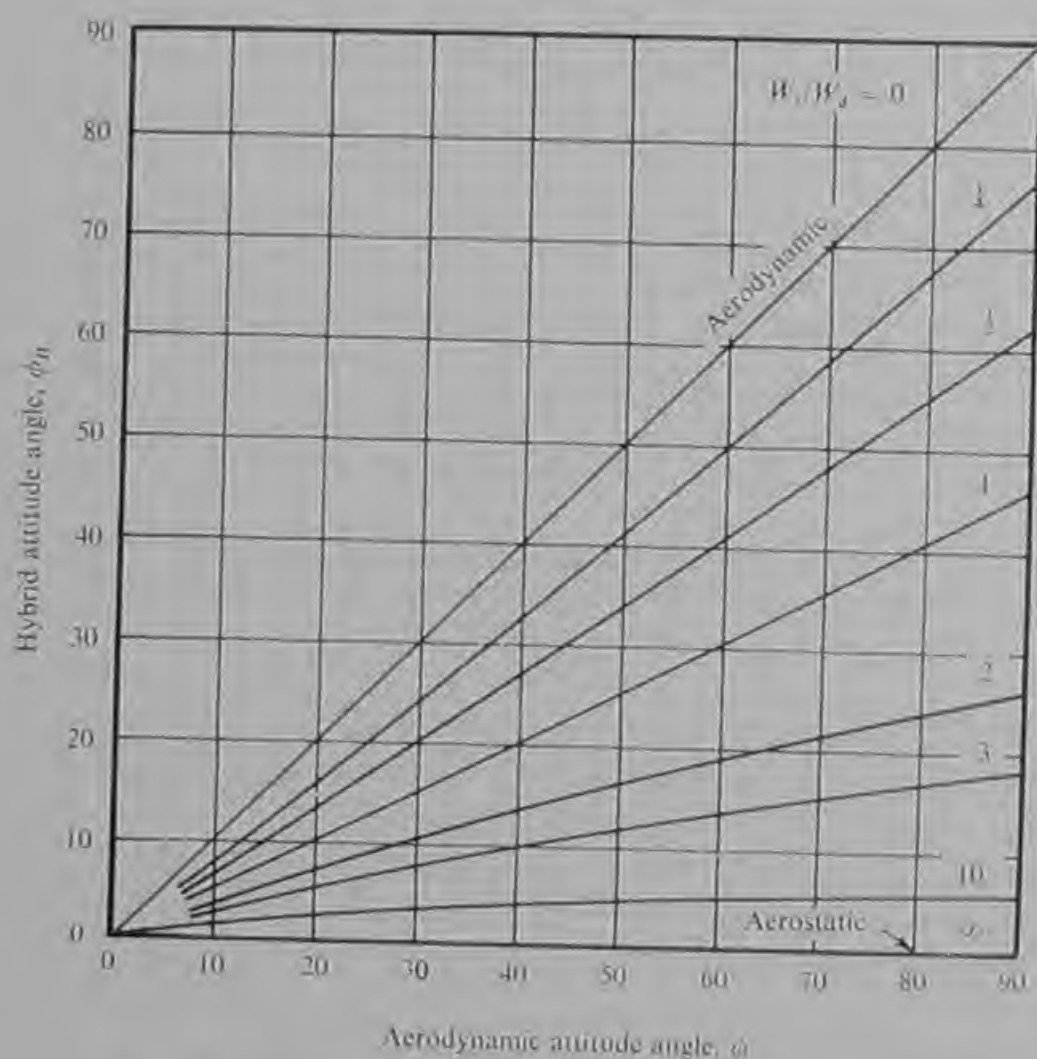
Fig. 5.10 Design of hybrid journal bearings—attitude angle

These calculations suggest that the required cutting loads can be carried. This result is confirmed in practice since the bearing is overloaded when a cutting load is applied in excess of 5 ozf. This represents a bearing load of 10·9 ozf and suggests that the bearing touches down at an eccentricity ratio near 0·7.
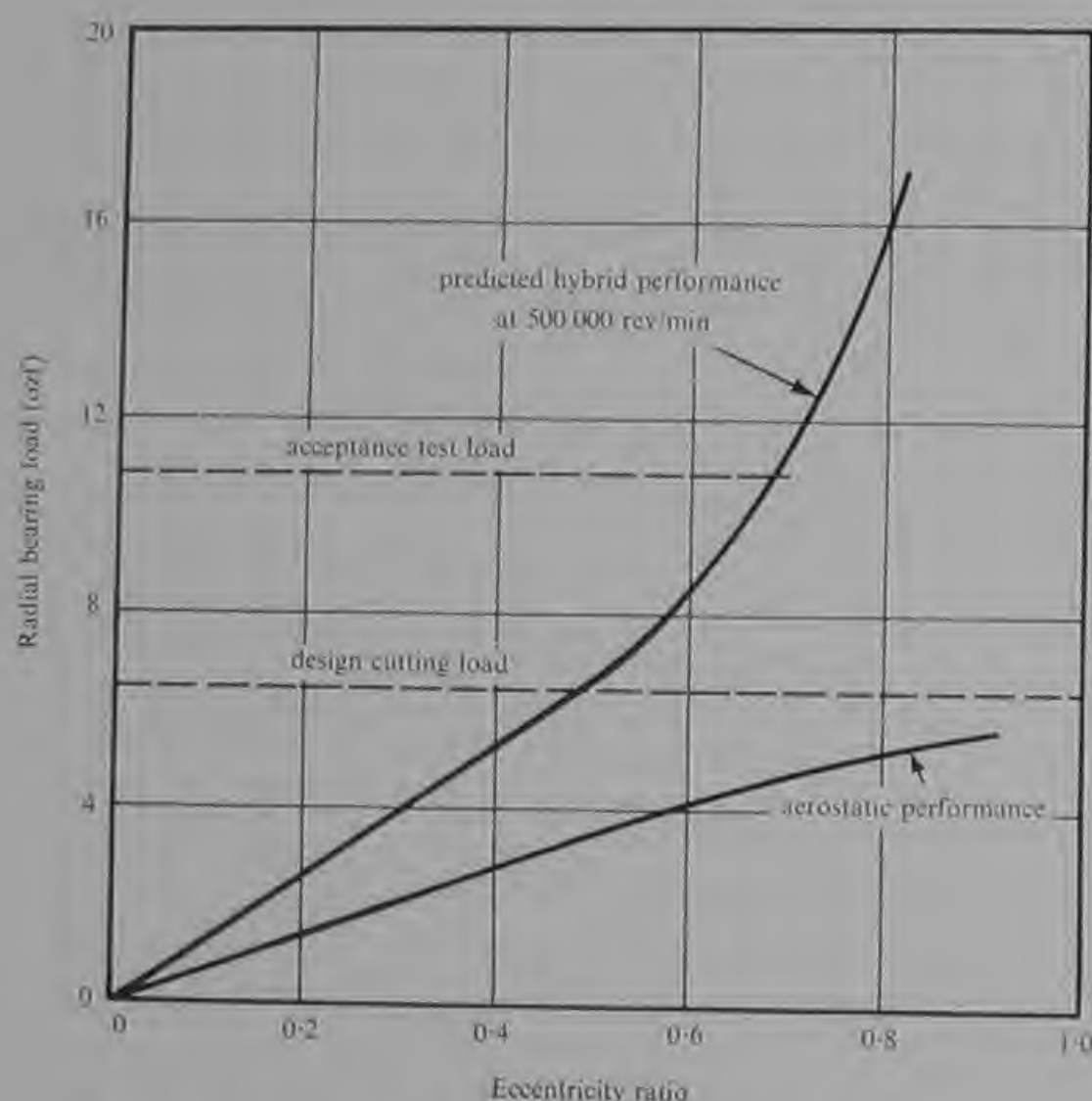
Fig. 5.11 Predicted performance of dental drill bearing compared to acceptance test load and design cutting load

The predicted performance of the bearing is shown in Fig. 5.11. The load capacity at higher eccentricity ratios is obtained by repeating the same calculations with aerostatic and aerodynamic loads appropriate to the eccentricity ratio. The design cutting load and the acceptance test load are also shown. No account is taken of dynamic loads since at these high speeds the rotor spins about its mass centre and is said to be inverted. However, the rotor does orbit in the bearing with a small amplitude and this accounts for part of the lost bearing clearance. The remainder is accounted for by geometric errors in the bearing surfaces and misalignment between the two journal bearings.

This example is of interest because it illustrates that the design method can usefully be applied in an extreme case of small size and high speed. If only aerostatic performance had been considered the project might well have been abandoned at the feasibility stage.

A larger lower speed bearing A second example of this design procedure considers a bearing with the following dimensions:

Diameter	2·0 in	
Length	4·0 in	$L/D = 2·0$
Mean radial clearance, h_o	0·000 62 in	
Design supply pressure	50 lbf/in^2 gauge	
Exhaust pressure	15 lbf/in^2 gauge	

Feed holes—one row of eight simple orifices with circular pockets at half station;

Feed hole diameter 0·005 8 in.

From Fig. 3.8(c) it can be seen that for the same gauge pressure ratio K_{go} the jet diameter at a length-to-diameter ratio of two is 0·7 of the jet diameter at an L/D of one. Thus the equivalent jet diameter for an L/D of one

$$= \frac{0·005\ 8}{0·7}\ \text{in}$$

$$= 0·008\ 3\ \text{in}.$$

Using this jet diameter together with the diametrical clearance of 0·001 24 in in Fig. 3.7 indicates that the bearing operates at a gauge pressure ratio of about 0·75. This value is within the recommended design range and the aerostatic performance can be derived from the design charts given in Chapter 3. From Fig. 3.15 it can be seen that the load coefficient based on diameter $C_L' = 0·24$ at $\varepsilon = 0·5$.

Thus

$$W_s = 0·24 \times 2^2 \times 50\ \text{lbf}$$

$$= 48\ \text{lbf}.$$

$$\frac{a}{h_o} = \frac{1}{0·000\ 62}$$

$$= 1·16 \times 10^3.$$

From Fig. 5.9 it can be seen that for this value of $\dfrac{a}{h_o}$, $\Lambda_H = 0·1$ at a speed of 5 800 rev/min. Thus

$$\text{at 2 500 rev/min, } \Lambda_H = 0·043;$$

$$\text{at 5 000 rev/min, } \Lambda_H = 0·086;$$

and

$$\text{at 7 500 rev/min, } \Lambda_H = 0·129.$$

At 2 500 rev/min and $\varepsilon = 0.5$, Fig. 5.4(b) gives $\dfrac{P}{P_m} = 0.12$, and Fig. 5.5(b) gives $\phi = 74°$.

Thus

$$\overline{W}_d = 0.12 \times 2 \times 4 \times 40 \text{ lbf} = 38.5 \text{ lbf}$$

and

$$W_d = k\overline{W}_d = 0.7 \times 38.5 \text{ lbf} = 27 \text{ lbf};$$

at

$$\varepsilon = 0.5 \quad \frac{W_s}{W_d} = \frac{48}{27} = 1.68.$$

Using this value together with $\phi = 74°$ in Fig. 5.10 gives $\phi_H = 28°$. Then from equation (61)

$$\text{the total load } W = 48 \cos 28° + 27 \cos 46° \text{ lbf}$$

$$= 61.5 \text{ lbf}$$

Repeating the calculation at 5 000 rev/min gives $W = 83$ lbf and $\phi_H = 32°$. Repeating the calculation at 7 500 rev/min gives $W = 107.5$ lbf and $\phi_H = 34°$.

These design predictions are compared to the measured bearing performance in Fig. 5.12. The measured aerostatic load with no shaft rotation was some ten percent in excess of the predicted load. However, the predicted hybrid loads are in good agreement with the measured loads and it is of interest to note that at 7 500 rev/min the load capacity and radial stiffness are double the standstill values. The measured attitude angles in the hybrid bearing are in approximate agreement with the design predictions and show the same trend of increasing attitude angle with speed.

5.5 Application of design method

There is no rigorous theoretical foundation for the prediction of hybrid journal load capacity by the method of linear superposition which has been described. However, in the absence of an alternative its application can be justified on the following grounds.

(a) It predicts qualitatively the variation of load capacity and attitude angle with speed, clearance, bearing dimensions and mean pressure.

(b) It permits the prediction of load capacity to an accuracy of ten percent by the application of empirical correction factors. For bearings of length-to-diameter ratio of two a factor of 0.7 has been established. There is some experimental evidence that this factor may apply approximately at other length-to-diameter ratios.

(c) The method is quick and simple, needing only the design charts and a slide rule.

Upper chart labels:
- $D = 2.0$ in
- $L = 4.0$ in
- $h_0 = 0.000\,62$ in
- $P_o - P_a = 50$ lbf/in^2
- $P_a = 15$ lbf/in^2
- $n = 8$, at half station
- $d = 0.005\,8$ in
- $K_{go} = 0.75$

Upper chart axes: Radial load (lbf) vs Eccentricity ratio
Curves: 7500 rev/min, 5000 rev/min, 2500 rev/min, aerostatic

Lower chart axes: Hybrid attitude angle (degrees) vs Eccentricity ratio
Curves: 7500 rev/min, 5000 rev/min, 2500 rev/min
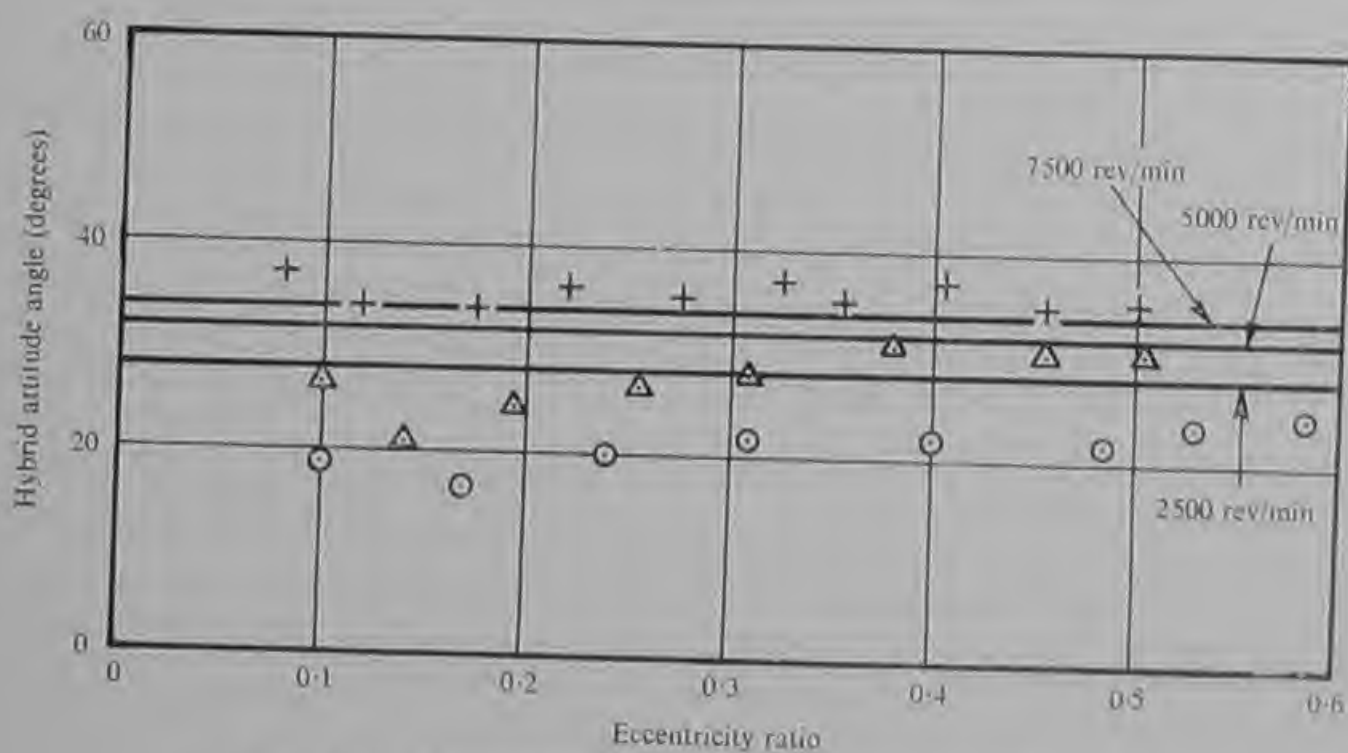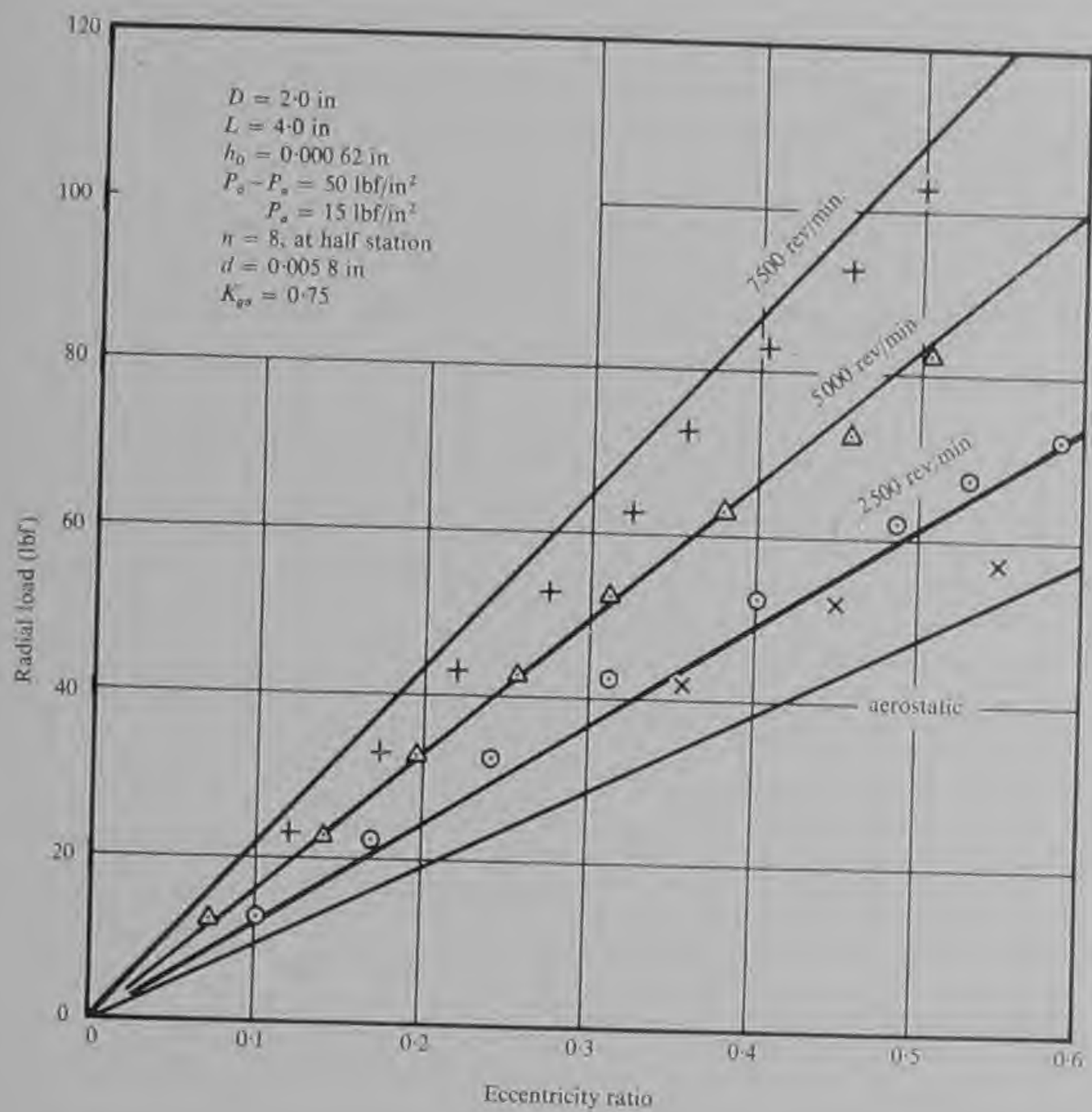
Fig. 5.12 Comparison of design prediction with tested performance of a hybrid air journal bearing

(d) It has provided satisfactory bearing performance predictions in numerous instances and in the author's experience has not been found seriously in error.

There are many applications of aerostatic bearings in which aerodynamic effects are negligible and need not seriously be considered at the design stage. Such applications include cases where a rotational speed of less than 3 000 rev/min is combined with a clearance ratio $\left(\dfrac{a}{h_o}\right)$ of less than 10^3 and a length-to-diameter ratio of less than 1·0. In other applications where the principal loading is static and applied at all speeds including standstill, the bearing must be designed to carry this load aerostatically and any aerodynamic augmentation of load capacity only serves to offset the dynamic loading which arises owing to unbalance or other effects.

There are some applications, of which the air turbine dental drill is an example, where the required bearing performance could not be achieved purely aerostatically. In such cases the bearings must be designed from the outset as hybrid bearings and consideration must be given to adjusting the bearing dimensions to achieve a high aerodynamic contribution. In this connection it may be necessary to design at a smaller clearance or at a greater length-to-diameter ratio than would optimize the bearing aerostatically. The design procedure becomes more complex and requires a greater number of trial configurations before the final design evolves.

Designing a hybrid gas journal bearing usually implies that the bearing will operate at moderate or high speeds. This in turn involves a consideration of the effect of unbalance forces, bearing film critical speeds and self-excited whirl instabilities. These factors are described in Chapter 7 which may be read in conjunction with the present chapter to cover most aspects of the design of bearings for high-speed machines.

CHAPTER 6

DESIGN OF AEROSTATIC MACHINES

6.1 Introduction

In machines in which it is intended to employ aerostatic bearings it is essential that the requirements of the bearings are considered at every stage of the machine design. It is seldom possible and almost always unsuccessful to take an existing machine design with conventional bearings and to engineer aerostatic bearings within the same space and shape. In aerostatic machines the bearings invariably occupy a larger proportion of the total volume than in machines with conventional bearings. This does not necessarily imply that the machine with aerostatic bearings is any larger or heavier than its counterparts. For example, in high speed electric motors the reduced bearing friction usually permits a smaller motor to be used to provide the same output power. In small turbo-compressers used in the temperature control systems of aircraft the change from ball bearings to air bearings involves no increase in weight since, although the structure of the air bearings is heavier, a sump with several pounds of oil is no longer required.

Aerostatic bearings have been employed in machines driven by most types of electric motors and most types of turbine. They have also been employed in a wide range of machine tool spindles driven by various types of belts and flexible couplings. In all these cases the driving torque is evenly and smoothly applied and, excepting the case of driving by means of a belt, the drive does not apply large loads to the bearings. Aerostatic bearings are most successful when operating under these conditions. They are much less likely to be successfully applied to machines with pulsating drives which impose large internal loads on the bearings. Thus aerostatic bearings have not found application to reciprocating machines or rotating vane machines and future designers should approach such applications with caution.

6.2 Alternative configurations

It would be impossible to consider all the possible configurations of machines with aerostatic bearings, but it is intended to give a general guide to the application of these bearings based on experience of a wide range of applications. It is hoped by this means at least to prevent the reader repeating the mistakes of the author and at most, provided enough mistakes have been made from which a lesson has been learned,

to provide a reliable basis for the future widescale utilization of
aerostatic bearings.

The simple machine tool spindle consisting of a shaft, bearings and
body exhibits most of the features pertinent to the successful applica-
tion of aerostatic bearings. A study of this simple aerostatic machine
forms a sound basis upon which the designer can build when con-
sidering machines with integral drives. Fig. 6.1 shows the basic con-
figuration and the important design factors. The shaft extends at both
ends of the body. One end carries a tool, for example a grinding wheel,
to which both radial and axial loads are applied. The other end carries
a pulley driven by a belt. It is essential that from the outset the applied
loads are known with regard to magnitude, direction and point of
application. Unbalance will also constitute an additional radial load
but this will be small in relation to the applied loads since the spindle
will need precise dynamic balancing to limit the run-out of the tool.
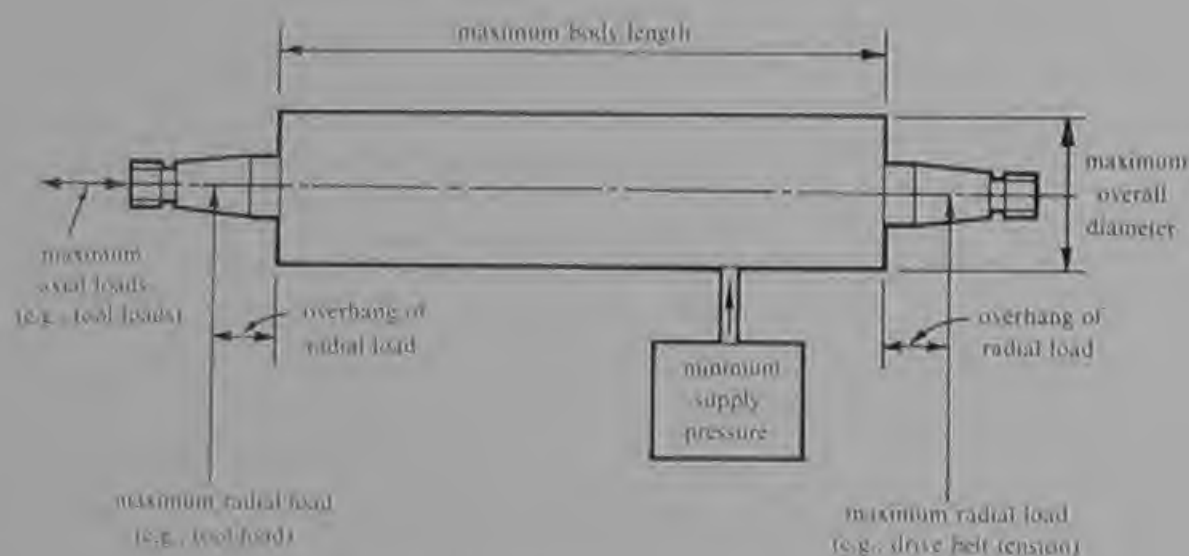
Fig. 6.1   Factors limiting the design of a machine tool
spindle with aerostatic bearings

The load capacity and rigidity that can be provided within the
spindle will be limited by the maximum permissible overall dimensions
and the minimum supply pressure at which the bearings are required
to operate. Having established these external limitations the designer
can proceed to establish whether the required performance is possible.
There are numerous possible bearing configurations from which to
choose, some of which are shown in Fig. 6.2. In each case two journal
bearings and two annular thrust bearings are used. The annular thrust
bearings are dictated by the need for the shaft to extend at both ends
of the body.
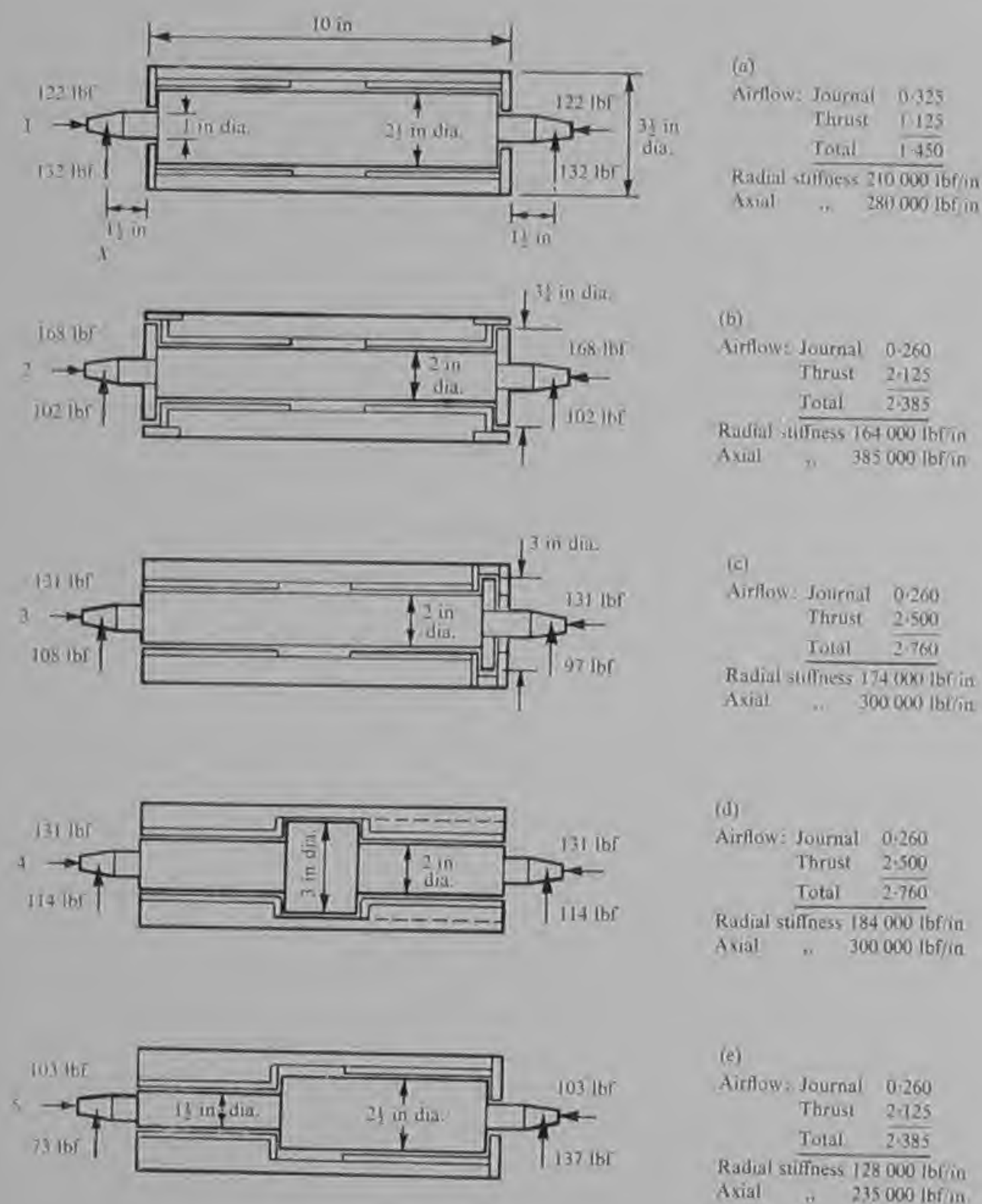
Maximum loads and airflow given for 80 lbf/in² gauge supply pressure.
All air film thicknesses 0·000 5 in at zero load.
All dimensions equal to those given for 1 unless stated.
Airflow given in c.f.m. free air volume. Radial stiffness given at 'X'.

Fig. 6.2 Some possible bearing configurations for a machine tool spindle

In order to provide a numerical basis of comparison it is assumed that the outside body dimensions in all cases are 10 in long and 3·5 in diameter and that the radial loads are applied 1·5 in from the ends of the body. In each case the radial load capacity is calculated for a journal bearing eccentricity ratio of 0·8. All gas film thicknesses are taken as 0·000 5 in when no load is applied to the shaft. The thrust loads are those calculated to bring the bearing surfaces into contact. For the sake of simplicity all the journal bearings are taken to be 3·5 in long and to be fed by two rows of eight feed holes with circular pockets at one-quarter stations.

The load capacity and the airflow of the journal bearings can be quickly assessed at the feasibility study stage by reference to Fig. 3.2. In all cases the values of load are corrected to an air supply pressure of 80 lbf/in² gauge, which would be typical of most machine tool applications, and are multiplied by 1·49 to give the load at 0·8 eccentricity ratio. In calculating the radial load carried on the shaft ends it is assumed that the bearing lift operates on the centre line of the bearing. The thrust bearing performance can be quickly assessed by reference to Fig. 4.2. In all cases two thrust bearings are loaded one against the other and in accordance with Fig. 4.8 the ultimate load is taken to be twenty-five percent greater than the design load given by Fig. 4.2. Again the values obtained are corrected to an air supply pressure of 80 lbf/in² gauge.

In the first configuration the primary design objective might be the provision of the largest possible radial load capacity. To achieve this end the journal bearing is of the largest practicable diameter. With such an arrangement the outside diameter of the thrust bearing is limited to the diameter of the journal bearing and so the axial load capacity and stiffness are low in comparison at least with the second configuration. However, the ratio of the outer thrust bearing diameter to the inner diameter at 2·5 is the largest value of any of the five designs considered and as a result the air consumption of this configuration is the lowest. It is of interest to note that this result is achieved in spite of the journal bearing airflow being greater than in the four other examples. This illustrates the overriding influence of the thrust bearings on the total air consumption.

The first configuration has much to commend it and was chosen in several of the early designs which first demonstrated the advantages of using air bearings on precision grinding machines. This work was carried out at the National Engineering Laboratory at East Kilbride, Glasgow, by H. L. Wunsch and others (Ref. 14). However, this configuration has several major disadvantages when one considers the manufacture and installation of more than a few prototype spindles. One disadvantage is the thin body wall which is particularly vulnerable

to distortion when fixed into a machine casting. Radial clamping, which is a popular means of retaining conventional machine tool spindles, is undesirable with any air bearing and is practically impossible with this thin-walled design. The fixing problem can be overcome by fitting the spindle into an accurately machined bore and retaining by bolting through a flange on the spindle body. However, the thin-walled body still remains vulnerable to distortion if the material is not completely stress-relieved.

Another undesirable feature which the first configuration shares with the second is the long distance between the thrust faces. This raises two problems. Firstly, it is difficult to set the end float precisely during manufacture and the assembly procedure invariably involves two or three trial builds alternating with grinding to adjust either the shaft length or the body length. Secondly, the end float is likely to vary with changes of temperature due to differential thermal expansion. It has been found with spindles of either of the first two configurations that if the total end float is less than about 10^{-4} inches per inch of thrust bearing separation the effects of differential expansion can be significant even when the same material is used for the shaft and the body.

In fairness to the early N.E.L. designs it should be stated that both the journal bearing and thrust bearing clearances were twice the values given in this example. Thus the bearings were somewhat less vulnerable both to clamping stresses and to differential thermal expansion. Further, with these large bearing clearances with their resulting high airflows the first configuration becomes relatively more attractive since any of the alternatives would have further increased the airflow. An early N.E.L. design is shown in Fig. 6.3.
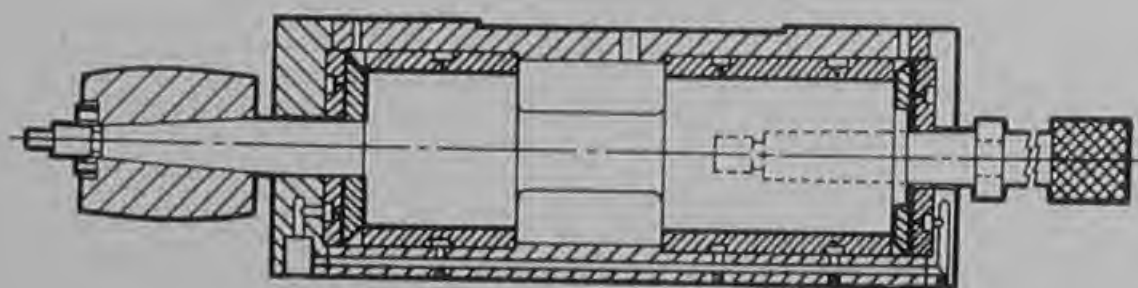

Fig. 6.3 Air bearing wheelhead for internal grinding designed at the National Engineering Laboratory, East Kilbride, Scotland (Ref. 14)

In the second configuration some radial load capacity is lost in providing a higher thrust load capacity and higher axial stiffness. A significant sacrifice is made in terms of air consumption. This

configuration has the advantage of lending itself to engineering within a small body diameter since a part of the large thrust load capacity can be spared in reducing the outside thrust diameter. In some cases where the spindle body diameter is strictly limited it may offer the only solution which provides adequate radial and axial load capacity. However, this configuration has a number of shortcomings. It shares with the first configuration the difficulties associated with widely spaced thrust faces. Setting the end float is considerably simplified in this case by using a thin spacing washer locating on the shaft between the shaft shoulder and one thrust runner. The end float is then adjusted during assembly by surface grinding or lapping the washer to the appropriate thickness.

The second configuration has been applied in several machine tool applications but except where the body diameter is limited it is not recommended. The shaft structure is complex, requiring two true running thrust runners. One thrust runner can be made integral with the shaft but it is debatable whether there is a net advantage owing to the difficulties of grinding into the corner with the required precision, and the need to use considerably larger bar stock material. This type of configuration has successfully been applied to vertical spindle roundness measuring machines. In this case only one thrust bearing was used and many of the difficulties were consequently avoided.

The third configuration offers lower radial load capacity than the first and lower axial load capacity than the second. It also demands the highest airflow. However, from most practical aspects concerning manufacture and installation it is the most attractive configuration. The advantages are derived from the location of both thrust bearings at one end of the spindle on opposite sides of the single thrust runner. Setting the end float is no longer a trial-and-error procedure since the end float can be pre-set by grinding the spacing ring to a thickness exceeding the thickness of the thrust runner by the desired amount. It is interesting to note that on a spindle of the size and clearances used in this example the free axial movement of the shaft after assembly is a few ten thousandths of an inch less than the difference between the thickness of the spacing ring and the thickness of the thrust runner.

Another advantage of this configuration is that the thrust bearing assembly consisting of two static thrust plates, the spacing ring and the thrust runner can be produced as a matched set independently of the spindle body and shaft. This considerably simplifies the final assembly of large batches of spindles since selective assembly is eliminated by the ability to assemble any matched thrust set to any matched body and shaft. It also provides the possibility of quickly changing *in situ* any thrust bearing parts which become damaged in use through accidental overload.

The third configuration does not suffer from variation of end float due to differential thermal expansion since the thrust faces are close together and not separated by the whole length of the body. As a result, the choice of materials for the body and shaft is considerably widened. Air feed holes must invariably be drilled through the body, so that a stainless steel is needed to avoid corrosion and a free cutting grade to make some of the long drillings a practical proposition. The shaft, on the other hand, usually requires to be hardened to provide wear resistance on the tapered or parallel tool locations. The shaft, however, only requires to be corrosion resistant on the actual bearing surfaces and this can be achieved, for example, by hard chromium plating. Thus if the shaft and body are to be made from the same material there is considerable difficulty in effecting a satisfactory compromise. The hardenable stainless steels are not as free cutting as the non-hardenable (austenitic) grades. When hardened they are not as hard and wear resistant as, for example, a nitrided surface. There is also the problem that if heat treated in air the surfaces exposed during hardening are no longer corrosion resistant so that the surface skin must subsequently be removed. This presents considerable difficulties in relation to internal drillings. By using the third configuration all these problems are avoided by the use of a free cutting grade of austenitic stainless steel for the body and a nitriding steel for the shaft with hard chromium plating on the bearing surfaces. Differential thermal expansion in the radial direction does not often provide a serious problem unless wide temperature variations are encountered. With the material combination mentioned the journal bearing clearance will increase with increasing temperature which is the preferred direction for most machine tool applications. Temperatures below about 10°C are seldom encountered although considerably higher temperatures may occur owing to atmospheric variation and heat conduction from motors and other equipment located on the same machine. Some increase in clearance will not generally reduce the radial load capacity although it must inevitably be accompanied by some reduction in radial stiffness.

To date the third configuration is the one which has been most widely employed in machine tool spindles of all types, including those powered by an integral motor or turbine as well as those driven by a belt or coupling. Fig. 6.4 illustrates an excellent example of this configuration. It shows a sectioned side elevation of an aerostatic workhead designed by the Precision Products Group of the British Aircraft Corporation. The workhead fits a Studer machine and is driven by means of a belt running vertically upwards. This spindle is capable of generating workpiece surfaces which are round to within a 5×10^{-6} in annular zone.
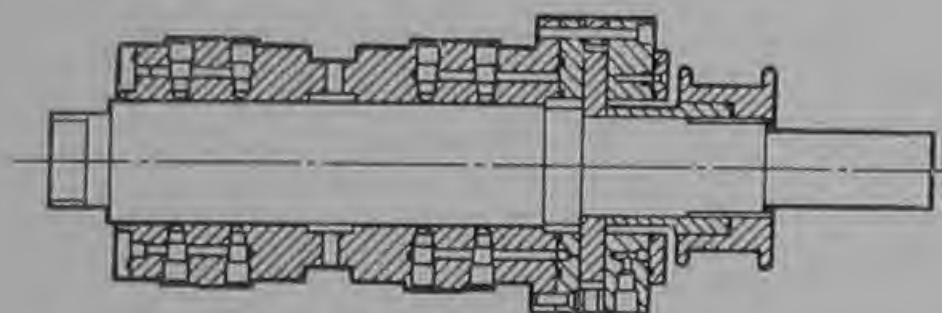
Fig. 6.4 Section of workhead for Studer cylindrical grinding machine designed by the Precision Products Group of the British Aircraft Corporation (Ref. 15)

The first three configurations all share one important advantage from the manufacturing viewpoint. The journal bearing bores can be machined in one continuous operation in the finished body and bearing assembly and are not subsequently disturbed in any way. Thus the greatest possible accuracy of bearing bore is achieved in terms of straightness, parallelism and alignment. This advantage is not shared by the last two configurations. The fourth configuration requires that the journal bearing alignment be disturbed subsequent to finish machining in order to permit the assembly of the shaft into the body.
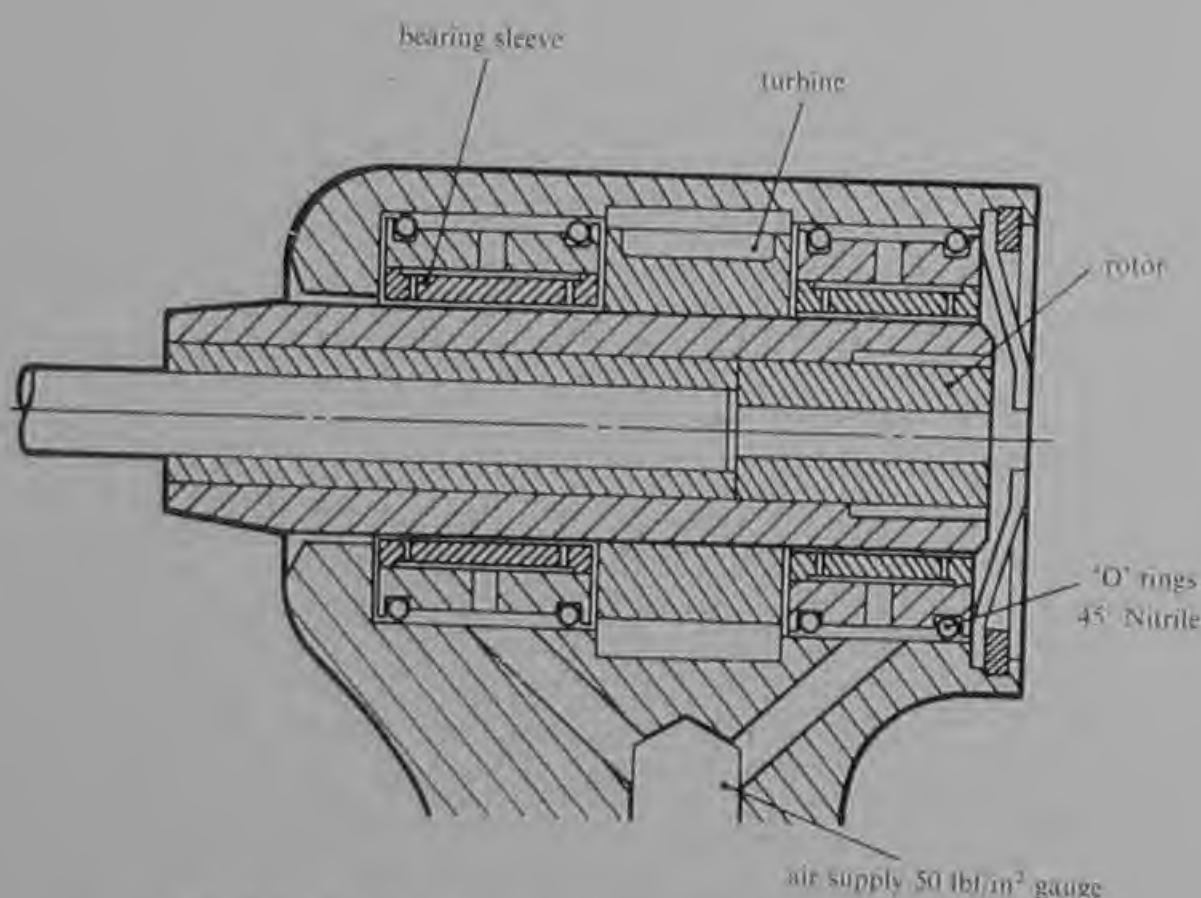
Fig. 6.5 Air bearing dental turbine developed by Micro Turbines Ltd. (Ref. 16) (British Patent No. 1,018,300)

This can be effected either by making one (or both) bearings removable from the body or by permitting the body to be split near the centre and dowelling the two halves to maintain alignment. The fifth configuration has journal bearings of unequal diameter which present difficulties both in producing and in checking the alignment.

The fourth configuration would not generally be suitable for a machine tool spindle for the reasons already mentioned. However, it has successfully been employed in high-speed hand tools, one example being the air turbine dental drill shown in Fig. 6.5. In such cases it is usual to make both bearings removable locating in an accurately machined bore with the air passages sealed by rubber 'O' rings. This configuration has an advantage when the overall length of the bearing assembly is restricted since it provides the widest possible journal bearing spacing and optimizes the radial load capacity at the tool. In some cases the bearings can be arranged to locate on the 'O' rings and, provided that a soft rubber is used, the bearings will self align when pressurized. The dynamic properties of this type of assembly are described in the next chapter.

The fifth configuration can perhaps be described best as illustrating how not to design an aerostatic spindle. It would be difficult to manufacture and offers low load capacity with no substantial saving of air flow. Its only useful feature is its high radial load capacity at one end. However, the author knows of no application of this configuration and other configurations involving journal bearings of unequal diameter have been used only in one or two isolated cases.

The list of possible bearing configurations is by no means complete and others will occur to the ingenious designer seeking a solution to a particular problem. However, it is hoped that the study of the examples given has highlighted the need to consider all aspects of bearing performance, materials selection, manufacturing techniques, assembly and installation from the earliest stages of the machine design.

6.3 Spindles driven by a belt

In most machine tool spindles driven by a pulley and a belt, the greatest single load imposed upon the bearings is the tension of the belt. In general practice belts tend to be tensioned much more than is required to transmit the driving torque. It is essential therefore that where aerostatic bearings are used the correct belt tension must be set and maintained to prevent overloading. The designer must first calculate the belt tension required to transmit the full torque of the motor at all operating conditions. He must take into account the centrifugal forces acting on the belt which will reduce the effective tension at high speeds. This effect is aggravated by the use of a heavy

belt or a small pulley; in high speed applications a light belt must be used and the pulley diameter kept as large as possible consistent with the attainment of the correct running speed. A porous belt is also advantageous since it prevents a film of air being drawn between the belt and the pulley surface and further reducing the grip of the belt. The load capacity of the bearing must be well in excess of the load imposed by the belt when set at its correct tension. It is usually possible to provide a load capacity between two and three times greater than the correct belt loading in the case of spindles operating at normal wheel speeds for cylindrical and surface grinding machines. These speeds seldom exceed 5 000 rev/min and the effects of centrifugal forces on the belts are negligible. However, at higher speeds the required tension increases and it appears that a practical limit of speed for belt-driven aerostatic machine tool spindles is reached between 30 000 and 40 000 rev/min. This limit depends on a number of factors including the power to be transmitted and the available air supply pressure.

(a) Preferred arrangement, which gives small couple

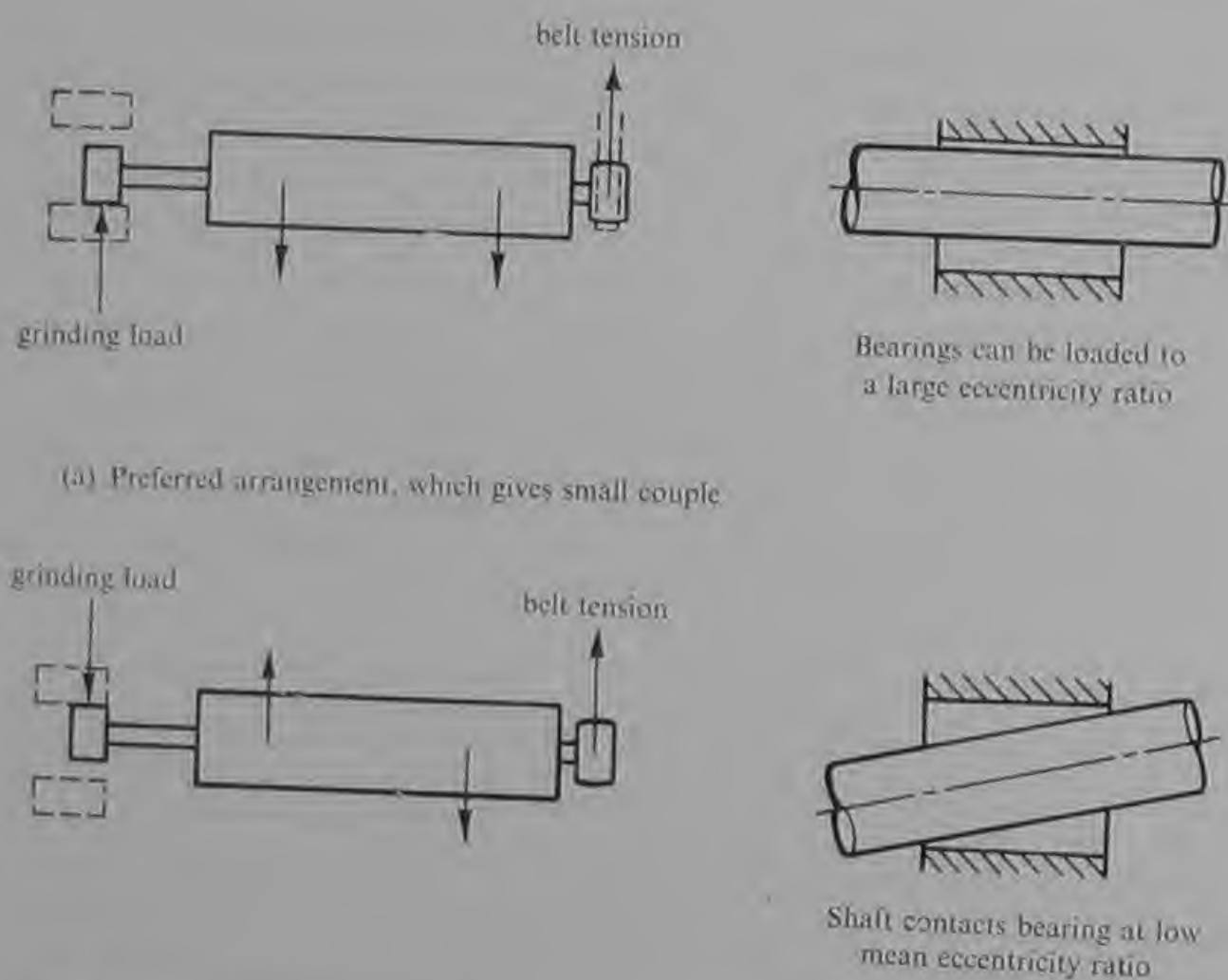(b) Alternative arrangement which imposes a large couple on bearings

Fig. 6.6 Importance of direction of belt tension in relation
to the direction of the applied grinding load

However, the designer is advised to consider all applied loads with extreme care if it is intended to use a belt-driven spindle in excess of the quoted speeds.

One problem which arises with spindles for surface grinding machines and some internal grinding machines is particularly difficult in the second case because of the high speeds which are also involved. Fig. 6.6(a) shows the arrangement on most British internal grinding machines in which the grinding load and the belt tension are in the same direction. This is the preferred arrangement since the aerostatic journal bearings are better suited to withstanding a centrally applied force than a couple. However, on most American and Continental internal grinding machines the workhead revolves in the opposite direction and the grinding takes place on the other side of the wheel. In such cases the grinding load and the belt tension form a couple, as shown in Fig. 6.6(b), and the effective bearing load capacity is reduced because the inclining of the shaft surfaces to the bearing surfaces means that the surfaces will come into contact at a lower mean eccentricity ratio. It is essential that this effect is taken into account at the design stage.

If the direction of the belt tension is known with certainty, and if it can be ensured that the spindle will always be correctly installed in the machine, it is possible to increase the load capacity of the pulley end bearing in the required direction. This is done by biassing the bearing by some means which destroys its load-carrying symmetry. There are several ways in which this can be achieved. Perhaps the

(a) Asymmetric feeding
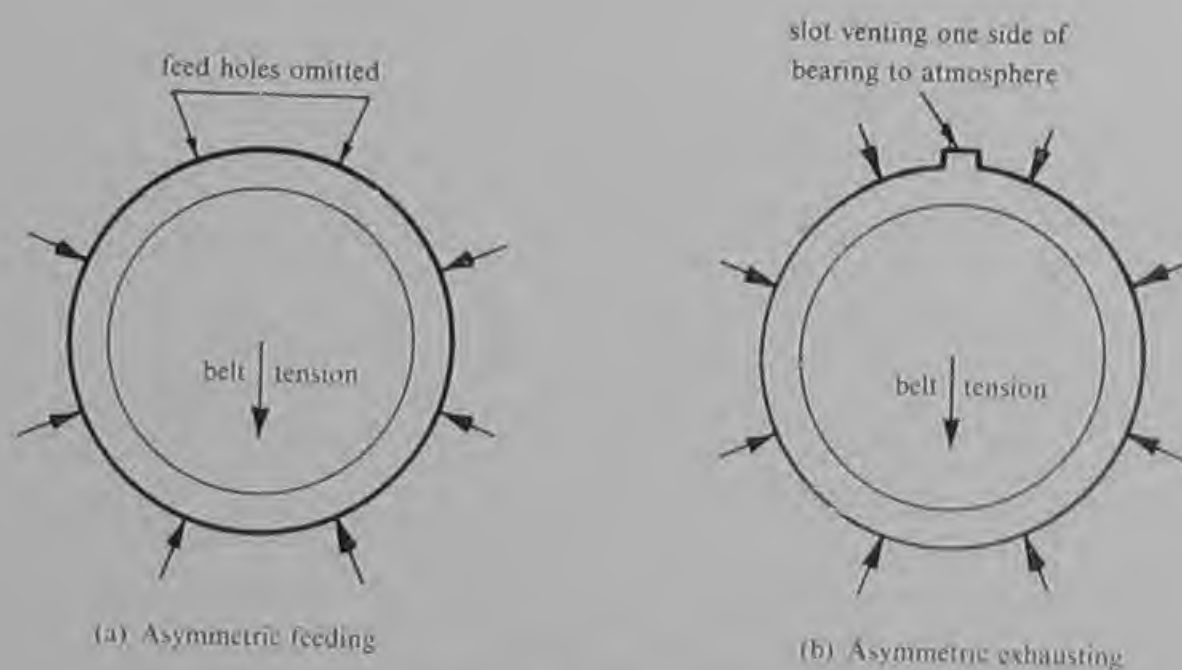
(b) Asymmetric exhausting

Fig. 6.7 Methods of increasing journal bearing radial load capacity in a preferred direction

simplest is to omit one or two feed holes in each row as shown in Fig. 6.7(a). This method has the advantage of reducing the airflow slightly. An alternative method which increases the air flow is to broach a slot in the journal bearing surface, as shown in Fig. 6.7(b). The slot vents that side of the bearing to atmosphere displacing the unloaded shaft towards the slot and increasing the load capacity away from the slot. This method has the doubtful advantage that if the precise direction of the belt load is not known at the design stage the slot can be machined at a late stage in the spindle's manufacture. There are several other possible methods of biassing a bearing. However, this technique must always be applied with caution since increasing the load capacity in one direction inevitably reduces it in another, which is another reason for studying all the applied loads under all possible operating conditions.

Whether the pulley end bearing is biassed or not it is essential that some means of accurately setting the belt tension is provided. In the case of the early N.E.L. spindles the belt tension was set by measuring the deflection of the shaft in its bearings using a dial gauge calibrated in 0·000 1 inch increments. This method tends to be time-consuming and to demand some skill on the part of the operator. A better method is to monitor the change of pressure in the air film as the load is applied. This system has been patented by Westwind Turbines Ltd. (British Patent No. 1,085,403).
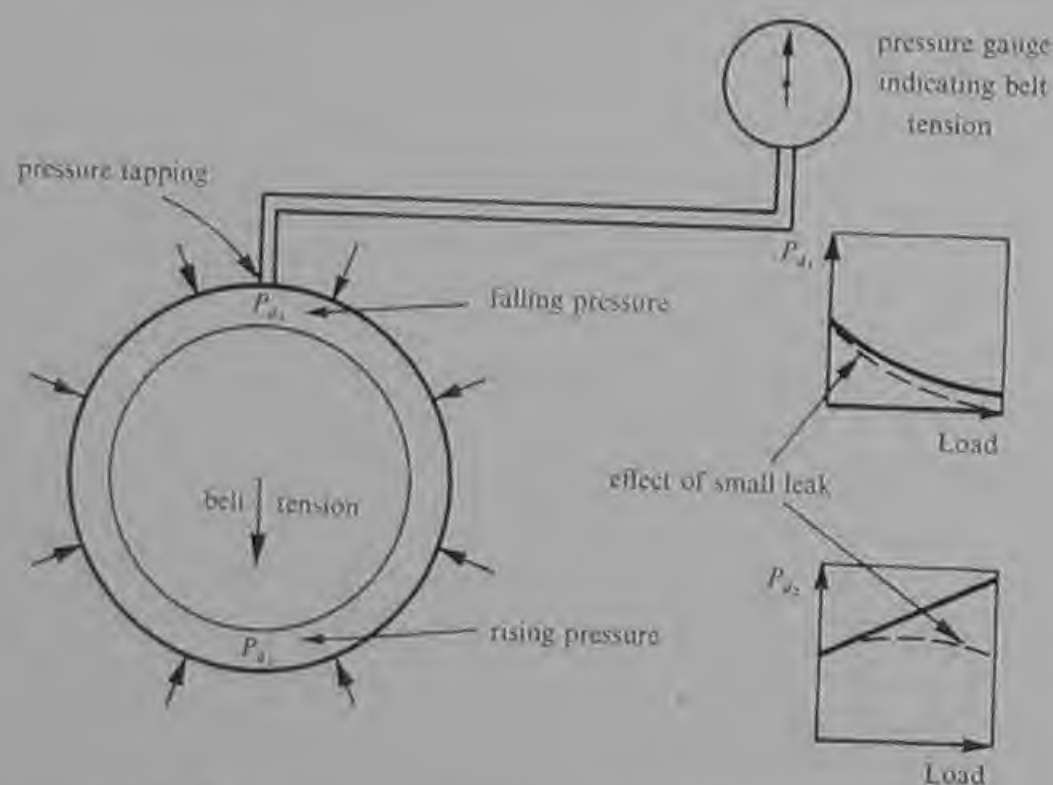
Tapping falling pressure is preferred since any error introduced by small leaks overestimates load and does not produce ambiguity. It is therefore a 'fail safe' arrangement.

Fig. 6.8 Method of setting belt tension

A pressure gauge connected to a tapping in the bearing wall will respond to changes of pressure caused by changes of load. The principle is shown in Fig. 6.8. The pressure rises in the direction of the shaft movement and falls in the opposite direction. In practice it has been found advantageous to tap the pressure in the region where it falls with increasing tension. One reason is because any leak developing in the connection to the pressure gauge indicates a higher belt tension and not a deceptively low tension. Another reason is because a falling supply pressure is also indicated as an apparent increase in belt tension which is the correct indication since in fact the safety margins are reducing in either event. The belt tension indicator is a very valuable addition which has eliminated what was by far the most common cause of failure in aerostatic machine tool spindles. The future designer is strongly recommended to employ this or some equally effective alternative device in all future applications of belt-driven aerostatic spindles.

6.4 Spindles driven through a flexible coupling

Aerostatic spindles adapted to be driven through a flexible coupling are essentially similar in construction to belt-driven spindles. However, as the side load associated with a belt is not present there is no need for any journal bearing biassing or for a load indicator.

There are many proprietary couplings which are broadly classified as flexible, yet the majority of these are relatively rigid and impose large side loads if the spindle axis is not accurately aligned with the axis of the driving motor. Designers are recommended to select a coupling which is as flexible as possible and to pay attention to the alignment of the spindle and the motor. Any rotating side load arising at the coupling will produce orbiting of the shaft which will degrade the performance of the spindle in most machine tool applications.

When correctly engineered, aerostatic spindles driven through a flexible coupling can produce excellent results. In one application on the wheelhead of a thread grinding machine an aerostatic spindle is coupled to a hydrostatic motor. This arrangement combines the infinitely variable speed and smooth torque of the motor with the precise axis definition of the spindle. Equipped also with an aerostatic workhead this machine is capable of producing a wide range of work of the highest quality.

6.5 Spindles with air turbine drive

Aerostatic bearings are widely used in machine tool spindles and hand tools driven by air turbines. They have also been applied to more exotic devices including gas liquefying expansion turbines and prism spinners for use in laser research.
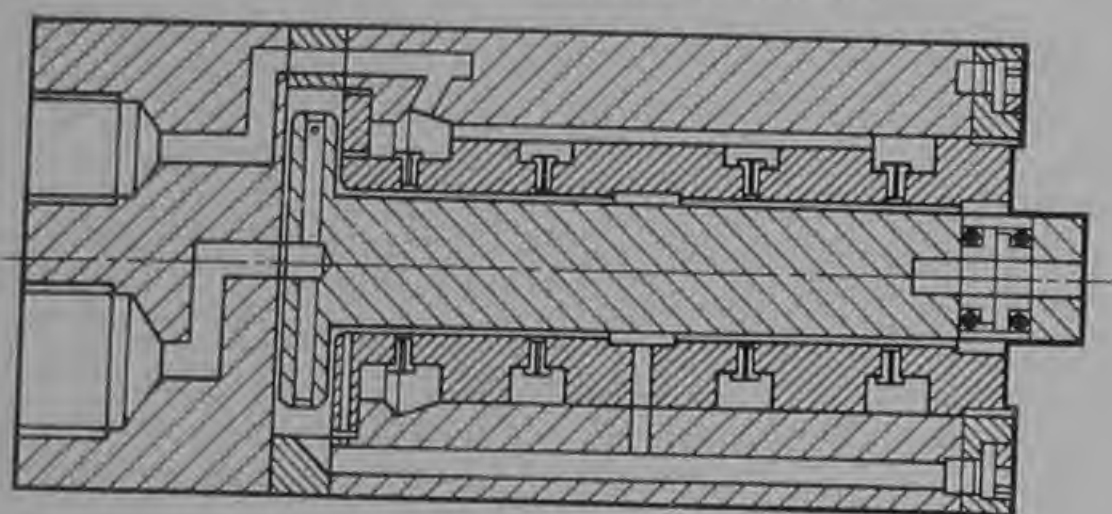
Fig. 6.9 High speed air turbine drilling spindle with aerostatic bearings developed by Westwind Turbines Ltd. for drilling electronic printed circuit boards (British Patent No. 1,013,351)

In most machine tool applications the third configuration of Fig. 6.2 is favoured. Typical of this category is the spindle developed by Westwind Turbines, Ltd., for drilling electronic printed circuit boards, and shown in Fig. 6.9. The turbine design is very simple and inexpensive to manufacture. Air is fed into the centre of the back face of the rotor, some leaking away radially to supply the rear thrust bearing. The driving air is discharged tangentially through six jets on the outside diameter of the thrust runner, providing an exceptionally smooth torque. A similar design produced by the Barden Corporation in the U.S.A. employs an air turbine of the Pelton wheel type.

It will be seen from the next chapter that in order to achieve stable journal bearing operation at high speeds it is necessary to use bearings of small radial clearance. It is usual to think of air bearings as running cold, and in most low speed applications the operating temperature is usually at or slightly below the ambient temperature. However, the combination of high speed and low clearance can result in the friction heating of even an air bearing becoming appreciable. If no attempt is made to carry the heat away from the bearing, high local temperatures can be reached which lead to problems of thermal stress and differential expansion. One important consideration is to ensure that the maximum possible surface area of the bearing sleeve is in contact with the spindle body. The temptation to design a simple spool-type journal bearing sleeve of the type shown in Fig. 6.10(a) must be avoided since the large area of air reservoir insulates the centre of the bearing and leads to high local temperatures. In a better design shown in Fig. 6.10(b) the air reservoir consists of two narrow grooves joined by an axial slot leaving a large area of metal to conduct away the heat.
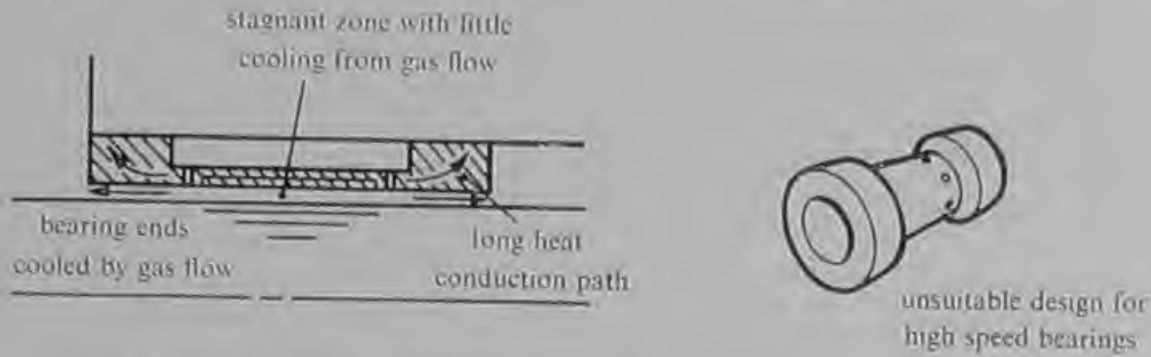
(a) High local temperature due to insulating effect of gas reservoir
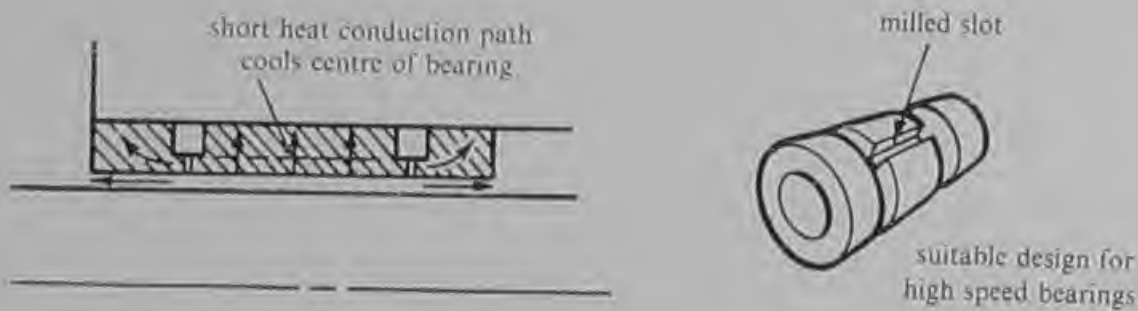
(b) Heat conduction improved by increased contact area of outside surface of bearing sleeve

Fig. 6.10 Heat dissipation in high-speed journal bearings

Proper design of the bearing sleeve can avoid the occurrence of very high local temperatures but in some spindles a large part of the body surrounding the bearings can still reach a temperature which is too hot to touch. This order of temperature, while not directly harmful to the bearings, is undesirable for several reasons. It constitutes a hazard to the operator, it can increase clamping stresses, and in an extreme case it can induce long-term material distortion through stress relieving. Compared to most metals, the stainless steels usually employed in aerostatic spindle bodies are poor conductors of heat and for this reason the use of some form of cooling is all the more necessary.

The bearing configurations (a) and (d) shown in Fig. 6.2 are the most popular for the application of aerostatic bearings to air turbine hand tools. When the first configuration is used a turbine of the Pelton wheel type is usually milled into the centre of the rotor between the two journal bearings. This arrangement provides a rotor of low mass supported in journal bearings of relatively large area and achieves stable bearing performance at very high speeds. The length of the

rotor seldom exceeds 3 in and differential thermal expansion in the axial direction does not usually present a problem.

Some of the advantages of the configuration (d) in relation to small high-speed hand tools have already been discussed. Another feature of the air turbine dental drill is the elimination of jet feeding to the thrust bearings and the use instead of journal bearing exhaust air. This arrangement provides low axial load capacity and stiffness in return for a considerable saving of air consumption. On small aerostatic machines the possibility of journal exhaust-fed thrust bearings should be considered wherever applied axial loads are small or where a low gas consumption must be achieved. This system can be applied to any of the first, second or fourth configurations shown in Fig. 6.2.

6.6 Spindles with electric motor drive

Electric induction motors are well suited to driving aerostatic spindles. With the elimination of brushes and any other form of rubbing contact the electric rotor and its shaft are freely supported to rotate smoothly about a precise axis. For most applications at both low and high speeds, the third configuration shown in Fig. 6.2 again represents the easiest arrangement from the manufacturing viewpoint. In such cases the rotor forms an extension of the shaft at either end of the assembly as shown in Fig. 6.11(a) and 6.11(b), or is built into the centre of the shaft as shown in Fig. 6.11(c). The arrangements shown in Fig. 6.11(a) and (b), are applicable at low and intermediate speeds, up to around 30 000 rev/min. It is usually necessary from considerations of bearing stability to use the arrangement shown in Fig. 6.11(c) at higher speeds.

There are several important factors to be borne in mind when using electric induction motors if the smoothest possible running is to be achieved. The first consideration is to ensure whenever possible that the motor is designed to operate at a low magnetic saturation. Such motors are usually termed 'low-noise motors' and are slightly larger for a given power output than the manufacturer's standard size. In many grinding wheelhead applications it is worthwhile having a motor specially designed if a suitable motor is not available off-the-shelf.

Even the best designed rotor-stator unit will not run smoothly unless the rotor is mounted accurately concentrically and axially within the stator. Concentricity is of the greatest importance and the designer will be rewarded for spending time and care on the means of locating the stator casing on to the spindle body.

The rotor surface can be ground assembled on to the shaft at the same time as the journal surfaces to ensure absolute concentricity of rotation. Finally, it is essential dynamically to balance the finished shaft and rotor assembly either in its own bearings or in a suitably designed balancing fixture with aerostatic bearings supporting the shaft journal surfaces.

rotor diameter smaller than
bore of thrust plate

(a) Rotor at thrust runner end

rotor diameter smaller
than journal bore

(b) Rotor at opposite end to thrust runner

(c) Rotor at centre of shaft
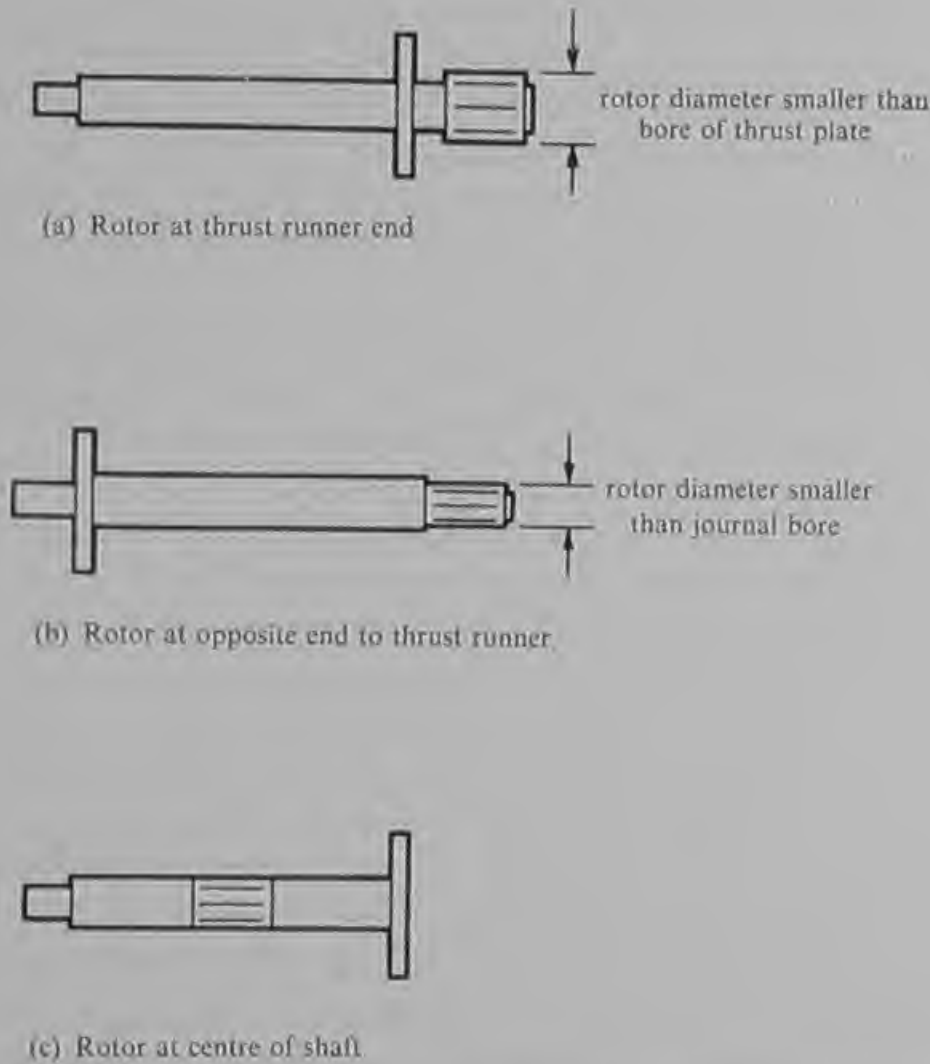
Fig. 6.11 High frequency motors—alternative rotor arrangements employing the bearing configuration shown in Fig. 6.2(c)

Heating is a problem with most electrically driven spindles. In low speed spindles operating on the mains frequency of 50 Hz (or 60 Hz in the U.S.A.), the heat dissipation is low and the bearing exhaust air directed through the motor casing often provides sufficient cooling. In this connection the arrangement shown in Fig. 6.11(a) is to be preferred since in this case it is simple to arrange for the exhaust air from the thrust bearings to flow into the motor casing.

The heating problem becomes more severe as the supply frequency and the rotational speed increase. The motors become less efficient due to increased iron losses and heat is generated in the bearings. It is always beneficial to use a light alloy motor casing with suitable finning to improve heat losses by convection in the surrounding atmosphere. In small motors up to about 0·5 h.p. and speeds up to about 30 000 rev/min this will often be sufficient, either alone or in combination with a little additional cooling air bled from the bearing supply. However, for larger motors and for small motors at higher speeds, it is necessary to employ either a cooling fan which forms part of the shaft assembly or water cooling. Using large quantities of bearing supply air for cooling is not an economical proposition although employing a little to drive a Coanda device which entrains large volumes of ambient air is sometimes an attractive means of providing cooling at low initial cost.

The next chapter deals with the problem of ensuring stable bearing operation in high speed machines and it is essential that this aspect of design is considered if a long and unexpected development programme is to be avoided. It is also equally important to ensure that the mechanical critical speeds of the shaft lie well beyond the operating speed range. It has been found that the most reliable method of predicting mechanical critical speeds of the shaft considers the shaft as a beam with pinned support at the journal bearing centres (i.e. using the pin-pin beam formulae). The shaft is usually capable of being broken down and approximated to a uniformly distributed mass together with a few point masses. Proper account must be taken of all factors affecting the stiffness of the shaft. This is particularly important in relation to shafts with a centrally mounted high frequency motor as shown in Fig. 6.11(c). A patented design manufactured by the Oberg Machine Company of Sweden provides induction motor rotors built integrally with the shaft. These rotors are of high rigidity as a result of being welded under high axial compression. However, when calculating the shaft critical speeds it is essential that allowance is made both for the loss of modulus of elasticity arising because the structure is partly steel and partly copper, and for the loss of second moment of area constituted by the axial slots milled in the rotor.

Conventional induction motor rotors which are provided with a parallel bore for locating onto the shaft are best suited to either of the arrangements shown in Fig. 6.11(a) and (b). In either case, in the calculation of the mechanical critical speeds the rotor can usually be considered as a point mass at its centre of gravity. Some manufacturers of induction motors recommend that the rotors are shrink-fitted onto the shaft with interferences of up to 0·003 in/in of rotor bore diameter. These large interferences can lead to shaft bending due to stress

relieving which is accelerated by the heat produced in the rotor during operation. It is recommended that, except in the case of very high-speed motors where considerations of dilation may be over-riding, the degree of interference is limited to well below this value. Any danger of the rotor's turning due to large starting torques or running torques is better dealt with by keying or pinning than by increasing the interference.

Many of the points raised in connection with induction motors apply equally to other types of electric motors. The shaft arrangements shown in Fig. 6.11(a) and (b) are well suited to any motors employing commutators or slip rings since these can be situated at the end of the motor casing with easy access for assembly and brush replacement. It has been found that the precise axis definition and smooth running properties of aerostatic bearings reduce brush noise and extend the life of the brushes. However, the need to replace brushes makes this type of motor aesthetically less pleasing than the induction motor with aerostatic bearings which, correctly applied, needs no routine maintenance. This factor may contribute to the present situation in which a brush-type electric motor with aerostatic bearings is a rare bird. However, there are several potentially attractive applications of d.c. motors with aerostatic bearings, of which the machine tool work-head with infinitely variable speed is an example, and so this situation may change in the future.

6.7 Static shaft bearings

So far this chapter has dealt with journal bearings of the conventional type in which a shaft rotates within a bush. The gas supply is fed to feed holes or slots in the stationary member which in this case is the bearing bush. However, it is sometimes necessary to employ a bearing in which the shaft is stationary and the bush rotates. In this case the gas supply is fed to feed holes or slots in the shaft surface. Fig. 6.12 shows two examples of the numerous possible static shaft configurations. Fig. 6.12(a) shows the simplest arrangement of a single journal bearing with thrust faces fed by the exhaust gas. This arrangement has successfully been applied to pulleys for fibre and plastic film processing and to a range of turbine flowmeters for gases. It offers a low but useful load capacity, the ability to support small light rotors running at high speeds and a very low gas consumption which is often of the order of 0·1 s.c.f.m. supplied at 20–30 lbf/in^2 gauge.

The second arrangement shown in Fig. 6.12(b) is one possibility for providing a static shaft arrangement for a considerably heavier duty. Two journal bearings are employed together with two jet-fed thrust bearings. This type of arrangement is used for supporting grinding

thrust faces fed by journal exhaust
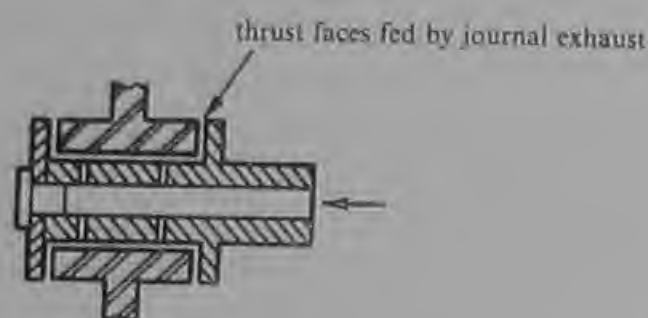
(a) The simplest air bearing arrangement, as used in low friction textile
pulleys and pivots and turbine flowmeters
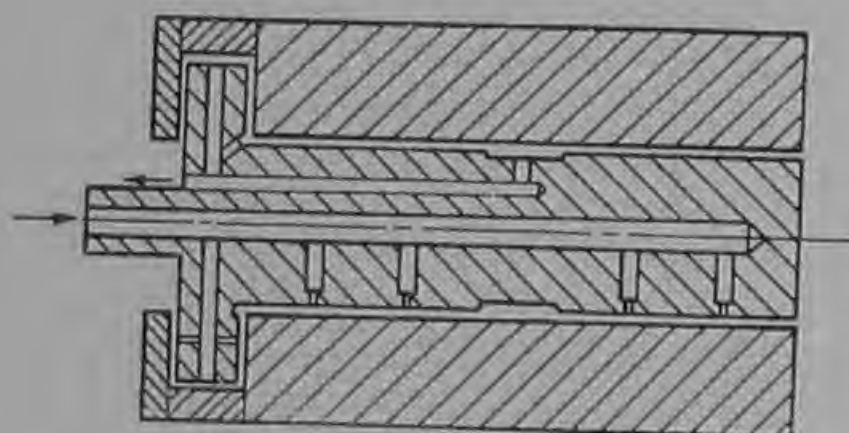
(b) Heavier duty arrangement with two journal bearings and jet-fed
thrust bearings as used in some grinding machine applications

Fig. 6.12　Arrangements of aerostatic bearings with static
shafts

wheels in the form of a sleeve which are used in machines for sharpening
surgical blades. In this case part of the outside of the rotor is formed
as a pulley and a parallel location is provided for the grinding wheel.

When designing the more complex arrangements of static shaft
bearings it is important to remember to provide suitable exhaust
passages to allow the gas to escape from the spaces between the bearings.
These passages can be difficult to provide at a late stage of design or
manufacture if overlooked in the initial design. It will be noticed that
in Fig. 6.12(b) all the exhaust gas needing ducting is taken through a
single hole in the static member. This is a general principle which is
strongly recommended in the design of all machines with aerostatic

bearings for two good reasons. Firstly, any air passing through a rotating member is liable to generate noise. Secondly, and very important, the single exhaust passage permits a restriction easily to be applied by means of a jet inserted in the exhaust hole. This can be of great value in damping aerostatic instability and is dealt with in more detail in Chapter 10.

BEARINGS FOR HIGH-SPEED MACHINES

7.0 Introduction

In many respects aerostatic bearings are ideally suited for use in high-speed machines. Their low friction provides high mechanical efficiency and minimizes bearing heating problems. They are quiet and smooth running and do not add to the sound and vibration levels of the machine in the way that high-speed ball bearings do. However, the advantages of aerostatic bearings in high-speed machines will be fully realized only by the designer who appreciates both their unique properties and their limitations. In particular, much attention must be paid to a study of the various critical speeds that can arise and to the possible onset of self-excited bearing film whirls.

Consider a rotor supported in aerostatic bearings which is steadily accelerated from rest. At low speeds it runs very smoothly with an undetectable level of vibration. However, the effect of any residual unbalance will become apparent as the speed increases. Instead of rotating about the axis through the journal bearing centres the rotor will orbit about this axis. The whirl orbit will grow almost imperceptibly with speed until quite rapidly it will grow large and then decay again. The rotor will have accelerated through its lower natural frequency and the effect is very like any other mechanical resonance. If the unbalance is large the whirl will reach an amplitude at which the bearing surfaces contact and the attainment of higher speeds is prohibited. However, a balanced rotor will accelerate through one or two resonances without damage. As the rotor continues to accelerate it will again be found to be running smoothly. The speed continues to climb until suddenly a large-amplitude uncontrolled whirl develops which inevitably results in the rotor coming instantly to rest with its bearings seized. It is usually noticed that the speed at which the disaster occurred is twice the speed of the first resonance. Repeating the experiment slowly with the necessary instrumentation will reveal that the frequency of the self-excited whirl is half the rotational speed. A resonance is excited at the lower natural frequency when the shaft is rotating at twice that frequency. This phenomenon has become known as half-speed whirl. To predict its onset speed in any particular machine requires a knowledge of the dynamic stiffness and damping forces present in the bearings. The purpose of this chapter is to enable

the designer to ensure that his machine will either operate well below its critical speeds or will incorporate some device to permit these speeds to be exceeded with impunity.

7.1 Dynamic stiffness and damping

The dynamic properties of all rotor-bearing systems are determined by the stiffness and damping forces arising in the bearings. The stiffness influences the frequencies at which resonances occur, excited by, for example, unbalance forces or externally impressed vibrations. The damping limits the amplitude of vibration or whirl arising at resonances and at any condition at which the damping becomes zero self-excited instabilities arise.

The influence of stiffness and damping and the dynamic characteristics of aerostatic journal bearings can best be understood from a study of a simplified bearing system. The following assumptions are made.

(a) The shaft is rigid and the bearings are rigidly supported so that the only finite stiffness and damping present arise in the bearing.

(b) Aerodynamically the bearings are considered to operate in the incompressible region. That is, the aerodynamic force acts at $90°$ to the displacement from the centre of the bearing. In practice this implies that the bearings are of relatively large clearance ratio (h_o/a greater than 0.002). It therefore follows that the stiffness arises from aerostatic action only and the dynamic stiffness is taken to be equal to the aerostatic stiffness and to be independent of speed.

(c) Damping forces arise from squeeze film action and aerodynamic action only and are not influenced by the external pressurization. In practice this limits the present discussion to bearings with annular orifice feeding, slot feeding, or simple orifice feeding with small shallow pockets. The presence of pockets or other storage volume within the bearing clearance reduces the damping present. In an extreme case the damping can be zero at zero speed leading to self-excited vibrations known as pneumatic hammer.

(d) In order to simplify the mathematics in this preliminary analysis, for purposes of considering squeeze film and aerodynamic effects the bearing is considered to be a segment of an infinitely long bearing. Thus end leakage effects are ignored.

(e) All whirl orbits are assumed to be circles centred on the bearing centres. This corresponds to neglecting the weight of a horizontal rotor or to considering a vertical rotor.

Tully (Ref. 17) has shown that applying these assumptions the

dimensionless damping force $\overline{W}$ can be defined as

$$\overline{W} = \frac{W}{LDP_a}$$

$$= \overline{W}_{sf} - \overline{W}_d \qquad (64)$$

where $\overline{W}_{sf}$ is the dimensionless squeeze film damping force given by

$$\overline{W}_{sf} = \frac{6\pi}{(1-\varepsilon^2)^{\frac{3}{2}}} \cdot \frac{r}{h_o} \left(\frac{\Lambda}{\omega}\right) \omega^*. \qquad (65)$$

Also $\overline{W}_d$ is the dimensionless aerodynamic force given by

$$\overline{W}_d = \frac{6\pi}{(2+\varepsilon^2)(1-\varepsilon^2)^{\frac{1}{2}}} \cdot \frac{r}{h_o} \left(\frac{\Lambda}{\omega}\right) \omega, \qquad (66)$$

where

$$\Lambda = \frac{\mu\omega}{P_a} \left(\frac{a}{h_o}\right)^2,$$

the compressibility number as before, ω is the angular velocity of the shaft, ω^* is the angular velocity of any whirl or vibration of the shaft, ε is the eccentricity ratio and r is the radius of the whirl orbit or half the amplitude of planar vibrations.

It can be seen from equation (65) that the squeeze film damping force is independent of shaft rotation and is proportional to the frequency of shaft whirl or vibration. Thus the squeeze film damping is present to damp the vibrations of the stationary shaft. Such vibrations could be forced vibrations, or free vibrations following a shock loading or the sudden release of a displaced shaft. A squeeze film number σ is often used where

$$\sigma = 12 \left(\frac{\Lambda}{\omega}\right) \omega^*. \qquad (67)$$

The aerodynamic damping force is proportional to the angular velocity of the shaft and is independent of the frequency of whirl or vibration. It is a negative quantity and for conditions of constant squeeze film damping causes the net damping force to reduce as the speed increases.

The damping arising from squeeze film and aerodynamic effects can be used together with the aerostatic stiffness to predict the dynamic behaviour of high speed rotors supported in aerostatic journal bearings. In particular it is possible to study the influence of unbalance forces and the occurrence of self-excited whirl instability.

7.2 Whirl induced by unbalance

Residual unbalance causes the rotor to orbit in its bearings at the same speed as its speed of rotation and hence the phenomenon is often called synchronous whirl. Considering the damping under these conditions by substituting $\omega^* = \omega$ in equation (65) and also putting $\varepsilon = 0$ for no static load on the bearing yields:

$$\overline{W}_{sf} = \frac{6\pi r}{h_o} \left(\frac{\Lambda}{\omega}\right) \omega$$

and

$$\overline{W}_d = \frac{3\pi r}{h_o} \left(\frac{\Lambda}{\omega}\right) \omega.$$

Thus

$$W = LDP_a \frac{3\pi r}{h_o} \left(\frac{\Lambda}{\omega}\right) \omega \qquad (68)$$

from equation (64). Since the net damping is proportional to angular velocity it is possible to define a damping coefficient C by dividing equation (68) by $r\omega$ and substituting for Λ. Thus

$$C = 6L\pi\mu \left(\frac{a}{h_o}\right)^3 \qquad (69)$$
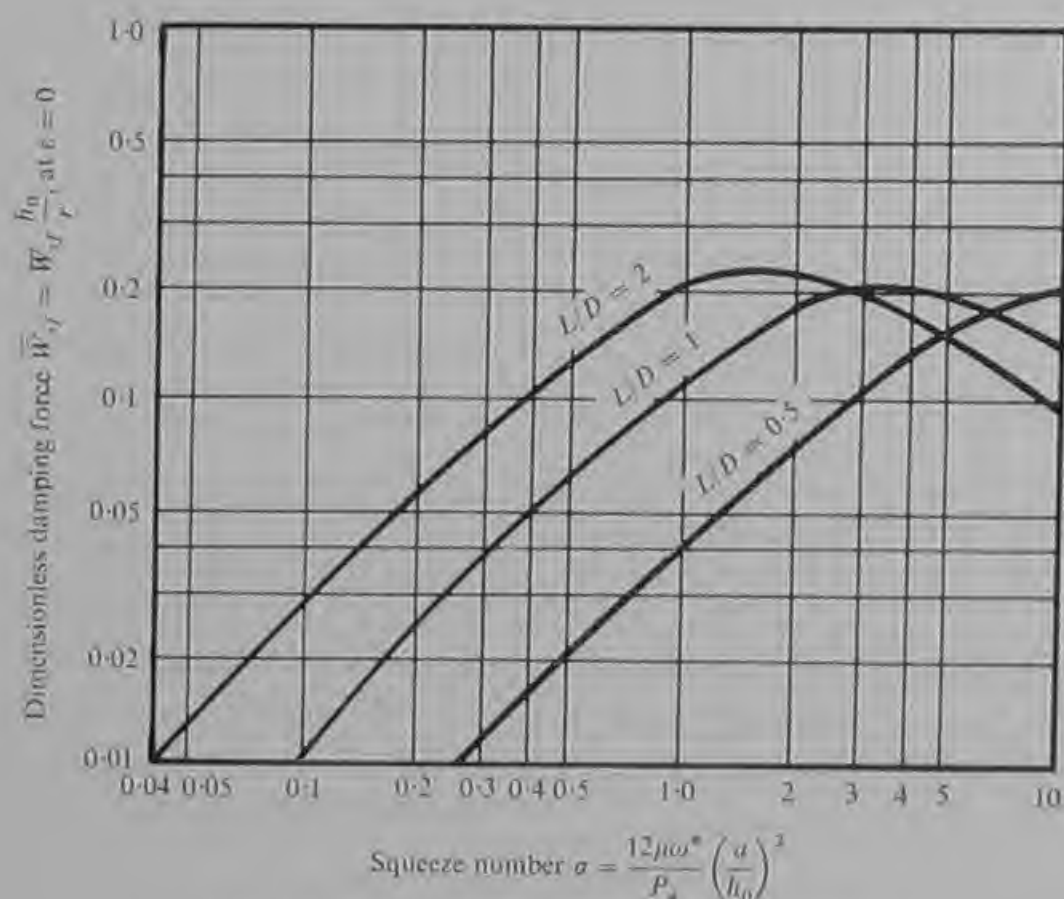
Fig. 7.1 Theoretical squeeze film damping

for an infinitely long bearing

or
$$C = \frac{LDP_a}{2r\omega}\,\overline{W}_{sf}$$
(70)

for a finite length bearing if the dimensionless squeeze film damping is known. Mullan and Richardson (Ref. 18) have computed a numerical solution of the full Reynolds equation for the squeeze film behaviour of initially concentric journal bearings. Their solution for bearings of length-to-diameter ratios of 0·5, 1, and 2 is given in Fig. 7.1. In this case $\overline{W}_{sf} = \overline{W}_{sf}\,\dfrac{h_o}{r}$ is plotted against the squeeze number σ. Thus the damping coefficient is given by:

$$C = \frac{LDP_a}{2\omega h_o}\,\overline{W}_{sf}.$$
(71)

In the incompressible region the real bearing of $L/D = 2$ has approximately half the damping of an equal segment of an infinitely long

rotor mass m_g
polar moment of inertia I_0
transverse moment of inertia I

Section A–A
During cylindrical whirl rotor centre O' orbits bearing centre O under the influence of static unbalance λ.

Fig. 7.2 Symmetrical rotor-bearing system

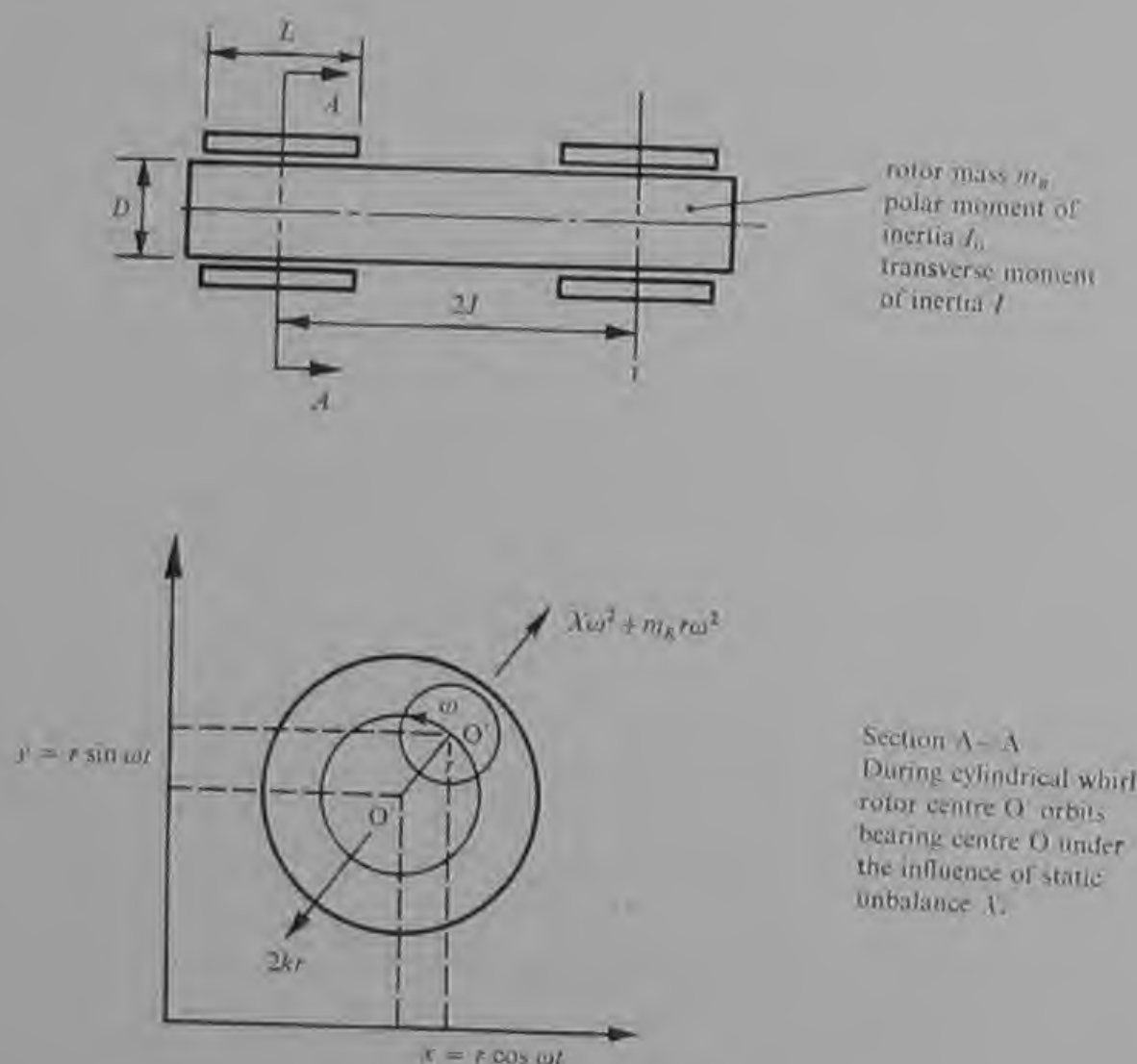bearing. It can be seen that the influence of compressibility reduces the squeeze film damping at high squeeze numbers and in theory the damping becomes zero at $\sigma = \infty$.

Having established the nature of the damping and using the aerostatic stiffness it is possible to investigate the dynamic behaviour of a rotor supported in two journal bearings. This system is shown in Fig. 7.2 and it is assumed that the system is wholly symmetrical. The axis of the rotor is forced to generate a cylindrical or conical form depending upon the type of unbalance present. It can be seen from Fig. 7.3(a) that if only static unbalance is present the rotation produces a single

(a) Cylindrical whirl generated by static unbalance force

(b) Conical whirl generated by dynamic unbalance couple

(c) General form of whirl generated by residual static and dynamic unbalance
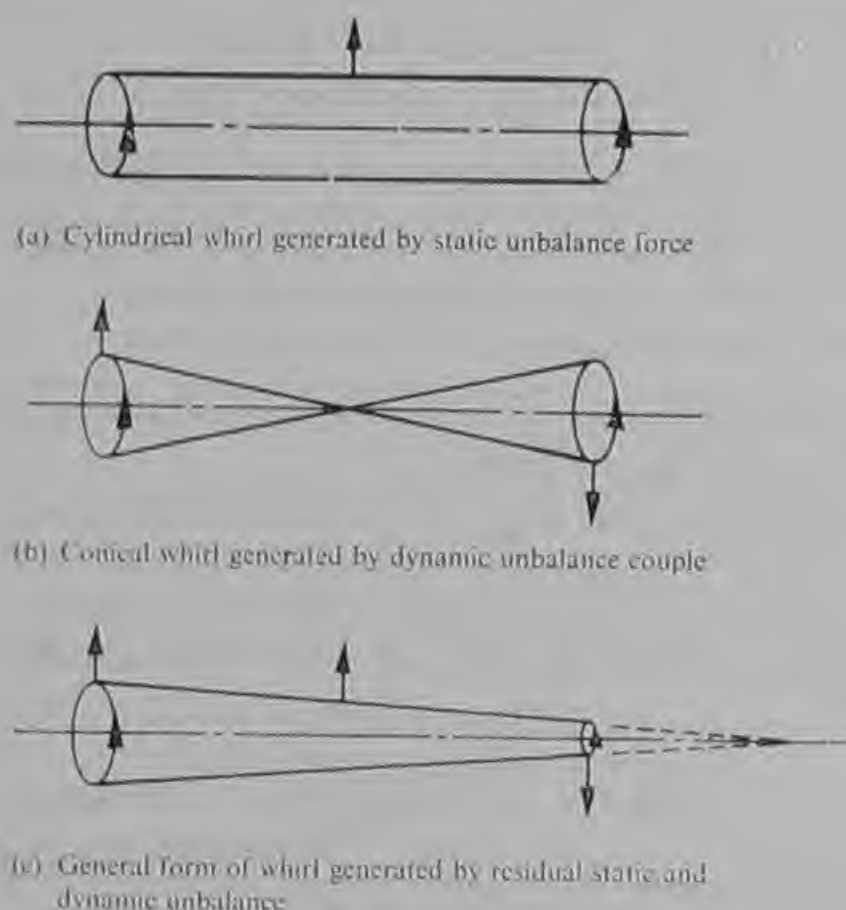
Fig. 7.3 Modes of rotor whirl

force acting on the centre of gravity of the rotor. If only dynamic unbalance is present the rotation produces a couple which causes the axis of the rotor to generate two cones with a common apex at its centre of gravity (Fig. 7.3(b)). Fig. 7.3(c) shows the generalized form of whirl produced when both static and dynamic unbalance are present.

Referring again to Fig. 7.2 it can be seen that the circular movement of the rotor can be considered as the sum of two sinusoidal vibrations in mutually perpendicular planes:

$$x = r \cos \omega t$$

and
$$y = r \sin \omega t$$

The forces acting on the rotor in the x plane can be represented as shown in Fig. 7.4(a). The amplitude and phase of the synchronous whirl can be calculated by equating the forces acting upon the centre of gravity of the rotor and taking moments about the centre of gravity, as follows.

$$m_R \frac{d^2 x}{dt^2} + 2m_R \eta \frac{dx}{dt} + 2Kx = X\omega^2 \sin \omega t \qquad (72)$$

$$(I - I_o) \frac{d^2 \beta}{dt^2} + 2m_R \eta J^2 \frac{d\beta}{dt} + 2KJ^2 \beta = Y\omega^2 \sin \omega t, \qquad (73)$$

where X is the static unbalance of the rotor;

Y is the dynamic unbalance of the rotor;

K is the aerostatic stiffness of one bearing;

$\eta = \dfrac{C}{m_R}$ is the damping constant per unit rotor mass per bearing;

I is the transverse moment of inertia of the rotor;

I_o is the polar moment of inertia of the rotor;

and $2J$ is the distance between the bearing centres.

I_o is included because during conical whirl the gyroscopic forces act in opposition to the inertial forces.

Similar equations to (72) and (73), but 90° out of phase, describe the motion of the rotor in the perpendicular plane. Equations (72) and (73) are of the same form as the standard differential equations for forced damped harmonic motion and the solutions can be written as follows:

$$x = \frac{X\omega^2 \sin(\omega t - \delta_1)}{m_R[(\omega_1^2 - \omega^2)^2 + 4\omega^2 \eta^2]^{\frac{1}{2}}}; \qquad (74)$$

$$\delta_1 = \tan^{-1} \left[\frac{2\omega\eta}{m_R(\omega_1^2 - \omega^2)} \right]; \qquad (75)$$

and $\qquad \omega_1^2 = \dfrac{2K}{m_R}; \qquad (76)$

and also

$$\beta = \frac{Y\omega^2 \sin(\omega t - \delta_2)}{(I - I_o)\left[(\omega_2^2 - \omega^2)^2 + \dfrac{4m_R^2 \eta^2 J^4 \omega^2}{(I - I_o)^2}\right]^{\frac{1}{2}}}; \qquad (77)$$

$$\delta_2 = \tan^{-1} \left[\frac{2m_R \eta J^2 \omega}{(I - I_o)(\omega_2^2 - \omega^2)} \right]; \qquad (78)$$

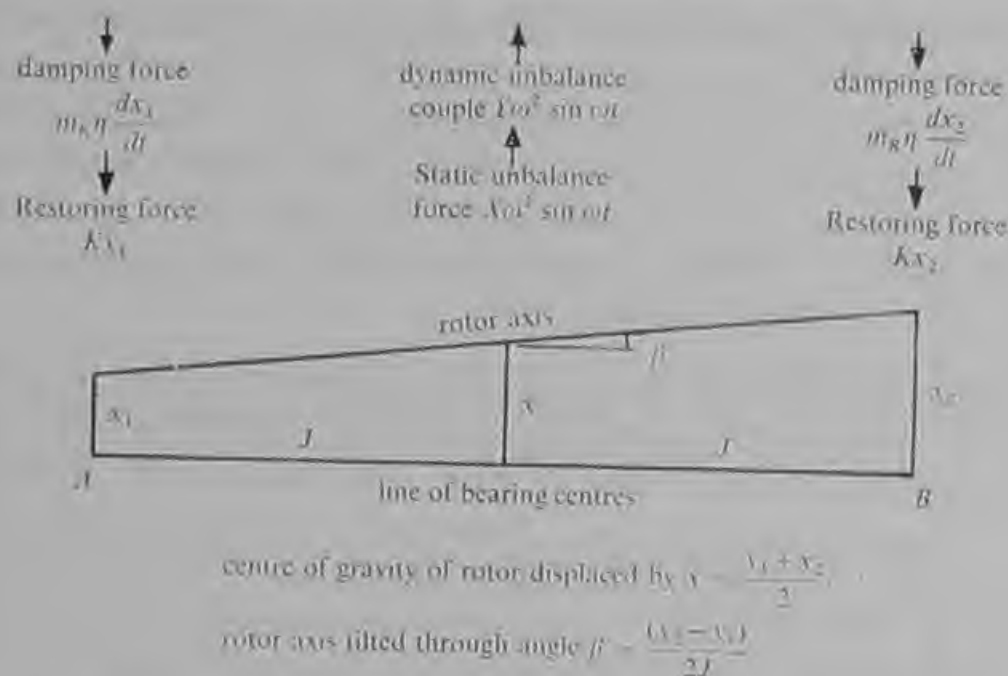$$\omega_2^2 = \frac{2KJ^2}{(I - I_o)}. \qquad (79)$$

Fig. 7.4a Forces acting on rotor during synchronous whirl
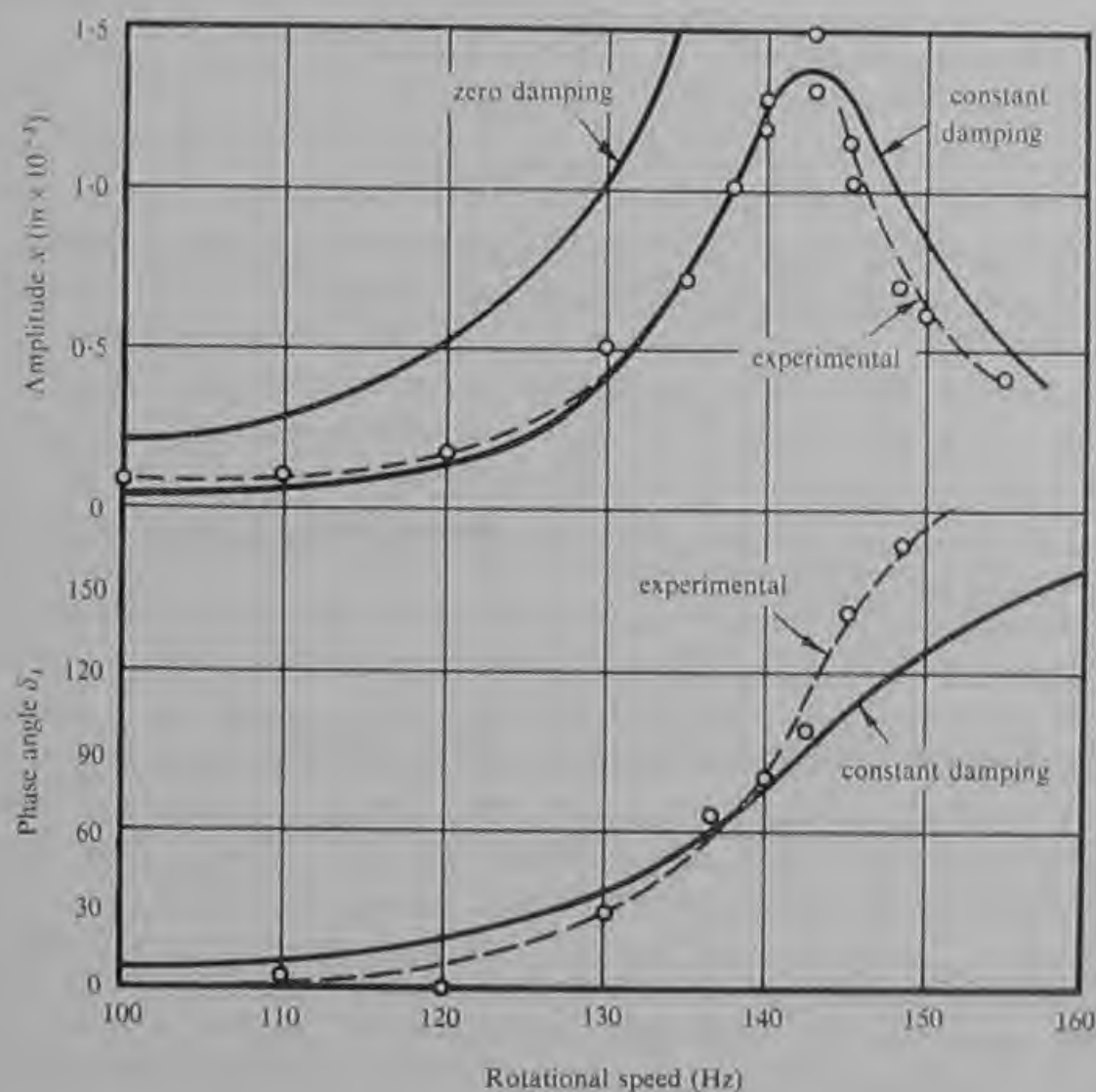

Fig. 7.4b Cylindrical synchronous whirl of a rotor supported in two aerostatic journal bearings

The corresponding solutions in the perpendicular plane are similar, except for the 90° phase difference, and the two solutions combine to describe fully the circular motion of the rotor axis. The three equations (74), (75) and (76) describe the cylindrical whirl and for small damping ($\eta < \omega_1$) a resonant speed is defined by equation (76). Equations (77) to (79) describe the conical whirl and for small damping the resonant speed is given by equation (79).

The predicted variation of synchronous whirl amplitude with speed for the two cases of zero damping and small damping are compared with experimental data in Fig. 7.4(b). It can be seen that the real bearing, of large clearance ratio, behaves in a manner similar to that predicted using a constant damping coefficient. In the absence of damping the whirl amplitude increases very rapidly as the resonant speed is approached. This is because at the resonant speed the stiffness force is exactly balanced by the centrifugal force acting on the rotor. Referring again to Fig. 7.2 and considering static unbalance only the radial forces acting on the rotor in the absence of damping are

$$2Kr = X\omega^2 + m_R r \omega^2, \tag{80}$$

giving
$$r = \frac{X\omega^2}{(2K - m_R \omega^2)}. \tag{81}$$

It can be seen that the whirl radius r approaches infinity as $(2K - m_R \omega^2)$ approaches zero. This occurs when

$$\omega_1^2 = \frac{2K}{m_R}, \tag{76}$$

Thus at the cylindrical resonance the unbalance force must be balanced by the damping force.

$$X\omega_1^2 = 2Cr\omega_1,$$

and the radial amplitude of the whirl orbit is given by

$$r = \frac{X\omega_1}{2C}. \tag{82}$$

Using equation (82), if a safe limit is established for the whirl radius a limiting value for the tolerable residual static unbalance can be calculated. Equation (82) can be derived from equation (74) by putting $\omega = \omega_1$, $x = r$ at $(\omega t - \delta_1) = \frac{\pi}{2}$ and $C = m_R \eta$.

A tolerable limit of dynamic unbalance can be established using equation (83):

$$\frac{r}{J} = \beta$$

$$= \frac{Y\omega_2}{2CJ^2}. \tag{83}$$

Equation (83) can be obtained by equating the moment generated by the dynamic unbalance and the moment of the damping forces of the two bearings or by making the appropriate substitutions in equation (77).

Equations (82) and (83) enable limits to be established for the residual imbalance in the rotor in order that the cylindrical and conical resonances can safely be run through. Strictly, a limit should be established from a consideration of the vector sum of the two whirl components but if the two resonant speeds do not occur close together this is not essential.

7.3 Inversion

It can be seen from equations (74) and (75) and equations (77) and (78) that at high rotational speeds the limiting value of x is X/m_R and the limiting value of β is $Y/(I - I_o)$. This condition represents the shaft rotating about a mass axis, and no unbalance forces arise. In practice this condition is rapidly approached at speeds beyond the synchronous resonances. It can be seen from Fig. 7.4(b) that the phase and amplitude change rapidly once the resonant speed is exceeded. With less than a ten percent increase in speed the phase shift from $90°$ to $180°$ is completed. This rapid shift to a condition approximating to rotation about the mass axis is a characteristic of rotors supported in aerostatic bearings and is called inversion.

The lower or more pronounced of the two synchronous resonances has often been called the inversion speed. This is rather a loose description since a complete inversion cannot occur until both resonances are exceeded. In many rotor-bearing systems only one synchronous resonance is observable due to the onset of self-excited whirl intervening between the resonant speeds. However, in machines capable of rotating at very high speeds, with the whirl suppressed, unbalance does not present a problem at speeds above the synchronous resonances and the level of external vibration in such machines is usually undetectably low.

7.4 Self-excited whirl

It has already been stated that if a condition is reached at which damping becomes zero a self-excited instability arises. From an

examination of equations (65) and (66) it is apparent that the damping becomes zero when

$$\frac{\omega}{\omega^*} = \left(\frac{2+\varepsilon^2}{1-\varepsilon^2}\right). \tag{84}$$

Following a shock loading or sudden disturbance a rotor supported in two journal bearings will vibrate at one of its two natural frequencies defined by equations (76) and (79). In the absence of forced vibration ω^* can take the values ω_1 or ω_2 only. Thus by substituting ω_1 and ω_2 in equation (84) two possible onset speeds of self-excited whirl are
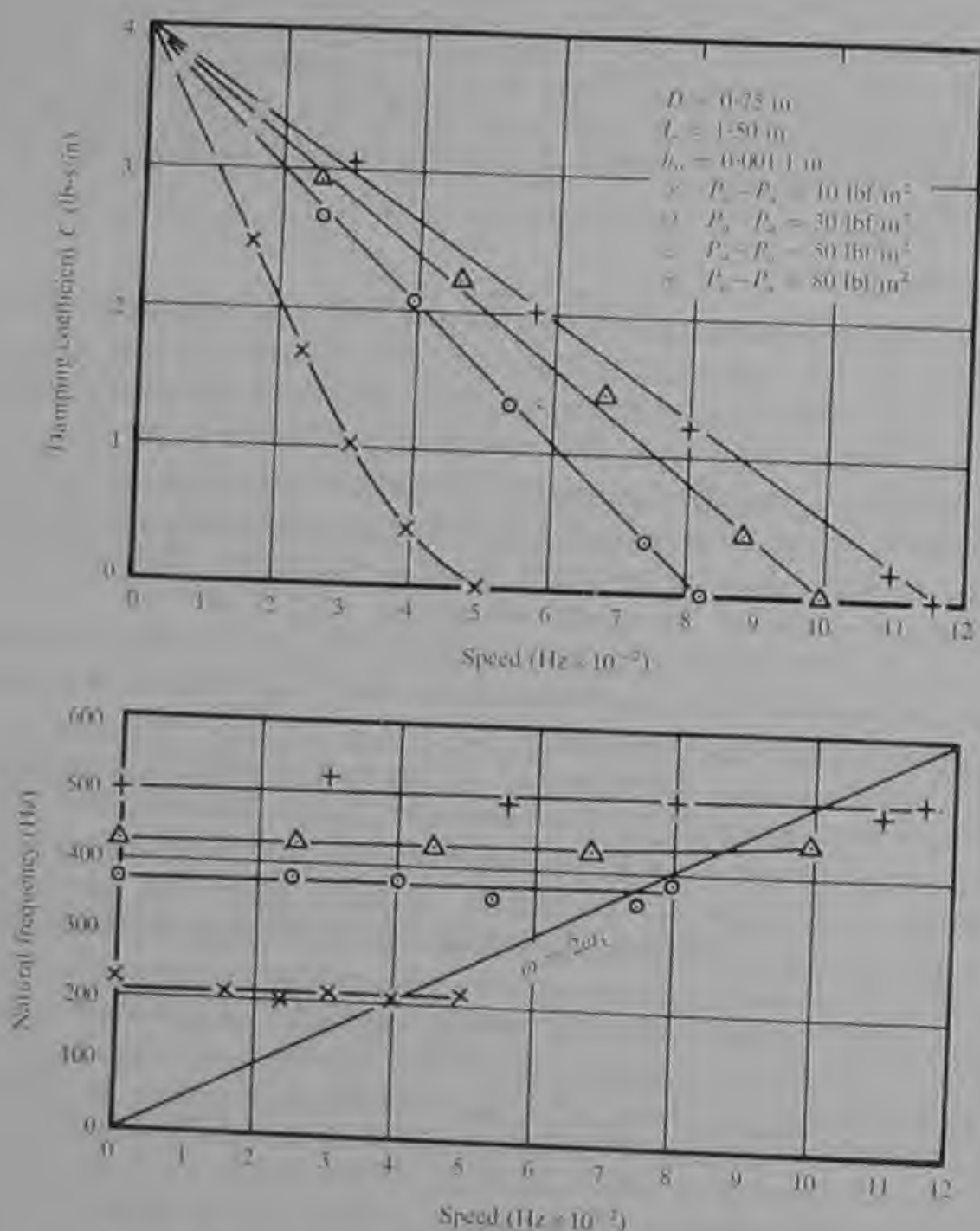

Fig. 7.5 Variation of natural frequency and damping with speed for large clearance bearing (after Tully, Ref. 17)

obtained. In practice only the lower is observable since the onset of self-excited whirl normally sets a maximum speed for the rotor. Theoretically a disturbance is required to start the whirl but in practice only a minute disturbance or vibration is needed and this is always present.

Assuming that the lower natural frequency is in the cylindrical mode, the onset speed of self-excited cylindrical whirl is obtained from equation (84) as

$$\omega_c = \omega_1 \left(\frac{2 + \varepsilon^2}{1 - \varepsilon^2} \right), \tag{85}$$

which for $\varepsilon = 0$ reduces to $\omega_c = 2\omega_1$. This is the onset speed of the well-known half speed whirl which is often met in aerodynamic bearings. During half-speed whirl the rotor orbits the bearing centre at a frequency (ω_1) equal to half its rotational speed (ω_c). Following its onset, the whirl amplitude increases very rapidly with any further increase in speed and the bearing surfaces come into violent contact.

Tully conducted a number of experiments in which he applied a shock load to a shaft supported in two journal bearings and measured the damping coefficient from the decay of the ensuing free oscillations. His data for bearings of large clearance ratio are shown in Fig. 7.5. It can be seen that the damping reduced linearly with speed. Self-excited whirl commenced at the speed at which the damping became zero. The linear fall in damping is predictable from a study of equations (65) and (66). Since the frequency of free vibration remained constant throughout the experiments the squeeze film damping remained constant. The aerodynamic damping increases linearly with speed and so the net damping would be expected to fall linearly with speed.

The data presented in Fig. 7.5 shows that the value of squeeze film damping at zero speed appears to be independent of the air supply pressure. This would be expected for Tully's bearings with annular orifice feeding. It is also shown that the natural frequency was sensibly independent of rotational speed but rose with increasing supply pressure. This confirmed that the dynamic stiffness was predominantly aerostatic, and Tully observed that the measured dynamic stiffness was equal to the aerostatic stiffness measured by applying static load at zero speed.

It can be concluded that for bearings of large clearance ratio the simplified theory gives a correct qualitative prediction of the bearing performance. It enables an accurate prediction of unbalance resonance speeds to be based upon the aerostatic stiffness and also provides an accurate prediction of the half speed whirl onset for lightly loaded bearings.

at the half speed whirl condition no aerodynamic stiffness is generated, leaving only the aerostatic stiffness to determine the natural frequency.

It must be emphasized that the data presented in Fig. 7.7 are an extreme case in which the aerostatic performance is almost lost. The gauge pressure ratio is in the region of 0·95 and consequently the aerostatic load capacity and stiffness are very low. The apparently disproportionate increase in stiffness between the data for 50 lbf/in² gauge supply pressure and 80 lbf/in² gauge supply pressure is due to the reduction in gauge pressure ratio at the higher pressure compounding the increase in stiffness resulting from the increase in pressure. If the feed hole diameter was reduced to reduce the gauge pressure ratio to say 0·6, the initial natural frequency at 50 lbf/in² gauge would be approximately 600 Hz and at 80 lbf/in² gauge approximately 750 Hz. In this case the initial rapid fall in damping and natural frequency would be somewhat less marked and the region of very low damping on 50 lbf/in² gauge supply pressure would be avoided.

Although a complete theory has yet to be developed fully to explain the performance of low clearance aerostatic journal bearings some important design recommendations can be made based on experience and experimental data.

(a) Avoid designing at gauge pressure ratios in excess of 0·8, the value for maximum stiffness for fixed feed hole diameter. This will assist in avoiding the more pronounced aerodynamic characteristics shown in Fig. 7.7 and in particular the region of very low damping.

(b) The onset speed of self-excited whirl can still be estimated to be beyond twice the lowest natural frequency of the shaft calculated from equation (76) or (79) using the aerostatic radial stiffness.

(c) The resonances excited by residual unbalance occur at a low rotational speed. This is a beneficial condition because unbalance forces are low and damping forces are relatively high. Tolerable limits of unbalance are difficult to estimate, but experience has shown that an adequately low level of residual unbalance is easily achieved using commercial dynamic balancing machines.

7.6 Design procedure for high-speed machines

At an early stage in the design of any high speed machine with aerostatic bearings it is essential to calculate the natural frequencies of the rotor in its cylindrical and conical modes. It can be seen from equations (76) and (79) that very few factors are involved. The aerostatic radial stiffness of the journal bearings will be known from the bearing design calculations. The distance between the bearing centres 2J will also be known. It is only then necessary to calculate the mass

of the rotor, its polar moment of inertia and its transverse moment of inertia. In the case of a solid cylinder the polar moment is given by:

$$I_o = m_R \frac{D^2}{8},$$ (86)

and the transverse inertia about the centre of gravity by

$$I = m_R \left(\frac{L^2}{12} + \frac{D^2}{16}\right).$$ (87)

In the case of a hollow cylinder the polar moment is given by

$$I_o = \frac{m_R(D^2 + D_i^2)}{8},$$ (88)

and the transverse inertia about the centre of gravity is given by

$$I = m_R \left(\frac{L^2}{12} + \frac{D^2 + D_i^2}{16}\right).$$ (89)

In equations (86) to (89) L is the length of the cylinder, D is the outside diameter and D_i is the inside diameter of a hollow shaft.

From equations (76) and (79) it can be seen that the lowest natural frequency will be in the cylindrical mode if

$$m_R J^2 > (I - I_o).$$ (90)

Having calculated the lower of the two natural frequencies this can then be compared to the maximum design speed of the machine. It will then be seen whether the machine can be designed to operate at speeds below its lower natural frequency. This is a desirable condition in many applications of aerostatic bearings. For example, in most machine tool applications, grinding wheels, cutting tools and other unbalanced masses are connected to the rotor and the overall degree of balance can only be controlled within broad limits. It is therefore important that the resonant speeds which are excited by rotor unbalance are not reached during the normal operation of the machine. In the majority of cases in practice this condition can be realized, and the machine tool spindles operate at speeds which are only a small fraction of the lowest natural frequency. In such cases the damping can be large. An important parameter is the damping ratio, ξ, where

$$\xi = \frac{C}{2} \left(\frac{2}{K m_R}\right)^{\frac{1}{2}}.$$ (91)

The damping ratio determines how quickly a free vibration dies away and an optimum value is near 0·6.

It is always advisable to calculate the squeeze number σ based on the lower natural frequency of the rotor where

$$\sigma = \frac{12\mu}{P_a}\left(\frac{a}{h_o}\right)^2 \omega_1,$$

or

$$\sigma = \frac{12\mu}{P_a}\left(\frac{a}{h_o}\right)^2 \omega_2,$$

whichever is the lower. Using this value the squeeze film damping at zero speed can be estimated from Fig. 7.1. Then for large clearance bearings the damping of the lower natural frequency at finite speeds can be estimated by assuming a linear fall from the squeeze film value at zero speed to zero damping at twice the lower natural frequency. In many applications the operating speed is less than ten percent of the lower natural frequency. In such cases this method affords a workable approximation even for bearings of smaller clearance ratio and it is often found that the damping ratio far exceeds the optimum value. The damping is reduced by the use of simple orifices with pockets, and by control of the pocket depth it is possible to achieve the optimum damping ratio. However, this result can be achieved at present only by empirical methods and must be checked by prototype testing. Some experimentally measured damping coefficients with pockets of varying depths are shown in Fig. 7.8.

It is sometimes necessary to investigate ways of raising the lower natural frequency of the rotor. This can be achieved only by either
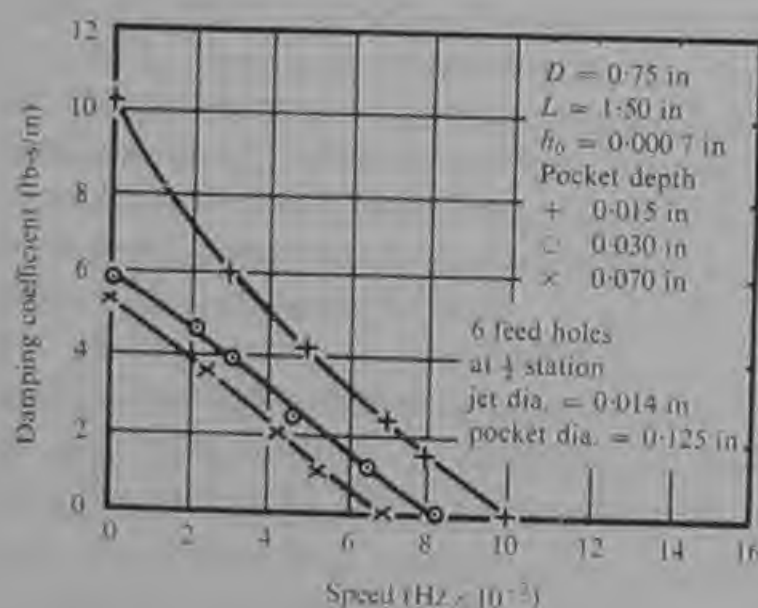

Fig. 7.8 Variation of damping coefficient with speed for various pocket depths in a journal bearing with simple orifice compensation

increasing the radial or the angular stiffness of the bearings or by reducing the mass or transverse moment of inertia of the rotor. Radial stiffness can be raised by increasing the plan area of the bearing, reducing the clearance or raising the gas supply pressure. Angular stiffness is raised by all these changes and in addition by increasing the bearing spacing. The mass and inertia of the rotor can be reduced by such devices as changing the rotor material or replacing a solid shaft by a hollow one.

When considering conical synchronous resonance it is worth remembering that the thrust bearings can make a contribution to the total angular or tilt stiffness of the bearing system. This is not often large compared to that of the journal bearings but can become significant in short machines with large diameter thrust bearings.

While considering the dynamic properties of the thrust bearings it is important to check that the natural frequency of the rotor in the axial direction is well beyond the maximum operating speed. The axial resonance is defined by

$$\omega_3^2 = \frac{K_A}{m_R},\tag{92}$$

where K_A is the combined axial stiffness of the two thrust bearings and $K_A = 2 \cdot 88 \dfrac{W^*}{h^*}$ from Fig. 4.8.

In some machines which either operate at ultra-high speeds or must operate on low gas supply pressures it soon becomes apparent that the design speed lies well beyond the natural frequencies of the rotor and possibly even beyond the half-speed whirl onset. Such instances arise in high-speed hand tools, textile spindles and some small, very high-speed drilling and internal grinding spindles. In these cases it is essential to introduce additional damping into the bearing system in order to withstand externally impressed vibration and shock loads and also to prevent the onset of destructive whirl.

7.7 Rubber stabilized bearings

One of the most effective and widely applied methods of increasing the damping in gas bearing systems is to mount the journal bearings resiliently on rubber. This method of suppressing the self-excited whirl of high-speed rotors was discovered by Montgomery and Sterry (Ref. 19) at Harwell in 1956. Montgomery and Sterry used aerostatic bearings with the air fed through porous bronze bushes to support the shaft of a turbine rotating a mirror for a high-speed camera. Later the same method was applied successfully by Kerr at the National Engineering Laboratory to stabilize aerodynamic bearings. Rubber stabilized bearings found widescale commercial use when the air

bearing dental turbine was introduced in 1963, and since that time their application has increased to include textile spindles, small turbo-compressors, high frequency motors for machine tool applications and a variety of scientific instruments.

In almost all cases to date the rubber mounting has been applied in the simple form of two rubber 'O' rings surrounding the bearing bush. In addition to providing resilience and damping, the 'O' rings also serve to seal the air reservoir around the bearing. The method is so powerful that the simple introduction of the rubber 'O' rings more often than not completely eliminates the destructive effect of self-excited whirl and makes possible speeds several times greater than the whirl onset speed for rigidly mounted bearings. However, commercially available rubber 'O' rings differ widely in the type of rubber compound used, the hardness number, the percentage of carbon filler and other factors. The following information will be of help to the designer.

The behaviour of rubber can best be explained by supposing it to exhibit a complex stiffness

$$S = A(\omega) \, e^{i\delta(\omega)}, \tag{93}$$

where A is called the stiffness modulus and δ is the loss angle. Both A and δ are frequency dependent. The in-phase or stiffness component is given by

$$S' = A(\omega) \cos \delta(\omega), \tag{94}$$

and the quadrature or damping component is given by

$$S'' = A(\omega) \sin \delta(\omega). \tag{95}$$

The energy loss per cycle per unit volume of rubber is given by Payne and Scott (Ref. 21) as

$$\text{energy loss} = \pi A_f A_e \sin \delta, \tag{96}$$

where A_f is the amplitude of the stress cycle,
and A_e is the amplitude of the strain cycle.

Now since the force must be transmitted to the rubber through the bearing:

$$A_f \propto \varepsilon h_o K \quad \text{(the radial force)}$$

and $A_e \propto \dfrac{\varepsilon h_o K}{A}$ (the deflection produced in the rubber).

Thus the energy loss per cycle is proportional to $(\varepsilon h_o K)^2 \dfrac{\sin \delta}{A}$. This forms a basis upon which to compare different rubbers. It also indicates that increasing the bearing stiffness has a powerful effect upon increasing the rate of energy absorption in the rubber.

Property	Rubber material				
	Natural	Butyl	Nitrile	Silicone	'Viton'
Hardness range (° BS)	30~100	35~85	40~100	40~85	70~90
Loss angle at 20°C	4·6	9·0/26·5*	6·0~9·0	5·1	—
Loss angle at 70°C	3·4	4·6	5·1~6·3	4·6	—
Working temp. (°C)					
Minimum	−55	−50	−20	−45	−45
Maximum	+70	+125	+120	+250	+220

* Stone and Andrews.

After Payne and Scott, *Engineering Design in Rubber* (Maclaren, 1960).

Fig. 7.9 'O' ring material data

A rubber with good damping will possess a high loss angle. Fig. 7.9 gives data for some available rubber compounds used for 'O' rings. It can be seen that the highest loss angles are achieved using butyl rubber. Nitrile and viton (data not available) rubbers offer better damping than natural rubber or silicone compounds. However, the properties of rubbers are affected by several factors, the more important of which are

(a) hardness number

(b) percentage of filler

(c) temperature

(d) frequency of vibration

(a) *Effect of hardness number* Both stiffness modulus and loss angle tend to increase with hardness number. However, the important factor $\dfrac{\sin \delta}{A}$ always falls with increasing hardness number indicating that soft rubbers are superior to hard rubbers. Data for natural rubber are shown in Fig. 7.10.

(b) *Percentage of filler* Increasing the percentage of filler in rubber compounds increases the stiffness modulus. The effect on damping properties is still the subject of some doubt.

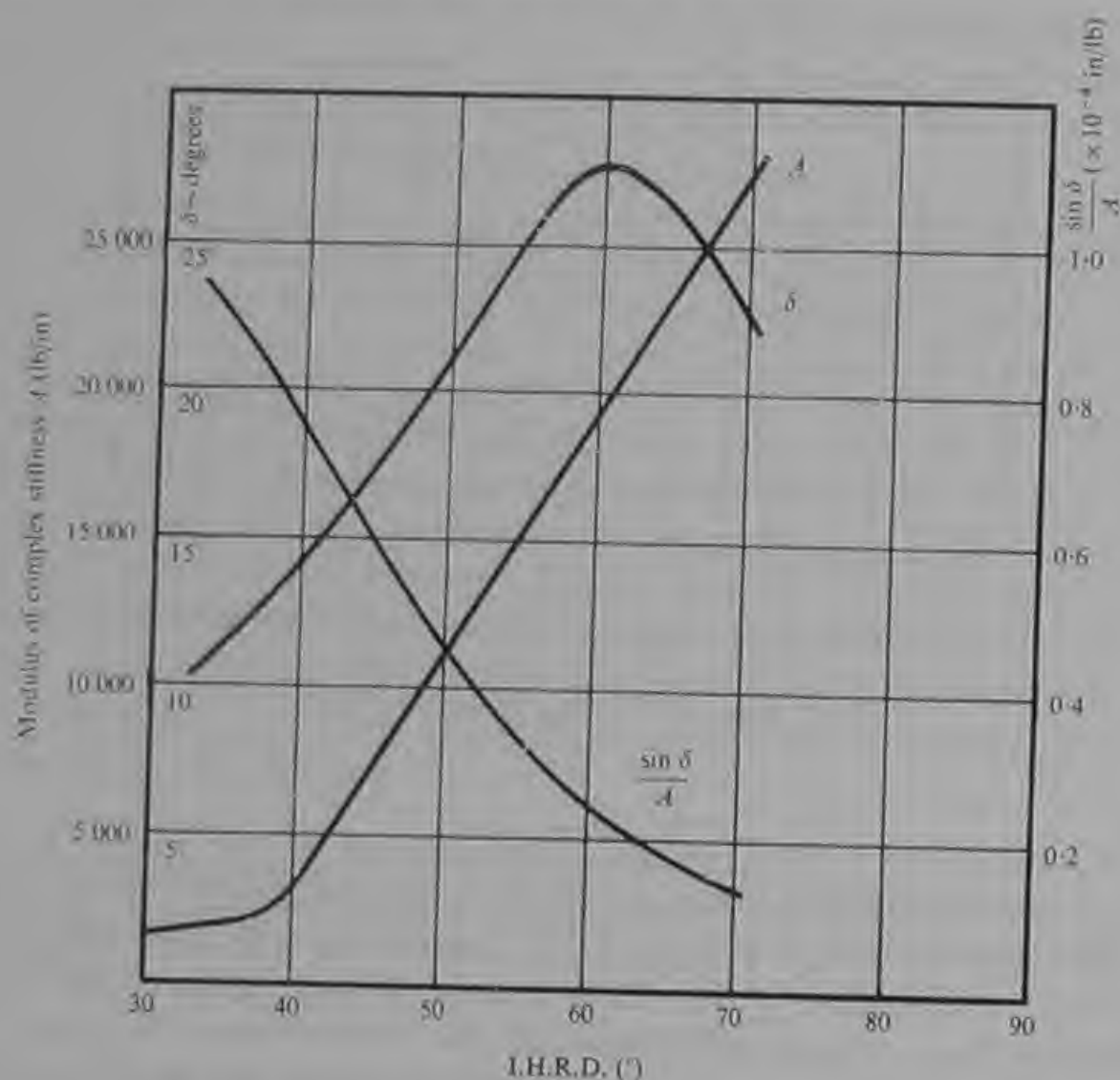(c) *Effect of temperature* Both the stiffness modulus and the loss angle

Fig. 7.10 Variation with hardness number of the dynamic
properties of natural rubber 'O' rings

fall with temperature. However, the net result is a fall in $\dfrac{\sin \delta}{A}$ as shown
in Fig. 7.11 for natural rubber and butyl rubber. It is therefore indicated
that the effectiveness of rubbers reduces with temperature and this has
been demonstrated in practice. For example whirl has been induced
in a high-speed rotor stabilized by butyl rubber 'O' rings by raising
the rubber temperature from 20°C to 70°C. It has been found that
viton and silicone rubbers have the best high temperature properties
and can be applied at temperatures up to 200°C.

(d) *Effect of frequency of vibration* The stiffness modulus of rubbers
increases with the frequency of the impressed vibration. The loss
angle increases at low frequencies but becomes nearly constant over a
broad band of higher frequencies. This suggests that for whirl suppres-
sion rubbers are likely to be less effective at higher frequencies due to
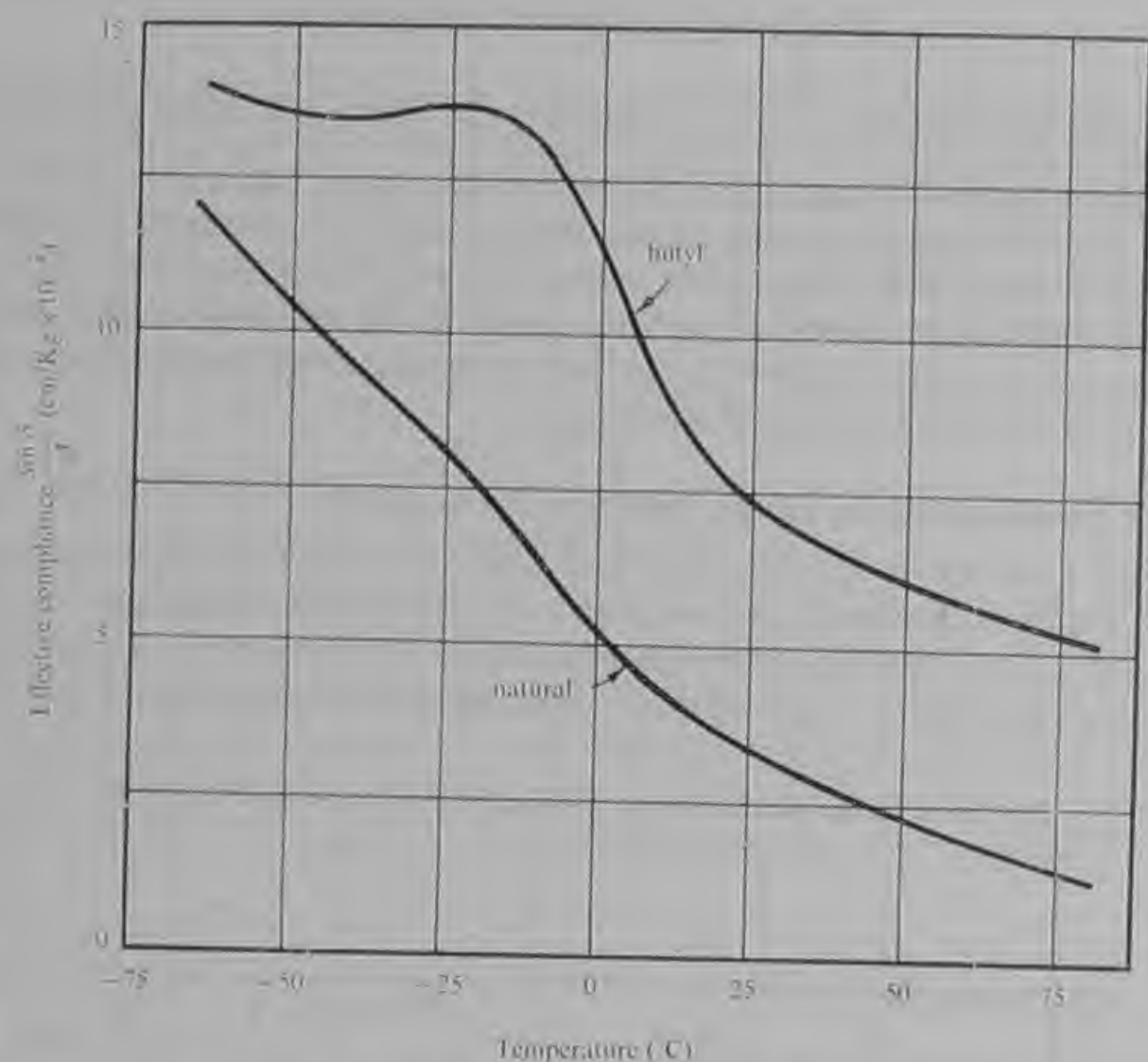
Fig. 7.11 Variation with temperature of the dynamic properties of natural and butyl rubber
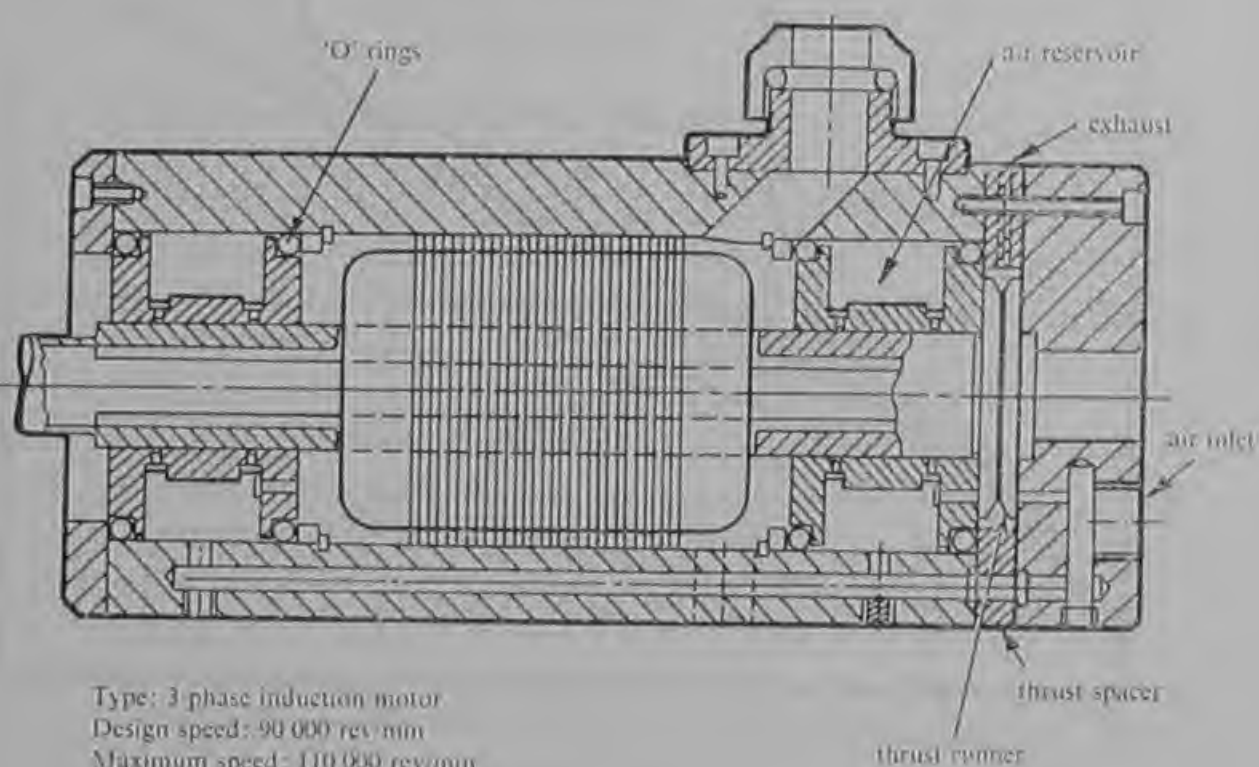

Fig. 7.12 High frequency motor with rubber stabilized air bearings (*Reproduced by permission of Westwind Turbines Ltd.*)

the reducing value of $\frac{\sin \delta}{A}$. However, this does not often present a practical limitation upon the use of rubber since in any one machine only one self-excited whirl is usually observed and for a constant supply pressure the whirl frequency remains constant irrespective of the rotational speed. Thus the rubber needs to be effective at the whirl frequency but not necessarily at the rotational frequency which can be up to an order of magnitude higher.

7.8 Characteristics of rubber stabilized air bearings

Fig. 7.12 shows a cross-sectioned view of a high-frequency motor with rubber stabilized air bearings. This machine was used by the author in an evaluation programme of 'O' rings made of various rubber compounds. The method of testing was to accelerate the rotor
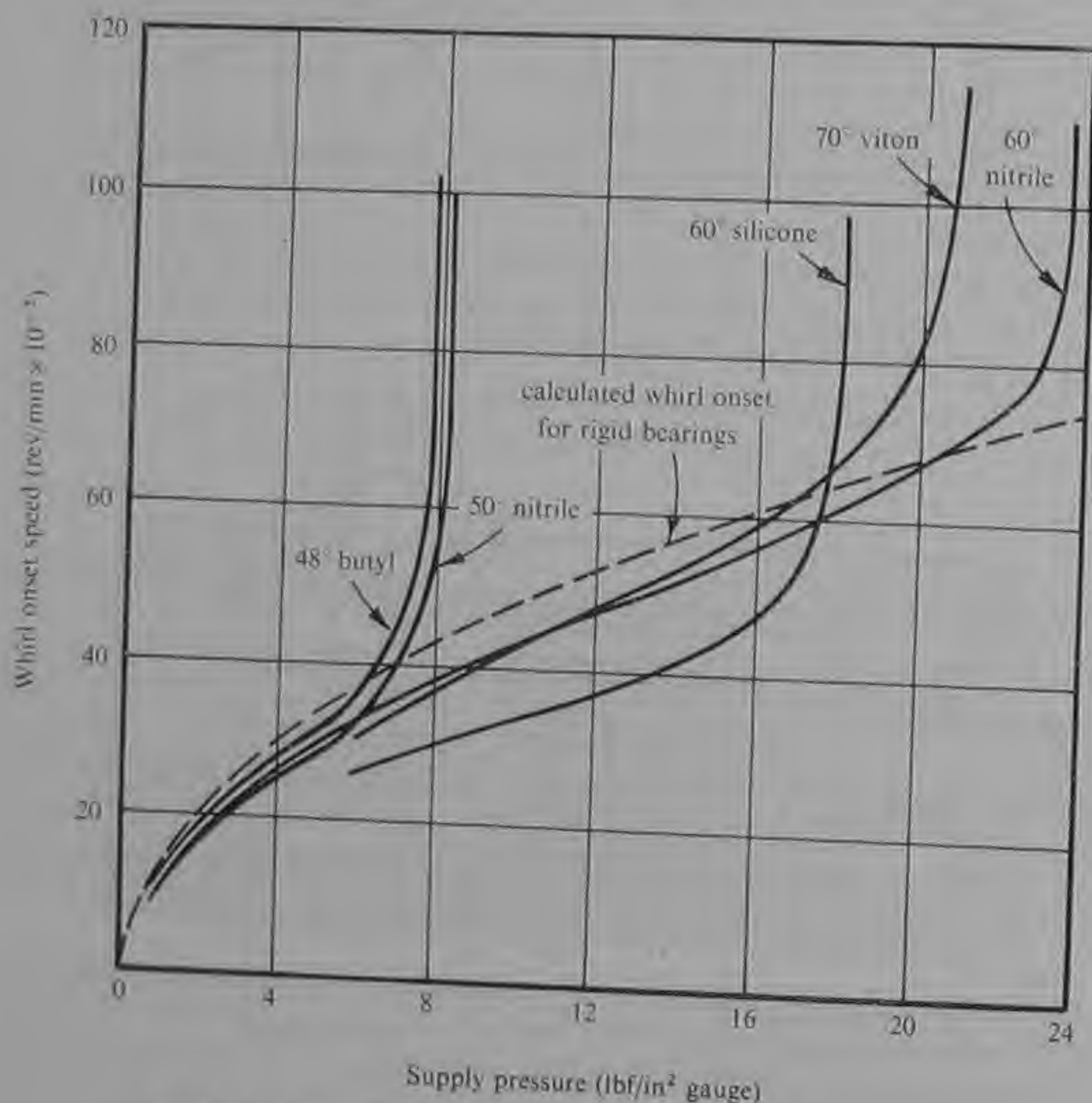

Fig. 7.13 Comparison of 'O' rings at ambient temperature

until the onset of whirl was observed and for each rubber the test was repeated at several bearing supply pressures. Some typical results are shown in Fig. 7.13 in which the whirl onset speed is plotted against supply pressure for various rubber compounds. It was found that at low supply pressures the whirl onset speed increased approximately with the square root of the supply pressure. This is what one expects for rigidly mounted bearings since

$$\omega_1 \propto (K)^{\frac{1}{2}}$$

and approximately

$$\omega_1 \propto (P_o - P_a)^{\frac{1}{2}}.$$

In this region the rubber is not effective since the gas film is not stiff enough to produce sufficiently large deflections in the rubber before contact occurs between the shaft and the bearing. However, for each rubber tested there existed a critical pressure above which the rubber became effective and no whirl onset speed could be reached within the capability of the motor. The stability diagram for rubber-mounted
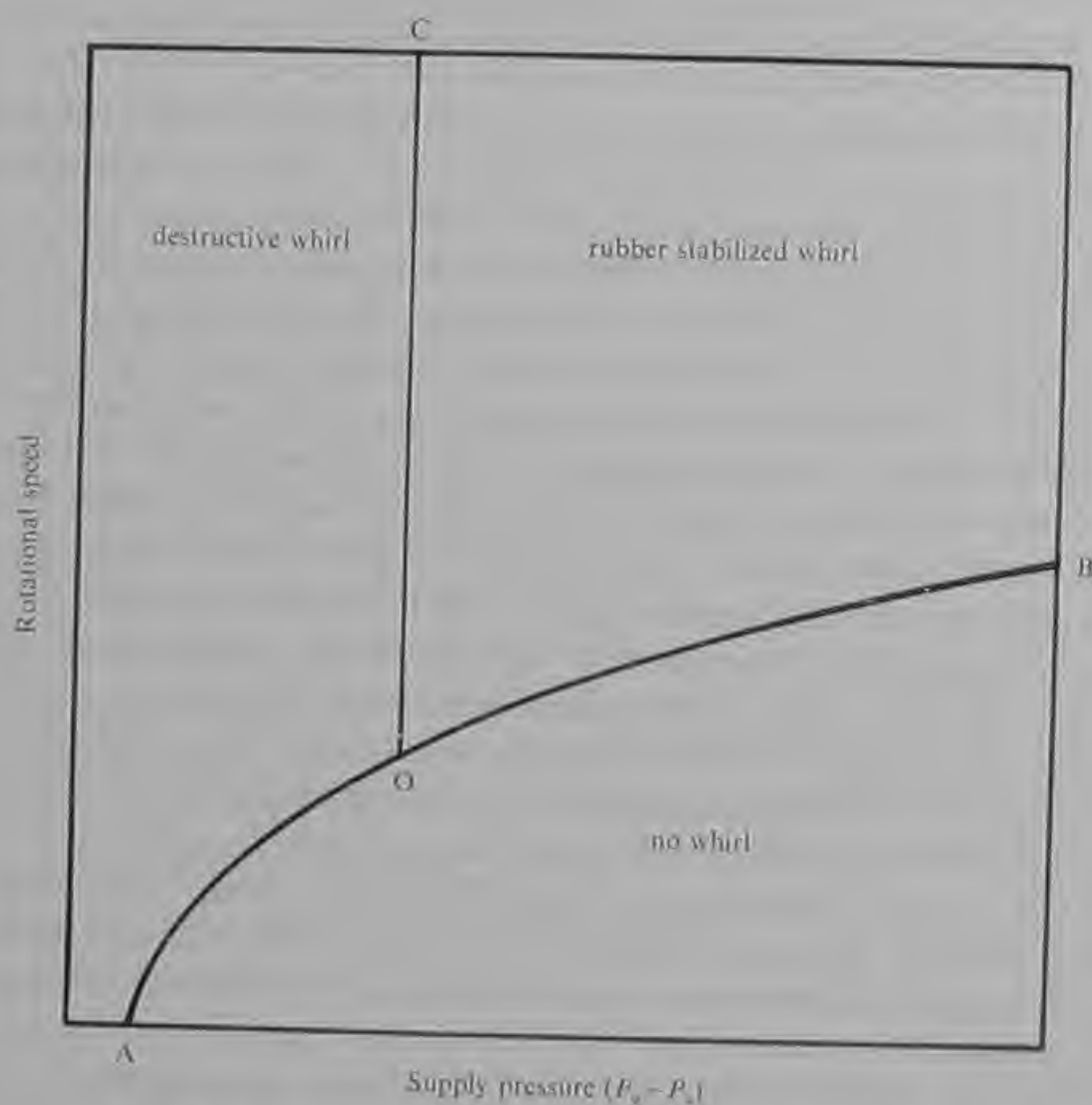

Fig. 7.14 Stability diagram for rubber mounted bearing systems

bearing systems is shown in Fig. 7.14. Below the line AOB, which is equivalent to the whirl onset boundary in a rigid system, no whirl exists. The critical pressure is shown by the vertical line OC. To the left of OC the whirl is destructive since the rubber is non-effective. To the right of the line OC and above the line OB the whirl exists but is contained at a small amplitude. For any one machine rubbers can be graded according to their critical pressure. For example, in the author's tests the data shown in Fig. 7.15 were obtained. It can be

Rubber Compound	Hardness Number (B.S. degrees)	Critical Pressure (lbf/in^2 gauge)
Butyl	48	8
Nitrile	50	8
Silicone	60	18
Viton	70	21
Nitrile	60	24
Butyl	75	> 60

Fig. 7.15 Experimental comparison of rubber compounds in a high speed machine with rubber stabilized air bearings

seen that the hardness number was more important than the rubber compound and that all compounds tested were effective in their softer grades. It is probably best to select the rubber on the basis of chemical compatibility and tolerance to high or low temperatures where necessary and to achieve stability by selecting a suitably soft grade. Butyl rubbers, for example, while possessing excellent damping properties are inclined to swell when attacked by oil contamination in the compressed air supply. This problem is also encountered with natural rubbers but not generally with nitrile, viton or silicone compounds.

In the early days of the use of rubber stabilized air bearings some doubts were expressed concerning the effect of the compliance of the rubber in hand tools and machine tool spindles. It was found that in the dental turbine and other hand tools the tactile sense was not impaired. There also does not seem to be any serious restriction on the use of rubber stabilized bearings in such applications as high-speed drilling spindles and small high speed internal grinding spindles. Tests conducted by the author with a high-frequency motor for small bore grinding showed that the presence of the rubber did not adversely affect the results achieved in respect either of workpiece geometry or surface finish.

Rubber 'O' rings can simply and effectively be applied to a wide range of machines with aerostatic bearings. They offer a form of construction which is simple to manufacture and to assemble. Because

whirl is stabilized, bearings of large clearance or supplied at lower supply pressures can often be used. In the future, bearings for 'O' ring mounting offer some promise of being available 'off the shelf' in the way that ball bearings have been for many years.

The list of rubber compounds mentioned is by no means comprehensive and new compounds are constantly appearing. If in any doubt the designer is advised to contact the 'O' ring manufacturers and obtain full details of the rubber compounds available.

7.9 Other methods of delaying whirl onset

Stabilization by rubber is the simplest and most effective method of obtaining whirl stabilization over a very wide speed range. However, there are many methods of delaying the onset of whirl by a greater or lesser degree. Several of these methods involve the introduction of some asymmetry into the bearing with a view to forcing the shaft to run eccentrically in the bearing. It has been shown that the greater the quasi-static eccentricity the higher is the whirl onset speed (see equation (85)). The assymetry can be achieved in a variety of ways, such as by the use of unequal spacing or diameter of feed jets or by venting one side of the bearing to atmosphere by means of a hole or slot. At best these methods achieve only a limited increase in whirl onset speed and always at the cost of a loss in static load capacity in one direction.

An effective method of eliminating self-excited whirl which can be applied at temperatures above or below those possible using rubber has been described by Sixsmith (Ref. 21). In this system the centre of the journal bearing is vented to atmosphere by a series of cavities with exhaust jets which are spaced symmetrically around the bearing between the feed jets. The whirl frequency can be tuned-out by adjustment of either or both the exhaust jet diameter and the cavity volume. Sixsmith successfully employed this method on liquefaction turbines for hydrogen and helium with the bearings operating on the process gas at temperatures below $50°K$. The major disadvantage of the use of tuned cavities is the sacrifice of radial load capacity. Another disadvantage is the additional manufacturing complexity. However, Sixsmith's bearing offers the most effective method of whirl stabilization for use at very high and very low temperatures and in other applications where the use of rubber is precluded.

Another series of methods of delaying the onset of whirl consists of introducing the feed gas tangentially into the bearing so that it is induced to swirl in opposition to the shaft rotation. This is achieved using tangential feed jets of slots. This method has been demonstrated (Ref. 22) to be effective in large clearance bearings but is of doubtful effect in small clearance bearings where gas inertia effects are small.

CHAPTER 8

SELECTION OF MATERIALS

8.1 Properties required of gas bearing materials

Much of the early research and development of aerodynamic bearings was concerned with the search for suitable combinations of materials for the bearing surfaces that would tolerate the rubbing contact which occurred at starting and stopping. This work has been reported widely and for detailed information on this aspect of materials selection the reader is referred particularly to References 11 and 12. There has been a tendency for this aspect to colour all thinking on the subject of materials selection for gas bearings, whereas in most applications of aerostatic bearings there are several more important considerations. The designer who relies upon materials with low friction and anti-seize properties to bestow reliability and long life upon his bearings will fail more often than he succeeds. The rubbing in the early experiments with aerodynamic bearings was limited to relatively light loads and occurred only at very low speeds. However, when an aerostatic bearing is overloaded this inevitably occurs at a much higher loading and often at a very high rotational speed. It has been found that very few materials can withstand these conditions and the exceptions only occur in very small machines where the kinetic energy to be dissipated in stopping the rotor is small.

With the exception of very small machines and some applications where rotational speeds are low the designer of aerostatic bearings will be wise to assume that any contact between the bearing surfaces will result in seizure, and to design to avoid contact occurring. This involves ensuring that adequate load capacity exists to deal with accidental overload and providing for such eventualities as a sudden loss of supply pressure. To a bearing designed in this way any seize resistance which can be provided acts as an additional safeguard rather than being fundamentally necessary for its reliability.

It has been found possible to ensure that damaging accidents are rare occurrences in most applications of aerostatic bearings. It is also possible by a suitable selection of materials to provide bearings that can be repaired quickly and easily several times without any replacement of parts being necessary. Aerostatic bearings are essentially 'go—no go' devices. They either function perfectly or, if damaged, they will not function at all. In many applications this property is advantageous

provided that rectification is cheap and simple. It avoids a period of gradual deterioration in performance during which results are unsatisfactory but the cause of dissatisfaction is not apparent.

The emphasis on rubbing properties has tended to focus attention on the selection of materials for the bearing bush and the shaft journal surfaces. However, in aerostatic machines it is important to select carefully the materials used for almost all the component parts. In this connection the following factors must always be borne in mind.

(a) *Material stability* All structural parts which can in any way influence the geometry of the bearing surfaces should be made from stable material in the fully stress-relieved condition.

(b) *Corrosion resistance* All component parts which are in contact with the supply gas and exhaust gas must be corrosion resistant. Materials used in machines with air bearings must be corrosion resistant in damp air and have the smallest possible electrical potential difference. The designer is recommended not to use materials which differ in electro-chemical potential by more than 0·25 V. Values of electro-chemical potential for some engineering materials are given in Fig. 8.2.

Material	Density (lb/in³)	Modulus of Elasticity (lbf/in² × 10⁶)	Coefficient of Thermal Expansion (× 10⁻⁶/ deg C)	Thermal Conductivity (c.g.s. units)	Max. Service Temperature (°C)
Ceramics Aluminium oxide	0·135	46·7	6·3	0·054	1 400
Silicon nitride	0·08–0·09	22	2·6	0·024	1 200
Tungsten carbide	0·55	80–100	1·1	—	450
Plastics Nylon	0·04	0·41	45–80	0·000 6	120
p.t.f.e.	0·08	0·05	55	0·000 6	260
Cast epoxy resin	0·04	0·40	50	0·01	65 cold cured 100 hot cured

Fig. 8.1 Properties of non-metallic materials

(c) *Thermal expansion* The influence of differential thermal expansion on the design of aerostatic machines is discussed in Chapter 6. It is wise to endeavour to match expansion rates as far as is practicable. Where a precise matching is not possible it is necessary to study the

Material	Density (lb/in³)	Modulus of Elasticity (lbf/in² × 10⁶)	Coefficient of Thermal Expansion (× 10⁻⁶/ deg C) (20–100°C)	Thermal Conductivity (c.g.s. units)	Electrode Potential Relative to Saturated Calomel Electrode in Sea Water (V)	Max. Service Temperature (°C)
Aluminium	0·098	10	23·5	0·57	−0·75	—
Aluminium alloys	0·095–0·102	10–10·5	20–24·5	0·35	−0·90 to −0·60	200–300
Brass, yellow, hard	0·306	15	20	0·29	−0·30	
Bronzes, lead	0·323–0·335		17·4–18·2		−0·20	—
Bronzes, phosphor	0·320	16	17–18	0·20	−0·20	
Copper, annealed	0·322	17	17	0·94	−0·20	
Iron, cast, grey	0·260	13	11·7	0·13	−0·70	
Nickel, annealed	0·321	30	13	0·21	−0·15	
Magnesium	0·062	6·4	26	0·38	−1·60	
Magnesium alloys	0·063–0·067	6·4	26–27·5	0·19–0·37	−1·60	200–300
Steel, mild	0·283	30	10	0·12	−0·75	
Steel, stainless (EN57) martensitic	0·278	30·5	10	0·06	−0·35	650
Steel, stainless (EN58) austenitic	0·286	29	17	0·036	−0·20	300
Titanium alloys	0·160	15–18	8·0–8·9	0·017–0·04	−0·09 to +0·06	500–550

Fig. 8.2 Properties of metals and alloys

consequences in terms of changes of bearing clearances and the stresses arising over the anticipated temperature range. Some subsequent adjustments to mean clearances or structural features may improve the design compromise.

(d) *Machinability* Provided that the conditions of stability, corrosion resistance and thermal expansion have been satisfied the available material with the best machining characteristics should always be chosen. This is important because in most cases some difficult machining operations are involved, and also because the problem of achieving high precision in the finished part is greatly simplified if the material is easy to handle. Although not strictly 'machinability', under this heading should also be considered ease of heat treatment and surface coating by plating or metal or ceramic spraying where appropriate. Unless there is a good case for trying a new material the designer is advised to use a material with which he is familiar.

(e) *Thermal conductivity* It is advantageous in all high-speed machines to provide a low resistance path for heat to flow away from the bearings and any other heat sources such as electric motor parts. It is unfortunate that the stainless steels which are ideally suited to use in structural parts in contact with the gas supply are poor conductors of heat. Aluminium alloys are some ten times better than stainless steels and are useful for such parts as motor casings. However, aluminium alloys are not generally suitable for parts in contact with the supply gas due to their large negative electrode potential and the strong probability of electro-chemical corrosion. Values of the thermal conductivities of metals, alloys, ceramics and plastics are given in Figs. 8.1 and 8.2.

With the desirable properties listed above uppermost in mind it is possible to consider in turn each of the major components of the aerostatic machine and to suggest some suitable materials. This discussion is based principally upon the various alternative configurations shown in Fig. 6.2 which can be considered for material selection under four headings:

(a) body materials;
(b) bearing bush materials;
(c) shaft materials; and
(d) materials for thrust plates.

8.2 Body materials

The term 'body' denotes the main structural member of the aerostatic machine which normally takes the form of a hollow cylinder in the bore of which are located the journal bearing bushes. It usually includes

drilled holes through which the supply gas passes on its way to the bearing surfaces. The two most desirable properties of the body material are stability and corrosion resistance. It should also possess a high modulus of elasticity in order to minimize any distortion arising from fixing to a support structure or a machine casting.

The most popular body materials are the stainless steels. The austenitic grades are denoted by the number EN58 in the British Standard Specifications. They have good corrosion resistance and are obtainable in free machining grades. They are not hardenable and are non-magnetic. The best corrosion resistance is offered by EN58J which is resistant to attack in marine atmospheres and is the only stainless steel used in surgery for implants in the human body. It is notoriously difficult to machine although a free cutting grade (a relative term!), EN58JM, is available. It is generally only necessary to employ EN58J in machines lubricated by or handling corrosive gases or in machines for marine applications. For most purposes either of the austenitic stainless steels EN58AM or EN58BM can be used. The letter 'M' denotes the free cutting grades and these two materials are the easiest stainless steels to machine.

Austenitic stainless steels have high coefficients of thermal expansion and this may present difficulties in some applications. According to grade and condition the coefficient can vary from 16×10^{-6}/deg C to $18 \cdot 5 \times 10^{-6}$/deg C. This compares to a typical value of between 10×10^{-6}/deg C and 11×10^{-6}/deg C for most shaft materials. Thus austenitic stainless steels are not generally suitable for use in either of the first two bearing configurations shown in Fig. 6.2 due to the large variations of end float which would occur with variations of temperature. However, EN58AM and BM are widely used in machines of the third or four configurations shown in Fig. 6.2.

Austenitic stainless steels can be stress relieved by heating to 800–850°C for two hours. In the stress-relieved condition their long-term stability is good. They have a high modulus of elasticity (29×10^6 lbf/in^2).

In machines in which it is necessary to match the rate of thermal expansion of the body to that of the shaft the martensitic stainless steels EN57 or EN56 can be used. These steels are magnetic and hardenable and in many applications can be used for both body and shaft. However, their corrosion resistance is not as good as the austenitic stainless steels and difficulties may be encountered with surface corrosion after hardening in air unless the oxidized surface of the metal is completely removed.

EN57(S80) is widely available and most engineers are familiar with its heat treatment. However, it is hardenable only to between forty and forty-five on the Rockwell C scale and is not particularly stable

in the hardened condition. Its use should be avoided wherever extreme hardness or wear resistance is required or where thin sections must be employed.

EN56 steels contain thirteen percent chromium and some types are called stainless irons. They have fair corrosion resistance and can be hardened to over sixty on the Rockwell C scale. They are stable in the hardened condition when properly heat-treated and may be useful as body materials where hardness or wear resistance is required.

There are some applications of aerostatic bearings where stainless body materials need not be used. These include instances where dry inert gases are used or where the supply gas can be fed to the bearings by some means which avoids contact with the exposed surface of the body material. The latter condition can sometimes be achieved by the insertion of tubes of stainless materials or by plating or other surface treatments. Materials such as mild steel or cast iron have been used in this way in some applications. However, as the consequence of the presence of any corrosion in the gas supply is eventually bearing failure due to blockage of the feed passages or the bearing clearance, if there is any doubt that these conditions can be met the designer is strongly recommended to use stainless materials.

8.3 Bearing bush materials

The traditional oil bearing bush materials, the bronzes, have much to commend them for use in aerostatic bearings. Lead bronzes have been used widely. They are corrosion resistant, easily machined and easily soldered or brazed so that the pressure-tight fixing of the numerous feed jets is a relatively simple procedure. They are ideally suited for use in combination with austenitic stainless steel body materials. The coefficients of thermal expansion are well matched, thereby avoiding thermal stress problems, and the electro-chemical potentials are identical so that no electro-chemical corrosion can occur. Lead bronzes also have fair anti-seizure properties and, particularly with the slight oil contamination which is often present in industrial compressed air systems, they will often survive an occasional accidental overload or failure of air pressure. They are also easily and quickly rectified when damaged.

Lead bronze bearing bushes are normally employed in the form of relatively thin walled cylinders shrink fitted into the body bore with a light interference. Used in this way they gain their strength and stability from the body material. Prior to grinding and fitting to the body any residual stresses set up in machining can be relieved by heating to 170–300°C for between one and three hours depending on the specification of the bronze.

In some applications of aerostatic bearings it is necessary to make the bearing bushes as separate components which are inherently strong and stable. This may be necessary, for example, where the bearings are flexibly or resiliently mounted. In such cases it is usual either to make the bearing entirely from hardenable stainless steel or to make the bearing in two parts: an outer sleeve to afford strength and stability and an inner sleeve to provide wear resistance and anti-seizure properties. The second approach is often adopted in small high-speed machines. For example, the air turbine dental drill employs bearings composed of an outer sleeve of EN58AM stainless steel and a thin inner sleeve of sintered tungsten carbide. The shaft surface is flame plated with tungsten carbide and these surfaces will withstand in excess of 10 000 near instantaneous stalls from the full running speed of 500 000 rev/min with less than 0·000 1 in wear and without seizing. During development this performance could not be approached with any combination of metal bearing surfaces. Unfortunately, however, the use of tungsten carbide bearing surfaces does not bestow comparable seizure resistance on larger machines due presumably to the greater kinetic energy to be dissipated. Another drawback is the high cost of large sintered tungsten carbide bushes. However, larger bearing bushes can be flame plated in the bore provided that the length-to-diameter ratio is unity or less.

In this connection it is worth noting that tungsten carbide and other ceramic materials can be sprayed onto metal surfaces by two processes; thermo-spraying and plasma spraying. The most dense, well bonded and seizure-resistant surfaces have been achieved using the thermo-spraying process. The plasma process is more versatile in that it can spray a wider range of coatings onto a wider range of base materials. It can also be applied with only a small rise of temperature incurred in the base material which avoids the problem of cracking due to phase changes as the base materials cool after spraying. For example, considerable difficulty is encountered in thermo-spraying martensitic (hardenable) stainless steels due to the phase change from austenite to martensite which causes cracking in the sprayed coating even when the cooling occurs very slowly. This problem can be overcome by plasma spraying or better still be thermo-spraying onto an austenitic steel which does not undergo a phase change. Details of metal spraying processes can be obtained from Metco Ltd., of Chobham, Surrey.

There are a few other seizure-resistant materials which can be used for bearing bushes on small aerostatic machines to provide good anti-seizure properties. The most widely-used material which has been applied to both aerodynamic and aerostatic bearings is the DU material manufactured by the Glacier Metal Company Ltd. This material consists of steel backing supporting a porous bronze matrix impregnated

with p.t.f.e. It is available as flat strip or rolled into split bearing bushes. In the latter form it can be pressed into a steel outer sleeve. The two sleeves can then be drilled radially and feed jet plugs inserted to leave a pocket in the bearing bore. The bearing must be diamond bored to remove the free layer of p.t.f.e. and to expose a mottled surface which is part bronze and part p.t.f.e. This surface is extremely seizure-resistant. The excess p.t.f.e. must be removed because with rubbing it tends to roll up and jam the bearing clearance.

With the journal jet plugs retained and sealed using high-temperature epoxy resin adhesive (e.g., C.I.B.A.'s Araldite), bearings with DU bushes can be applied at temperatures up to 150°C. The temperature range can be extended up to beyond 200°C if the jet plugs are retained by a solder with a melting point in the range 260–280°C. However, the soldering must be carried out with great care and not using a naked flame since p.t.f.e. burns, giving off toxic gases.

Another material with seizure-resistant properties which has been applied to small aerostatic machines is the Deva Graphite Bronze manufactured by Deventer-Werke GmbH of Allendorf, W. Germany. This material consists of a sintered porous bronze matrix with the porosity filled with graphite. It is easily machined although care must be exercised since it is rather brittle. Its best rubbing performance is achieved against hard metal surfaces such as stellite. Deva bronze is not easily soldered and as fine holes cannot be drilled in it directly it is usually necessary to insert jet plugs which are retained by epoxy resin adhesive. The adhesive again limits the permissible operating temperature to about 150°C.

There are numerous other materials with anti-seizure properties that have been tested for use in aerodynamic bearings. These include a range of filled graphites and carbons, some containing molybdenum disulphide, which are manufactured by Morganite Carbon Ltd. These may find limited use in aerostatic bearings in view of their chemical inertness and ability to operate at temperatures up to 400°C. However, they are difficult to machine and handle due to their brittleness and tend to be less attractive than alternative materials for most applications.

Very hard materials, including ceramics, are easier to apply to journal bearings with inlet slots than to bearings with jet feeding, since in the former case no radial drillings are required. Thus in applications involving corrosive fluids or high temperatures ceramic bearings with slot feeding will often present the most attractive solution. The use of silicon nitride in this type of bearing has been described by Shires and Dee (Ref. 12). Silicon nitride is extremely corrosion resistant and can be used at temperatures up to 1 200°C. It has the great advantage of being machinable on a lathe in the green state. Dimensional

changes during firing are extremely small and any subsequent grinding, honing or lapping is minimized. The wear-resisting and anti-seizure properties of two silicon nitride surfaces are good and approach those of tungsten carbide surfaces under atmospheric conditions. Techniques for spraying silicon nitride onto a variety of materials have been developed by the Admiralty Materials Research Laboratory at Horton Heath, Dorset, to whom reference may be made for further details.

8.4 Shaft materials

The choice of materials for the shaft of an aerostatic machine is very wide. The need for corrosion resistance is limited to the journal surfaces only or the journal surfaces and thrust surfaces if a shaft with integral thrust runner is used. These bearing surfaces can be protected by a wide range of surface treatments, including plating or spray coating using the wire spraying, thermo-spraying or plasma spraying technique.

The most widely used plated surface is hard chromium. Its properties and applications are familiar to most engineers and it can be applied to most steels including tool steels and stainless steels. In many applications the cheapest and simplest solution is provided by the use of a mild steel or low alloy steel shaft with hard chromium plating on the journal surfaces and a bolted-on thrust runner of hardened stainless steel or high-chromium tool steel. In applications requiring a hardened tool location on the shaft ends a nitriding steel can be used which is nitrided on the tool location and hard chromium plated on the journal surfaces. This is an attractive combination because the nitriding steels are extremely stable due to the very effective stress relieving which occurs during the nitriding process. The recommended manufacturing procedure is as follows:

(a) Turn, screw cut, drill and tap, mill keyways, etc.

(b) Nitride harden to required depth (roughly 0·01 in deep per 24 h of process) with threads protected.

(c) Grind between centres to remove nitrided surface from shaft journal diameter.

(d) Hard chromium plate shaft journal diameter with all other surfaces protected.

(e) Finish grind shaft all over between centres.

Other hard and corrosion-resistant metal coatings which can be applied by plating or by wire or powder spraying techniques include stellite, tungsten and molybdenum. Any of these may have advantages in particular applications but with the possible limited exception of

stellite they are unlikely to rival hard chromium for air bearings used at atmospheric conditions in a normal industrial environment.

Mention has already been made of spraying ceramic coatings onto steel shafts. These are normally required on smaller machines where a degree of seizure resistance can effectively be achieved when two ceramic surfaces are used in combination. Normally the same ceramic is used for both surfaces since this limits the number of processes involved in the manufacture of the machine. Combinations of different ceramics have been used experimentally and may offer advantages in some applications. The most promising ceramic materials are tungsten carbide, silicon nitride, aluminium oxide, chromium oxide and titanium carbide.

The alternative to using a mild steel or low alloy steel shaft with plating to provide corrosion resistance is to use a corrosion-resistant material for the shaft. Some part of the shaft must often be hardened to provide wear resistance on a tool location and it is desirable for the journal surfaces to be hardened to minimize the risk of damage in handling during finish machining and assembly. These factors appear to limit the choice of materials to the martensitic stainless steels. The EN57 steels can offer only a limited hardness which is not suitable for many machine tool applications. The thirteen percent chromium EN56 steels are harder but have inferior corrosion resistance. In practice it has been found preferable to use a high chromium (seventeen percent) tool steel such as Balfour and Darwin's SC45 or Firth Vickers' F.H.M. steel. In normal industrial environments these materials have a corrosion resistance at least equal to that of EN57; they can be hardened to near sixty on the Rockwell C scale and are very stable materials in the hardened condition. They are particularly suitable materials for shafts with an internal taper or an integral thrust runner. Both these features are often required on shafts for internal grinding spindles and machine tool workhead spindles adapted to accept a range of collets.

In an increasing number of instances the designer is asked to produce high-speed machines, usually with air turbine or high-frequency motor drive, for a variety of scientific and industrial purposes involving the spinning of mirrors, prisms, optical chopping discs and atomizing spray discs. In the majority of cases no loading is involved other than unbalance forces and the only requirement is that the rotor should run at a constant high speed or accelerate repeatedly to a high speed. There are often two special requirements for the materials of rotors in these machines. Firstly, it is usually desirable that the rotor should be as light as possible, and secondly (and this particularly if a hollow rotor is used to save weight), the dilation of the journal diameter at running speed must be limited to well below the journal bearing

clearance. The dilation of a hollow shaft can be derived from the following equation:

$$\delta_1 = \frac{\rho \omega^2}{4gEX}(D^3 X - tD^2 + t^2 D^2),\qquad (97)$$

where δ_1 is the increase in diameter, E is Young's modulus of the shaft material, ρ is the density of the shaft material, σ is Poisson's ratio of the shaft material, ω is the angular velocity of the shaft, D is the nominal journal diameter, t is the shaft wall thickness, and $X = \dfrac{1}{3+\sigma}$ and g is the acceleration due to gravity. Thus in choosing a material for hollow cylindrical rotors it is necessary to consider both the density and the ratio of Young's modulus to density $\dfrac{E}{\rho}$. Fig. 8.3 lists these properties for some possible shaft materials.

Material	Poisson's ratio, σ	Density, ρ (lb/in^3)	Youngs modulus, E (lbf/in^2 $\times 10^6$)	$\dfrac{E}{\rho}$ (lbf in/lb $\times 10^6$)
Aluminium	0·33	0·098	10	102
Aluminium alloys	0·33	0·095–0·102	10–10·5	103
Magnesium	0·29	0·062	6·4	103
Magnesium alloys	0·30	0·063–0·067	6·4	95–102
Low alloy steels	0·27	0·283	30	106
Stainless steels	0·30	0·286	29	101
Titanium alloys	0·32	0·160	15–18	94–113

Fig. 8.3 Materials for high-speed rotors

Light alloys are often used for small high-speed rotors where rubbing contact of the bearing surfaces can be avoided. They offer the lowest densities and $\dfrac{E}{\rho}$ values as high as those of other shaft materials. The values of $\dfrac{E}{\rho}$ for the materials tabulated show little variation. For

purposes of comparison the value for hard yellow brass is only forty-nine and for grey cast iron fifty.

It is also necessary to calculate the effect of dilation on interference fits where these are employed on composite rotors. This is almost always the case in machines with high-frequency motor drive. The dilation in the bore of a hollow shaft is given by:

$$\delta_2 = \frac{\rho \omega^2}{16gEX} \left(D^2 D_i + \frac{X}{Y} D_i^3 \right), \tag{98}$$

where δ_2 is the increase in the bore diameter, $Y = \frac{1}{1-\sigma}$ and D_i is the bore diameter.

The dilation of a solid shaft is given by:

$$\delta = \frac{\rho D^3 \omega^2}{16gEY}. \tag{99}$$

Poisson's ratio σ can be taken as 0·3 for most metals. Values of Young's modulus, density and Poisson's ratio are given in Fig. 8.3.

8.5 Materials for thrust plates

Under this heading are included not only the static thrust plates in which the gas feed passages and pockets or grooves are formed but also the thrust runner and spacing ring where appropriate. In each case the component takes the form of a thin plate with numerous drilled holes, and all are in contact with the gas lubricant either on outside surfaces or within internal drillways. The requirements are for corrosion resistance and stability preferably combined with surface hardness to provide protection in handling during finish machining and assembly. The most attractive materials are again the hardenable stainless steels or a high chromium tool steel. The latter is often preferred for its greater stability when used hardened in the form of a thin plate.

When using hardened steel thrust plates the feed holes can be either drilled prior to hardening or provided by inserting brass jet plugs into larger holes in the manner described for journal bearing bushes. However, as the jet diameter changes slightly in hardening, and drilling fine holes in even soft steel is considerably more difficult than drilling in brass, it is normally preferable in bearings for use at atmospheric temperature to use brass jet plugs for jets smaller than about 0·015 in diameter.

In general, non-corrosion-resistant materials are not suitable for static thrust plates or spacer rings with their numerous internal holes through which the supply gas and exhaust gas flow. Mild steel and

other materials could be used for thrust runners provided that bearing surfaces were protected by plating, but there is little or no advantage in terms of performance, cost, or ease of manufacture to be gained.

There are some instances where it may be preferable to use an austenitic stainless steel for the static thrust plates with hard metal or ceramic plating on the bearing surfaces. This may be necessary where brass jet plugs are undesirable due to high temperature or corrosion problems, or in small machines where it is necessary to provide a degree of seizure resistance on the thrust faces. In such cases it is always advisable to use a free cutting grade such as EN58AM or EN58BM to facilitate the fine hole drilling.

With care thrust surfaces can be manufactured flat to within one optical fringe ($11 \cdot 6 \times 10^{-6}$ in for helium light). This degree of flatness, however, will not necessarily be retained under operating conditions since distortion can arise from the effects of changes in pressure and temperature. These effects can be minimized by care in design and materials selection. Static thrust plates usually incorporate an annular groove from which the supply gas is fed to the ring of jets or slots. There is much inducement to minimize the thickness of material through which the jets are drilled and consequently there is a danger that when the supply pressure is applied the material can bulge to a significant degree. The problem is overcome by keeping the annular supply groove as narrow as possible and avoiding using a material of low modulus of elasticity. It is also advantageous to avoid using thin wall sections wherever possible, either by counterdrilling behind the feed jets or by using separate jet plugs.

A problem of static thrust plate distortion is often met with in aerodynamic thrust bearings and could arise in aerostatic thrust bearings of low clearance. The heat generated in the gas film is partly conducted axially through the thrust plate, causing an axial temperature gradient. The effect is to distort the thrust face convex towards the gas film. Although the gas flow in aerostatic bearings provides some cooling the latter may not be sufficient to prevent distortion in bearings operating at high speeds. Materials which combine a high thermal conductivity with a low coefficient of expansion will distort the least. Molybdenum is one of the best materials in this respect. Another approach is to insulate the back of the thrust plate to force most of the heat to flow radially. Alternatively the plates can be made slightly concave so that they become flat on warming up. This approach, however, is not recommended because not only are there difficulties in design and manufacture but also concave thrust surfaces are prone to the aerostatic instability described in Chapter 10.

The range of materials available to the engineer is constantly increasing with the appearance of new materials with improved properties.

No discussion of materials within the space presently available could be comprehensive and no such claim is made in this instance. However, it is hoped that a sufficient understanding will have been gained of the essential properties to be looked for in materials for aerostatic machines to enable the designer to effect a suitable choice. The selection of materials is probably influenced more by personal preferences based on previous experience than any other aspect of design. Impressions of some materials are coloured by difficulties experienced in heat treatment or surface treatments due to shortcomings in equipment or technique. However, these shortcomings may persist, and for this reason whenever possible materials should be chosen with which the designer has a background of good experience. In materials for aerostatic machines this is of particular importance, for example, in relation to corrosion resistance and in relation to the stability of materials in the hardened and tempered condition.

CHAPTER 9

MANUFACTURING METHODS AND CONTROL

9.1 Introduction

The first action of the designer of an aerostatic bearing should be thoroughly to acquaint himself with the available manufacturing and inspection processes particularly in relation to their limitations of capacity and accuracy. Whilst every effort should be made to improve manufacturing techniques and to incorporate any proven refinements into the bearing design, it is wise not to anticipate such improvements. The most successful designs are likely to evolve from a close collaboration between the bearing designer and the production engineer. The designer then appreciates better the difficulties of manufacture and inspection and the production engineer understands that significant improvements in bearing performance can result even from an apparently marginal improvement in the geometry of the bearing components.

No unique manufacturing processes are involved in the production of aerostatic bearings and most engineers are familiar with the machine tools and techniques which must be applied. However, it is essential to think clearly about the desired result of each stage of manufacture in order to ensure that the available equipment is applied in the best possible way. For example, the fact that an aerostatic bearing defines an extremely precise axis of rotation should never be overlooked and many processes can considerably be improved in terms of geometric accuracy by rotating the workpiece, the cutting tool or both on aerostatic spindles.

9.2 Geometric accuracy

Before discussing particular manufacturing processes in relation to the production of bearing components it is useful to consider the various features of geometric accuracy which are sought and the methods by which they can be measured. The principal features to be considered are

(a) absolute size,
(b) parallelism,
(c) roundness,
(d) straightness,

(e) concentricity,
(f) squareness of faces to axis of rotation,
(g) flatness, and
(h) surface finish.

These are illustrated in Fig. 9.1.

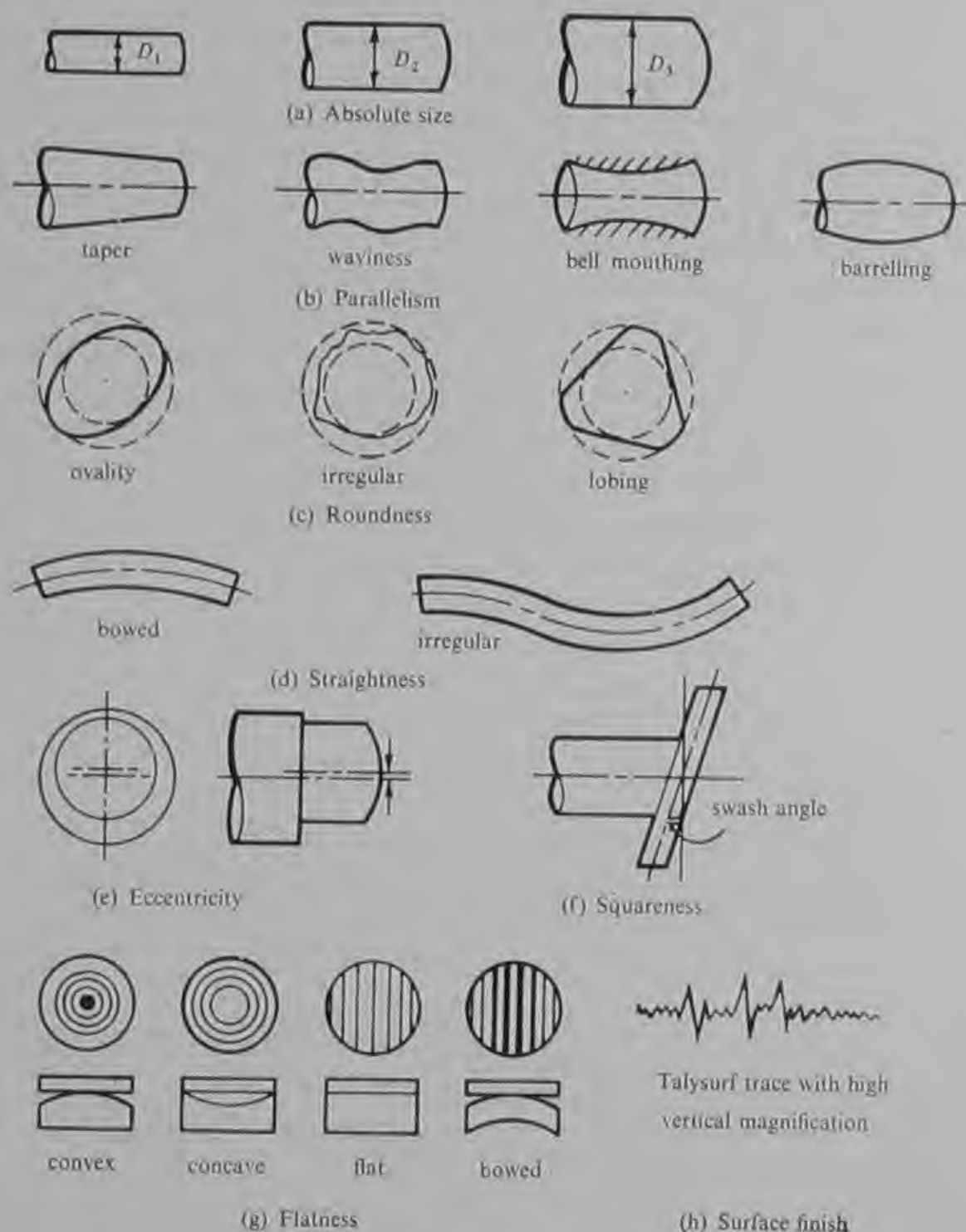(a) Absolute size

taper   waviness   bell mouthing   barrelling

(b) Parallelism

ovality   irregular   lobing

(c) Roundness

bowed   irregular

(d) Straightness

swash angle

(e) Eccentricity   (f) Squareness

convex   concave   flat   bowed

Talysurf trace with high
vertical magnification

(g) Flatness   (h) Surface finish

Fig. 9.1 Features of geometrical accuracy

(a) *Absolute size* While most engineers are very familiar with the concept of absolute size and are constantly using measuring instruments such as micrometers it is not generally appreciated that as all engineering measurements are relative, absolute size is seldom known to the degree

of accuracy which the number of digits after the decimal point leads one to assume. For example, although it is possible to read a vernier micrometer to 0·000 1 in (a tenth of a thou), it is doubtful if when all sources of error are considered absolute sizes can confidently be established under average workshop conditions within better than 0·000 5 in. However, the relative sizes of two components measured at the same temperature and differing by 0·000 5 in can be established to within about 0·000 1 in. Gas bearing components need to be measured to a higher degree of accuracy than is met in general engineering and as a result the importance of understanding the difference between absolute size and relative size is even greater.

The finished sizes of gas bearing components cannot generally be established with sufficient accuracy by mechanical devices such as micrometers and instruments employing dial gauges. High magnification instruments such as air gauges and electronic comparators employing inductance probes are more suitable. Air gauging equipment is manufactured by Mercer, Solex, Sigma and Teddington and electronic comparators by Mercer and Rank Taylor Hobson. In each case the instruments are set up relative to setting gauges such as precision slips (preferably tungsten carbide for durability and low thermal expansion) or specially manufactured plug or ring gauges. The diffi-
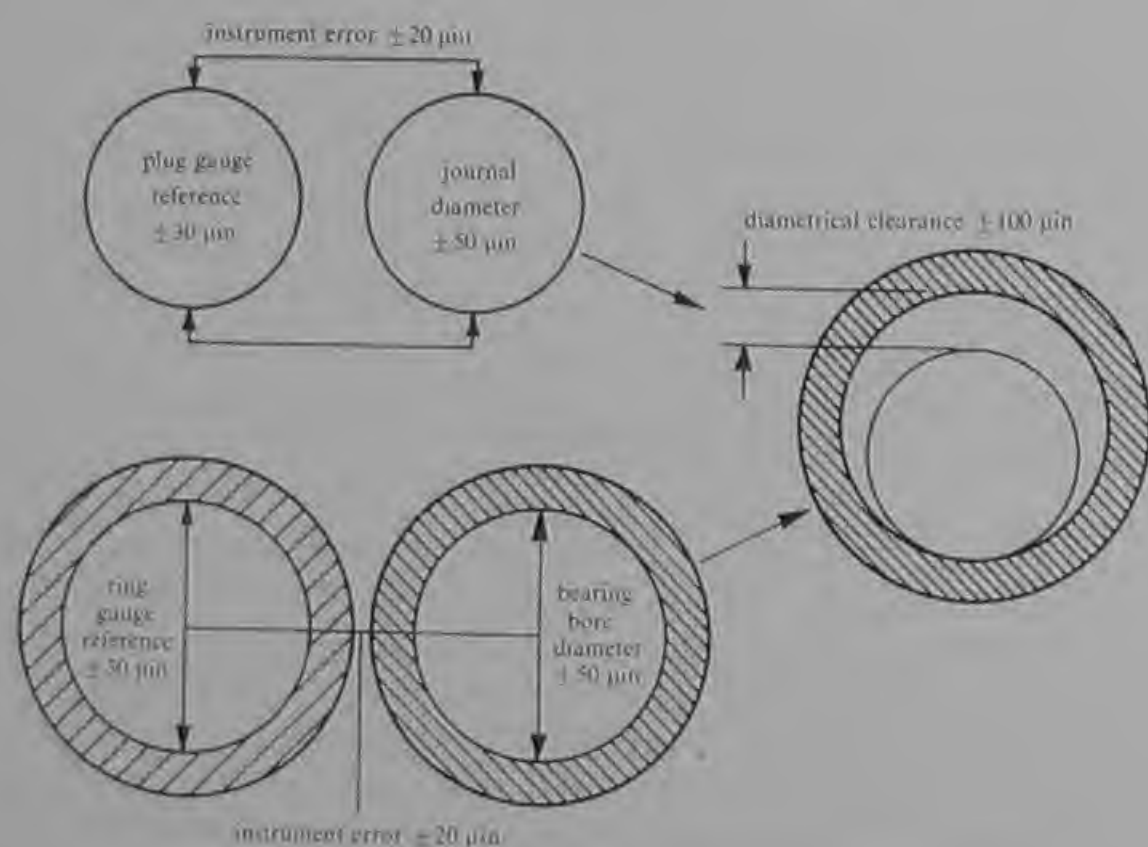
Fig. 9.2 Measurement of journal bearing clearance by attempting to establish size of the journal diameter and bearing bore diameter

culty of establishing absolute size is again emphasized by the fact that even with certification by the National Physical Laboratory the sizes of plug or ring gauges are usually at best given to not better than ± 30 µin.

Fig. 9.2 helps to indicate the difficulty in controlling bearing clearance by attempting to establish the absolute sizes of the journal diameter and the bearing bore diameter. The figures given are typical for good conditions with temperature control, certificated reference gauges, high magnification air gauges and adequate thermal soaking of the component parts. It can be seen that the accumulation of errors leads to a significant degree of doubt concerning the diametrical clearance in the bearing. When a manufacturing tolerance is added for each component it soon becomes apparent that two nominally identical bearings could easily differ in clearance by up to fifty percent of a total design clearance of 0·001 in. Selective assembly eliminates one manufacturing tolerance but the problem remains particularly in relation to bearings of smaller clearance.

In practice it is necessary to combine measurement of the component parts with a measurement of the bearing clearance. The simplest and often the most convenient method is to measure the 'mean effective clearance' between the shaft and the bearing by measuring the total free radial movement of one component relative to the other. One arrangement by which this can be accomplished is shown in Fig. 9.3
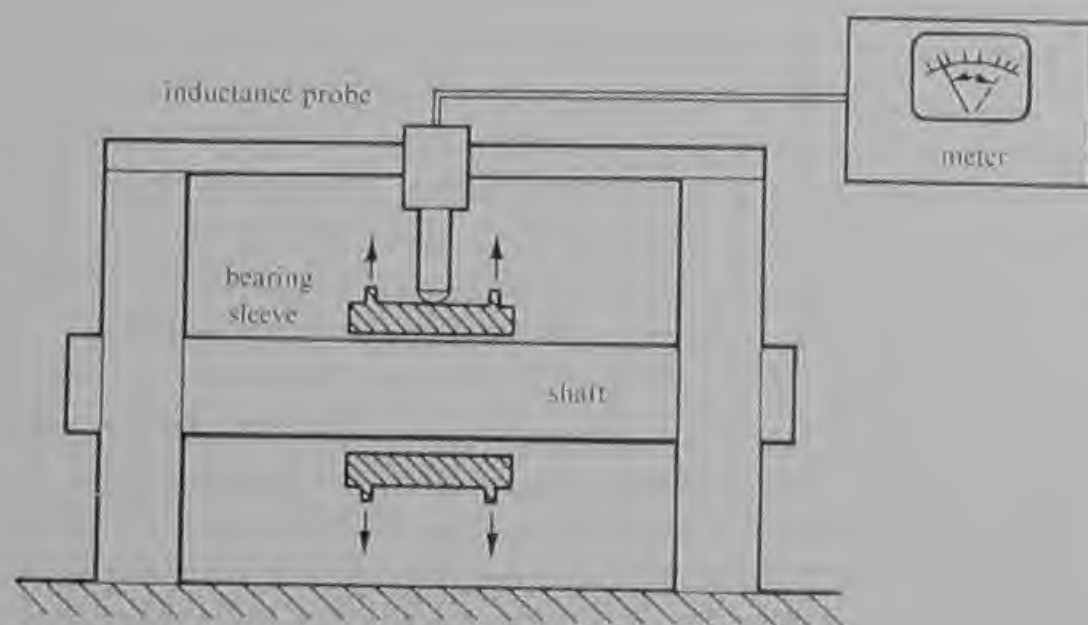
Provided that shaft and probe are rigidly supported and that only light pressure is applied to the bearing sleeve, the mean effective clearance can be obtained from the change in meter reading as the bearing is raised and lowered.

Fig. 9.3 Measurement of mean effective clearance

but there are numerous other methods. The figure shows a single bearing sleeve but where two bearings are rigidly located in a single body structure the same basic method can be used or the total radial movement of each end of the shaft can be measured from which the clearance of each bearing can be calculated. The mean effective clearance measurement should always be used in combination with other measurements of component sizes and geometry. If the geometry of the two components is good in terms of roundness, straightness and parallelism the mean effective clearance measured will be close to the true total clearance. However, the measured mean effective clearance will always be less than the true clearance and the difference will increase with increasing geometric errors in the components. When measuring the diameter of the bearing bore and the journal diameter it is necessary to take numerous measurements spaced both circumferentially and axially in order to find realistic mean sizes. The variations in these measurements provide some indication of the geometric accuracy of the components although one must be cautious of forming wrong conclusions on this basis. If little variation is found in either component it is likely, though not quite certain, that the measured mean effective clearance closely approaches the true clearance in the bearing. The error in the mean effective clearance measurement is of the order of the error in the measuring instrument plus the sum of the variations in the diameters of the two components. This error will usually be less than the error in arriving at the clearance from the difference in the measured component diameters.

Measuring the airflow through a finished assembled bearing provides an accurate comparative method of checking the effective clearance. The method is very sensitive and gives close control of clearance even with relatively inaccurate flow-measuring devices. Variable-area meters are convenient to use and give an accuracy of $\pm 2\%$. It is necessary to ensure that the bearing is supplied at an accurately-controlled pressure and that the pressure and temperature at the airflow meter is in agreement with the calibration requirements. A suitable arrangement is shown in Fig. 9.4.

Setting the thrust bearing clearance can be somewhat easier than setting the journal bearing clearance in designs of the type shown in Fig. 6.2(c) and Fig. 6.4. Here the total clearance of two thrust bearings is the difference in thickness between the spacer ring and the thrust runner. The thickness of the two components can be measured on the same instrument and at the same setting so that the difference in the readings is known to within the accuracy of the instrument. Using a high magnification air gauge or an electronic comparator the error could be below 20 μin. It is also comparatively simple to measure the free axial movement or 'end float' of the assembled machine to

read flowmeter pressure

read bearing
supply pressure

change-over valve

to bearing

set bearing supply pressure

10

1·0

variable area flowmeters individually
calibrated at 50 lbf/in² gauge
and 20°C in c.f.m. of free air;
accuracy ±2%

1·0

0·1

supply of dry
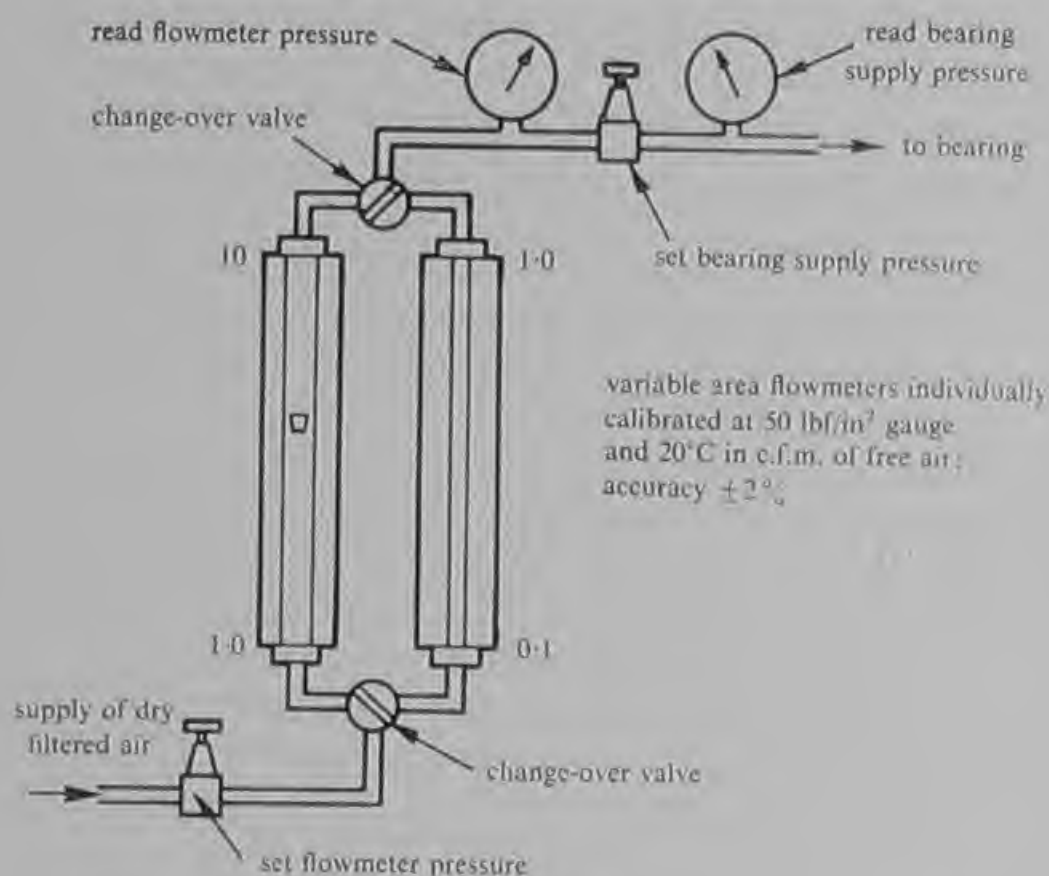filtered air

change-over valve

set flowmeter pressure

Fig. 9.4 Measurement of airflow provides a production
control of bearing clearances

provide confirmation of the total thrust clearance or to investigate
the accuracy of the assembly.

(b) *Parallelism* It is possible to check parallelism by the means used
to measure the absolute size of the component. If the diameter of a shaft
or bearing bore is measured at several points axially spaced in one
radial plane the difference in the readings gives the parallelism error
in that plane. The process should be repeated in several radial planes
if a true impression of the parallelism of the component is to be
realized.

The most common parallelism error is the bell mouthing of bearing
bores which have been finished by honing or lapping. Measuring the
bore using an air plug gauge is a simple and effective means of checking
for bell mouthing. Another parallelism error which is sometimes
encountered is the barrelling of shafts. This error occurs in long thin
shafts due to flexure during the grinding process. It is usually traced to
a loaded and glazed grinding wheel which because of its low coefficient
of friction will grind only with a high radial load between the wheel
and the shaft.

Parallelism must not be confused with straightness which cannot be
checked by size measurements. It is possible for a component to be
parallel but not straight, like railway lines on a curve in the track.

7*

(c) *Roundness* Three forms of roundness error are shown in Fig. 9.1(c). Some indication of ovality and irregularity will be indicated by several measurements of diameter spaced radially around the component in an axial plane. However, if no variation in diameter is found it is wrong to assume that the component is round. The component can be badly lobed and still indicate a constant diameter. Three lobes are frequently encountered in bores and the error can often be traced to holding in a three-jawed chuck at some stage of manufacture and not necessarily at the finishing operation.

Measurement of roundness is essentially a measurement of radius and the roundness error is the difference between the minimum and maximum radii measured in one axial plane of the component. Roundness measuring instruments are available and the best known is the Talyrond manufactured by Rank Taylor Hobson Ltd. Another instrument employing a reference axis defined by an aerostatic bearing was developed at the National Engineering Laboratory and is manufactured by Optical Measuring Tools Ltd. Both of these instruments are capable of detecting roundness errors down to a limit of about 3 µin. They are also capable of measuring surface finish and the familiar round paper tracings produced provide a permanent record of both quantities.

Achieving a high order of roundness is seldom a major difficulty in the production of aerostatic bearing parts. On a cylindrical grinding machine equipped with aerostatic wheelhead bearings shafts ground between dead centres are usually round to better than 10 µin and with care can be better than 5 µin. A similar degree of precision can be achieved in the bores of workpieces rotated on an aerostatic workhead.

(d) *Straightness* Of all the qualities required in aerostatic bearing components straightness is probably both the most difficult to produce and to measure. Traditionally the measurement of the straightness of both bores and outside surfaces has been achieved by means of an autocollimator technique. Light is reflected from a small mirror mounted perpendicularly to the axis of the component and moved in turn to several axial positions along the component. Deviations from a straight line in the progression of the mirror are indicated by vertical movements of the reflected light. This method is somewhat lengthy and tedious.

A straightness measuring machine which is both accurate and relatively simple to use was devised by Tempest and Munday of Bristol Siddeley Engines Ltd and is shown in Fig. 9.5. The machine employs an optical flat as a reference surface with air gauge jets reading from the surface of the optical flat and the surface of the component. The second air gauge jet is mounted on an arm to permit traversing through bores. For ease of operation and the elimination of stick-slip
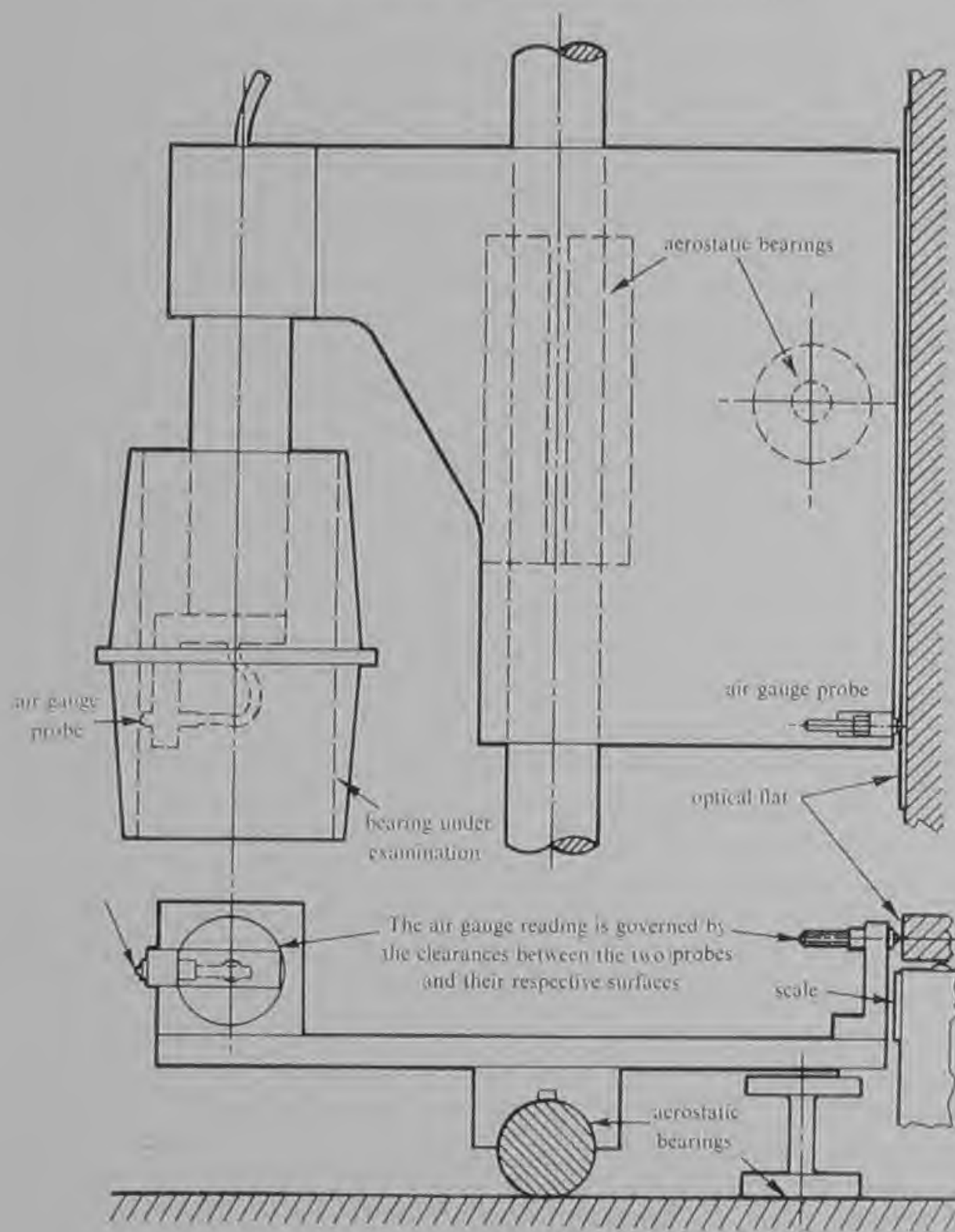
Fig. 9.5 Straightness measuring machine developed by Tempest and Munday

effects the gauging heads are mounted on a carriage which traverses on an aerostatic slide composed of a half journal bearing and a flat bearing. This machine can be used to check the straightness or alignment of two journal bearings and this is a most important consideration in aerostatic machines.

(e) *Concentricity* In the construction of aerostatic machines it is often necessary to ensure concentricity between two diameters. This is

certainly necessary where two bearings of unequal diameter are
employed. More commonly it is necessary to ensure that a tool or
collet location is concentric to the journal surfaces. Concentricity
can be measured using a roundness measuring machine but recourse
to one of these is seldom essential. Since one diameter is invariably a
bearing surface it is usually a simple matter to support that diameter
in its aerostatic bearing and to monitor the rotation of the other
diameter using an air gauge or an electronic comparator. This is an
especially simple and effective procedure in the case of tool or collet
locations on machine tool spindles where the diameters in question
can precisely be checked by rotating the assembled spindle by hand.

(f) *Squareness of faces to axis of rotation* In all aerostatic machines it
is essential that both the rotating and static thrust faces are square
to the axis of rotation defined by the journal bearings. Since the shafts
are normally ground between centres it is usually sufficient to check
the run-out of the faces of the thrust runner with the shaft supported
between centres. Once again an air gauge or an electronic comparator
can be employed and swash down to below 20 μin total indicated
reading can be detected.

The measurement of the squareness of the static thrust faces usually
requires the construction of a special fixture. A typical arrangement
is shown in Fig. 9.6. The spindle body with the journal bearings assem-
bled and finished in the bore is placed on a shaft with a central air
feed so that the body is supported radially and axially on aerostatic
bearings. The body can than be rotated freely by hand. An air gauge
probe or an inductance probe monitors the swash of the upper face
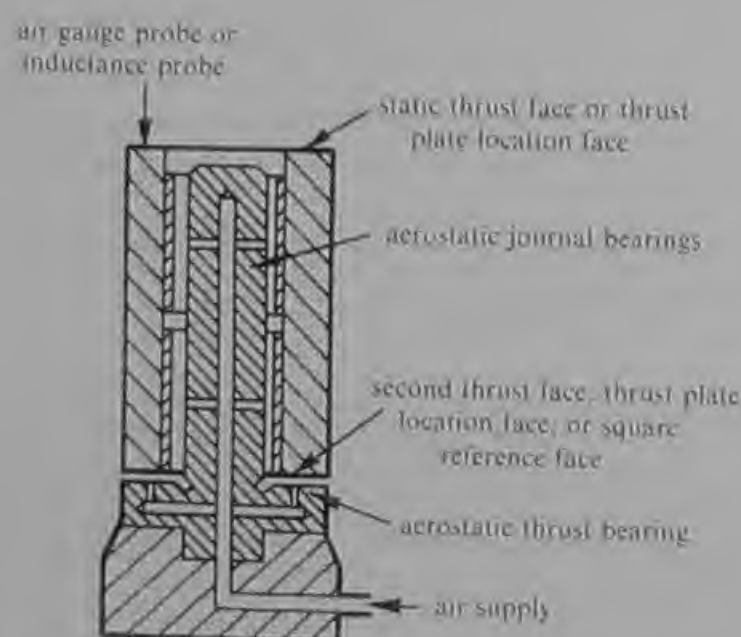
Fig. 9.6 Measurement of squareness of static thrust faces

of the body as it rotates. It is necessary for both faces of the body to be ground square to the bore to enable the measurement to be made. However, the error in the lower face is reduced by at least a factor of four by the averaging effect of the aerostatic thrust bearing and does not confuse the measurement of the upper face. If the lower face is also checked by up-ending the body and repeating the measurement it soon becomes apparent which face, if any, is in error. Again the limit of detectable swash is below 20 µin total indicated reading.

(g) *Flatness* It is always necessary to ensure that the thrust surfaces are flat, not only to provide the optimum bearing performance but also to provide some means of checking for distortion due to fixing stresses or stress relieving effects. Optical flatness measuring devices are widely used and are comparatively inexpensive. The surface to be checked must be clean and polished so that light is reflected. An optically flat glass plate is placed on the surface. When illuminated by a monochromatic light source such as from a helium-filled tube a flat surface is distinguished by a series of parallel dark lines called interference fringes. If the fringes are curved the surface is not flat and the flatness is graded according to the number of fringes cut by a straight line across the component tangential to a fringe. Each fringe represents an error in the surface of half the wavelength of the monochromatic light. In the case of helium light with a wavelength of 23·2 µin each fringe represents an error of 11·6 µin.

Prior to assembly most thrust plates can be checked using a large round optical flat. Optical flats of narrow rectangular section are useful for checking assembled parts or the faces of a thrust runner manufactured integrally with the shaft. After assembly a flat plate may be distorted by fixing stresses and this is immediately apparent from a flatness check.

Flat plates are usually produced by surface grinding followed by lapping. It is interesting here to note that on surface grinding machines in good condition, and equipped with an aerostatic wheelhead, small plates can be ground flat to better than one optical fringe. Subsequent lapping is reduced to a light polishing operation to improve the light reflection and facilitate the flatness measurement.

(h) *Surface finish* Surface finish is seldom a primary consideration in the manufacture of aerostatic bearing parts. However, a good surface finish is almost always produced by the means employed to ensure good geometry. Where necessary surface finish can be measured using a Talysurf machine manufactured by Rank Taylor Hobson Ltd. The value normally obtained is a centre line average (c.l.a.) of the small irregularities of the surface expressed in µin. Surfaces ground with wheels supported on aerostatic bearings will almost always be better

than 3 μin c.l.a. Subsequent honing or lapping operations produce further improvements.

9.3 Manufacturing techniques

Having discussed the various features of geometric accuracy and the methods by which each can be measured it is possible to proceed to consider some of the manufacturing techniques by which a high order of accuracy can be achieved. It is not intended to dwell on primary machining operations such as turning and milling except to say that the workpiece should always be held in such a way that stress and distortion are minimized. Large geometric errors introduced early in manufacture can often be difficult to eradicate later through requiring an excessive amount of material to be removed during the finishing operations. Cooper (Ref. 23) has observed that the errors of early machining operations can persist unseen through subsequent work to be revealed only during final lapping.

(a) *Grinding operations* Most gas bearing components require grinding during the later stages of manufacture. The basic geometrical accuracy is usually determined by the grinding operation since the small material removal during the final honing or lapping operation is insufficient to remove other than minor imperfections. There are a few important considerations in connection with grinding operations which ensure that the best results are achieved with the available equipment. The machines in the best mechanical condition should be employed. It is particularly important that the slideways are in good condition and properly lubricated. The condition of the wheelhead and workhead bearings determines the quality of the roundness and surface finish produced but errors from slideways can cause much more trouble. Before taking a cut it is necessary to run the machine with the slides operating until lubrication is normal. This care can reduce errors of straightness and parallelism by up to ninety percent.

As the grinding operation nears completion cuts must be reduced to a very low level such as 0·000 2 in. This allows for the correction of earlier errors and minimizes thermal effects which degrade measurements and possibly the material. The grinding of hard chromium plate requires light cuts at all times in order to avoid burning and the consequent degradation of hardness and adhesion.

The cleanliness of the atmosphere surrounding the grinding machine is of some importance. Airborne particles can upset the location of the component in its fixture at set up. Airborne particles also cause more damage to the surface finish than coolant-borne particles. In a general workshop a cover for the grinding machine can do more good than expensive filtration of the coolant and on no account should

dry dressing of grinding wheels be carried out in the vicinity of the grinding machine.

When grinding shafts between dead centres the roundness is determined by the quality of the centres. It is more important to use small centres in the workpiece than to grind or lap the centres, although both are beneficial. The male centres on the machine must always be in good order. Roundness is also influenced by the precision of the wheelhead bearings and aerostatic wheelhead bearings are very good in this respect. The roundness of bores is determined by the quality of the workhead bearings and here again improvements result from the use of aerostatic bearings. On any precision grinding machine in good condition and fitted with aerostatic bearings on the workhead and wheelhead it should be possible to grind both internally and externally round to within a 5 μin annular zone. The straightness and parallelism of the workpiece is dependent upon the precision of the slideways but on most machines in good order errors should not be greater than 100 μin/ft.

(b) *Honing and lapping* Ideally these operations should be used only for the final bringing to size, with some improvement of surface finish and with the removal of less than 0·000 1 in of material. If there are local errors of this order to be corrected (such as lobing, taper or waviness) lengthy and careful work is needed. Extra time spent on grinding operations, ensuring the generation of true surfaces which reduces the amount of correction by honing or lapping, is time well spent. In quantity manufacture it is essential to keep the time spent on these skilled finishing operations to a minimum.

Honing and lapping are complementary: on cylindrical components honing is effective in removing lobing but lapping is better for removing waviness and taper. Flat surfaces are finished by lapping.

Honing can set up cavitation on certain materials such as hard steels. The cavitation originates in surface defects, usually grinding flecks, which enlarge to cavities and the débris produced damages the surfaces being worked. Materials which suffer from cavitation must be finished by lapping. Many materials do not cavitate during honing and these include brasses and bronzes, hard chromium plate and stainless steels.

Wet lapping is useful for stock removal but, if prolonged, leads to the degradation of the accuracy of all edges due to hydrodynamic action. Abrasive can also be carried to operate on surfaces at a different level from that intended to be cut. Dry lapping is superior for finish and accuracy but the lap must be soft and free from hard particles. Cooper recommends lead in preference to cast iron since the cast iron contains hard particles which scratch the work. Lead laps are useful

for thrust bearings with surface features and for aerodynamic bearings of the pivoted pad type. However, full cylindrical journal bearings are probably best finished using solid cast iron laps in spite of their shortcomings. These can be finished to a high order of accuracy and are less easily damaged than lead laps. Expanding laps can be used to cover a wider range of sizes but are not as accurate as solid laps. Provided that the lapping is kept strictly to a minimum and the material removed is less than 0·000 1 in in diameter, in quantity manufacture most aerostatic bearings can be finished by wet lapping using a solid cast iron lap. This method is particularly useful for finishing two journal bearings precisely in line.

(c) *Single point boring* An effective method of finish machining two journal bearing bores round and accurately in line has been developed by Westwind Turbines, Ltd. The basic machine is a precision boring machine with an accuracy of slideway better than 0·000 1 in/ft. The spindle body complete with its journal bearings is mounted into the bore of a carrier which is itself supported in aerostatic bearings. With the body rotating at 2 000 rev/min for a 1·75 in bore the bearings are bored in line using a single point diamond tool. A second tool can be used to machine the front face of the body to provide an accurately square location for the thrust bearings. This process is capable of producing bores round to within 10 μin and with errors of straightness and parallelism through the two bearings not exceeding 70 μin for an 8-in long spindle body. At the same time a surface finish of the order of 5 μin is produced and a thrust bearing location face is provided which is square to within 20 μin total indicated reading on a 3 in diameter. Subsequent lapping is required only to improve straightness and parallelism further.

Development of the single point boring process using an aerostatic workhead offers considerable promise of producing precision aerostatic bearings inexpensively in large quantities. The process is considerably simpler, quicker and less expensive than precision bore grinding and yet achieves an equal or higher degree of accuracy.

9.4 Other manufacturing processes

In addition to those manufacturing processes required to ensure a high order of geometric accuracy of the bearing surfaces there are a few other techniques which, while not unique to aerostatic bearing production, are nevertheless somewhat more refined or specialized here than in general precision engineering.

These techniques include:

(a) the production of fine jets
(b) the production of fine slots

(c) machining ceramic materials

(d) dynamic balancing.

(a) *The production of fine jets* The oldest and still the most widely used method of producing holes is by means of a rotating drill and this method can be used down to very small diameters. Steel twist drills are available down to 0·1 mm (0·003 94 in) diameter and pivot drills down to 0·03 mm (0·001 2 in) diameter. These drills are produced by Müller on a common shank diameter of 1 mm and cost only a few shillings each. When correctly applied they can produce in excess of 2 000 holes at a rate in excess of 500 per hour. However, in order to achieve this performance the following factors are essential.

(i) The material must be free cutting, preferably brass.

(ii) The depth of drilling must be minimized by counter drilling at a larger diameter. Preferably the depth of drilling should not exceed three diameters.

(iii) The run-out of the drilling spindle bearings and collet must be very small, preferable below 0·000 1 in.

(iv) The optimum drilling speed depends upon the drill diameter and the material drilled but is often in the range 20 000 to 60 000 rev/min.

(v) The feeding of the drill must be very smooth and a hydraulically controlled feed is superior to manual feeding.

A drilling head has been developed by Westwind Turbines, Ltd., to fulfil the last three requirements. The spindle runs in aerostatic bearings driven by an air turbine at speeds up to 120 000 rev/min. The run-out of the bearings is negligible and the collet runs true to 0·000 1 in. A pneumatic cylinder provides the feed which is smoothed and controlled by a hydraulic cylinder coupled in series. With units such as these the drilling of fine holes in free cutting materials becomes a fast and inexpensive process.

Where hard materials must be used the production of jets is more difficult and this is one reason for choosing slot feeding where, for example, ceramic materials are employed. However, fine holes can be drilled in ceramics and at fairly high production rates. For example, holes of 0·006 in diameter are drilled in the tungsten carbide bearing bushes on a machine designed for drilling watch jewels. The bearing bush is vibrated at high frequency in a vertical plane under a wire of 0·006 in diameter rotating at 100 000 rev/min. Fine diamond paste fed under the wire enables it rapidly to penetrate the ceramic. The spindle rotating the wire on this machine also runs in aerostatic bearings.

Spark erosion can also be used to drill holes in ceramics and other hard materials. At the time of writing the smallest possible hole diameter is in the region of 0·01 in but smaller holes may become possible in the future. Another possibility for the future is the application of the laser provided that cost does not remain a barrier to its wider utilization.

(b) *The production of fine slots* The production of fine slots should not present severe problems provided that the slots are formed at the abutment of two bearing parts. The most obvious method is to surface-grind the slots into one of the abutting faces. Alternatively the slots can be produced by one of the methods used for machining shallow grooves on the faces of spiral groove aerodynamic thrust bearings. These methods include photo-chemical etching and powder blasting, both of which can be controlled to produce shallow features and therefore very fine slots. In the case of ceramic materials the most practical method is to produce the slots by surface grinding using a diamond wheel. Powder blasting is possible only if a ceramic powder can be found which will abrade the workpiece. Aluminium oxide powder is commonly used for powder blasting and this will abrade most other ceramics but the rate of material removal may be impractically slow in some cases.

(c) *Machining ceramic materials* Although some ceramic materials, notably silicon nitride, can be turned on a lathe in the 'green' state prior to firing, machining ceramic is most often a matter of grinding the fired material using diamond impregnated wheels. In this connection the use of aerostatic wheelhead bearings is strongly recommended. The true rotation ensures full utilization of the periphery of the wheel and prolongs the wheel life by up to fifty percent compared to that achieved with conventional spindles. Diamond wheels are very expensive and consequently the saving is a vital factor in the economic manufacture of precision ceramic components. Bearing surfaces can be finished by honing using diamond stones or lapping using diamond lapping paste. All these processes utilizing diamond tend to be expensive and ceramic components should therefore be designed for a minimum of machining in the fired condition.

(d) *Dynamic balancing* The last manufacturing process on a rotor prior to assembly, and often subsequent to assembly, is dynamic balancing. Provision should always be made in the design of the rotor to enable material to be removed at either end in an effective and unobtrusive manner. Effectiveness is achieved by the use of a large diameter at the balancing positions so that the amount of material removed is minimized. Unobtrusiveness is achieved either by balancing

within the casing of the machine or by removing material by neat drillings.

The object of dynamic balancing is to attempt to make the mass axis of the rotor coincide with its geometric axis. The geometric axis is defined by the cylindrical journal surfaces, and so, in order that the rotor is balanced about the correct axis, it must be supported in aerostatic bearings locating on these journal surfaces during the balancing process. The simplest solution is to balance the assembled machine. Where this is not possible, due to the inaccessibility of the rotor, a special balancing fixture should be made. This should incorporate journal bearings of the same length and diameter as those employed in the machine but can employ a larger clearance together with larger and fewer feed jets or slots. The balancing fixture should be kept as light as possible and can often be made of light alloy.

The balancing can be carried out on any commercial dynamic balancing machine which has been adapted to carry either the complete machine or the balancing fixture. A wide range of balancing machines is available, most with high sensitivity, and the final selection often hinges on considerations of adaptability and ease of operation. Some machines cover a wide range of work and are ideal for research and development purposes. Others are more limited in capacity but their ease of operation suits them for the rapid production of large batches.

CHAPTER 10

THE PROBLEM OF AEROSTATIC INSTABILITY

10.1 Introduction

A most important consideration in the design of any gas bearing system is to ensure that it is stable. If it is unstable, it is clearly of little value to study other aspects of the design until the instability has been eliminated. Designed with no consideration of stability, a substantial proportion of aerostatic journal bearings and the majority of aerostatic thrust bearings would probably exhibit self-excited vibrations which occur at all speeds including standstill. These vibrations are usually audible, often loudly so, and can also be detected by touch. They have been called by several names, including 'air hammer', 'pneumatic hammer', 'self-excited resonance' and more popularly 'moan'. There are probably two or more distinct types of instability which can be identified, but for the present purpose the term aerostatic instability is taken to include all self-excited vibrations of aerostatic bearings which can occur independently of relative rotational movement of the bearing surfaces.

The basic mechanism of aerostatic instability can be described with reference to Fig. 10.1 which shows a cross-section through a circular thrust bearing with central feed hole and pocket. Under steady load conditions the flow into the pocket m_1 is equal to the flow out of the pocket m_2. Thus if the upper plate is loaded the bearing clearance is reduced which in turn reduces m_2 and m_1, causing the pocket pressure P_d to rise to support the increased load. If the upper plate is forced to execute sinusoidal vibrations about its equilibrium position, as shown by the variation of y with time t in Fig. 10.1(a), and if the condition $m_1 = m_2$ were to persist throughout then the resulting change in pressure δP_d would be 180° out of phase with y as shown in Fig. 10.1(c). This is a condition equivalent to a mass vibrating on a spring in the absence of damping. However, in practice two other effects are manifest which result in the flow into the pocket no longer necessarily being equal to the flow out of the pocket at any given instant. Firstly, the squeeze film effect influences the flow out of the pocket, reducing the flow as the plate falls. The pressure changes arising from this effect are proportional to the velocity of the upper plate and provide pure damping. Taken alone the pressure changes arising from squeeze film action are represented in Fig. 10.1(b). It can be seen that the

(a) motion of upper plate

(b) squeeze film damping effect

(c) quasi-static response

(d) pocket volume effect
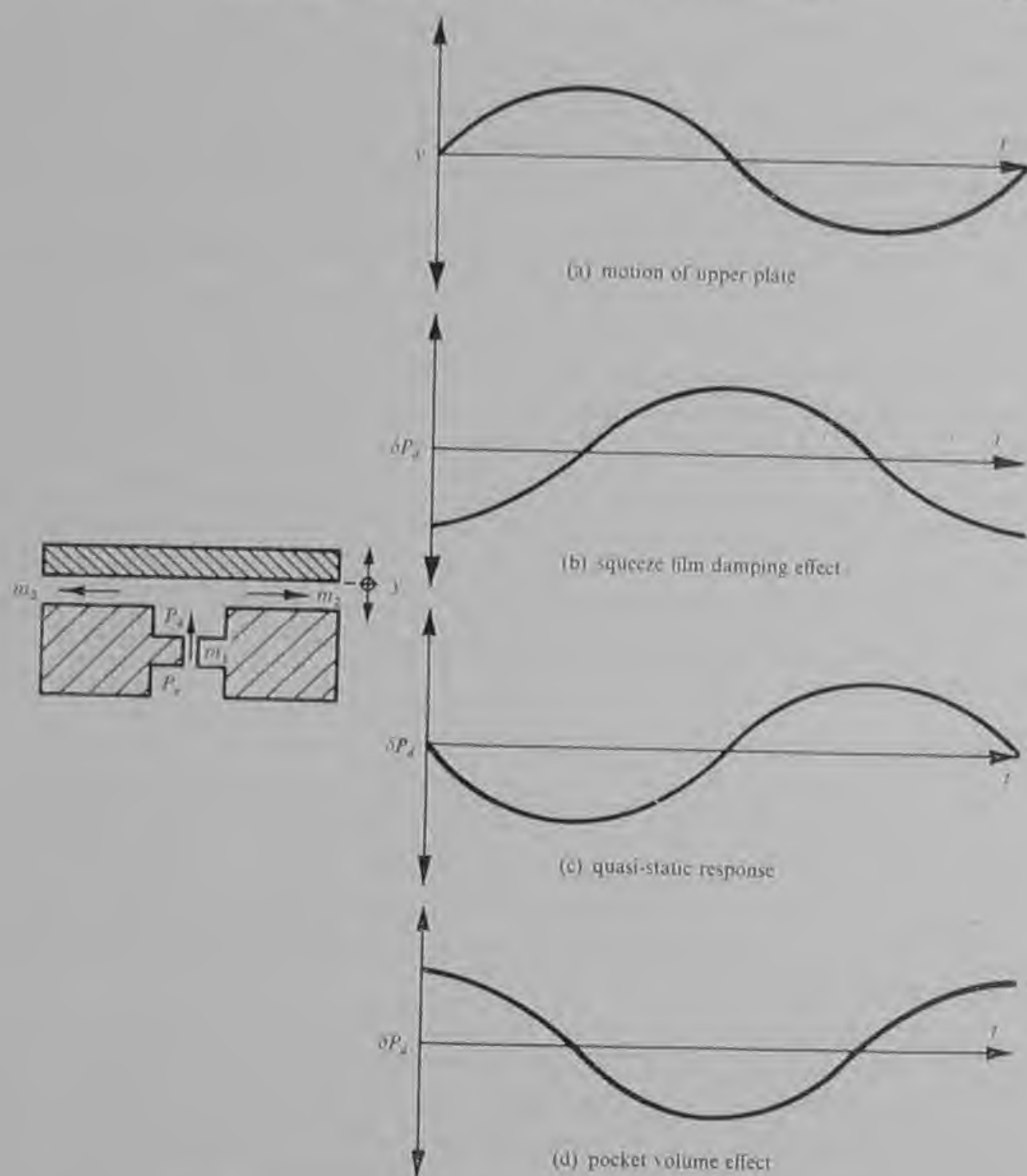
Fig. 10.1 Aerostatic instability in a simple thrust bearing

effect of this pressure variation is to resist the motion of the plate. When the plate is falling the pressure is positive and when the plate is rising the pressure is negative. If no other effect were present in the bearing apart from the quasi-static stiffness and the squeeze film damping, the bearing would always be stable and vibrations would die out when the forcing ceased. However, a second effect which causes instantaneous inequality of flow into and out of the pocket tends to reduce the damping and can lead to instability. The finite volume of the pocket ensures that the pocket takes a finite time to fill and to empty, and as a result the pocket pressure variations tend to lag behind the

movement of the upper plate. Taken alone this effect produces a pressure variation as shown in Fig. 10.1(d). The effect of this pressure variation is to drive the vibration. The change in pressure is positive when the plate is moving up and negative when the plate is moving down. This action is opposite to the squeeze film damping and represents negative damping.

If the pocket volume effect is greater than the squeeze film effect the net damping in the bearing is negative and the bearing is unstable. Following a disturbance from the equilibrium condition a vibration of increasing amplitude develops. Only a minute disturbance is required, and as some turbulence is always present at the feed-hole exit and at the pocket exit the vibration is self-excited from these sources. In an extreme case of a bearing with a large pocket volume the vibration diverges in amplitude until the bearing surfaces come into intermittent contact. This condition is observed in practice as a low-frequency vibration with audible metallic contact. The driving of the vibration can be very powerful and can result in damage to the bearing surfaces.

10.2 Theory of aerostatic instability

Many researchers have concerned themselves with the problem of aerostatic instability and several theoretical analyses of simple bearing geometries have been published. However, as the mathematics is generally protracted and the results are of limited application, space considerations preclude their inclusion here and the reader is referred to the bibliography.

A comprehensive investigation of aerostatic thrust bearings of both circular and rectangular plan form was carried out by L. Licht and H. G. Elrod (Ref. 24). In summarizing the results of their theoretical analysis they concluded that within the limitations imposed upon the design of the bearing by other considerations, the following parameters or combinations of parameters should be treated as shown in order to ensure stability:

(a) depth of pockets
(b) difference between supply and pocket pressures } minimized.
(c) vibrating mass

(d) supply nozzle diameter
(e) length (radial) of annulus
(f) area ratio of annular to pocket regions } maximized.

It can be seen that all of these recommendations tend to reduce the pocket volume effect (a), (b) and (d) or increase the squeeze film effect (c) and (e) or achieve both (f). The vibrating mass influences the resonant frequency of the system and a lower mass leads to a higher

frequency. Aerostatic instability is a type of resonant condition and as the squeeze film damping increases with frequency a low mass is clearly beneficial. The value of a small difference between supply pressure and pocket pressure may not immediately be obvious. However, it is at this condition that the flow into the pocket responds most rapidly to changes in pocket pressure and hence minimizes the extent by which the pocket pressure lags behind the motion of the upper
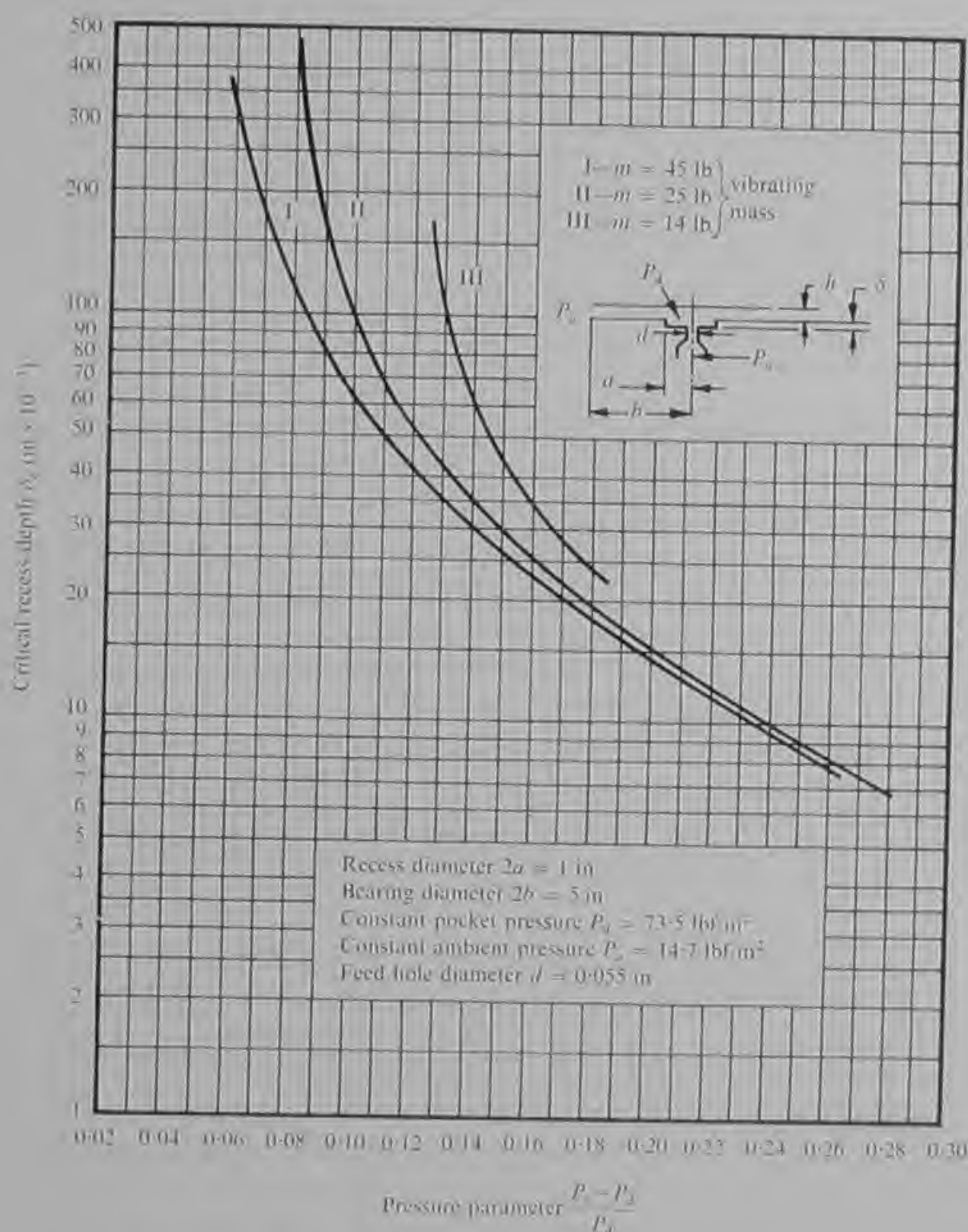
Fig. 10.2 Typical experimentally derived stability boundaries for a simple thrust bearing (after Licht and Elrod, Ref. 24)

plate. A large pressure difference causes the feed hole to become choked and at this condition the flow into the pocket becomes independent of the pocket pressure. For this reason, and also to avoid turbulence associated with shock waves, choked feed-hole conditions should always be avoided.

Typical stability boundaries for a circular thrust bearing with a central pocket are shown in Fig. 10.2. The effects of varying pocket
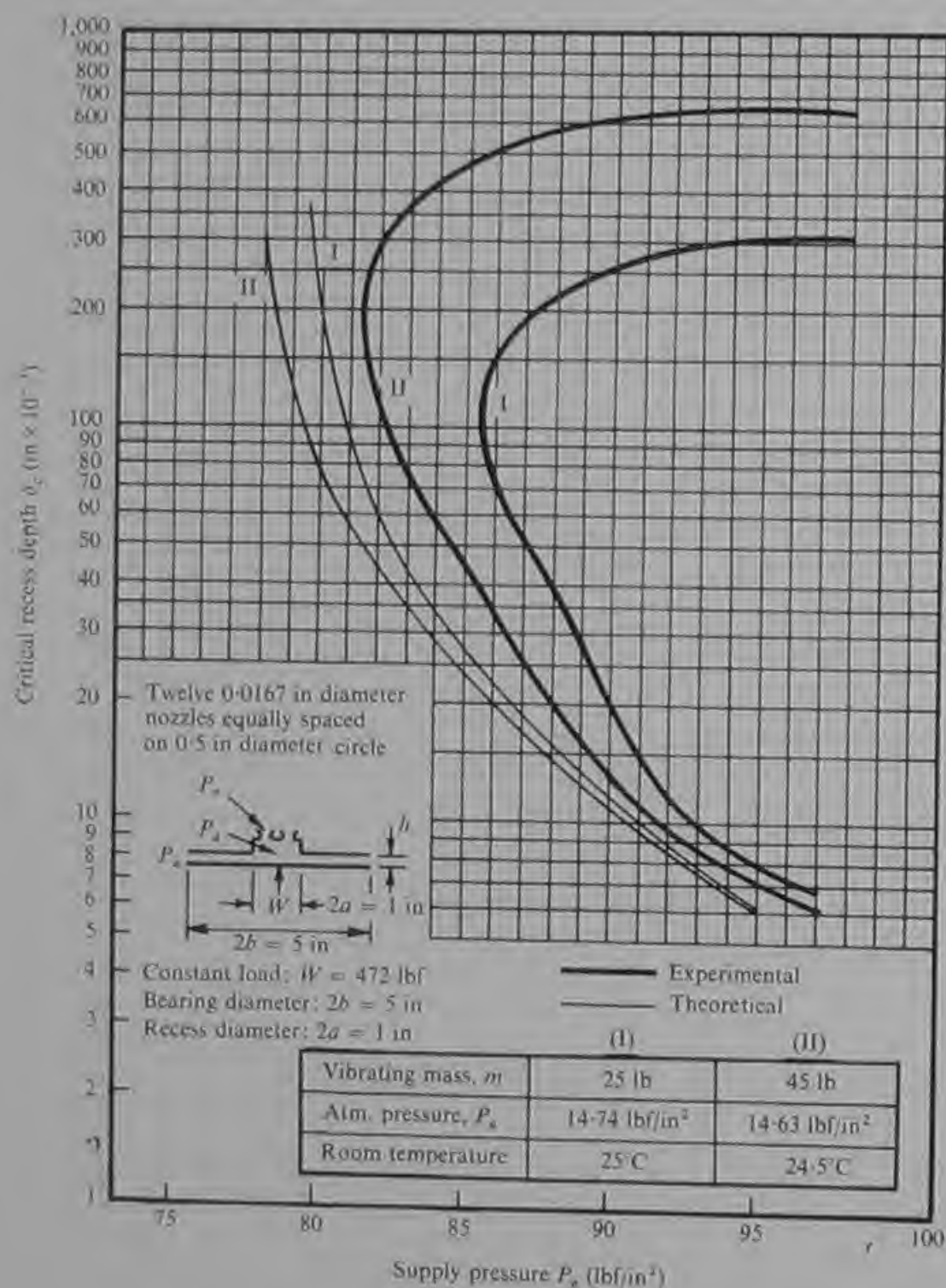
Fig. 10.3 Experimentally derived stability boundaries for a simple thrust bearing with twelve holes feeding a central pocket (after Licht and Elrod, Ref. 24)

depth, pocket pressure, supply pressure and mass are shown. Theoretical predictions are compared to experimental data in Fig. 10.3. The agreement is reasonably good over most of the range but the theory fails to predict the stability exhibited by the real bearing at very large pocket depths. In practice one is most interested in pocket depths in the range 0·005 to 0·020 in and here the theory is reliable and errs on the safe side.

10.3 Avoidance of aerostatic instability

In machines with aerostatic bearings the prediction of areas of instability is complicated by the number of bearings and the complexity of their geometries. The stability is also influenced by the stiffness and damping of the support structure. The analysis is extremely difficult and necessitates the use of a digital computer even in cases where simplified geometry and operating conditions make a solution possible. In practice it has been found advisable to design all bearings in relation to a set of rules which ensure stability in the great majority of cases. It is also wise to incorporate in the design certain features which enable instabilities arising in the minority of cases to be eliminated at the prototype testing stage.

While in theory any storage volume within the bearing including the clearance space can lead to instability, in practice, bearings without pockets or grooves in either of the bearing surfaces are almost invariably stable. Thus bearings with annular orifice or slot feeding are unlikely to exhibit aerostatic instability except in an extreme case such as, for example, when a rotor of large mass is supported on a narrow annular thrust bearing. For this reason bearings with annular feed orifices or feed slots are recommended wherever their lower stiffness and load capacity can be accepted. However, simple orifice feeding usually provides a higher stiffness and in the many applications where this consideration is of paramount importance simple orifice feeding can be used provided that the following rules are observed.

(a) *Thrust bearings*

1 Avoid using pockets wherever possible and achieve the effect of a pocket by feeding into narrow grooves which outline the required pocket area. The width and depth of a groove is determined by the diameter of the feed jets as illustrated in Fig. 10.4. Therefore in order to minimize the volume of the groove a large number of small jets is better than a small number of large jets.

2 Design at a value of gauge pressure ratio of 0·69 or above. Do not design at lower gauge pressure ratios and always avoid choked feed hole conditions.

3 Avoid using narrow annular thrust bearings wherever possible.
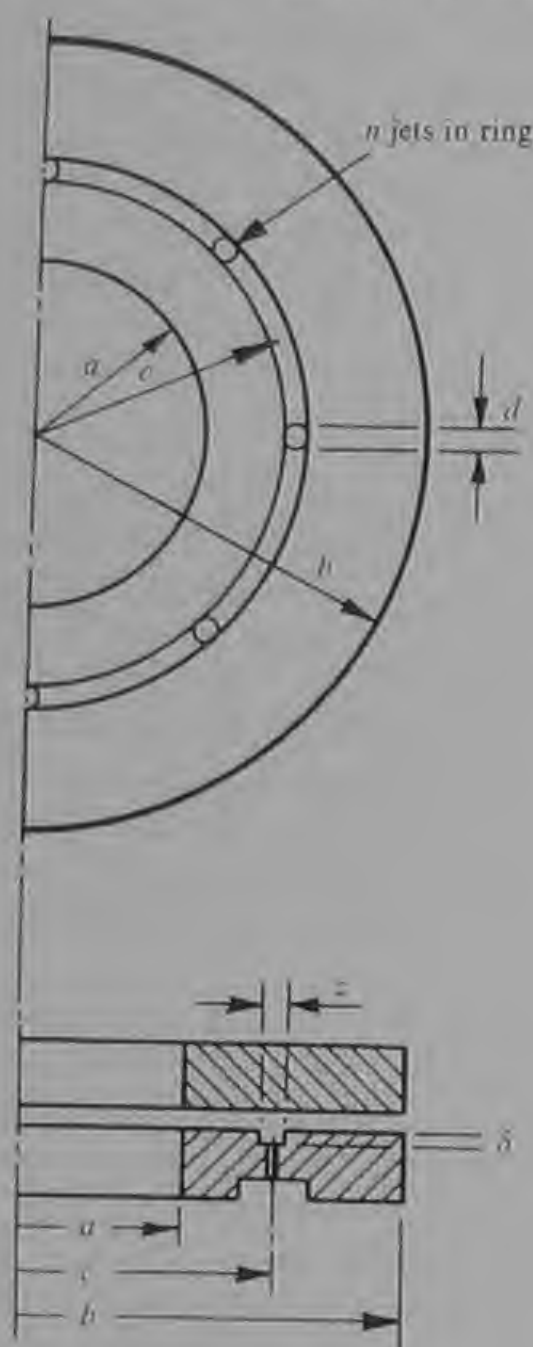
Volume of groove, $V = 2\pi c z \delta$.

For choking in jet   minimum $z = \dfrac{\pi d}{2}$,

minimum $\delta = \dfrac{d}{4}$,

Therefore minimum $V = \dfrac{\pi^2 c d^2}{4}$.

For all other factors to be constant $n d^2 = $ constant for simple orifice feeding.

Therefore $V \propto \dfrac{1}{n}$ and so the greater the number of jets the better will be the bearing stability.

Fig. 10.4 Determination of thrust bearing groove dimensions for maximum stability

The ratio of outer radius to inner radius $\left(\dfrac{b}{a}\right)$ should exceed 1·5 and preferably 1·75.

4 Geometric errors have an adverse effect on stability. The worst condition is concavity in one or both of the bearing surfaces. Every effort must be made to ensure that the faces are flat and mounted parallel to one another. Any residual flatness error should tend towards convexity rather than concavity.

5 Always ensure that the gas supply to the bearing is not throttled or restricted by using the largest possible feed passages. Any restriction in the supply close to the bearing tends to increase the pocket volume

effect in retarding the response of the pocket pressure to changes of bearing clearance.

(b) *Journal bearings* The squeeze film damping is relatively more effective in creating stability in journal bearings than in thrust bearings due to the larger effective area of gas film. Journal bearings are therefore generally less troublesome than thrust bearings. However, aerostatic instabilities can occur particularly in cases where a rotor has a large mass overhung beyond the bearings. In such cases the transverse inertia of the rotor is high and an angular form of instability often arises which is related to the self-excited conical whirl of high speed rotors. The following precautions are of value.

1 Since the machining of grooves in the bearing bore is a difficult and expensive procedure pockets are more often used as these can be easily formed by inserting a jet plug into a hole in the wall of the bearing bush. It is important that the pocket depth should be minimized and again the minimum effective depth is equal to one-quarter of the jet diameter. The number of pockets is equal to the number of jets and is therefore determined by considerations of load capacity and the manufacturing limitations on the minimum jet diameter. The pocket diameter should be chosen so that the total area of the pockets does not exceed fifteen percent of the plan area of the bearing.

2 A high gauge pressure ratio is again beneficial for the stability of journal bearings. Gauge pressure ratios in the range 0·6 to 0·8 are recommended. Choked feed hole condition should be avoided.

3 Bearings of length-to-diameter ratio below unity show a greater tendency to instability than bearings of larger length-to-diameter ratios. Very short jet-fed bearings should be avoided and slot-fed bearings used instead. Short slot-fed bearings not only exhibit better stability but also provide greater load capacity due to the elimination of dispersion effects.

4 Geometric errors have an adverse effect on stability. The worst condition is ovality in the bearing bore and this can be particularly troublesome if caused by clamping stresses. Particular attention should therefore be paid to the method of fixing the machine or spindle in order that radial distortions of the bearing surfaces are minimized. Barrel-shaped bearing bores can also lead to instability, and any residual parallelism error should tend towards bell mouthing rather than barrelling.

10.4 Methods of damping aerostatic instability

Even when all the recommendations which have been made are incorporated into the design of the aerostatic bearings it is still not possible to be absolutely sure of a stable system. For this reason

several methods of eliminating aerostatic instability have been developed. Two of these which combine the advantages of effectiveness and simplicity involve the use of a damping cavity and a controlled exhaust.

(a) *Damping cavity*   The damping cavity method of eliminating aerostatic instability has been described by Lehmann *et al* (Ref. 25). It is shown in its simplest form applied to a circular thrust bearing with central feed hole and pocket in Fig. 10.5. The pocket is connected to
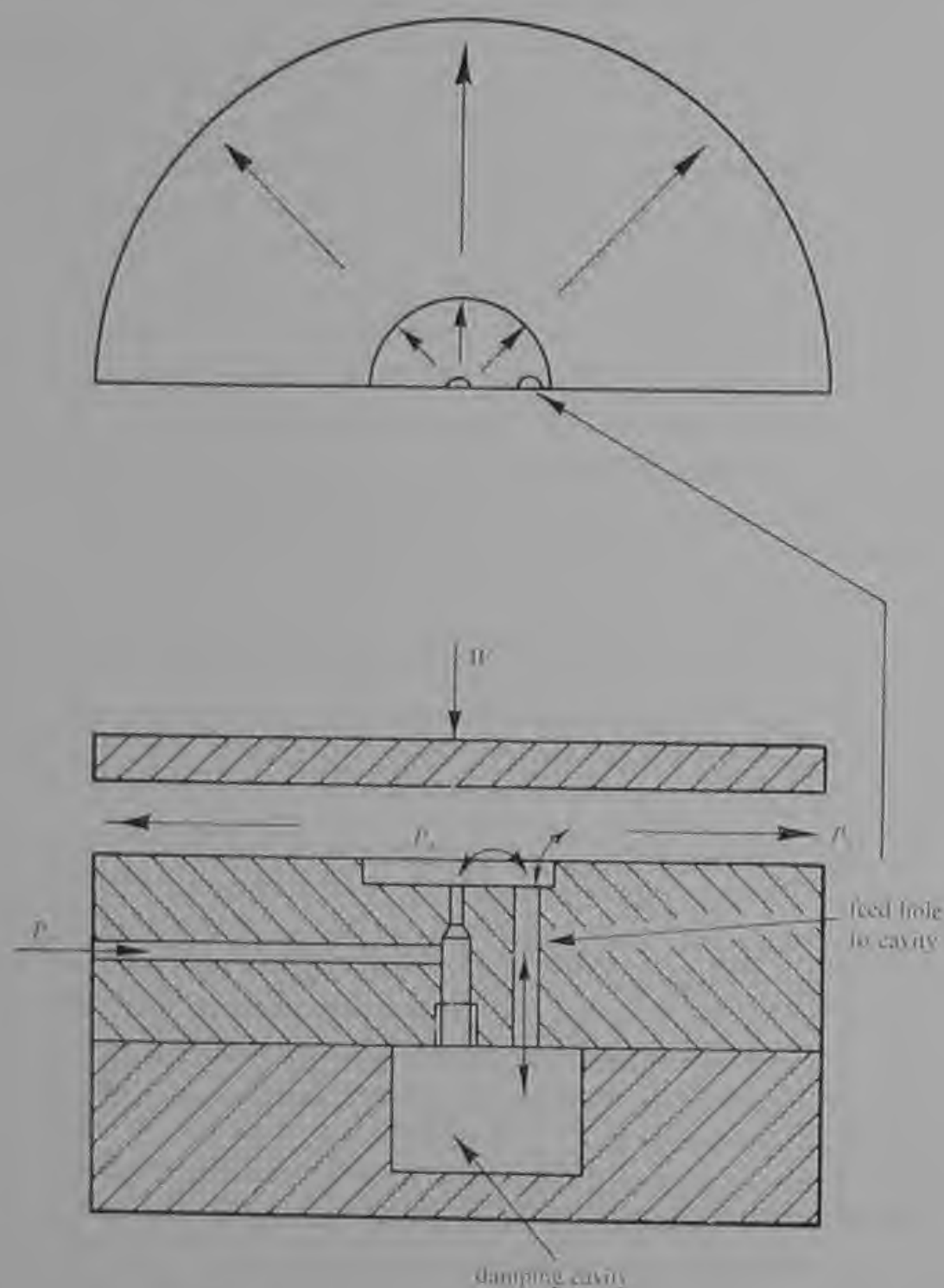
Fig. 10.5 Simple thrust bearing with damping cavity

the damping cavity by means of a hole which is normally rather larger in diameter than the feed hole from the gas supply. Any variation in the pocket pressure, such as arises during vibration, causes gas to flow into or out of the damping cavity. The cavity is completely closed apart from its feed hole from the pocket and its presence does not affect the static load capacity or static stiffness of the bearing in any way. A damping cavity applied to an annular thrust bearing is shown in Fig. 10.6. In this case the cavity is also of annular form and is
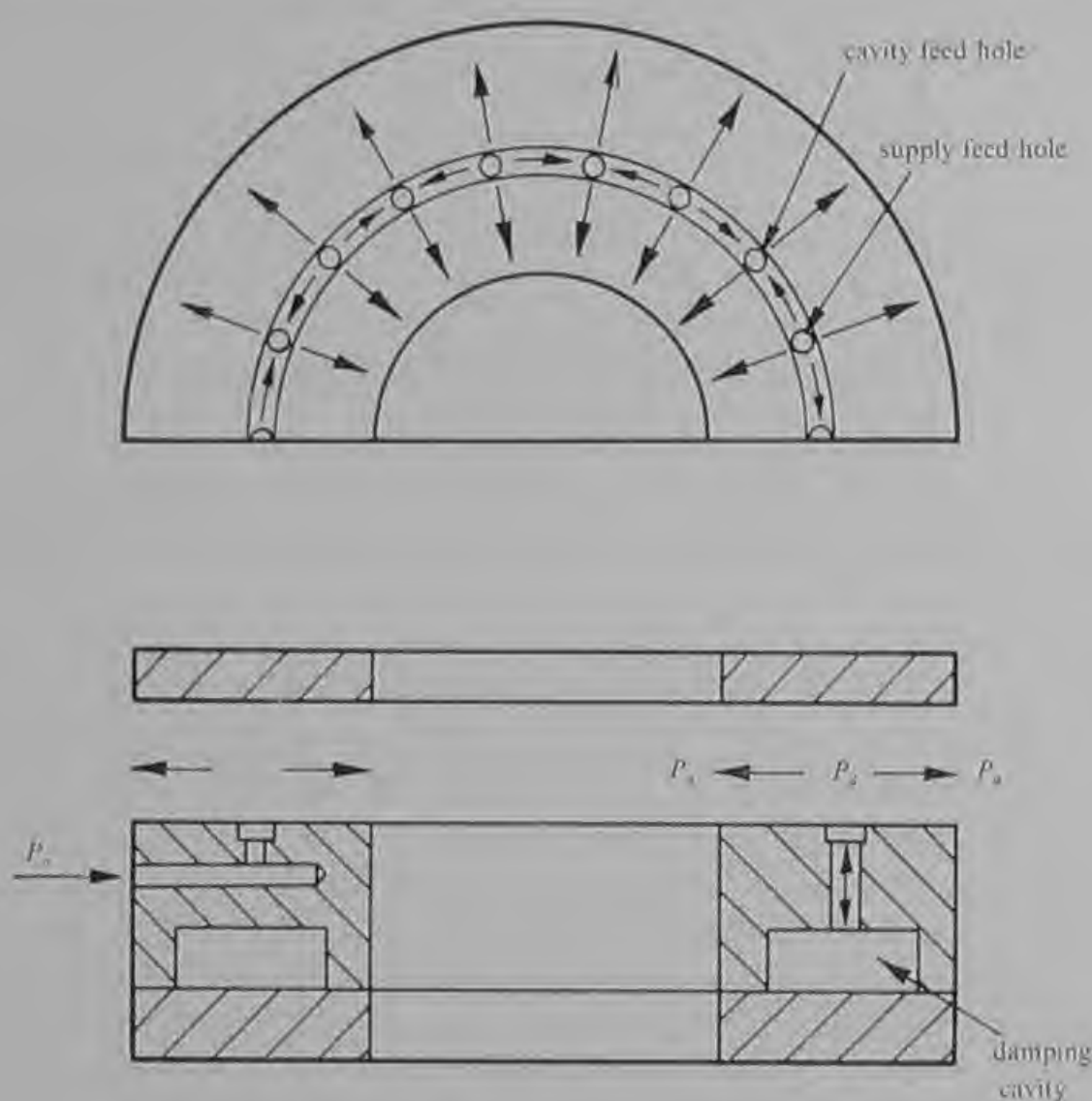
Fig. 10.6 Annular thrust bearing with damping cavity

connected to the bearing groove by a number of holes interspersed between the feed holes. The number of holes into the damping cavity need not be equal to the number of supply feed holes but can, for example, equal half that number or even less in some cases.

The precise mechanism by which the damping cavity achieves its effect is not certain. Lehmann *et al* offer an explanation based on tuning out the resonant frequency of the instability. They suggest that

the cavity volume and feed hole diameter can be adjusted to achieve
this effect, and this has been demonstrated experimentally with simple
bearings with central feed hole and pocket. However, experiments
conducted by the author with an annular thrust bearing have suggested
that the range of stable bearing performance is extended by increasing
both the cavity volume and the feed hole diameter. Continuing to
increase both quantities yielded a diminishing return but there was no
optimum combination to suggest a tuning-out effect. However, little
gain resulted from increasing the cavity volume beyond one thousand
times the groove volume or the feed hole diameter beyond twice the
groove width.
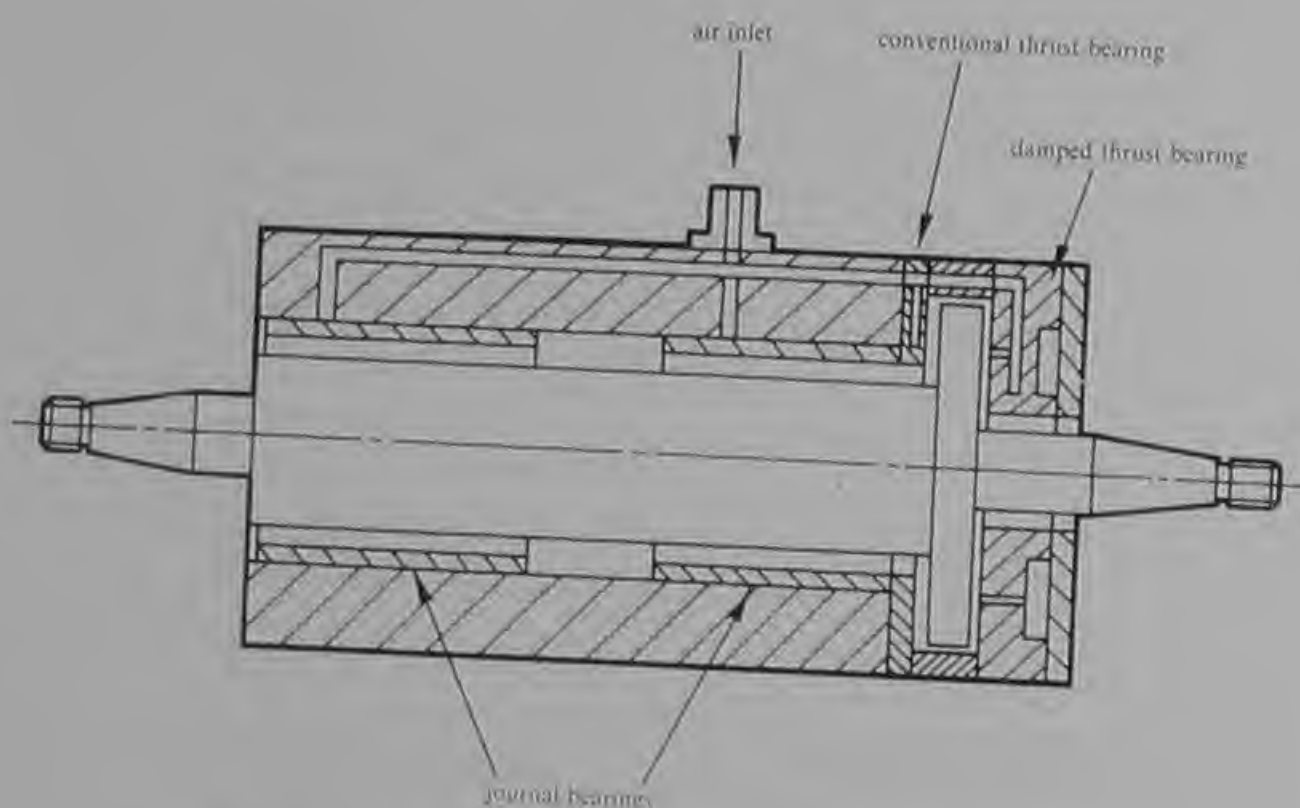
Fig. 10.7 Aerostatic machine tool spindle with damping
cavity on one thrust bearing

The majority of aerostatic machines employ two thrust bearings
but the damping cavity is effective even if applied only to one of the
thrust bearings. A simple aerostatic spindle with one stabilized thrust
bearing is shown in Fig. 10.7. The use of the damping cavity has the
advantage of increasing manufacturing tolerances particularly in
relation to total axial clearance, the geometry of the thrust bearing
surfaces and the width and depth of the pockets or grooves. It also
extends the range of application of the machine, permitting stable
operation with a wider range of support structures and with a wider
range of masses coupled to the rotor. These considerations are

important in, for example, a general purpose machine tool spindle which might be applied to a wide variety of machines and to carrying a wide variety of tools, grinding wheels and pulleys.

(b) *Controlled exhaust* The aerostatic bearing designer has already been advised to channel the exhaust air from each bearing through a single hole, or a small number of holes, before permitting it to escape to atmosphere. This simple expedient affords a powerful method of combating aerostatic instability. If a prototype machine is found to exhibit instability under some operating condition the following procedure may be adopted.

1 Set the condition at which audible instability occurs.

2 Temporarily throttle the exhaust flow from each of the bearings in turn.

3 Note which exhaust when throttled causes the vibration to fade. If throttling the journal bearing exhaust reduces the vibration, and throttling the thrust bearing exhaust has no effect, the instability is in a radial mode. The reverse indicates an axial instability.

4 Permanently throttle the effective exhaust.

5 Provided (4) is effective and the vibration has ceased the load capacity of the bearings should be measured by means of applied static load.

The controlled exhaust method of eliminating aerostatic instability is probably effective for the following reason. When the bearing clearance increases the gas flow increases. Since the flow must pass to atmosphere through the exhaust passage the pressure drop across the control throttle placed in the passage is increased. This means that the effective exhaust pressure at the bearing rises and tends to lessen the increase in the flow. When the bearing clearance is reduced the effect of the throttle is to lessen the reduction in flow. The throttle therefore acts to even out fluctuations in the gas flow through the bearing and hence exercises a stabilizing influence.

The controlled exhaust method is remarkable when first encountered not only because of its effectiveness but also because it can be effective while at the same time not seriously reducing the load capacity and static stiffness of the bearing. Losses in load capacity are usually less than five percent and only rarely greater than ten percent. The method is equally effective with both thrust bearings and journal bearings and can also be used in the rare instances where aerostatic instability occurs in journal bearings at high speeds of rotation. Unlike self-excited whirl, aerostatic instability in high-speed journal bearings is usually audible and non-destructive. It is therefore easily detected and simply eliminated.

The damping cavity and controlled exhaust methods of eliminating aerostatic instability can be used singly or in combination. While the author has experience of many bearing systems which were violently unstable he has yet to meet one which could not be mastered by one or a combination of both of these methods. If the design rules given earlier in this chapter are closely followed, very few bearings will be found to be unstable. These few can be stabilized by the methods described.

CHAPTER 11

INSTALLATION DESIGN

11.1 Introduction

Irrespective of the quality of the design of the aerostatic bearings and the machine of which they form part, the success or failure of an application is often determined in the end by the quality of the installation design and the care with which the installation is executed. Many aerostatic bearings have failed in the past due to such installation defects as clamping a machine or spindle body in such a way as to cause distortion of the bearing surfaces, or failing to make adequate provision for controlling the load imposed by a driving belt. Other failures have resulted from shortcomings in the design of the gas supply installation and more particularly from inadequate filtration. There are also factors to be considered which, while they seldom cause bearing failure, can nevertheless seriously detract from the bearing performance in relation to a particular application. For example, any factor which causes vibration can be detrimental to a machine tool spindle. Thus the performance of an aerostatic spindle driven by a belt is dependent upon the accuracy of the pulleys, the quality of the belt and the degree of dynamic unbalance in the driving motor.

The problems of installation design are most difficult in the case of the machine tool spindle driven by a belt and supplied from a workshop compressed air supply. The problems are invariably less severe where the drive is provided by an integral motor or turbine or where the gas supply is provided from an alternative source. For example, in applications where gases other than air are used, filtration is made easier because the bearing supply gas is often available in an uncontaminated condition as a result of chemical or nuclear considerations. For these reasons the present discussion is centred around a typical grinding machine wheelhead spindle fed from the workshop air supply and driven by a belt.

11.2 Mechanical installation

(a) *Spindle body location* Some typical methods of locating machine tool spindles are shown in Fig. 11.1. While it is obvious that the first two methods can and usually do cause radial distortions in the bearings, whatever types of bearing are used, they are still widely employed.
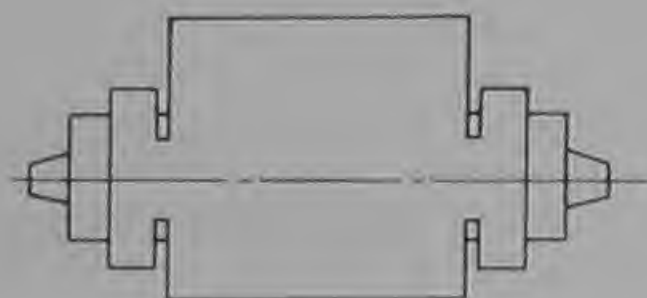
(a) Slit clamp
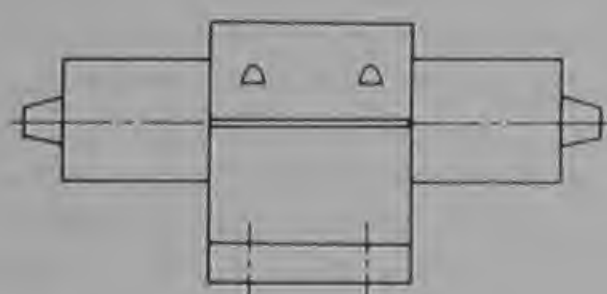
(b) Saddle clamp

(a) and (b) not recommended
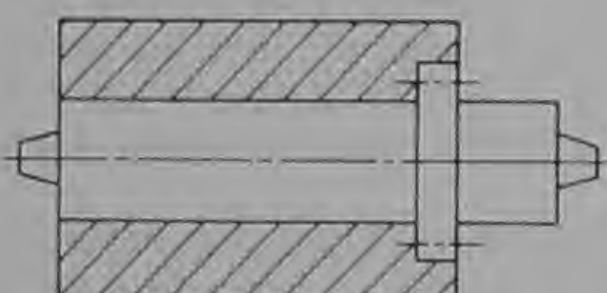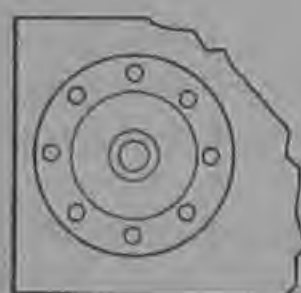
(c) Bolted flange
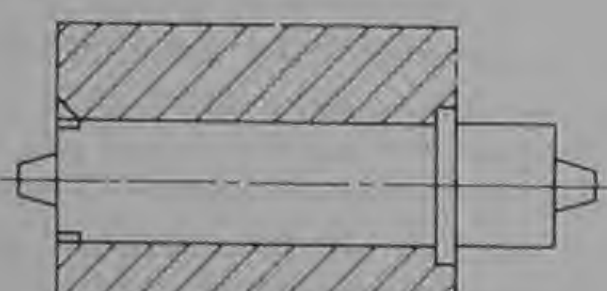
(d) Flange and tapered nut

(c) and (d) recommended

Fig. 11.1   Some commonly used methods of locating machine tool spindles

presumably on account of their simplicity and their ability to accommo-
date a relatively wide variation in the spindle body diameter. However,
they cannot be recommended for aerostatic spindles. The combination
of a thin body wall and a fine bearing clearance can enable an over-
enthusiastic fitter to clamp the shaft firmly in its journal bearings.
Even if the shaft remains freely supported after clamping it is probable
that some distortion has occurred that will weaken the radial load
capacity in certain directions. This effect is illustrated in Fig. 11.2.

clamping forces

reduced load
capacity in
this plane

distortion of
bearing surface
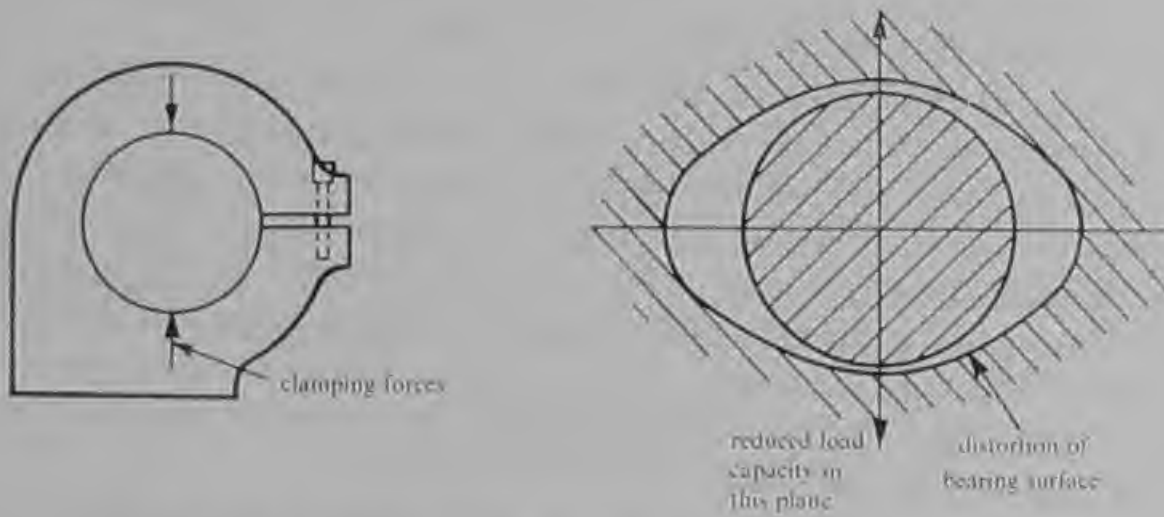
Fig. 11.2 Loss of load capacity due to distortion caused
by radial clamping of machine tool spindle

The best method of locating an aerostatic machine tool spindle is
by means of a bolted flange as shown in Fig. 11.1(c). This method
reduces radial and axial clamping stresses to negligible proportions and
hence enables the full bearing performance to be realized. It has one
disadvantage in requiring the spindle body diameter to be a close fit
in the casting bore. Typical clearances are in the range 0·001–0·002 in
in order to avoid movement of the spindle body or distortion under
load. Somewhat larger clearances can be used if the grinding wheel
is mounted at the flanged end and the pulley, with its belt tension
constant in magnitude and direction, at the other end.

In cases where a close clearance between the spindle body and the
casting bore cannot be used for manufacturing reasons, or where space
considerations preclude the use of a flange large enough for bolting
through, a smaller flange and tapered nut can be used. The tapered
nut located in a conical seating at the end of the casting bore provides
radial support for the spindle preferably at the wheel end. If a close
clearance can be maintained between the spindle body and the casting
bore, the tapered nut can be replaced by a plain nut locating on the
end face of the casting. This method is less satisfactory than the

bolted flange because it puts the spindle body into axial tension and can cause distortion of the thrust bearing surfaces. This problem can be minimized by locating the single-ended thrust assembly at the flanged end and outboard of the flange. The method is not generally suitable for double-ended thrust designs.

Distortion of the bearing surfaces can arise not only from clamping stresses but also from stresses caused by temperature changes. In applications of aerostatic bearings involving either high or low temperatures this consideration must be studied and the problem eliminated either by matching rates of thermal expansion or by providing a degree of flexibility in the means of location.

Whatever the method of location, an effective means of checking for distortion is to measure the radial load capacity in at least four directions at both ends of the spindle. The axial load capacity should be measured two or three times in all directions, turning the shaft between each measurement. Distortion is signified by unevenness of load capacity or a reduction of the measured values below the acceptance test level. The measurements can be made using an accurate spring balance and if the shaft is rocked by hand the point of metallic contact can be detected by a sudden increase in friction.

An alternative method is to use an electrical measurement of the resistance between the shaft and the spindle body to indicate by a short circuit when metallic contact has occurred.

(b) *Setting belt tension* It is essential that where aerostatic spindles are driven by means of a belt care is exercised in the selection of the correct belt and some provision is made for the correct adjustment of the belt tension during installation. Thin flat belts are most suitable for providing a smooth drive and imparting the least influence to the spindle. Thicker types of belts of the 'V' or poly 'V' types should be used only where dictated by considerations of power transmission. The type of material used for the belt is also important and some materials which form a permanent set when left stationary overnight must be avoided. It is also important to use a belt of the endless type without any localized thickening or join.

Before the belt is placed on the pulleys the pulley surfaces should be checked for run-out by means of a dial gauge indicator graduated in 0·000 1 in divisions. Any run-out in the spindle pulley is reflected in a run-out at the other end of the spindle diminished by a factor of the order of 100. This factor therefore usually only becomes of major significance in belt-driven workhead spindles where an extremely high degree of rotational accuracy is required. In such cases the spindle pulley can often be ground *in situ* on the machine by turning the spindle by hand during the grinding process.

When the belt is placed over the pulleys, the pulleys should be at their closest centre distance. This avoids scuffing the bearing surfaces through turning at the condition of very high tension as the belt rides onto the pulley. The belt is then tensioned usually by moving the driving motor on its slide by means of a lead screw to increase the centre distance of the pulleys. During this process it is essential that some means is used to measure the load imposed on the bearings.
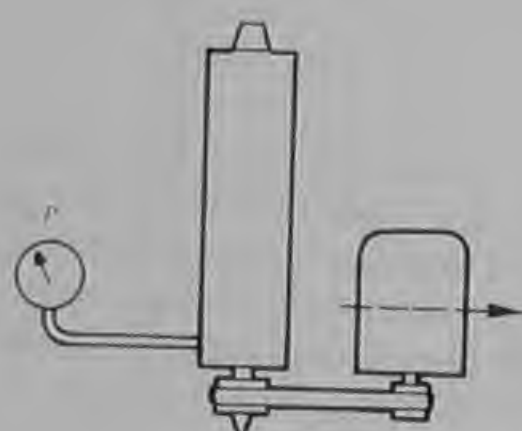
(a) Pressure measurement
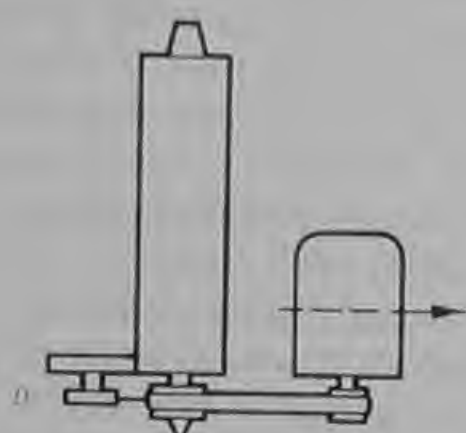
(b) Dial gauge
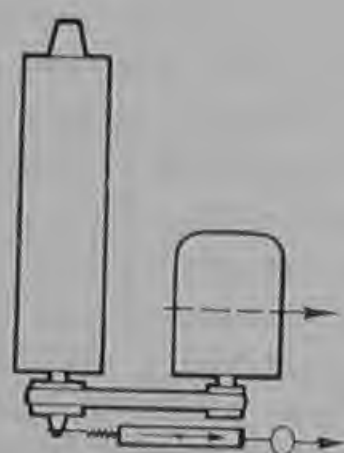
(c) Spring balance
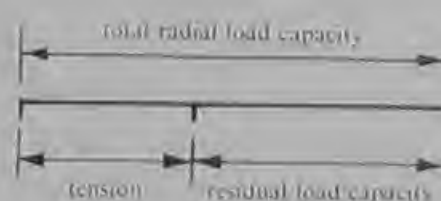
Fig. 11.3 Methods of setting the correct driving belt tension on an aerostatic machine tool spindle

The best method is to monitor the change in pressure in the pulley end journal bearing as already described in Chapter 6. Another method (shown in Fig. 11.3) is to measure the deflection of the bearing by means of a dial gauge indicator measuring on the pulley. However, this method requires great care and skill as the reading can be confused by a variety of factors. A somewhat more satisfactory alternative method is to use a spring balance to measure the residual bearing load capacity after a tension has been set. The belt tension is then obtained by subtracting this value from the value measured before the belt was placed on the pulleys.

11.3 Air supply installation

(a) *Filtration* If an aerostatic bearing is to achieve its full design performance over a long period of time it is essential that the gas supply is free of solid, liquid and gaseous impurities which can detract from that performance. It is difficult to imagine a gas supply which is more contaminated with impurities than the average industrial compressed air supply. All types of impurities are present. Solid particles originate from dust particles in the atmosphere which are small enough to penetrate the filter on the compressor. Liquid impurities consist of condensed water vapour and lubricating oil which originates in the compressor. Gaseous impurities consist of water vapour and also of oil vapour in some cases where certain oils with constituents of low vaporization temperature are used in the air compressor. Clearly filtration problems are less where the air originates from a well-designed compressor which is maintained in good working order and equipped with an efficient aftercooler. The installation of the air supply piping can also contribute to the quality of the compressed air, particularly in relation to the provision of drain taps for liquid impurities. Some of the more important features of a compressed air installation are shown in Fig. 11.4. Although in the past these features have been often overlooked, they are now regarded by many as common practice. In the future the increasing use not only of aerostatic bearings but also of pneumatics, fluidics and air gauging will demand a higher standard of design, installation and maintenance of compressed air systems.

Solid particles are the easiest impurities to remove from a compressed air system. Many types of porous filter elements are available made from sintered bronze or ceramic, woven stainless steel wire, fabric or paper. Filter elements are usually graded according to their mean pore diameter expressed in microns (μm), where 1 micron = 10^{-3} mm = 0.000 040 in. Filter elements suitable for aerostatic bearing applications usually lie in the range from 1 to 25 microns. The smallest dimension in the bearing is usually the clearance between the bearing surfaces and a useful guide to the selection of a suitable filter element
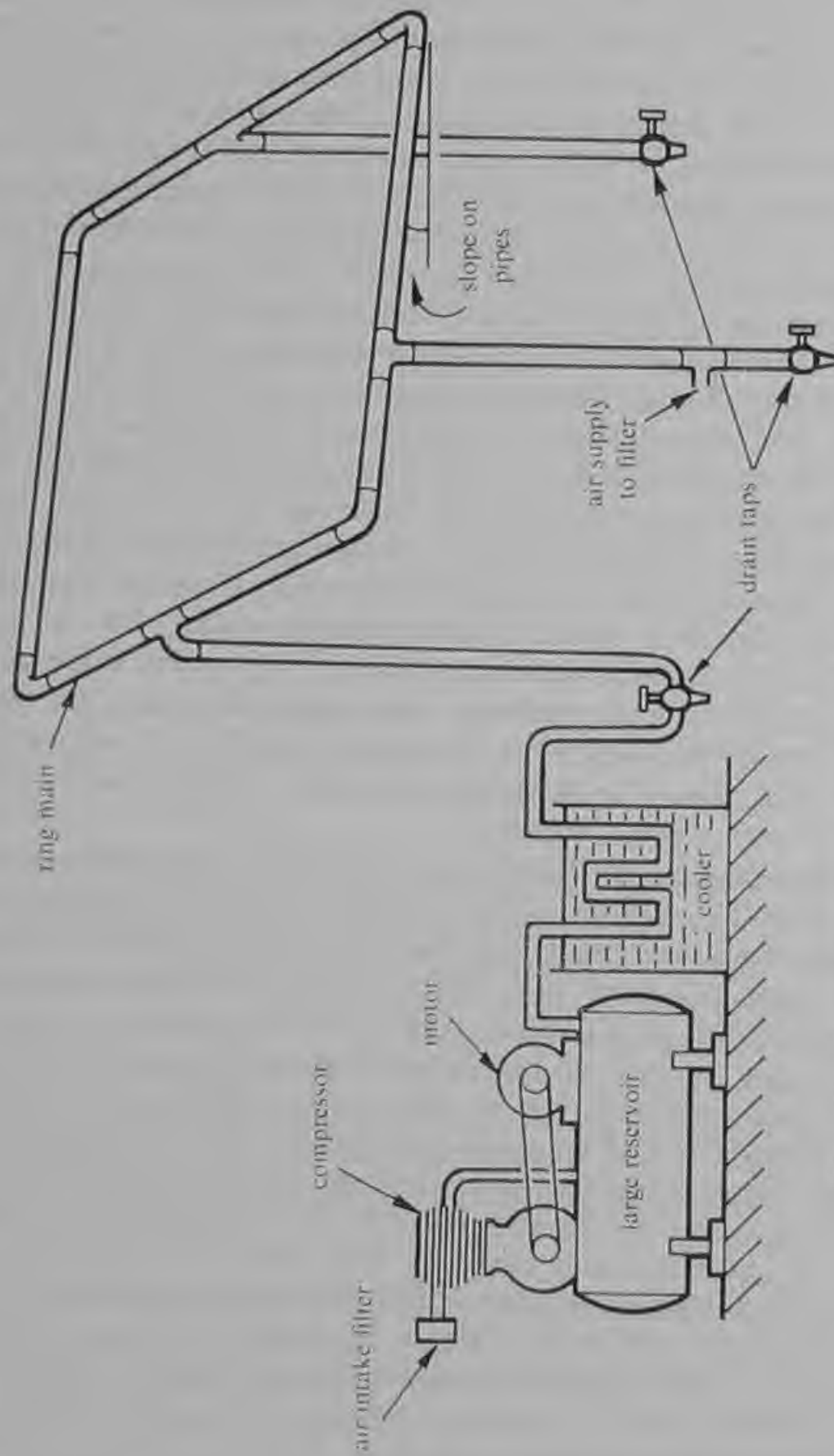
Fig. 11.4 Some important features of a compressed air installation

is to make the mean pore diameter equal to less than half the clearance. For example, in practice a 5 μm filter element has been found to be suitable for bearings of clearance around 0·000 5 in. Of the various materials available for filter elements only sintered ceramic elements require special care in use. They are prone to shed ceramic powder which can cause severe scoring of the bearing surface and for this reason they should be used only for coarse filtration where a fine filter of another material is installed downstream. In industrial environments, where there is heavy contamination by solid particles, it is advantageous to use two filters in series. The first filter of coarse porosity, e.g. 25 or 50 μm, prevents the second filter of fine porosity from becoming blocked quickly. Whatever type of filter element is used it is essential that it is inspected regularly and changed or cleaned as necessary. Metal and ceramic elements can be effectively cleaned by immersing in industrial solvent while agitating in an ultrasonic cleaner. Fabric and paper filter elements are normally discarded after use.

Commercially available filters of the inexpensive type can be employed with aerostatic bearings. However, the user is advised to inspect such filters for general cleanliness, particularly for the presence of metal swarf, and for adequate sealing to prevent some gas flow short circuiting the filter element. Filter manufacturers are generally willing to undertake special assembly or cleaning procedures free of charge in the case of substantial quantities or at a small additional cost in the case of small quantities.

The removal of liquid impurities is generally more difficult than the removal of solid particles. The presence of water, however, seldom impairs bearing performance provided that it is not present in excessive quantities and provided that only corrosion-resistant materials are used downstream of the filter. Most of the water in a compressed air system can be removed by efficient aftercooling and by the proper provision and systematic use of drain taps. Much of the remainder can be removed by commercial air filters which incorporate some means of vortex generation to centrifuge out the liquid droplets. It is advantageous for the liquid receptacle to be fitted with an automatic drain, or a small constant bleed, so that the vortex generator is not prevented from functioning by an excessively high liquid level. Vortex separation is more effective in filters where the swirl is induced downstream of the filter element so that some advantage is taken of the reclassification of small droplets into larger droplets which occurs during flow through the filter element.

Liquid oil is more difficult to remove than water, because with its higher viscosity it tends to cling to walls of the air supply pipes and to make its way slowly but inevitably past all obstacles. A properly designed compressor in good mechanical condition should not intro-

duce large quantities of oil into the compressed air. However, there are very many compressors that do and many air bearings must inevitably operate on oil-contaminated air supplies. Most commercially available filters are considerably less efficient in dealing with oil than with water or solid particles. For this reason some additional provision often needs to be made for dealing with excessive oil contamination. There are several approaches to the problem but all have their limitations. A relatively large vessel filled with lambswool is effective for retaining oil but sooner or later it must be cleaned or refilled and this point is difficult to predict in advance of oil appearing at the bearing exhaust. Another school of thought reasons that liquid oil in limited quantities is unlikely to harm an aerostatic bearing. During normal operation it is blown through the bearing and exhausted to atmosphere where in the average industrial environment it is hardly noticed. Difficulties only arise when a bearing is left to stand with oil in the clearance spaces. Then there is a tendency for the oil to deteriorate into a semi-solid state between a wax and a grease which can block feed passages and clearance spaces. To prevent this occurring the bearing can be flushed through with a suitable solvent which is introduced into the air supply for between half and one minute before the air supply is shut off. Oil mist lubricators can be filled with paraffin or iso-propyl alcohol to perform this function. It is necessary to ensure that it is not inadvertently filled with oil, and that it is regularly used and replenished with solvent.

Oil vapour in the compressed air supply presents difficulties because of its tendency to condense into a wax-like deposit within the bearing clearances. This normally occurs immediately downstream of the feed holes due to the cooling resulting from isentropic expansion. The early stages of this form of contamination are signified by thin lines of yellow-brown wax deposited on the bearing surfaces opposite to the feed holes. The only effective way of preventing the oil vapour reaching the bearing is the use of an activated charcoal filter element. The charcoal must be replaced periodically but spent elements can be reactivated by heating in an oven.

(b) *Supply pressure regulation* The pressure available from a compressed air supply is liable to fluctuate over a considerable range determined by the differential pressure between the cut in and cut out points of the compressor and by variations in the demand for air in the locality of the aerostatic machine. Many applications require a constant supply pressure to the bearings; for example, the bearings in the wheelhead of a surface grinding machine must not cause the grinding wheel to rise and fall with fluctuations of the supply pressure. To achieve a constant supply pressure the air must be fed to the bearings

through a pressure reducing value which is set to a pressure lower than the base level of the supply pressure fluctuations. Simple reducing valves, depending for their action upon the balance of forces between an adjustable spring and a pressure-loaded diaphragm, will meet the needs of most applications. For those applications demanding more precise control of pressure, pilot-operated pressure reducing valves are available.

(c) *Provision for air supply failure* In most industrial applications of aerostatic bearings the designer is wise to make provision for a possible failure resulting from the compressor stopping due to overheating, mechanical or electrical breakdown or to being switched off without warning for maintenance purposes. In such a case the pressure in the system falls gradually over a period of several minutes. The only safeguard necessary is a pressure-sensitive electric switch wired into the machine overload relay circuit to cut off the electrical power to the machine if the pressure falls below a pre-set level. Electric pressure switches are inexpensive, reliable and in widescale use and most can easily be adjusted to operate at the required pressure level.
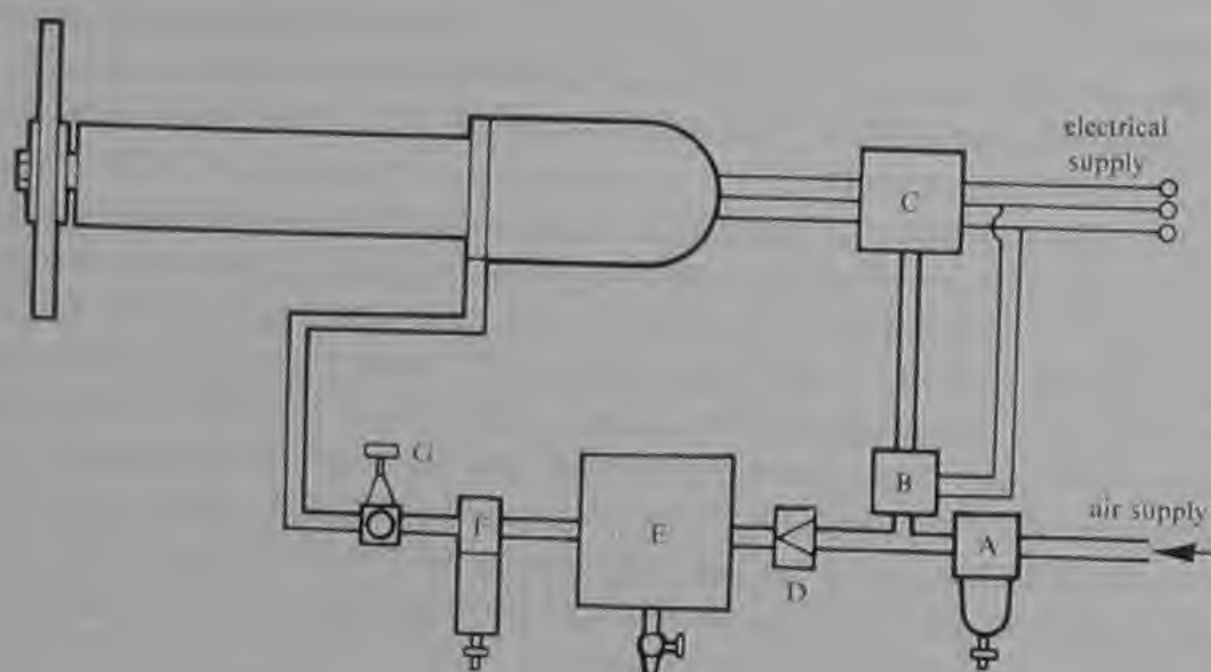
A   Filter to remove solid particles and liquid oil and water
B   Electric pressure switch to operate relay if supply pressure falls
C   Relay, often with on-off buttons, connected in three-phase
    motor supply
D   Non-return valve
E   Storage volume calculated to maintain bearing pressure until
    motor stops
F   Oil absorption filter
G   Pressure regulating valve

Fig. 11.5 Air supply installation for electrically driven
machines with aerostatic bearings

In addition to the slow loss of pressure normally associated with a compressor failure, in some applications a more rapid fall of pressure can occur. This usually results from a local event such as a burst supply pipe or an inadvertently operated shut-off valve. Such eventualities are best prevented by ensuring that the air supply piping is maintained in good condition and is correctly installed so that there is no possibility of accidental interruption of the supply. However, a sudden supply failure can be accommodated by the provision of a vessel of adequate storage volume fitted at the inlet with a non-return valve. The complete system is illustrated in Fig. 11.5. The required storage volume V is given by:

$$V = \frac{M_o RT}{P_o} \frac{(P_o + P_1)}{(P_o - P_1)} \cdot t,$$ (100)

where P_o is the normal supply pressure,
   P_1 is the minimum permissible supply pressure,
   M_o is the mass flow rate at pressure P_o,
and t is the time taken for the machine to come to rest.

If the gas flow rate is known in c.f.m. free air then the required storage volume is given by:

$$V = (\text{c.f.m.}) \frac{P_a}{P_o} \frac{(P_o + P_1)}{(P_o - P_1)} \cdot t.$$ (101)

Fig. 11.5 shows an air supply installation for electrically driven machines. An installation for a turbine-driven machine can be similar except that the pressure switch is replaced by a valve which senses the bearing supply pressure and cuts off the supply to the turbine if the bearing supply pressure falls below a pre-set level. Since in most
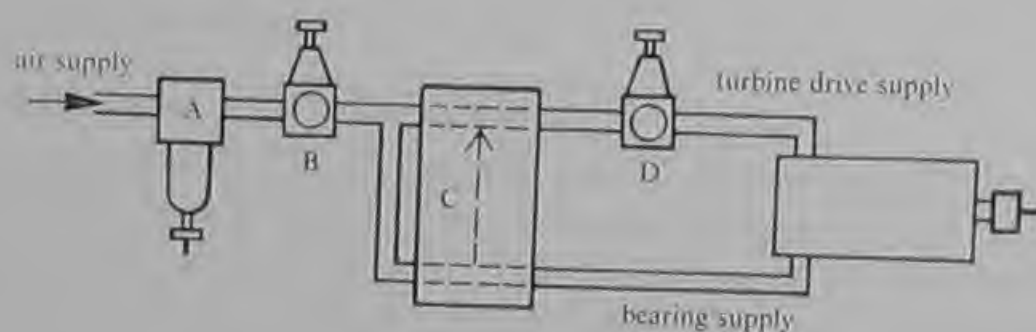
A Filter
B Pressure regulating valve to set bearing supply pressure
C Bearing pressure sensitive turbine cut-off valve
D Pressure regulating valve to control turbine supply

Fig. 11.6 Air supply installation for air turbine driven machines

small spindles for drilling and grinding applications the bearing supply and the turbine supply come from a common source, cutting off the turbine supply in the event of falling pressure conserves the available air to support the bearings for as long as possible. However, most small air turbine-driven spindles are found to be able to run down aerodynamically from full speed or near full speed and many can survive even an instantaneous air supply failure without damage to the bearing surfaces. For this reason the simple air supply installation shown in Fig. 11.6 will normally provide adequate protection by preventing the spindle being used on an inadequate bearing supply pressure.

APPLICATIONS OF AEROSTATIC BEARINGS

12.1 Introduction

A study of existing applications of aerostatic bearings is of value for three main reasons. Firstly it illustrates the advantages to be secured by the use of these bearings. Secondly, it stimulates ideas for future applications. Thirdly, it teaches how earlier designers have approached their problem of achieving a workable compromise between the required performance and the limitations imposed by manufacturing considerations and the available compressed gas supply.

One of the most important fields of application of aerostatic bearings is undoubtedly machine tools. For this reason, and because much of the author's experience has been gained in this field, many references have been made to problems relating particularly to machine tool spindles. However, the range of machine tool applications is very wide, and within it, most of the advantages of aerostatic bearings can be exploited and most of their problems have to be overcome. Fig. 12.1 summarizes the applications of aerostatic spindles to machine tools and lists the principal advantages which stimulated their adoption. Almost all of the benefits result from three properties of aerostatic bearings: low friction, precise axis definition and the absence of wear. In comparison with spindles with ball or roller bearings the lower level of vibration of aerostatic bearings is also advantageous. This is particularly so in relation to the production of good workpiece geometry and surface finish, and in ensuring a long life of the cutting tool, drill or grinding wheel.

12.2 Applications to grinding machines

An aerostatic workhead spindle for a Studer cylindrical grinding machine has already been referred to in Chapter 6 and a sectioned drawing is shown in Fig. 6.4. The performance of this spindle was described by B. T. Trayner of the British Aircraft Corporation in a paper presented to the Gas Bearing Symposium at the University of Southampton in 1965 (Ref. 15). While it is possible to grind external surfaces between dead centres to a degree of roundness within 5 μin annular zone, the roundness that can be achieved on internal surfaces is determined by the performance of the bearings in the workhead. Most present-day grinding machines employ either plain oil bearings

Process	Function	Operation	Principal Advantages
Grinding	Workhead spindle	Internal cylindrical, external and live centre cylindrical	P.A.D. provides a high order of roundness and concentricity A.W. provides freedom from deterioration
	Wheelhead spindle	External cylindrical, surface	L.F. eliminates thermal distortion
		Production of screw threads, splines, gears and surface forms	P.A.D. ensures good form and the grinding wheel holds its form longer
		Internal cylindrical	L.F. provides high mechanical efficiency A.W. provides long bearing life
Drilling	Drill spindle	Electronic printed circuit board drilling. Micro-hole drilling in metals	L.F. provides high speeds on low power P.A.D. ensures accurate hole size and minimizes burring and the smearing of resin in printed circuit board
Turning	Workhead spindle	Fine turning. Fine boring	P.A.D. provides a high order of roundness L.F. minimizes thermal distortion and assists accurate size control
Milling	Milling spindle	Production of fine slots, e.g. in recording heads. Facing with diamond cutting tools. Production of miniature components, e.g. watch and instrument parts	P.A.D. provides minimum burring and high order of surface finish A.W. enables higher speeds to be used with a resulting increase in productivity or further improvement of surface finish

L.F.   Low friction   P.A.D. Precise axis definition
            A.W.   Absence of wear

Fig. 12.1 Applications of aerostatic spindles in machine tools

or rolling contact bearings. A typical performance using either of these types of bearings is to produce a workpiece of roundness in the range 25 to 50 μin annular zone. However, aerostatic bearings can provide a degree of roundness equal to or better than that obtained when grinding between dead centres. Fig. 12.2 shows roundness measurements of components produced by Trayner's aerostatic bearing workhead and the plain oil bearing workhead originally supplied with the machine. The aerostatic bearings enabled a workpiece roundness within 5–8 μin annular zone consistently to be achieved and the ultimate capability appeared to be in the region of 2–3 μin annular zone.
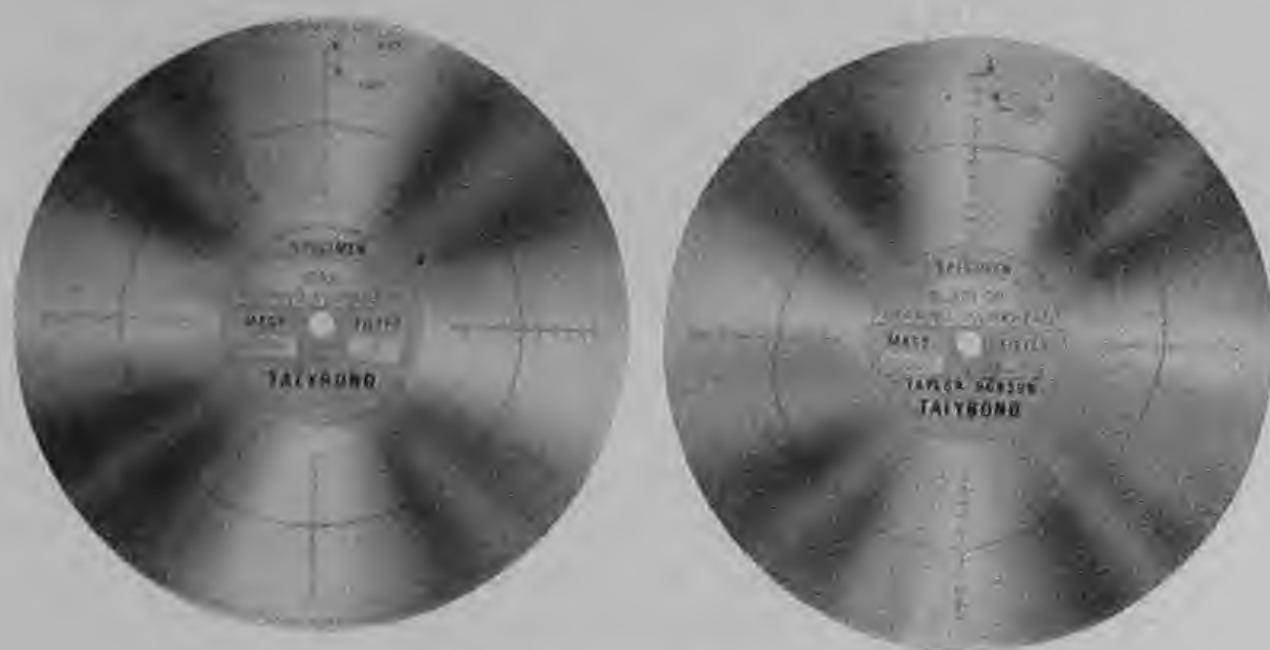
Fig. 12.2 Comparison of air bearing and plain oil bearing workheads—roundness of workpiece (after Trayner, Ref. 15)

However, it was reported that the presence of oil in the compressed air supply could derate the roundness produced by a factor of between three and four with a tendency to eight point lobing, presumably a function of the number of journal bearing feed jets.

Some details of the design of the aerostatic bearings of the workhead shown in Fig. 6.4 have been published. The bearings are designed at gauge pressure ratios chosen for maximum stiffness. The journal bearings have eight jets per row at approximately one third station and the mean radial clearance of the journal bearings is 0·001 in. The mean clearance of the thrust bearings is 0·000 5 in. The bearings are designed to operate on a supply pressure of 80 lbf/in^2 gauge and the air consumption is approximately 3·5 c.f.m. of free air. Comparative external grinding tests carried out using the test piece in Fig. 12.3 showed that the radial stiffness at the workpiece was comparable to

that achieved grinding between dead centres. Fig. 12.3 shows the deflections resulting from a plunge cut of 0·000 5 in (0·001 in diametrical reduction) applied suddenly by the machine handwheel. The immediate workpiece deflection was approximately 0·000 1 in in the case of both the aerostatic bearing workhead and dead centres. The spark-out was somewhat quicker in the case of the aerostatic bearing and this seems to be a characteristic found in most grinding applications of aerostatic bearings in both workheads and wheelheads.
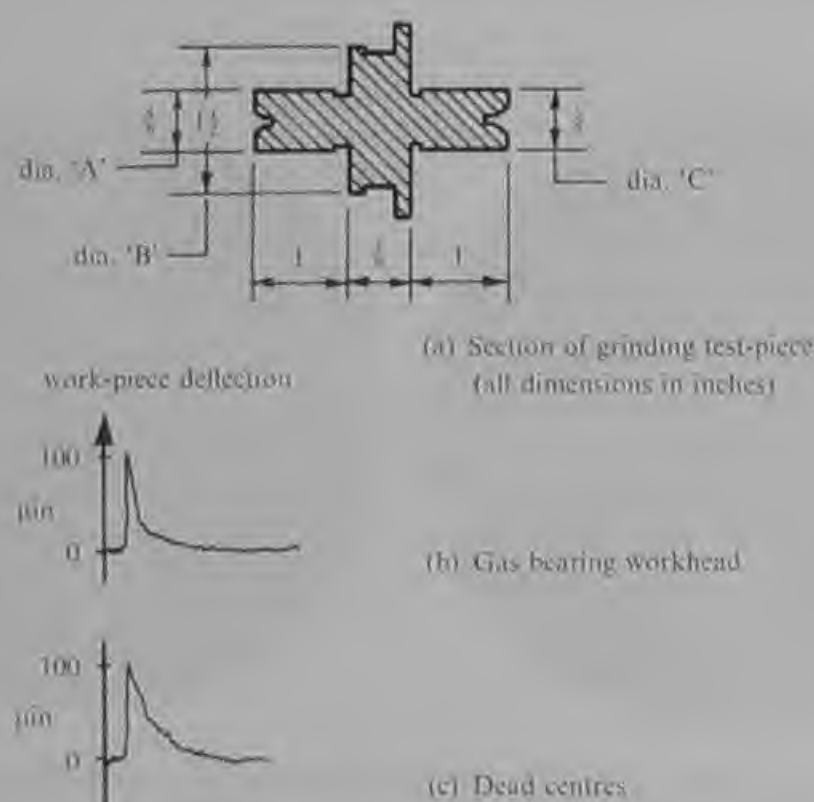
Fig. 12.3   Deflection of workpiece during grinding (after Trayner, Ref. 15)

Radial stiffness is a much discussed aspect of the performance of the various alternative types of workhead bearings which might be employed in future grinding machines. Dr. H. J. Renke of Fritz Studer A.G., the Swiss grinding machine manufacturers, has stated (Ref. 26) that a recently designed hydrodynamic or hydrostatic spindle which is small enough to fit a grinding machine may have a stiffness of about 620 000 lbf/in. It is a commonly held belief amongst machine tool manufacturers and users that aerostatic bearings cannot approach this order of stiffness. However, both the British Aircraft Corporation (Operating) Ltd. and Westwind Turbines Ltd. have produced aerostatic workheads with a front bearing radial stiffness of 600 000 lbf/in and the ultimate of development is far from being reached.
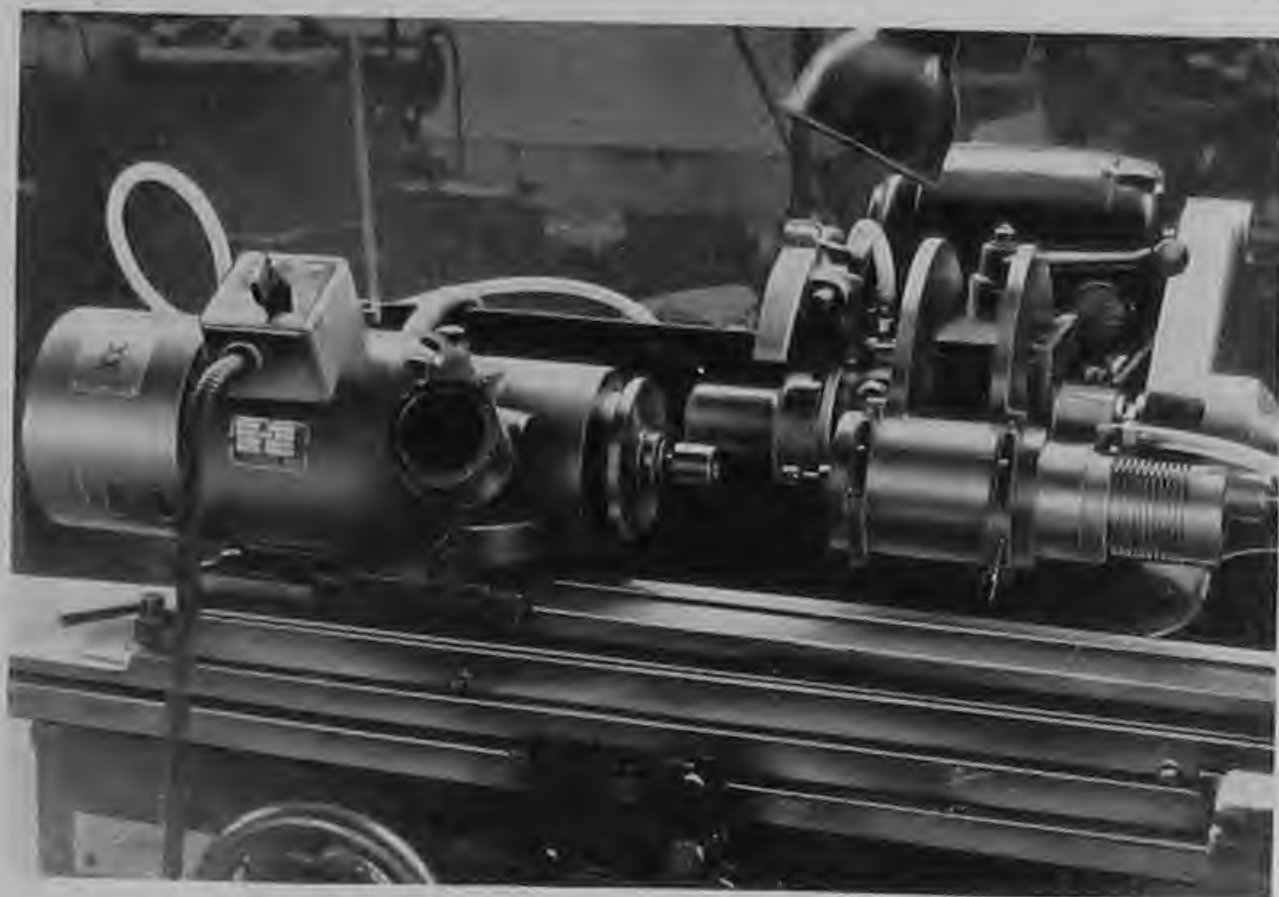
Fig. 12.4 Studer RHU 450 grinding machine with aero-
static bearings in the workhead, wheelhead and high fre-
quency motor driven internal grinding spindle. The machine
is shown set up for bore grinding a test piece. This machine
was converted by Westwind Turbines Ltd. for S. Smith &
Sons Ltd. who use it to produce aerodynamic gas bearing
components for gyroscopic instruments

Fig. 12.4 shows a Studer RHU450 universal grinding machine which
was converted to aerostatic bearings by Westwind Turbines Ltd. The
main wheelhead and workhead spindles were provided with aerostatic
bearings and each was driven by a belt from the original wheelhead
and workhead motors. The internal spindle was also provided with
aerostatic bearings but the driving belt was abandoned in favour of an
integral high-frequency motor. Some details of the three spindles
are given in Figures 12.5, 12.6 and 12.7. This machine was converted
to enable it to reach the high degree of precision needed in the manu-
facture of aerodynamic bearings for gyroscopes. It proved capable
of producing workpieces with both inside and outside diameters
round to within 3 μin annular zone and concentric to within 5 μin.
These results are obtainable under normal precision workshop con-
ditions and can be held throughout large batches of components.
Surface finishes of better than 1 μin c.l.a. can be achieved on both
internal and external surfaces.

Performance	
Air supply pressure	80 p.s.i.g.
Air consumption	5·5 c.f.m. free air
Radial load capacity	250 lb
Axial ,, ,,	125 lb
Radial stiffness	500 000 lb/in
Axial ,,	300 000 lb/in

Section 'A'—'A'
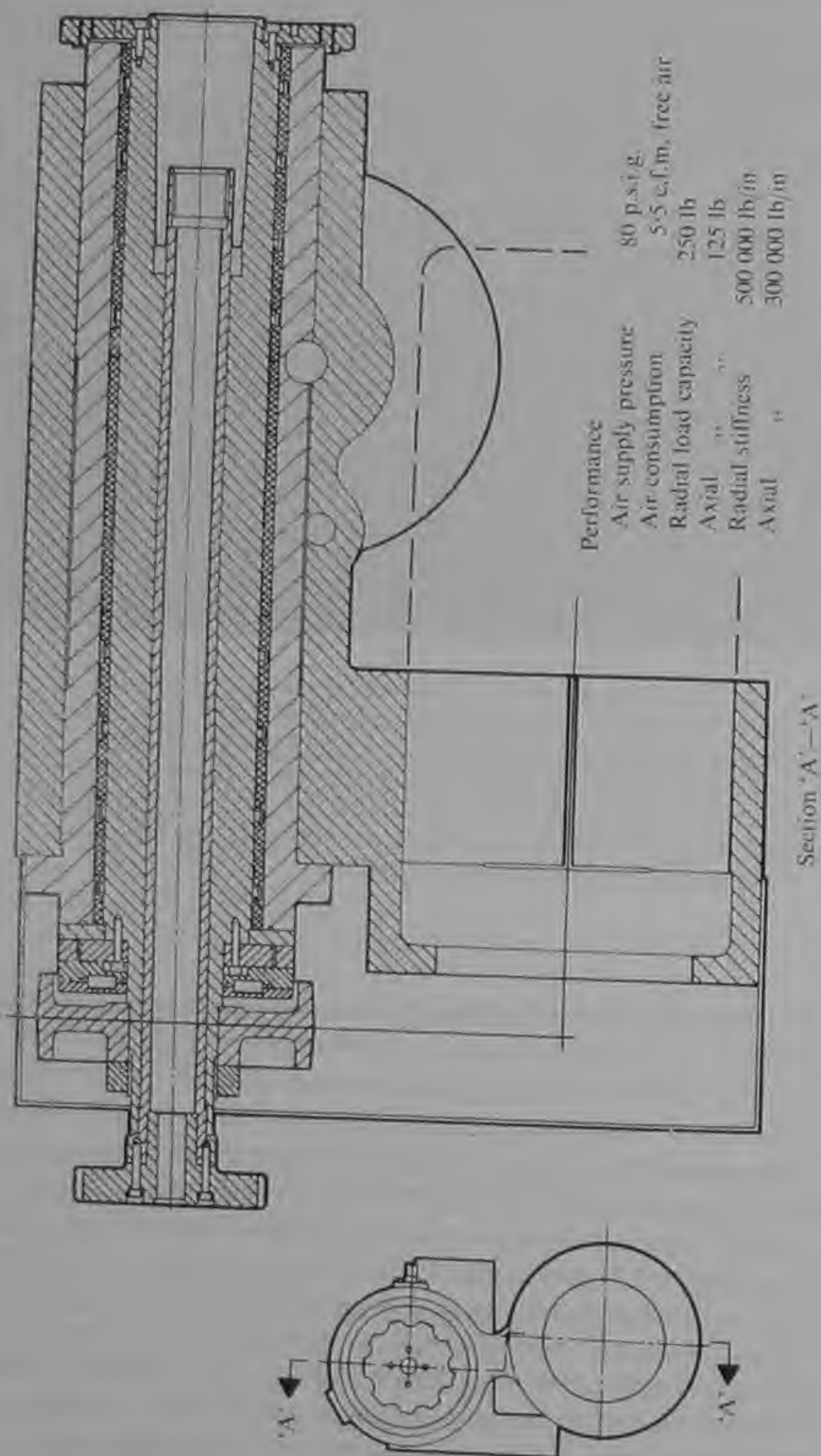
Fig. 12.5 Aerostatic workhead for Studer 450 grinding machine
(Reproduced by permission of Westwind Turbines Ltd.)

Section 'A'—'A'

Maximum radial load	120 lb	
Maximum radial stiffness	250 000 lb/in	at 80 p.s.i.g.
Maximum axial load	120 lb	bearing supply
Maximum axial stiffness	250 000 lb/in	pressure
Air consumption	4 s.c.f.m.	
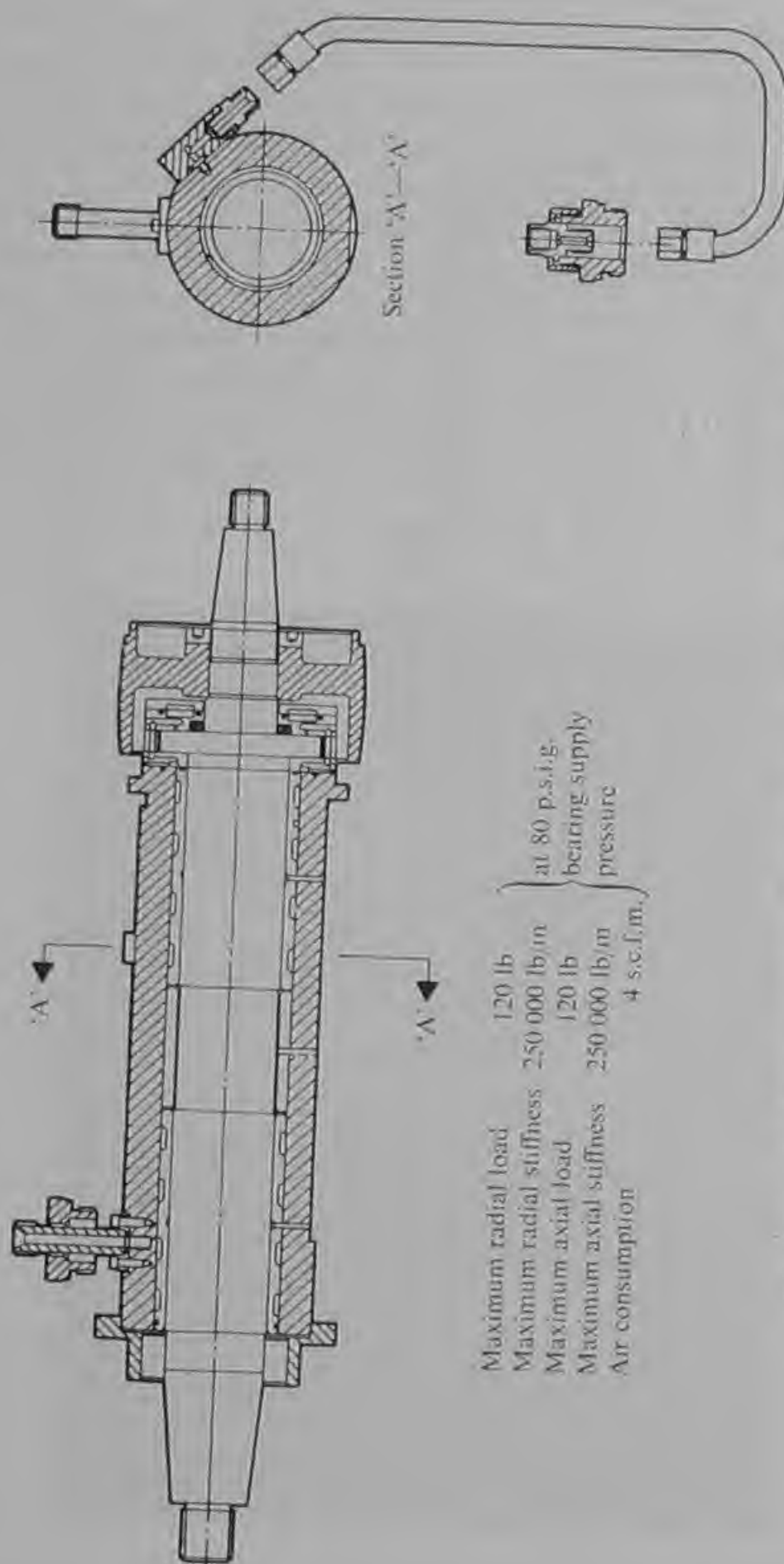
Fig. 12.6   Air bearing wheelhead for Studer 450 cylindrical grinding machine
(*Reproduced by permission of Westwind Turbines Ltd.*)

Speed	27 000 r.p.m.
Power	0·6 h.p.
Maximum radial load	55 lb
Maximum radial stiffness	200 000 lb/in
Maximum axial load	100 lb
Maximum axial stiffness	100 000 lb/in
Air consumption	5 s.c.f.m.

at 80 p.s.i.g.
bearing supply
pressure
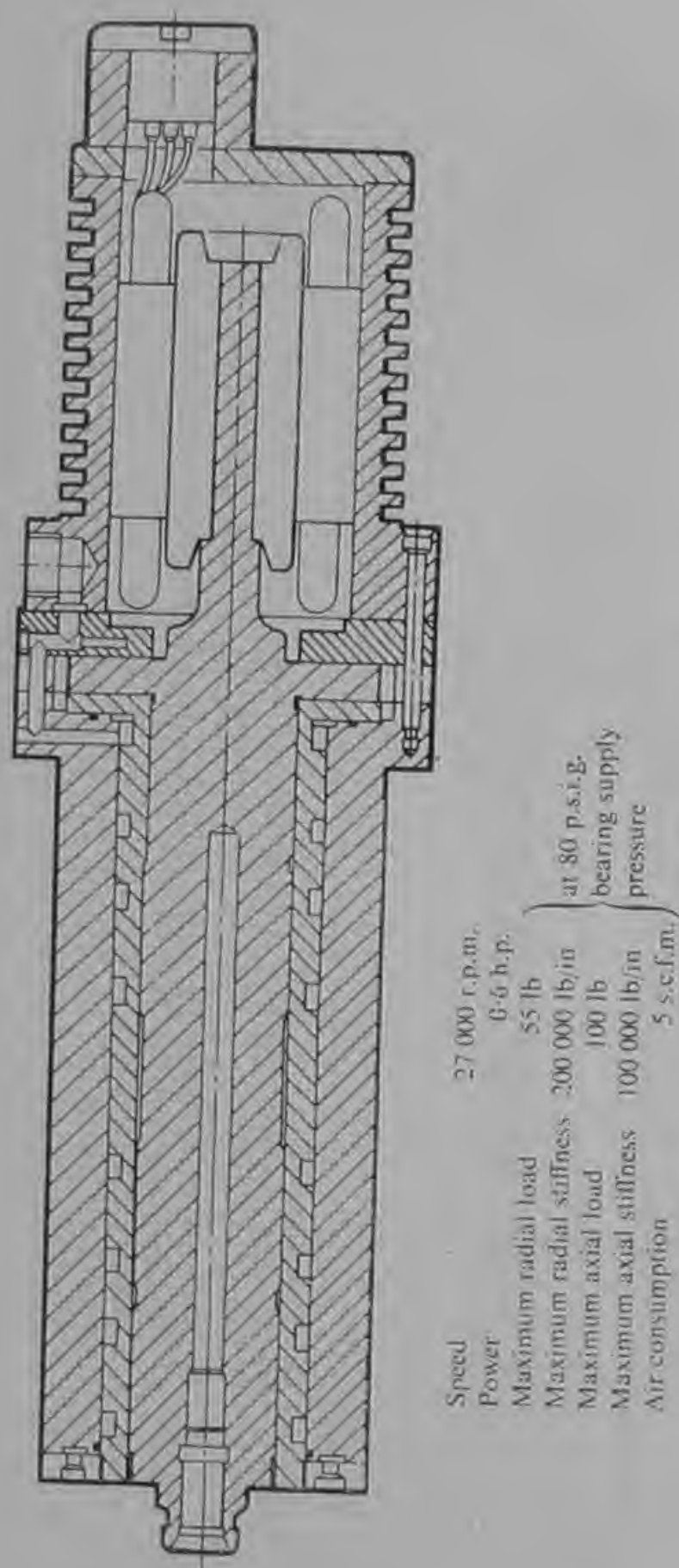
Fig. 12.7   Air bearing high-frequency motor driven internal grinding spindle
(*Reproduced by permission of Westwind Turbines Ltd.*)

One of the most successful applications of aerostatic bearings to precision grinding machines has been the wheelhead spindle developed by Westwind Turbines Ltd. for the Jones and Shipman range of 540 (see Fig. 12.8), 1540 and 1400 surface grinding machines. In the eighteen months following its introduction in March 1966 over 250 machines were converted. The majority of these machines were employed on grinding gauges and other high quality workpieces, such as electronic recording heads and tungsten carbide dies where the advantages conferred by aerostatic bearings are most pronounced.

On surface grinding machines with conventional wheelhead bearings one of the biggest problems is the thermal expansion caused by the heat generated in the bearings. During the first hour of running while the machine is warming up, the wheelhead temperature rises, making it
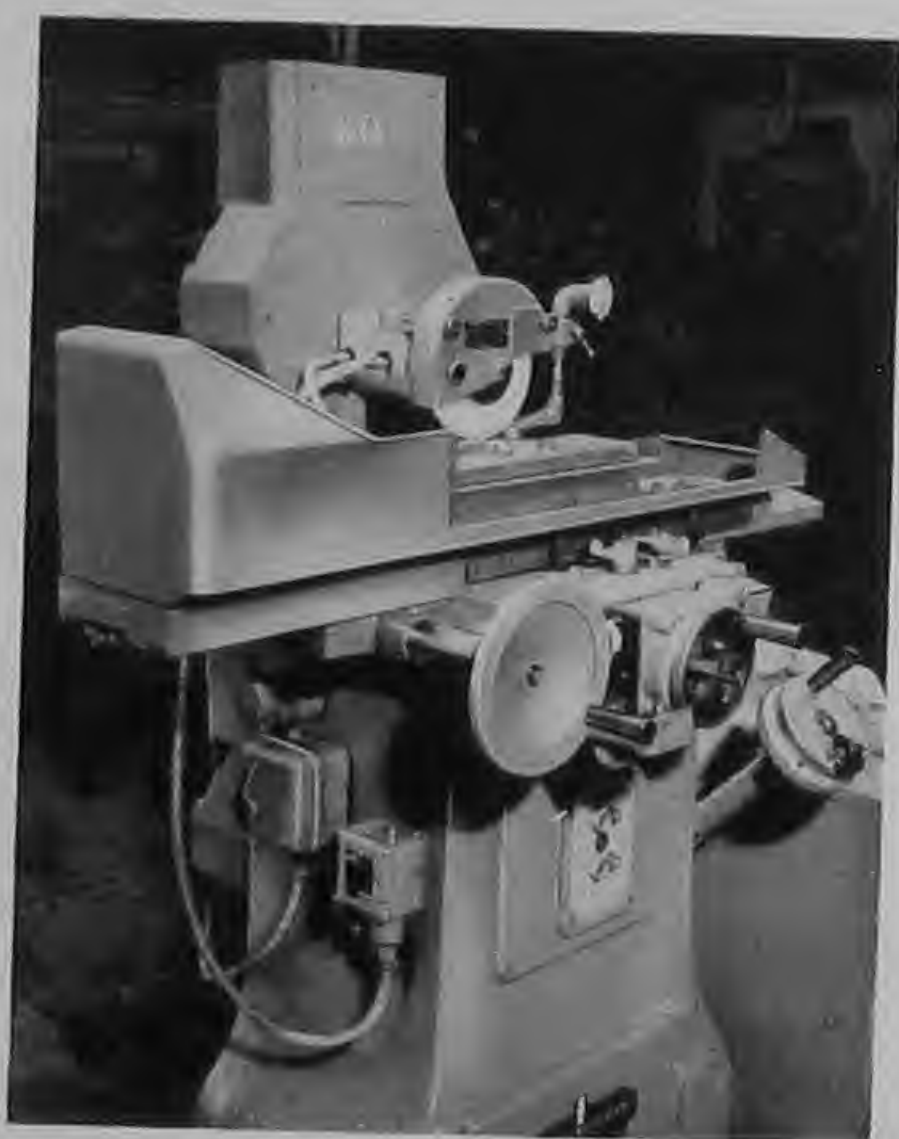
Fig. 12.8a A Jones and Shipman type 540 surface grinding machine which has been fitted with a conversion wheelhead produced by Westwind Turbines Ltd. The air bearing head is interchangeable with the conventional type and is belt driven

Fig. 12.8b An air bearing wheelhead for the Jones and Shipman type 540 surface grinding machine. The external design of the head permits of mounting the standard wheel dressing attachments and the knock-off unit for the power rise-and-fall mechanism

difficult for the operator to hold close tolerances. Fig. 12.9(a) compares the temperature rises occurring in plain oil bearings, ball bearings and air bearings. The measurements were made by Jones and Shipman Ltd. on three of their type 1400 surface grinding machines (Ref. 28). Fig. 12.9(b) compares the vertical movement resulting from thermal expansion during the first hour of running. It can be seen that the greatest temperature rise occurs with hydrodynamic oil bearings. Ball bearings are better, but with air bearings the problem is eliminated.

The low friction of air bearings ensures that the full motor power is available for grinding. This has been demonstrated by tests carried out on Jones and Shipman type 540 surface grinding machines in the gauge grinding shop of the Coventry Gauge and Tool Co. Ltd. It was found that a cut of 0·020 in would stop the grinding wheel on a machine equipped with conventional wheelhead bearings. However, machines with aerostatic wheelheads are frequently used on cuts of up to 0·030 in.

Another demonstration of the negligible friction power consumption of aerostatic wheelheads is given by measurements of the current drawn by the driving motor. The following data were obtained from tests on a Jones and Shipman 540 surface grinding machine.
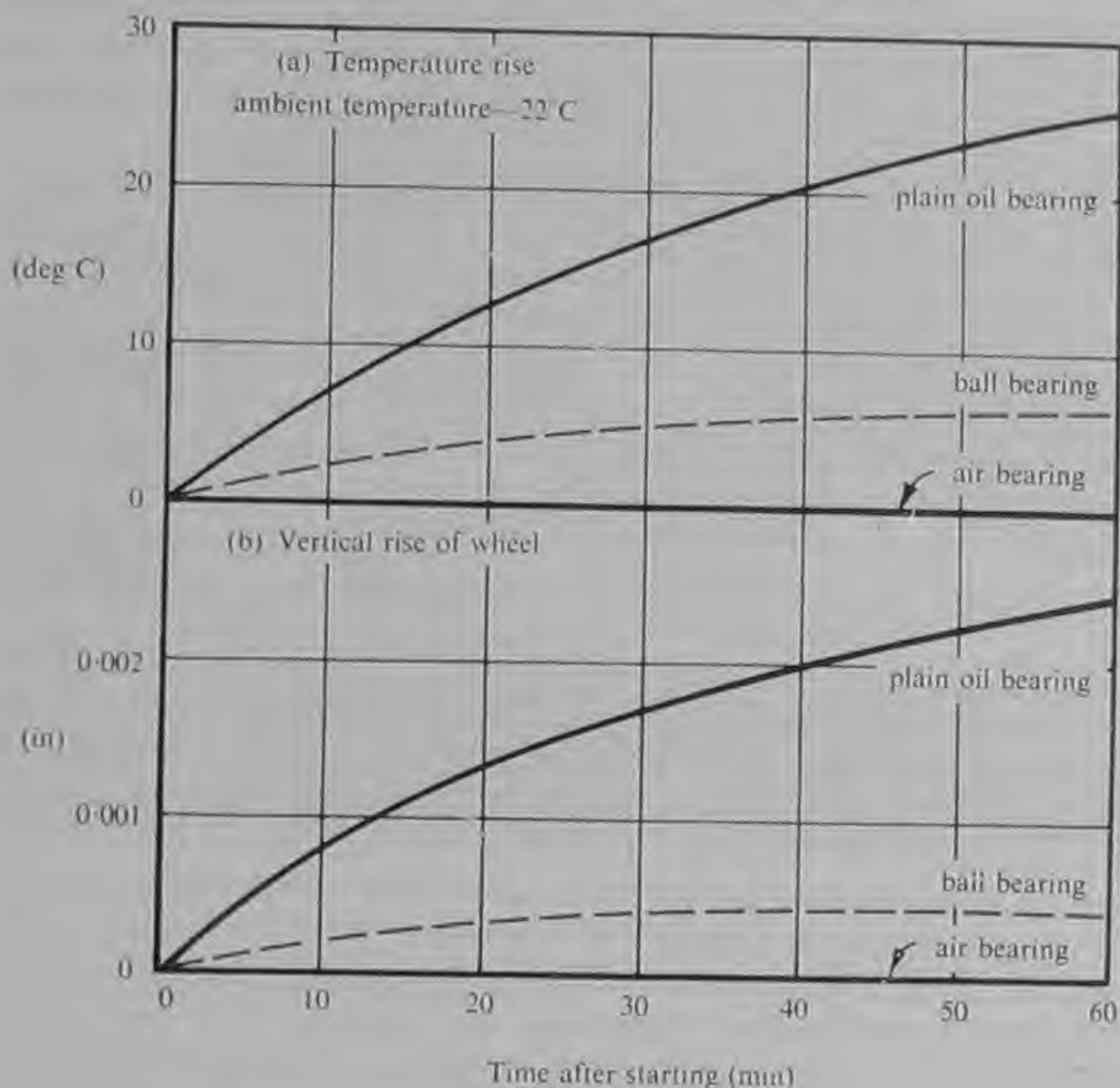
Fig. 12.9 Thermal distortion in surface grinding machines with various types of wheelhead bearings (Ref. 28)

(a) Current drawn by motor at 2 850 rev/min driving conventional wheelhead at 2 850 rev/min   1·2A

(b) Current drawn by motor alone at 2 850 rev/min   0·8A

(c) Current drawn by motor at 2 850 rev/min driving aerostatic wheelhead at 2 850 rev/min   0·8A

(d) Current drawn by motor at 2 850 rev/min driving aerostatic wheelhead at 5 000 rev/min   0·8A

Most grinding machine wheelhead motors run light for longer periods than they run loaded since grinding is essentially an intermittent process. For this reason a saving of thirty-three percent of the motor power consumption is of some economic significance and can partially offset the power expended in compressing the supply air. This factor, combined with the economic advantages arising from the absence of any warming-up period, longer wheel life and dressing diamond life,

higher metal removal rate, the elimination of wear and the reduction in routine maintenance, produces a considerable net economic gain in most applications of aerostatic bearings to grinding machine wheelheads.

Another important advantage of aerostatic wheelhead bearings on surface grinding machines is their ability to grind workpieces flat to within one optical fringe. This property probably arises from the fact that the stiffness of an aerostatic journal bearing is greatest at zero eccentricity, that is at the all-important condition of sparking out when the radial load on the bearing tends to zero. By contrast, a ball bearing spindle has up to 0·000 1 in of free movement and thus provides its lowest stiffness during sparking out.

Several British manufacturers have recognized the advantages of aerostatic spindles for precision grinding machines. In addition to those already mentioned the Churchill Machine Tool Co. Ltd. and Joseph Lucas Ltd. deserve special mention. Churchill have developed the work originated at the National Engineering Laboratory and now offer most of their range of precision grinding machines with air bearings as an alternative to conventional bearings. A large number of air bearing machines have been sold since their introduction in 1964–65. Joseph Lucas, following their early successes in applying aerostatic bearings to hydrogen liquefaction turbines, have developed a high speed air turbine driven internal grinding spindle. This spindle was developed for the specific application of grinding diesel fuel injector pump bores. It proved capable of grinding a 0·25 in diameter bore 1 in deep with a surface finish of 1 μin c.l.a.

12.3 Applications to drilling machines

Drilling machines provide a field of application which is second in scale only to that provided by grinding machines. Fig. 6.9 shows a small high-speed air turbine drilling spindle which was developed by Westwind Turbines Ltd., to fulfill a requirement of the International Business Machine Corporation (I.B.M.) of the U.S.A. I.B.M. were developing a twenty-four spindle tape-controlled machine (shown in Fig. 12.10) for drilling the electronic printed circuit boards of their 360 series computer. Each machine was to be capable of drilling a single circuit board with over six thousand holes in under a minute. In addition it was important that each hole should be clean and burr-free so that no de-burring operations were necessary subsequent to drilling and prior to plating through the holes. It was discovered that the combination of a precision tungsten carbide twist drill (developed by the Metal Removal Company of Chicago) and an air bearing drilling spindle enabled holes of excellent quality to be produced. After a

Fig. 12.10 International Business Machines Hydropad electronic circuit board drilling machine. Each machine incorporates twenty-four Westwind P.C.B.1 air turbine air bearing drilling spindles

good deal of experimentation the condition which produced the best quality holes of 0·030 to 0·045 in diameter, in combination with a long drill life, was found to be a drilling speed of 80 000 rev/min and a feeding rate of 2 in/s. During the development of the process speeds of up to 180 000 rev/min and feed rates up to 5 in/s were tested. Eventually a drill life in excess of 14 000 holes was achieved and this was to a large extent made possible by the true running and vibration-free performance of the aerostatic bearings in the drilling spindles. Performance data for the Westwind P.C.B.1 drilling spindle are given in Fig. 12.11. During two years of continuous operation at the I.B.M. plant at Endicott, N.Y., only one spindle out of a total of over three hundred had to be taken out of service because of bearing trouble. This performance illustrates that the long and wear-free life of which aerostatic bearings are theoretically capable can be realized in practice when they are applied under properly controlled conditions.

Since the adoption of aerostatic drilling spindles by I.B.M. many leading companies in the electronics and computer industries have followed suit. Several manufacturers of printed circuit board drilling

Performance data at 80 lbf/in² gauge bearing supply pressure:

maximum aerostatic radial load at collet nose	5 lbf
aerostatic radial stiffness	25 000 lbf/in
maximum axial load	25 lbf
mean axial stiffness	25 000 lbf/in

Turbine Drive Pressure (lbf/in² gauge)	Speed (rev/min)	Total Airflow (s.c.f.m.)
80	130 000	9·0
60	110 000	7·5
40	90 000	5·2

Fig. 12.11 Performance data of Westwind P.C.B.1 high-speed precision drilling spindle

machines have developed new machines to take full advantage of their high-speed capabilities. The machine built by Select-O-Matic in the U.S.A. (shown in Fig. 12.12) is typical of those designed for large scale production. It incorporates sixteen air turbine drilling spindles (Westwind type P.C.B.3) and the hole positioning is numerically
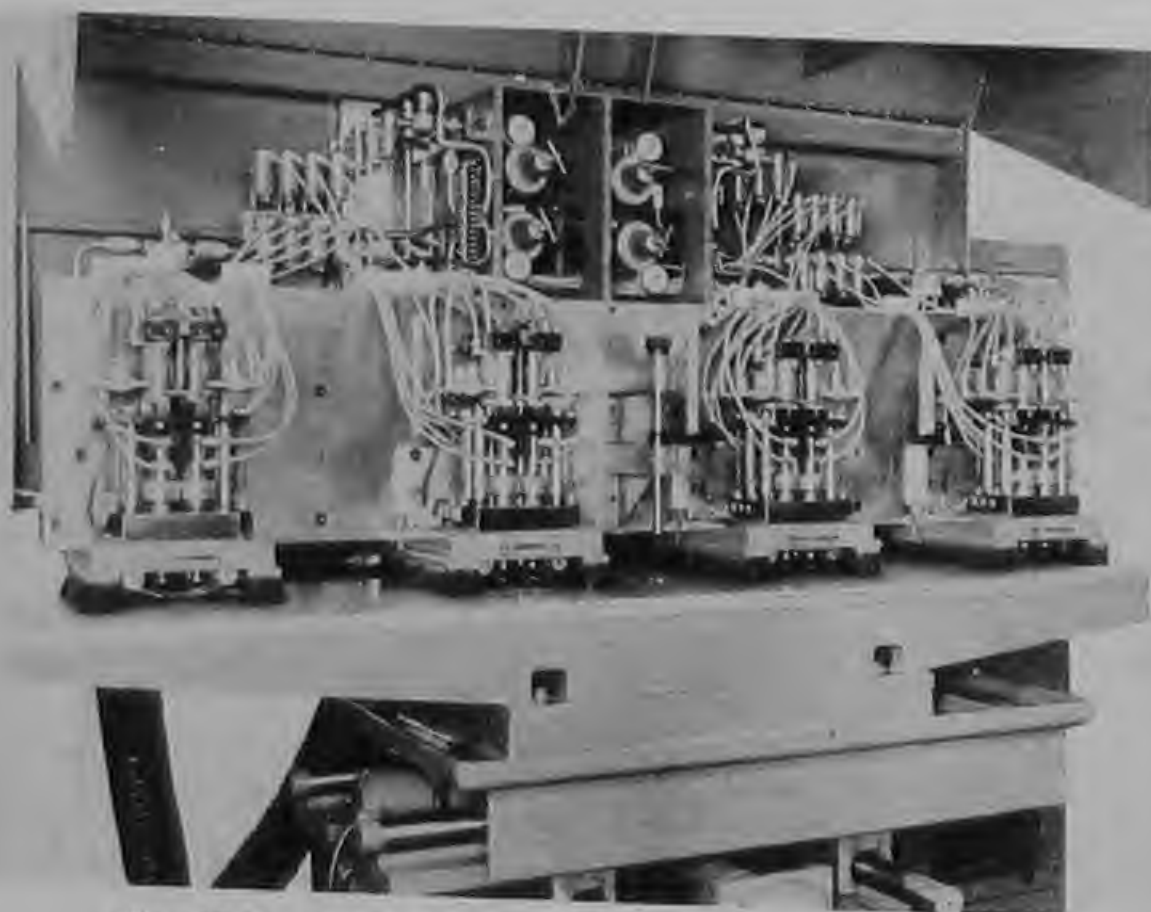
Fig. 12.12 Select-o-Matic circuit board drilling machine with sixteen air turbine drilling spindles with aerostatic bearings

controlled. A more modest manually operated machine produced by James White Printed Circuit Products Ltd. is shown in Fig. 12.13. This machine incorporates a single air turbine drilling spindle (Westwind type P.C.B.1) mounted beneath the table and drilling vertically upwards. It is representative of a class of machine ideally suited to prototype and small batch production work.

Fig. 12.13 James White Printed Circuit Developments circuit board drilling machine with high-speed air turbine air bearing drilling spindle

The successful drilling of holes of diameters below 0·010 in using spiral fluted drills demands the greatest precision in the drilling spindle bearings and in the collet holding the drill. It is also important to eliminate all sources of vibration in order to minimize the chances of drill breakage. Aerostatic bearings have proved to be ideal for micro-hole drilling. At Westwind Turbines Ltd. the development of spindles capable of drilling small holes at high production rates was stimulated by the demands of the aerostatic bearing production. The spindle which had been developed for drilling printed circuit boards was equipped with a precision collet and proved capable of drilling holes
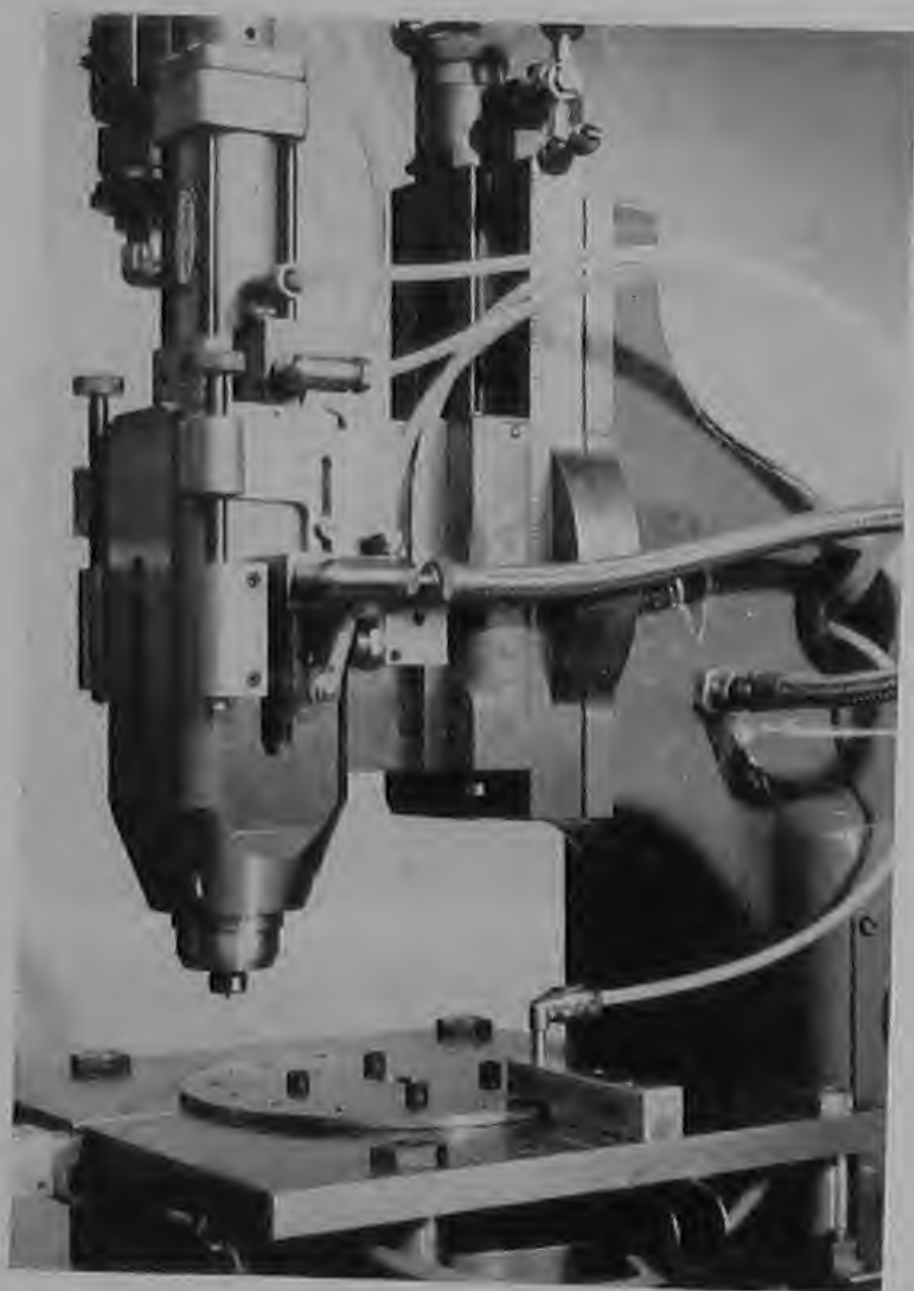
Fig. 12.14 Westwind brass jet drilling machine with air
turbine drilling spindle with aerostatic bearings

down to 0·002 in diameter. The Westwind brass jet drilling machine
is shown in Fig. 12.14. The machine is semi-automatic in operation,
requiring the operator only to load the jets into the slide feeding the
indexing plate. The machine indexes, drills and ejects drilled jets in
automatic sequence following the operation of the feeding slide. The
drilling spindle is advanced by a pneumatic cylinder with a hydraulic
cylinder in tandem to give a smooth motion at a controlled speed. The
following performance is typical:

operation: drilling holes of 0·1 mm (0·003 94 in) in brass;
                  depth of drilling 0·010–0·015 in
drilling speed: 40 000 rev/min
feed speed: 5 in/min

production rate: over 500 holes per hour
drill life: 1 500 to 2 000 holes
drill type: Müller carbon steel twist drill with 1 mm shank

Aerostatic drilling spindles have also been applied to drilling stainless steels and various plastic and composite materials. To date most applications have been concerned with small hole drilling, up to about 0·050 in diameter in metals and 0·100 in in printed circuit board. However, there is no reason to suppose that they could not produce the same high quality burr-free holes in larger sizes if such a performance were advantageous in any particular instance. A future development of some promise might involve the application of an aerostatic drilling spindle to a general purpose precision bench drilling machine. However, the traditional multi-pulley and belt drive would probably have to be abandoned in favour of a motor mounted directly on the drilling spindle, and some alternative means of changing speed would need to be provided.

12.4 Applications to lathes and boring machines

Unlike the applications to grinding and drilling machines, where in certain types of machines the use of aerostatic bearings is already established, the application of aerostatic bearings to metal turning and boring is still, at the time of writing, in its infancy. However, the experiments which have been undertaken offer much promise for the future and some manufacturers are already planning to produce precision lathes with aerostatic workheads. In Switzerland a watchmakers' lathe with an aerostatic spindle has been manufactured for several years.

In 1966 some experiments were carried out by the United States Atomic Energy Commission in relation to the diamond turning of aluminium cylinders. The cylinders were machined while rotating on an aerostatic spindle and were produced round to better than 5 µin with a 1 µin c.l.a. surface finish. Encouraged by this success, Westwind Turbines Ltd. produced aerostatic bearings for the headstock of their Stuart Davis precision boring machine. This machine is used for the finish machining of aerostatic bearing bores while the spindle body rotates in the headstock bearings. The ability to produce bores which are round, straight and parallel to a high degree of precision offers much promise for the future utilization of aerostatic bearings in boring machines. The elimination of friction heating makes size consistency easier to achieve, and the adoption of aerostatic bearings on, for example, machines for boring internal combustion engine pistons could eliminate the selective assembly of gudgeon pins in the motor industry.

Fig. 12.15 Two high-speed air bearing air turbine drilling spindles produced by Westwind Turbines Ltd. The Model P.C.B.1 (right) is widely used in machines for drilling printed circuit boards. The Model P.C.B.2 is only 1 in in diameter to permit close hole spacing on multi-spindle machines. Both spindles are capable of speeds of over 100 000 rev/min

Fig. 12.16 Sectioned air bearing dental turbine showing air passages, turbine and rubber stabilized air bearings (*Reproduced by permission of the Dental Manufacturing Co. (Sales) Ltd.*)

12.5 Applications to medical equipment

The high-speed air turbine dental drill has been mentioned already in earlier chapters. This development, which took place in 1962/63, represented the first large-scale British application of aerostatic bearings. In the four years following its introduction in 1963 over 20 000 units were produced and this success considerably encouraged later applications of aerostatic bearings in other fields. The original design shown in Fig. 12.16 is still being produced at a rate of about 150 units a week and production seems likely to continue for several years.

The original high-speed air turbine dental drill with ball bearings had three major disadvantages. It emitted an intense high-pitched note which could be damaging to the hearing, its bearings needed replacement on average twice a year and it exhausted atomized lubricating oil mist which when inhaled could present a health hazard.
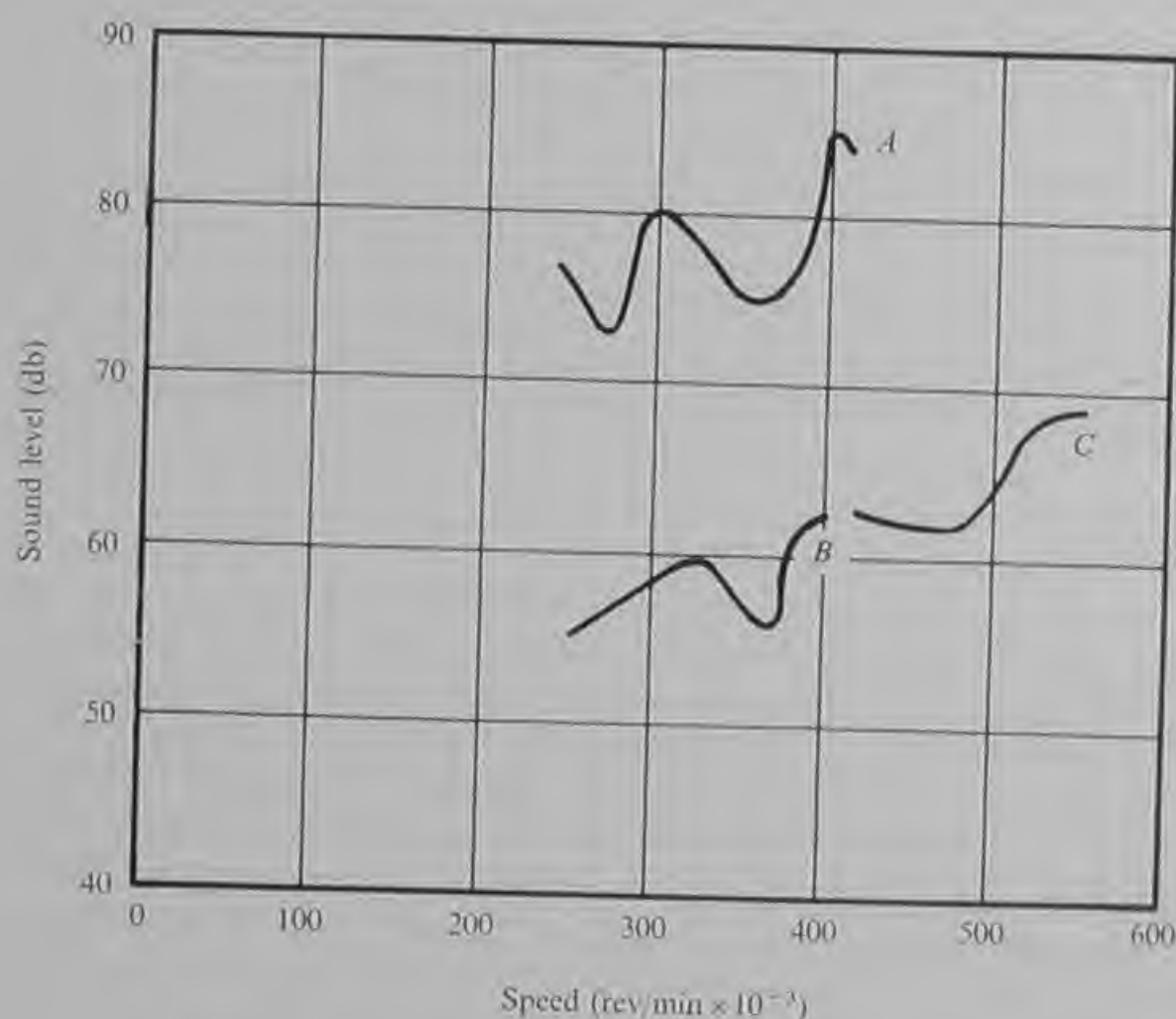
Measured at 12 in from turbine in a sound insulated cabinet using a
Bruel and Kjaer condenser microphone type 4133.
A Typical ball bearing unit
B Early unit with rigid air bearings
C Unit with rubber stabilized air bearings

Fig. 12.17 Sound levels of dental turbines

The introduction of aerostatic bearings overcame all three problems. Fig. 12.17 shows the reduction in sound level which was achieved. The early models with rigidly mounted air bearings were very quiet compared to the ball bearing supported turbines but were subject to some wear due to the occurrence of half-speed whirl. Turbines with rubber stabilized air bearings ran faster and with a slightly higher noise level. The final design which runs between 450 000 and 500 000 rev/min exhibits a noise level of around 63 db compared to about 80 db for a turbine with ball bearings.

The reduction in noise levels which can be achieved by the application of aerostatic bearings is likely to be of increasing significance in the future. The tendency towards higher rotational speeds in, for example, the textile industry is tending to raise noise levels while the introduction of new legislation is likely to demand a reduction below the existing noise levels. Part of the solution to this dilemma may lie in the introduction of aerostatic bearings.

Air bearings in dental turbines have established a considerable superiority over ball bearings in terms of reliability and long life. An analysis of the manufacturer's repair records has shown that on average five percent of dental turbines with air bearings are returned annually for reasons connected with the bearings. This compares to an average figure of 200 percent per annum for ball bearing units. Thus again it is demonstrated that the potential of long wear-free life can be realized even in an application where the bearings are frequently overloaded and caused to rub at high speeds. However, this result was only achieved by the use of ceramic bearing surfaces and could not be approached with any of the combinations of metal surfaces which were investigated during development testing.

A second medical application of aerostatic bearings is shown in Fig. 12.18. The Allen Powell air turbine was developed for use in orthopaedic surgery. It operates on bottled sterile nitrogen supplied at 100 to 110 lbf/in^2 gauge. Speeds above 100 000 rev/min permit bone to be cut without the risk of damage caused by heat generated by the cutting tool. Compared to traditional methods of bone cutting the use of the Allen Powell air turbine has been found to reduce post-operative pain by up to eighty percent. This advantage was demonstrated by tests carried out by the Royal Army Medical Corps on spinal fusion operations.

There were two factors to be considered in the design of aerostatic bearings for an orthopaedic instrument which are not often met in other applications. Firstly, the instrument had to be capable of sterilization by autoclaving in steam temperatures up to 150°C. To meet this requirement stainless materials were essential. Particular difficulty was experienced in providing a flexible air supply lead, which, as it was

connected to the instrument, also had to withstand the autoclaving process. Finally, a terylene covered silicone rubber tubing was found which met the requirement. The second special factor was the need for the turbine to stop quickly when the control lever was released. This is essential if, for example, a swab becomes caught up by the
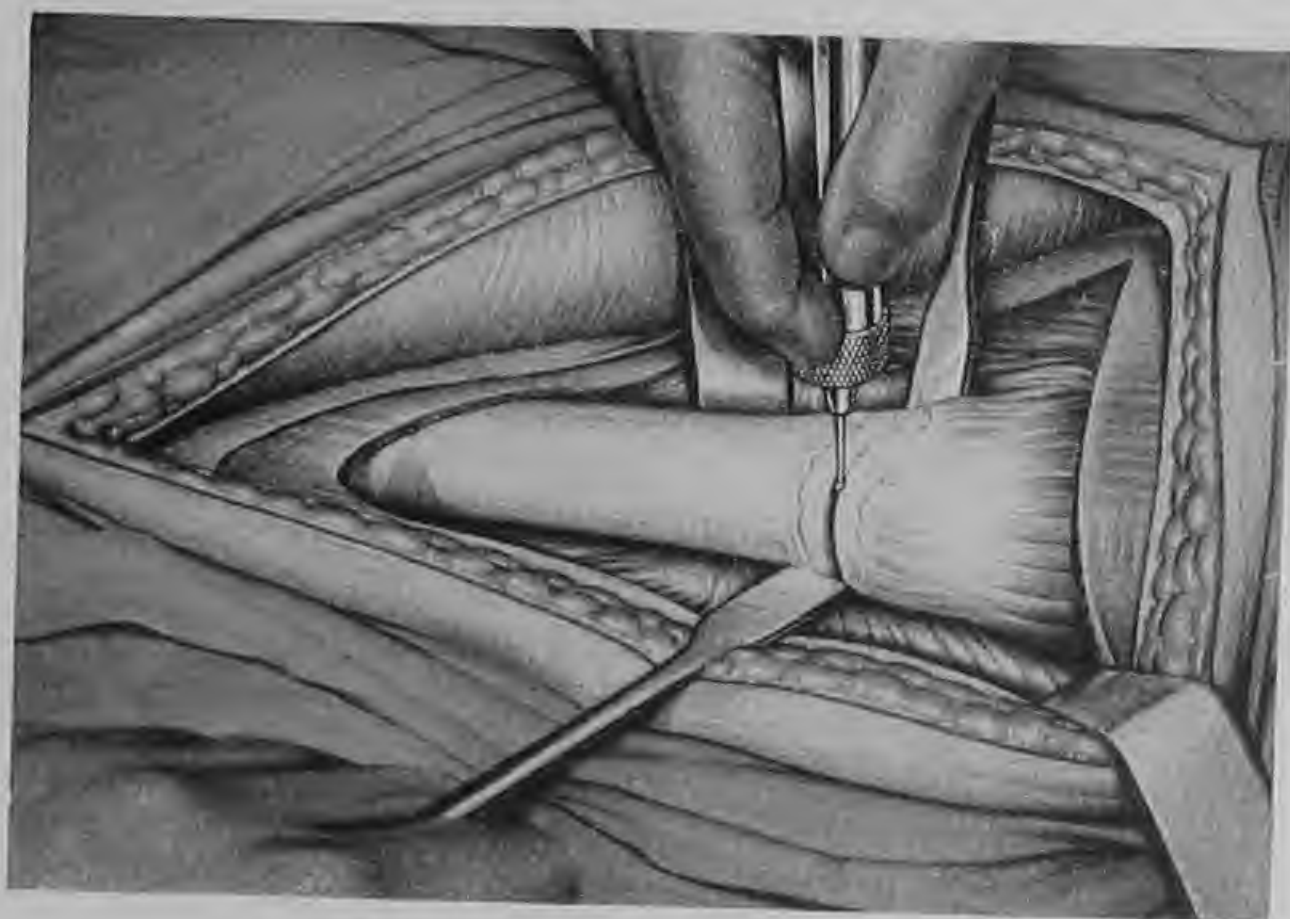
Fig. 12.18 Aerostatic bearings in orthopaedic surgery
(Copyright: Zimmer Orthopaedic Ltd.)

cutting tool. It was decided that stopping from full speed in less than three seconds was desirable. The braking action is achieved by the following method. The control lever operates a valve which supplies air to both the turbine and the bearings. When the lever is released the turbine and bearing supply is cut off and the bearings run down aerodynamically. A small bleed of air is allowed to leak through a metering jet from the air supply to feed the rear thrust bearing. The rotor is thereby forced forwards causing its front face to rub against the front thrust bearing face giving the required braking action. The two rubbing surfaces are coated with tungsten carbide to resist abrasion and wear. This is an interesting example of how unusual requirements can influence the design of a machine and its bearings. Such considerations can present great difficulty and lead to a protracted development period; however they also provide opportunities for a novel or ingenious approach which can be rewarding to the designer.

12.6 Applications to turbine flowmeters for gases

For many years the use of a turbine or propeller flowmeter has been an established method of metering the flow of liquid in pipes. The principle of operation is based upon the fact that over a wide range of flow the speed of the turbine is linearly related to the velocity of the flow. Thus, if a means of measuring the turbine speed is available the instrument can directly be calibrated in terms of volumetric flow rate or mass flow rate. It seemed logical to extend this technique to the measurement of gas flow. However, it was found that when rolling contact or dry rubbing bearings were tried the response of the turbine was non-linear and a relatively large gas velocity was necessary to start the turbine revolving. The defects were due to the high bearing friction in combination with a low turbine torque due to the low gas density. The solution was found in mounting the turbine on an aerostatic bearing. Then the turbine would turn in response to very low gas velocities, and the turbine speed increased linearly with gas velocity over a flow range exceeding 20 : 1.

The first turbine flowmeter for gases with an aerostatic bearing was developed in 1961 at the University of Southampton for the United Kingdom Atomic Energy Authority. The flowmeter is now manufactured by Westwind Turbines Ltd. under licence to the U.K.A.E.A. Fig. 12.19 shows a cross-section drawing of a turbine flowmeter for a 1 in diameter pipe. The flow range of this instrument is from 0·5 to 10 ft^3/min and it can be used at pressures up to 350 lbf/in^2 and temperatures up to 250°C. Within this range of conditions it maintains an accuracy of volumetric flow rate of the order of $\pm 1\%$. The bearing is normally supplied with the same gas as that being metered, but at a pressure between 10 and 50 lbf/in^2 above the pressure of the metered flow. A magnetic transducer head produces an electrical pulse from the passage of each of the five turbine blades. The turbine runs to 2 000 rev/min for every 1 c.f.m. flowing and so the output signal produces 10 000 pulses per cubic foot of gas flowed. Flowmeters of this type have been applied by I.C.I. Plastics Ltd. to integrate the total mass of gas consumed during various manufacturing processes. The volumetric flow output of the turbine is compensated by signals from linear temperature and pressure transducers in a specially developed mass flow calculator. The total mass flow integrated over periods of up to fifty hours has been proved accurate to within $\pm 1\%$ by experiments in which a condensable vapour was metered, then condensed and weighed.

Turbine flowmeters of the same basic type as that shown in Fig. 12.19 have been made in sizes up to 12 in diameter to meter flow rates up to 6 000 c.f.m. In addition to gas flow measurement they have been
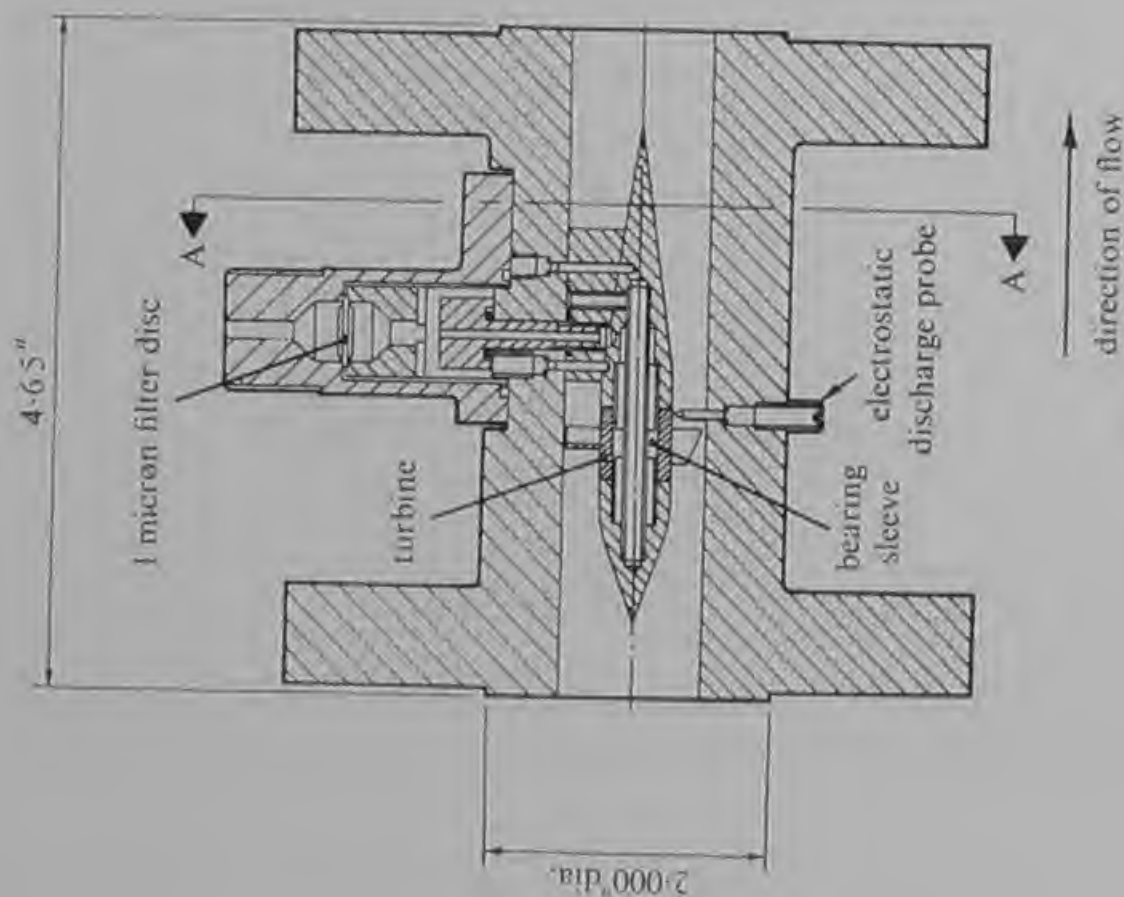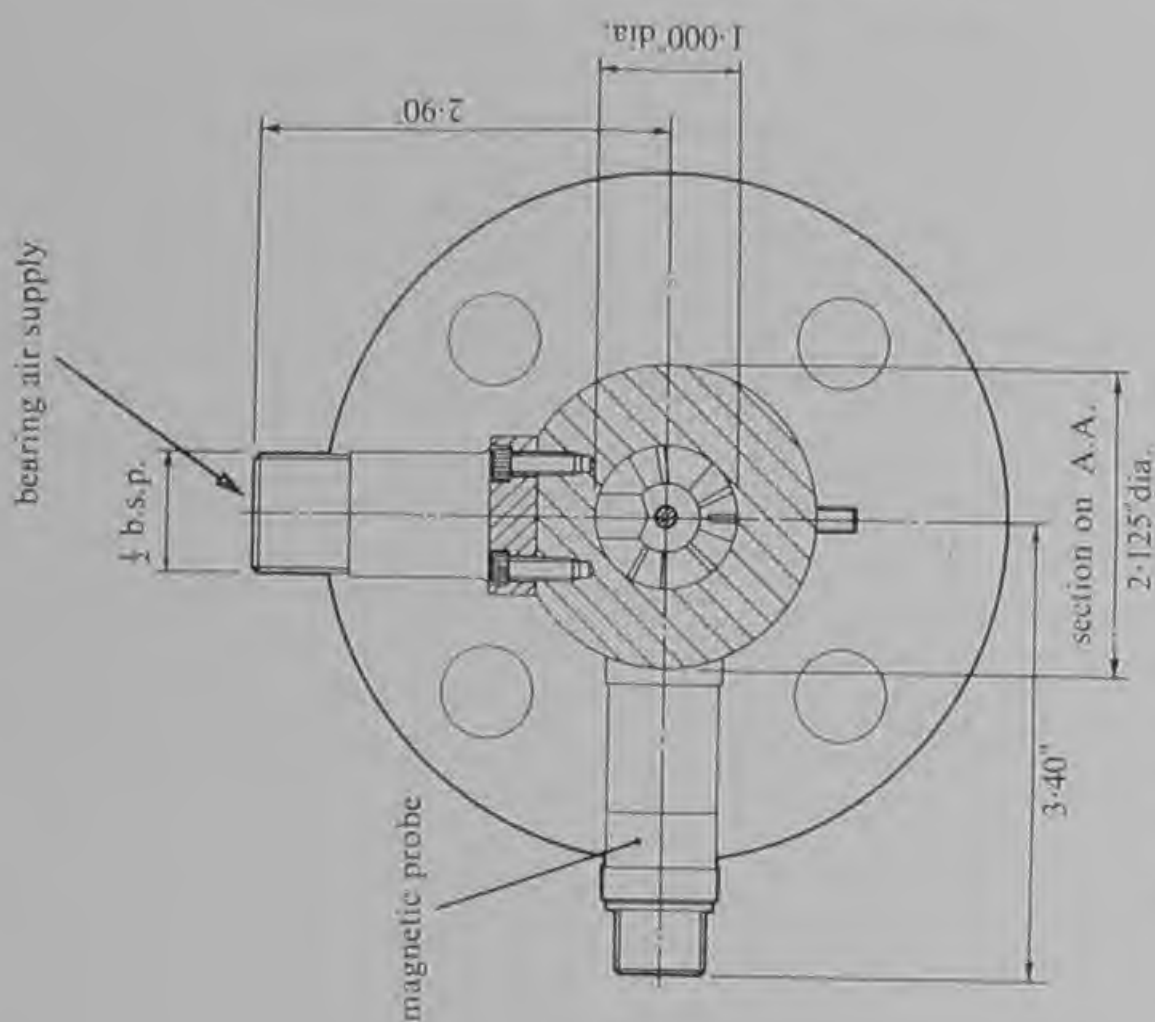
Fig. 12.19 Turbine flowmeter for gases with aerostatic gas bearings
(*Reproduced by permission of Westwind Turbines Ltd.*)

applied to the measurement of the flow of gas-borne dust suspensions where the outflow of gas from the bearing is essential to prevent dust intrusion. In one interesting application a 12 in turbine flowmeter was used in the testing of small gas turbine engines under simulated dust storm conditions. In such applications no special sealing of the bearings is necessary apart from that inherent in their construction. This fact illustrates an important advantage of aerostatic bearings which is not generally appreciated but which might more widely be exploited in the future.

Mounting the turbine on a small central journal bearing as in Fig. 12.19 has the advantage of minimizing the bearing friction. Thus the turbine responds to the gas flow with negligible slip and the ideal of a purely volumetric response is closely approached. The disadvantages of this type of construction are firstly that the small bearing requires a relatively high supply pressure, and secondly that since the configuration lends itself better to a jet-fed bearing design than a slot-fed bearing design the jet diameter has to be adjusted for each bearing gas and a completely universal model cannot be made. These two disadvantages are overcome by the turbine flowmeter devised by C. Dee of Aerostatic Ltd. In this design (shown in Fig. 12.21) the aerostatic

Fig. 12.20 An 8 in diameter turbine flowmeter with aerostatic bearings produced by Westwind Turbines Ltd. under licence to the U.K.A.E.A.
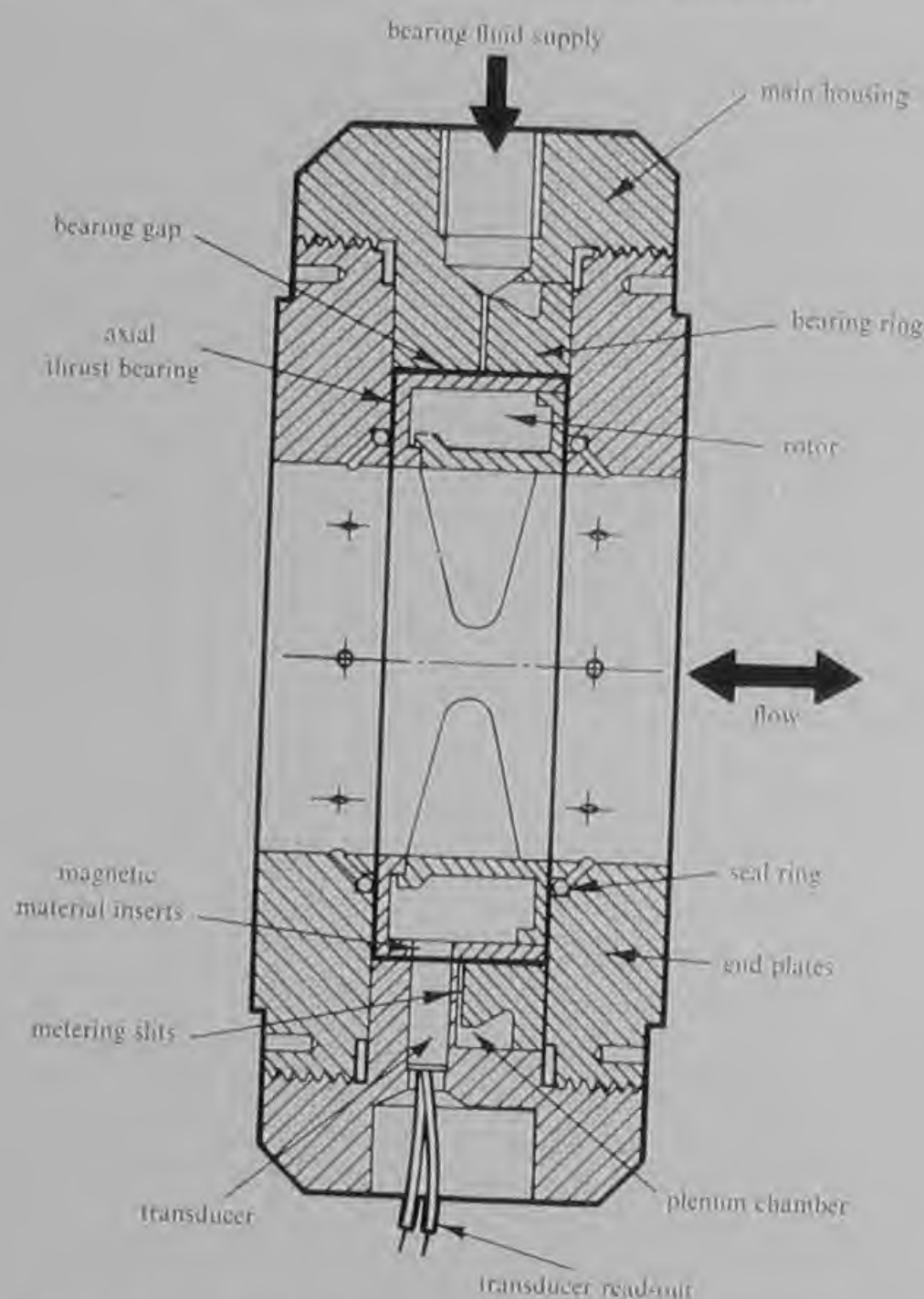
Fig. 12.21 Simplified drawing of the construction of the Dynaflow meter. The flowmeter uses the principle of slot inlet bearings (*Reproduced by permission of Aerostatic Ltd.*)

journal bearing surrounds the turbine. A slot-fed bearing design permits the use of the flowmeter on any gas, or indeed on any liquid, and the large bearing area enables the turbine to be freely supported on bearing supply pressures of only 1–2 lbf/in² above the pressure of the metered flow. However, the increased friction of the large bearing increases the slip of the turbine relative to the gas flow, and the higher inertia inherent in the rim around the turbine decreases the rate of response of the turbine to changes in flow rate. Clearly both types of turbine flowmeter have fields of application in which they excel but

in many applications either type could be employed. It is interesting to see how two designers have sought to solve the same problem by the application of aerostatic bearings and yet have evolved different and individualistic designs. This illustrates how in a new field of engineering, even though the general guide lines are already laid down, the designer can still find ample opportunity to exercise ingenuity and to imprint his work with his own personality.

12.7 Applications to scientific instruments

The applications of aerostatic bearings to scientific instruments are numerous. Fig. 12.22 lists some representative examples. One large

Type	Advantage	Application
Low-speed	Low friction	Balances Dynamometers Frictionless pivots and pulleys
	Precise axis definition	Roundness measurement
High-speed	Low friction power consumption and precise axis definition	Laser Q-spoilers Prism and mirror spinners Optical and infra-red choppers Neutron choppers Atomizing spray discs High speed cameras

Fig. 12.22 Applications of aerostatic bearings to scientific instruments

group of applications takes advantage of the effectively zero friction of aerostatic bearings at zero speed to eliminate the effects of 'stiction' which is often a problem in instrument bearings. Many early applications of air bearings belonged to this class including a variety of balances, wind tunnel balances, dynamometers, frictionless pivots and pulleys. Other low-speed applications have included roundness measuring machines which take advantage of the precise axis definition provided by aerostatic journal bearings.

Many high-speed scientific instruments have been designed with aerostatic bearings. One large family of applications involves the spinning of mirrors and prisms for purposes such as high-speed photography and laser 'Q'-spoilers. Two developments in the latter category are shown in Figs. 12.23 and 12.24. Both machines were developed by Westwind Turbines Ltd. for the National Physical Laboratory. The unit shown in Fig. 12.23 is an adaptation of an air turbine driven

Fig. 12.23 Air turbine with aerostatic bearings supplied to the National Physical Laboratory for rotating a large glass prism at 25 000 rev/min
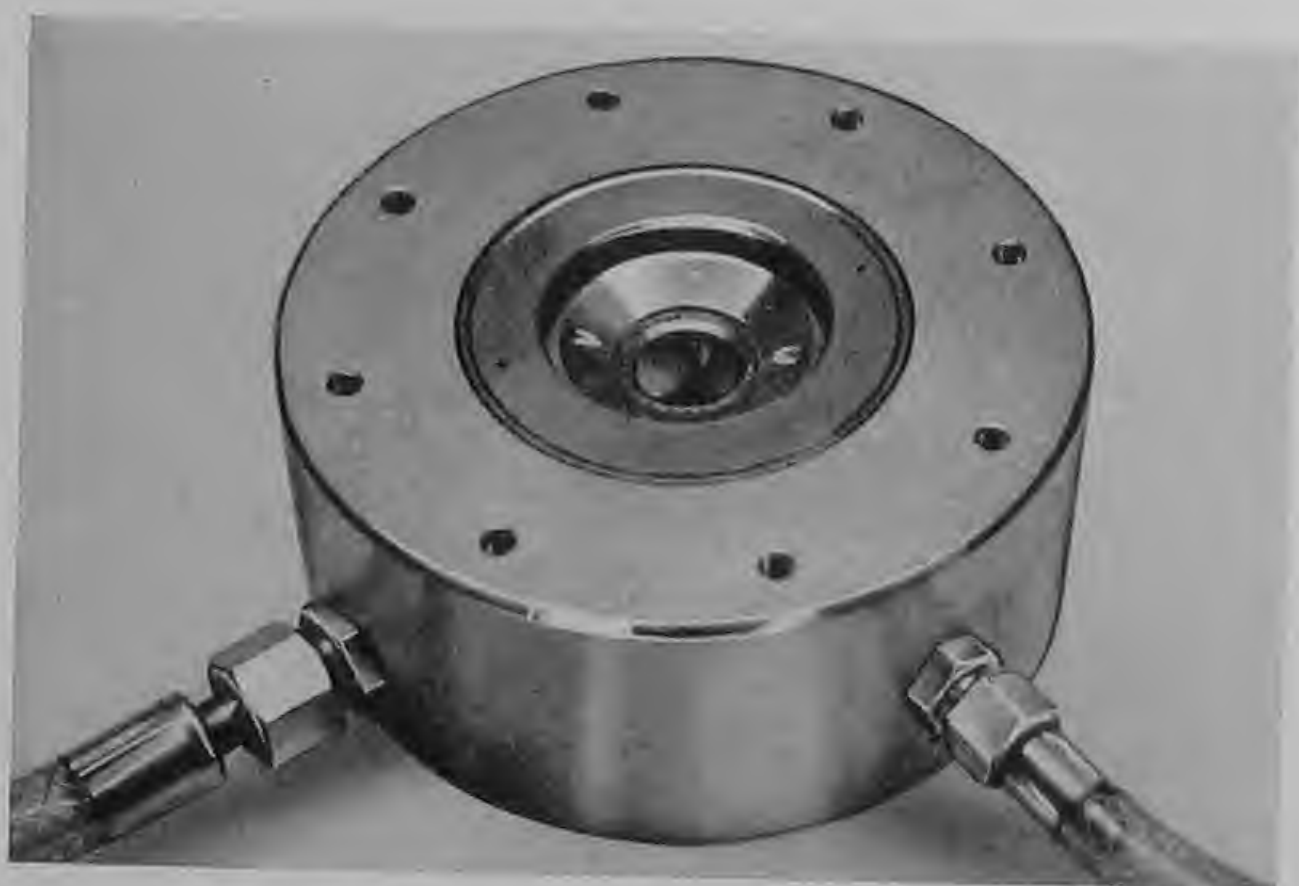
Fig. 12.24 Prism-spinning air turbine with aerostatic bearings developed by Westwind Turbines Ltd. for the National Physical Laboratory. This unit spins a pentagonal prism at 90 000 rev/min for use as a laser 'Q'-spoiler. A developed version runs at 130 000 rev/min

internal grinding spindle. It rotates a relatively large prism at 25 000 rev/min. The unit shown in Fig. 12.24 was specially designed to enable a prism to be mounted in a hollow rotor in such a way that light could be passed axially through the prism if entering and leaving within a cone of solid angle of 120°. This consideration imposed severe limitations on the design of the air turbine and the aerostatic bearings. Difficulties also arose through the radial dilation of the rotor and the need to mount the prism in such a way as to prevent stress concentrations which could cause polarization of the transmitted light. This development is typical of several where the application of aerostatic bearings has provided the research scientist with a tool of performance far in advance of that available hitherto. Another example is shown in Fig. 12.25. This miniature air turbine was designed to operate as an infra-red chopper in a remote temperature-measuring apparatus.

Fig. 12.25 Miniature air turbine infra-red chopper with aerostatic bearings (*Reproduced by permission of Westwind Turbines Ltd.*)

It ran at 150 000 rev/min and provided a chopping frequency of 5 kHz. The infra-red detector was cooled by liquid nitrogen produced from a bottle of compressed nitrogen. The gas exhausting from the infra-red detector amounted to only 0·5 c.f.m. of free gas volume at 10 lbf/in² gauge but this supply was adequate for the chopper turbine and bearings. The diameter of the unit was 0·5 in and its length was 0·75 in so that its volume represented less than one percent of the

volume occupied by the low-speed electric motor employed on an earlier model of the apparatus.

12.8 Conclusion

There are many other applications of aerostatic bearings but lack of space prevents their inclusion. It is hoped that the examples chosen will have provided the reader with some idea of their potential, both their numerous advantages and their adaptability in relation to limitations imposed by other aspects of the design of the machine in which they are used. It is hoped above all that the reader has been persuaded that the aerostatic bearing is no longer a delicate and temperamental device but has evolved into a reliable and effective part of mechanical engineering. Finally, to those readers who go on to design their own aerostatic bearings the author wishes every success stimulated by the same intense fascination which has spurred his own efforts.

APPENDIX

A.1 Physical Properties of Air, Gases and Vapours

1 *Viscosity*

Viscosity of air at 20°C = 181 micropoise (μP)
$$= 3 \cdot 8 \times 10^{-7} \text{ lbf-s/ft}^2$$
$$(100 \ \mu P = 2 \cdot 1 \times 10^{-7} \text{ lbf-s/ft}^2)$$

Viscosity (μP) of Gases and Vapours at Various Temperatures (°C)									
Gas or vapour	0	20	50	100	150	200	250	300	Sutherland's constant, C
Air	171	181	195	218	239	258	277	295	117
Argon	212	222	242	271	296	321	344	367	142
Benzene	70	75	81	94	108	120	—	—	
Carbon dioxide	138	146	163	186	207	229	249	267	240
Carbon monoxide	166	177	189	210	229	246	264	279	102
Chlorine	123	132	145	169	189	210	230	250	350
Chloroform	94	102	112	129	146	160	—	—	—
Ethanol	—	—	—	109	120	136	152	—	—
Ethylene	97	103	112	128	141	154	166	179	226
Helium	186	194	208	229	250	270	290	307	—
Hydrogen	84	88	93	103	113	121	130	139	72
Methane	103	109	119	135	148	161	174	186	164
Neon	298	310	329	365	396	425	453	—	56
Nitrogen	166	174	188	208	229	246	263	280	104
Nitrous oxide	137	146	160	183	204	225	246	265	260
Oxygen	192	200	218	244	268	290	310	330	125
Steam	—	—	—	128	147	166	184	201	650
Sulphur dioxide	117	126	140	163	186	207	227	246	306

	lbf s/ft²	lb/ft s	poise	centipoise	kgf s/m²	kg/m s
Conversion Factors for Viscosity						
lbf s/ft²	1	32·174	$4·788\ 0 \times 10^2$	$4·788\ 0 \times 10^4$	4·882 41	47·880 1
lb/ft s	0·031 081	1	14·881 6	$1·488\ 16 \times 10^3$	0.151 750	1·488 16
poise	$2·088\ 55 \times 10^{-3}$	0·067 197	1	100	0·010 197	0·1
centipoise	$2·088\ 55 \times 10^{-5}$	$6·719\ 7 \times 10^{-4}$	0·01	1	$1·019\ 7 \times 10^{-4}$	10^{-3}
kgf s/m²	0·204 817	6·589 79	98·066 5	$9·806\ 65 \times 10^{-3}$	1	9·806 65
kg/m s	$2·088\ 55 \times 10^{-2}$	0·671 97	10	10^4	0·101 97	1

From the kinetic theory, the viscosity of gases is expected to be independent of pressure and to vary as the square root of the absolute temperature. The first relationship is true except at very low and very high pressures; the second relationship requires certain corrections. If the viscosity μ_1 at temperature T_1 is known, the viscosity μ_2 at temperature T_2 is given by:

$$\mu_2 = \mu_1 \left(\frac{T_1 + C}{T_2 + C}\right)\left(\frac{T_2}{T_1}\right)^{\frac{3}{2}}$$

where C = Sutherland's constant.

2 *Density*

$$\text{Density of air at } 0^\circ C = 0{\cdot}080\ 6\ \text{lb/ft}^3$$
$$20^\circ C = 0{\cdot}075\ 4\ \text{lb/ft}^3$$
$$50^\circ C = 0{\cdot}068\ \text{lb/ft}^3$$

Density of Gases Relative to Air at 0°C	
Argon	1·38
Carbon dioxide	1·527
Carbon monoxide	0·965
Chlorine	2·49
Ethylene	0·97
Helium	0·138
Hydrogen	0·069 5
Methane	0·552
Neon	0·695
Nitrogen	0·967
Nitrous oxide	1·525
Oxygen	1·103
Sulphur dioxide	2·26

Density of steam relative to air at 100°C = 0·636

3 Specific Heats and Ratios of Specific Heats

Specific heat at constant pressure C_p
Specific heat at constant volume C_v

Ratio of specific heats $\gamma = \dfrac{C_p}{C_v}$

C_p and C_v given in J/g deg C at 20° C

Gas	C_p	C_v	γ
Air	1·006	0·718	1·401
Argon	0·523	0·312	1·667
Benzene	1·04	0·745	1·40
Carbon dioxide	0·835	0·641	1·300
Carbon monoxide	1·035	0·800	1·297
Chloroform	0·603	0·544	1·110
Ethylene	1·53	1·21	1·264
Helium	5·24	3·21	1·63
Hydrogen	14·1	10·05	1·407
Methane	2·16	1·64	1·313
Neon	—	—	1·642
Nitrogen	1·022	0·732	1·401
Nitrous oxide	0·892	0·671	1·324
Oxygen	0·92	0·655	1·400
Steam (100°C)	1·88	$\begin{cases} 1·66 \\ 1·45 \end{cases}$	1·135 (dry saturated) 1·30 (superheated)
Sulphur dioxide	—	—	1·26

4 *Gas Constant*

Universal gas constant = 2 780 ft lbf/lb mol deg K

For air, $R \simeq 96 \cdot 0$ ft lbf/lb deg K

Gas	R (ft lbf/lb deg K)
Argon	69·5
Benzene	35·7
Carbon dioxide	63·2
Carbon monoxide	99·4
Chlorine	39
Chloroform	23·2
Ethylene	99·5
Helium	695
Hydrogen	1 390
Methane	174
Neon	139
Nitrogen	99·4
Nitrous oxide	63·2
Oxygen	87
Steam	154·5
Sulphur dioxide	43·4

5 *Boiling Points of Gases at Atmospheric Pressure*

Gas	Boiling Point (°C)
Argon	−185·6
Benzene	80·1
Carbon dioxide	−78·2
Carbon monoxide	−191·3
Chlorine	−33·8
Chloroform	61·3
Ethanol	78·4
Ethylene	−103·7
Helium	−268·6
Hydrogen	−252·2
Methane	−161·5
Neon	−246
Nitrogen	−195·8
Nitrous oxide	−88·5
Oxygen	−183
Sulphur dioxide	−10

6 *Thermal Conductivity of Gases*

The thermal conductivity K of a gas is related to its coefficient of viscosity μ and specific heat at constant volume C_v by the equation

$$K = 0 \cdot 25(9\gamma - 5)\mu C_v,$$

where

$$\gamma = \frac{C_p}{C_v},$$

Coefficients of thermal conductivities given in J/cm s deg C (for Btu/ft h degF multiply by 57·78).

Gas	Variation of $K \times 10^4$ with Temperature (°C)			
	−100	0	100	500
Air	1·58	2·41	3·17	—
Argon	1·09	1·62	2·11	3·60
Carbon dioxide	—	1·45	2·23	—
Carbon monoxide	1·51	2·32	3·04	—
Chlorine	—	0·72	—	—
Ethylene	—	1·64	—	—
Helium	10·59	14·15	17·06	—
Hydrogen	11·23	16·84	21·6	38·9
Methane	1·88	3·02	—	—
Neon	—	4·65	5·70	—
Nitrogen	1·58	2·43	3·12	5·42
Nitrous oxide	—	1·51	—	—
Oxygen	1·59	2·44	3·25	—
Sulphur dioxide	—	0·77	—	—
Steam	—	1·58	2·35	5·7

References used in Appendix A1:

Kaye, G. W. C., and Labye, T. H., *Tables of Physical and Chemical Constants.* Longmans, 1966.

Mayhew, Y. R., and Rogers, G. F. C., *Thermodynamic Properties of Fluids and other Data.* Basil Blackwell, 1957.

A.2 Bibliography

1 Engineering Science Data Sheet No. 65007, 'General Guide to the Choice of Journal Bearing Type', Institution of Mechanical Engineers, 1965

2 Engineering Science Data Sheet No. 66023, 'Calculation Methods for Steadily Loaded Pressure Fed Hydrodynamic Journal Bearings', Institution of Mechanical Engineers, 1966

3 Powell, J. W., Moye, M. H., and Dwight, P. R., 'Fundamental Theory and Experiments on Hydrostatic Air Bearings', Institution of Mechanical Engineers, Lubrication and Wear Group Convention, May 1963

4 Shires, G. L., and Pantall, D., 'The Aerostatic Jacking of a Vented Aerodynamic Journal Bearing', Institution of Mechanical Engineers, Lubrication and Wear Group Convention, May 1963

5 Dudgeon, E. H., and Lowe, I. R. G., 'A Theoretical Analysis of Hydrostatic Gas Journal Bearings', National Research Council of Canada, Mech. Engineers' Report No. MT-54

6 Robinson, C. H. and Sterry, F., 'The Strength of Pressure-fed Air Lubricated Bearings, Parts 1 and 2', A.E.R.E. Reports E.D./R. 1672 and 1673, 1958

7 Shires, G. L., and Dee, C. W., 'Pressurised Fluid Bearings with Inlet Slots', University of Southampton, Gas Bearing Symposium, 1967, paper 7

8 Whitley, S., 'Review of Research in Gas Bearings in the United Kingdom Atomic Energy Authority', First International Symposium on Gas Lubricated Bearings, Washington D.C., October 1959, pp. 30-70

9 Powell, J. W., 'Experiments on a Hybrid Air Journal Bearing', A.S.M.E. 64-WA/LUB-11

10 Allen, D. S., Stokes, P. J., and Whitley, S., 'The Performance of Externally Pressurised Bearings Using Simple Orifice Restrictors', Trans. A.S.L.E., Vol. 4, No. 1, 1961

11 Grassam, N. S., and Powell, J. W. (ed.), Gas Lubricated Bearings, (Butterworth, 1964)

12 Proceedings of the 3rd Symposium on Gas Lubrication held at the University of Southampton, April 1967

13 Raimondi, A. A., 'A Numerical Solution for the Gas Lubricated Full Journal Bearing of Finite Length', Trans. A.S.L.E., Vol. 4, No. 1, 1961

14 Scoles, C. A., and Wunsch, H. L., 'The Use of Air Bearings in Grinding Machines', National Engineering Laboratory Report No. 156, East Kilbride, 1964

15 Trayner, B. T., 'Applications of Gas Bearings to Precision Grinding', University of Southampton, Gas Bearing Symposium, 1965, Paper 9b

16 Powell, J. W., 'A Review of the Experience of Producing over 20 000 Air Bearing Dental Turbines', University of Southampton, Gas Bearing Symposium, 1967, paper 10

17 Tully, N., 'The Vibration Characteristics of Hybrid Journal Gas Bearing Systems', Ph.D. thesis University of Southampton, 1966

18 Mullan, P. J., and Richardson, H. H., 'Plane Vibrations of the Inherently Compensated Gas Journal Bearings: Analysis and Comparison with Experiment', Trans. A.S.L.E., Vol. 7, 1964

19 Montgomery, A. G., and Sterry, F., 'A Simple Air Bearing Rotor for Very High Rotational Speeds', A.E.R.E. Report E.D./R. 1671, 1956
20 Payne, A. R., and Scott, J. R., *Engineering Design with Rubber* (Maclaren, 1960)
21 Sixsmith, H., 'The Theory and Design of Gas Lubricated Bearings of High Stability', First International Symposium on Gas Lubricated Bearings, Washington D.C., October 1959, p. 418
22 Tondl, A., 'Bearings with a Tangential Gas Supply', University of Southampton, Gas Bearing Symposium, 1967, paper 4
23 Cooper, S., 'The Manufacture and Operation of Self-acting, Gas Lubricated Journal and Thrust Bearings', Proceedings A.S.M.E. Spring Lubrication Conference, 1963
24 Licht, L., and Elrod, H. G., 'An Analytical and Experimental Study of the Stability of Externally Pressurised, Gas Lubricated Thrust Bearings', Franklin Institute Report I-A2049-12, 1961
25 Lehmann, R., Wierner, A., Thalkeim, E., and Vorberger Hond Walter, R., 'Die erste Taktstrabe mit luftgelagerten Transportschlitten für 4,5 Mp Tragkraft', *Neue Technik* 6/64 pp. 366-370 and 7/64 pp. 438-441
26 Renke, H. J., contribution to discussion, University of Southampton, Gas Bearing Symposium, 1967
27 Renke, H. J., 'Application of Gas Bearings or Hydraulic Bearings to Precision Grinding', paper presented at 8th International M.T.D.R. Conference at University of Manchester 1967 (Pergamon Press, 1968)
28 'Thermal Distortions of Three Types of Wheelhead that may be fitted to a Jones and Shipman 1400 Surface Grinding Machine'. R & D Department Report, A. A. Jones and Shipman Ltd., 1967
29 Stansfield, F. M., Machine Tool Industry Research Association, *Hydrostatic Bearings for Machine Tools and Similar Applications* (Machinery Publishing Co., 1970).

INDEX

)R
ld-famo

ACK

)

A DS T
E T

ua
CO LTD

B 1 4H

27th April 2014

Note from the uploader:

I found this book some years ago in a library and enjoyed reading it. I tried to find a paper copy for purchase but it was quite hard to get hold of. Recently I came across some webpages belonging to the author, which mentioned a way to contact him:
http://www.amazon.com/John-W.-Powell/e/B001KMI0DG
http://ezinearticles.com/?Gas-Lubrication:-The-Story-of-a-Book&id=6764942
http://www.ghanabooksjwp.com/aboutme.htm

I contacted the author to suggest making this book more widely available and he was helpful and supportive. I tried to determine whether the publisher had any copyright that might prevent me from placing the book on the internet, but the book was published so long ago that it is difficult to find records. It seems that The Machinery Publishing Company Ltd ceased publishing books in the early seventies, and the author was of the suspicion that Wiley may have taken over this book. The author contacted Wiley and received an e-mail stating that they had no knowledge of the book. I contacted Companies House and obtained a disc containing the financial records of the Machinery Publishing Company, which included a note from 1975 explaining that they were exiting the business of publishing books. The records also showed that the company was wound up around 1981, and showed entries relating to the assets of the company at that time. There was no specific reference to any copyright assets at that time, however the liquidator did receive £90.22 in exchange for a "deed of assignment" to the Industrial Press of the USA, without any information about which rights this related to.

I contacted the Industrial Press, and asked them about this book, and whether the payment they made in the early eighties had anything to do with this book. They did not find any records relating to it, and in any case they had no objection to me uploading the book.

Therefore after my best efforts to find any successor to the publisher, who may or may not have had some right over this book, I can find no such entity and therefore assume in good faith that only the author remains in a position to decide the conditions under which this book may be distributed. If I am mistaken and you can prove that you or your company has the rights to this book, please contact me with proof of your copyright claim, and I will assist you to take whatever actions are required.

The author has kindly provided me with the statement (overleaf).

If you find this book to be interesting or useful then I would encourage you to visit the author's website above and perhaps let him know.

Chris Jones

www.chrisj.org